Appendix F

Groundwater numerical modelling technical report

F1 Overview

This appendix summarises the 2024 updates to the Boggabri-Tarrawonga-Maules Creek Complex (BTM Complex) numerical model. It also presents the predicted cumulative impacts from approved mining at the BTM Complex and proposed extensions or modifications at Maules Creek Coal Mine (MCCM) and Boggabri Coal Mine (BCM). The BTM Complex model has been used to assess the potential impacts associated with projects proposed by individual members of the BTM Complex, which are described in the main report.

This appendix focuses on updates to the model, detailing the methods used for re-calibration and uncertainty analysis.

F2 History of BTM groundwater model

Regular groundwater modelling efforts have been conducted at the BTM Complex since 2006 to quantify the impact of mining on the groundwater regime. Several groundwater models have been developed for the region, each with different mines as the primary focus (Heritage Computing (2012), HydroSimulations (2018; 2019), adding to our knowledge of the system behaviour. This BTM Complex groundwater model version has been modified and improved in response to increasing information on the groundwater regime and different project and regulatory needs. This approach aligns with the fundamental guiding principle described by Middlemis (2004) that *"…model development is an on-going process of refinement from an initially simple representation of the aquifer system to one with an appropriate degree of complexity. Thus, the model realisation at any stage is neither the best nor the last, but simply the latest representation of our developing understanding of the aquifer system."*

Parsons Brinkerhoff (2005) developed the first groundwater model for the BTM Complex area in the BCM as part of the approval application. Parsons Brinkerhoff (2008) recalibrated the original MODFLOW model to evaluate the impacts of a new mine plan on the groundwater regime. This model was converted to MODFLOW SURFACT by Australasian Groundwater and Environmental Consultants Pty Ltd (AGE) (2010) as part of the 'Continuation of Boggabri Mine Project'. These early models were relatively simplistic, with limited detail regarding the coal seams in the Maules Creek sub-basin. At that time, little public information was available on the geometry of the coal seams outside the BCM area, particularly under the alluvial floodplain surrounding the site. Therefore, the early numerical models did not represent the coal seams individually; instead, the coal seams and interburden were lumped into layers with a transmissivity equivalent to that estimated for the coal seams.

During the planning stages for the Maules Creek Coal Project in 2010, it was recognised that, due to the proximity of the Maules Creek Coal Project, BCM, and the Tarrawonga Coal Project, quantifying cumulative impacts was important. This led to a data-sharing agreement in 2010 between the companies to facilitate a cumulative impact assessment. Combined geological models enabled the coal seams to be more accurately defined across the mining areas and alluvial plains. The groundwater model developed for the BCM was then updated with this data and used as the basis for a new model to simulate the entire mining complex for the Maules Creek Coal Project approval application (AGE, 2011).

An outcome of the approval applications for the BCM and MCCM was the installation of a network of bores to monitor cumulative impacts on the floodplains surrounding the area where mining occurs. The cumulative monitoring bore network, known as the BTM network, representing BCM, MCCM, and Tarrawonga Coal Mine (TCM), was installed between November 2013 and January 2014 under the supervision of MCCM geologists. At this time, the MCCM groundwater numerical model was also updated by AGE (2014).

The NSW Project Approvals for the BTM Complex mines set Environmental Performance conditions, including those related to groundwater. Each of the BTM Complex mines is required to prepare *'a Groundwater Management Plan, which includes …a program to validate the groundwater model for the project, including an independent review of the model every 3 years, and comparison of monitoring results with modelled predictions.'*

In 2018, the BTM Complex mines engaged AGE to validate the groundwater model to address the above condition of consent. The model was converted to MODFLOW-USG (MFUSG). The mesh was updated, and some limited changes were made to the model layering. The model parameters were then updated through a water level history matching process (i.e., model calibration).

Following the NSW Government's review of the 2018 model, the BTM Complex mines engaged AGE to further develop the numerical BTM Complex model. This work was largely undertaken between 2019 and 2021, with a final BTM Groundwater Model Update report issued in 2022 (AGE, 2022). The engagement involved thoroughly reviewing available data and revisiting the conceptual model. The rainfall recharge zones were updated to represent localised recharge occurring through the beds of the major drainage lines, and 15 model layers were added to further subdivide the coal seams within the model. The model was recalibrated, and updated water take and drawdown predictions were made. This model was then used to investigate BCM Mod 8 and the subsequent amendment. The evolution of the BTM Complex numerical model is summarised in Table F 1.

In January 2023, the BTM Complex mines engaged AGE to review the model to fulfil a condition of consent, which mandates this review to occur every three years. AGE was also separately engaged by BCM and MCCM mines to update the BTM Complex numerical model to assess the potential impacts of the new proposed extension and modification (Continuation Project and MOD10) on continuing mining operations at the complex. The main updates to the current BTM Complex model considered expanding the general-head boundary condition to layer 1 (Alluvium), changing the recharge model for an accurate representation of recharge processes along creeks and surface water features, swapping the horizontal flow barrier feature for a structural overlay to represent local faults, relaxing the relationship between hydraulic conductivity and depth to allow for more flexibility during calibration, and deactivating the low permeability barrier adjacent to the Tarrawonga Mine featured in the original model design. The effect of the fault on groundwater flow was changed to only influence Permian and volcanics, which previously included the Gunnedah alluvium. Additionally, prompted by updates to the mine site's geological model, some layer elevations were also adjusted to reflect the new data. This appendix provides a detailed outline of the updates made to the BTM Complex model for these purposes.

Table F 1 Historical model comparisons

Year	2010	2011	2014	2018	2022
Reference	AGE 2010	AGE 2011	AGE 2014	AGE 2018	AGE 2022
Purpose	Boggabri approval application	Maules Creek approval application	Maules Creek conditions	BTM Complex update	BTM Complex update
Model code	Surfact	Surfact	Surfact	USG	USG
Model area (km^2)	892	1,190	1,190	961	961
Grid	rectangular	rectangular	rectangular	Voronoi & rectangular	Voronoi & rectangular
Grid cell size (m)	50 x 50 – 100 x 100	50 x 50 – 500 x 500	50 x 50 – 500 x 500	100 x 50. 200 x 200, 115 – 650 diameter polygons	100 x 50. 200 x 200, 115 – 650 diameter polygons
Layers	5	12	12	19	34
Coal seams modelled?	No	Yes – 4 groups	Yes – 4 groups	Yes – 5 groups	Yes – 10 groups
Lowest seam modelled	Base of L3 set to the base of Merriown seam	Templemore group (L10)	Templemore group (L10)	Templemore group (L17)	Templemore (L32)
Calibration (SS/TR)	SS	SS	SS & TR 2006 – 2013, 31 quarterly SPs	SS & TR 2006 – 2014, quarterly SPs	SS & TR 2006 – 2024, quarterly SPs
Predictions	2006 – 2032, 107 quarterly SPs	2006 – 2032, 107 quarterly SPs	2014 – 2043, 119 quarterly SPs	2006 – 2032, 107 quarterly SPs	2006 – 2045, quarterly SPs
Sensitivity/ Uncertainty?	S	S	No	U	U

Notes: Y: Yes. N: No. L: model layer. S: sensitivity. SP: stress period(s). SS: steady-state. TR: transient. U: uncertainty. m: metres. km: kilometres.

F3 Guidance on groundwater modelling

The following guideline documents, which directly inform aspects of groundwater modelling, have been published by regulators since the BTM model was last updated:

- The NSW Groundwater Assessment Toolbox for Major Projects in NSW (NSW Department of Planning and Environment, 2022a), which includes a guideline entitled the Minimum Groundwater Modelling Requirements (NSW Department of Planning and Environment, 2022b) and other supporting guidelines.
- Federal Independent Expert Scientific Committee on Coal Seam Gas and Large Coal Mining Development (IESC) guidelines on:
  - Characterisation and modelling of geological fault zones (Murray & Power, 2021);
  - Assessing groundwater-dependent ecosystems (Doody & Moore, 2019);
  - Uncertainty analysis for groundwater modelling (Peeters & Middlemis, 2023); and
  - IESC Explanatory Note: Using impact pathway diagrams based on ecohydrological conceptualisation in environmental impact assessment (IESC, 2023).

The IESC explanatory note on ecohydrological models is not specific to groundwater modelling but focuses on approaches for identifying causal impact pathways and Quantities of Interest (QoIs). These pathways influence model design, prompting its inclusion as a guide for groundwater modelling.

The Groundwater Modelling Decision Support Initiative (GMDSI)[1] has been developing a range of guidance notes on groundwater modelling, mainly related to model complexity, uncertainty analysis and decision-making support. The GMDSI approaches provide tools that facilitate improved application of the IESC's uncertainty analysis guideline. While the GMDSI is not a government regulation, it influences the direction of groundwater modelling, and therefore, its approaches and recommendations have been considered.

The Groundwater Assessment Toolbox (GAT) offers high-level guidance on conducting groundwater impact assessments, with a focus on data acquisition for conceptual models. The Minimum Groundwater Modelling Requirements provide more technical detail on synthesising data into a groundwater model.

Whilst not a recent publication, the Australian Groundwater Modelling Guidelines (AGWMG) (Barnett, et al., 2012) is also an important document guiding groundwater modelling and was considered part of the model update.

[1] https://gmdsi.org/.

F4 Model plan and objectives

A Groundwater Modelling Plan (GMP) to update the BTM Complex model (AGE, 2023) was prepared in accordance with the Minimum Groundwater Modelling Requirements for SSD/SSI Projects – Technical Guideline (Minimum Groundwater Modelling Requirements)[2] (NSW Department of Planning and Environment, 2022b). The GMP considered both the Maules Creek Continuation Project (MCCP) and BCM Mod 10 and was presented to DCCEEW during an online meeting held on 17 May 2024 and subsequently submitted in writing.

The primary objective of the groundwater model described here is to assess the magnitude and likelihood of impacts caused by mining at the BTM Complex on proximal groundwater resources and/or groundwater-dependent ecosystems (GDEs). This is a broad statement that encompasses several modelling-specific objectives listed below (Table F 2), which are required by the Aquifer Interference Policy (AIP) and are consistent with previous modelling investigations for the entire BTM Complex. These modelling-specific objectives are related to QoIs discussed and identified in the main Groundwater Impact Assessment (GIA) report. It is noteworthy that the QoIs were developed in consultation with other disciplines, including surface water hydrologists and ecologists. Further details are provided in the Ecohydrological Conceptual Model (Section 7.9.2 of the GIA). Most notable is the groundwater "take" estimation from coal measures and alluvium for water licensing requirements.

Table F 2 Modelling specific objectives

Objective	Rationale
Evaluate cumulative drawdown at all identified receptors (including GDEs).	Determine if the impacts will exceed 'minimal impact considerations' as outlined in the AIP due to groundwater drawdown.
Evaluate incidental and passive water take from groundwater and surface water sources.	Estimate water take and determine water licensing requirements to account for predicted water take.
Address the Project-specific Secretary's Environmental Assessment Requirements (SEARs).	Evaluate whether the proposed project will comply with water-related SEARs.
Forecast the range of potential inflows into the approved and proposed expansions of open cut pits for each BTM Complex mine.	Continuation Project and MOD10 proponent's request.

The BTM Complex model aims to quantify the magnitude of cumulative impacts on the groundwater regime, surface water resources and groundwater-dependent assets. Additionally, it provides a tool for the sustainable and adaptive management of the aforementioned assets. A fit-for-purpose model provides predictions of future impacts useful for all stakeholders. This does not mean that the model can perfectly represent past and future changes within the groundwater regime, but simply that it is a useful tool for identifying the level of risk and assisting in decision-making and sustainable management of the groundwater regime.

The respective GIA report for each mine site lists project-specific QoIs for each proposed expansion project (Maules Creek Continuation Project and BCM MOD10). Therefore, this appendix does not describe project-specific QoIs of interest for each mine site.

[2] Minimum Groundwater Modelling Requirements for SSD/SSI Projects.

F5 Model assumptions and limitations

F5.1 Assumptions

The numerical model adopts the following assumptions:

- Pre-mining conditions are assumed to be prior BCM's start of operations in 2006.
- Groundwater in the model domain is represented as a single-phase fluid with constant density in a continuous porous medium.
- Hydraulic conductivity is heterogeneous and isotropic in the horizontal direction but anisotropic in the vertical direction.
- Upscaling and averaging aquifer properties to the dimensions of model grid cells is appropriate for the modelled area.
- Model layers accurately reflect the elevations and extents of geology/hydrostratigraphy.
- Discontinuities in model layers representing formation pinch-outs prevent horizontal flow.
- Model boundaries, where assigned, are reasonable approximations of the primary sinks and sources in both space and time.
- Groundwater flow through coal seams, regolith and alluvial formations is dominated by horizontal flow, while flow through interburden formations is dominated by vertical flow.
- Specifically, for the recharge model employed in this assessment, water leaching from the soil moisture model is assumed to reach the water table without any lag in timing within the defined stress period.
- Mean stresses (excluding mining operations) and hydraulic heads over the last two decades reasonably approximate system steady-state conditions.
- Prior probability distributions of model parameters capture epistemic uncertainty.
- The Conomos fault likely acts as a groundwater flow barrier; however, the 2024 numerical model has been updated to assess the potential for flow conduits. It was assumed to have no impact on layer 1 of the model, representing the alluvium and weathered regolith.
- The Hunter-Mooki Thrust Fault System, located at the boundary of the New England Fold Belt, is represented as a vertical no-flow barrier along the eastern edge of the model, spanning layers 3 to 34. It represents the boundary between the edge of the Maules Creek sub-basin and the non-coal New England fold Belt.
- The emplacement of spoils during mining progress was not represented in the model for all open cut pits until the end of calibration (June 2024).
- Other mining operations, such as the Vickery Mine and Narrabri Mine, occur within the region but are not within the extent of the numerical model. Given the distance, lack of continuity within the coal seams, and the boundary condition effect of the intervening alluvial system, these mines are unlikely to contribute to the cumulative impact on groundwater.
- The agricultural groundwater extraction represented in the model is sufficient for calibration and prediction purposes.

F5.2 Limitations

The numerical model limitations are the following:

- Processes at spatial scales smaller than 100 m must be aggregated.
- Processes at temporal scales smaller than 90 days must be aggregated.
- The stress on the system related to mining progression is approximated as step changes, which may differ in timing and location but are considered reasonable given the timescales associated with the predictions. For example, the stress simulated by mining in the model calibration period excludes any effects of spoil emplacement, which, if included, would yield different properties for similar hydraulic diffusivities.

- Future stresses on the system, other than those related to mining, are represented by mean values and exclude the effects of seasonal variability in recharge from flow events, stage changes in the Namoi River, and third-party water use.
- Uncertainty in predictions precludes aleatoric uncertainty. This means that uncertainty analysis might underestimate the full range of uncertainties (epistemic[3] and aleatoric[4] uncertainty).
- The model grid design reflects the underlying connectivity assumptions between the Permian and alluvium, placing an upper limit on the saturated thickness available for lateral flow. The effect of this assumption is explored below with a focus on the Maules Creek alluvium.
- Information available to constrain fluxes is highly uncertain and considered a soft target for calibration, thereby increasing the potential for non-uniqueness.
- Like many mining projects, detailed mapping and characterisation of regional faults within the model extent are sparse, although available sources generally agree that they are present to some degree. As such, the current representation of faulting in the numerical model may be limited relative to their actual presence. This potential under-representation is a common feature in numerical groundwater models, and it is an important aspect to highlight, given its implications for model calibration and predictions. Conceptually, this may contribute to the conservative predictions of drawdown that are inconsistent with observations outside the mining area.
- The timing and location of past and future mining in the numerical model contains uncertainty. Specialised literature refers to this as 'scenario uncertainty' (Middlemis and Peeters, 2018) in the context of future mining. Historical mining records can be difficult to obtain or are necessarily simplified, so assumptions about the progress of mining operations, particularly those from older times, are required. The exact advancement of future mining operations is also uncertain. All mining operations are subject to detailed mine design, market conditions, and other factors that can impact project progression and mining rates. Therefore, the historical and future mining represented within the numerical model should be considered a guide rather than an accurate representation.
- Despite these limitations, the model is considered to accurately reflect mining as it has historically occurred and is expected to continue in the future; however, there is a degree of uncertainty regarding the timing and elevation of the mining.
- The BTM Complex model incorporates two layers to represent the full thickness of the alluvium, with Layer 1 being the Narrabri alluvium, and Layer 2 being the Gunnedah alluvium. The Narrabri alluvium is laterally connected to Permian weathered regolith, while the Gunnedah Alluvium is laterally disconnected, limiting flow to the vertical direction through sub-cropped coal seams. This aligns with the current conceptual model of the system, which assumes that weathered regolith is the primary pathway for lateral groundwater flow from the alluvium.
- This assumption implies that lateral flow from the alluvium is limited by the regolith thickness, which was assessed using an analytical approach that considers the full saturated thickness of the alluvium being available for lateral flow. The Edelman Solution (Edelman, 1947) is a transient 1D solution that calculates hydraulic head response and changes in flux at a fixed distance from a step change in hydraulic head. This solution assumes constant transmissivity but can be applied to unconfined systems when the head change is less than 20% of the saturated thickness, as it produces solutions comparable to those of the linearised Boussinesq equation (Boussinesq, 1877). The application of the solution in this analysis assumes a 1.0 m head difference across 250 m (gradient of 0.004) as representative of the drawdown.
- Typical values of hydraulic conductivity, storage coefficient and saturated thickness (Table F 3) for the two alluvial formations were used to estimate the change in flux at equilibrium. A total flux from the alluvium into the Permian can be estimated by assuming a 10 km stretch of alluvium is affected by drawdown, resulting in 0.09 ML/d discharge from the Narrabri and 0.52 ML/d discharge from the Gunnedah. In a calendar year, this equates to approximately 219 ML, which remains well below the WALs held by the proponent of the Project. The 10 km length is approximately the same as the length of Upper Maules Creek alluvium affected by drawdown through the regolith, according to the numerical model.

[3] Epistemic uncertainty is related to known errors such as measurement error, model structural errors.

[4] Aleatoric uncertainty is related to the inherent randomness of the system and can be thought of as an unknown, unpredictable and unquantifiable error.

Table F 3 Analytical assessment parameters and results

Formation	Kh (m/day)	S (--)	Thickness (m)	Flux (ML/day)
Narrabri	1.0	0.01	10.0	0.09
Gunnedah	2.5	0.15	13.0	0.52

F6 Model construction and development

F6.1 Model code

The BTM Complex model uses the MFUSG modelling package based on the AGE (2022) model. MFUSG is considered superior to pre-2013 versions of MODFLOW, as it allows the use of an unstructured model mesh, ranging from triangles to n-sided polygons. This means the model grid can be designed to accommodate environmental features, such as rivers, water bodies, and excavations, with improved flexibility. MFUSG is relatively numerically stable and does not require continuous layers, meaning it can simulate geological units that pinch out or subcrop, such as coal seams. Therefore, flow transfer processes between layers that are not directly connected can be more realistically represented and simulated.

The amount of water level monitoring data available (264 monitoring bores/VWPs sensors) for the BTM Complex now means that trial-and-error selection of model properties is not an efficient method for calibrating the model. The typically faster run times associated with MFUSG mean the code is well-suited to automated calibration. In addition, MFUSG is not restricted by licence agreements, allowing numerous iterations of the model to be run simultaneously. This can reduce the time required for model calibration and uncertainty analysis, where applicable.

The model was created using Python and Fortran scripts, along with an MFUSG edition of the Groundwater Data Utilities by Watermark Numerical Computing. The model mesh remains consistent with AGE (2022) which was developed with Algomesh v2.0 (HydroAlgorithmics, 2016).

F6.2 Model design

The model domain is approximately 30 kilometres (km) wide and 40 km long, as shown in Figure F 1. The model domain was centred on the approved mining activities in the BTM Complex. The model encompasses the main receptors identified, including alluvial management zones and their associated GDEs located to the north, west, and south of the BTM Complex, as well as water users and surface water features such as the Namoi River and its tributary creeks. The eastern extent of the model is located at the Mooki Thrust Fault System, which represents the boundary of the Maules Creek sub-basin and marks a change in hydrogeological regime to an area less sensitive to environmental impacts from the BTM Complex due to distance and geology. The thrust fault is assumed to be vertical.

Other mining operations occur within the region but are not within the extent of the numerical model:

- The Vickery Mine is situated approximately 14 km south of the BTM Complex, with several intervening faults separating Vickery from the BTM Complex. A combination of distance, lack of continuity within the coal seams, and the boundary condition effect of the intervening alluvial system means that Vickery and the BTM Complex are considered unlikely to generate a cumulative groundwater impact. Groundwater modelling completed as part of the Environmental Impact Statement (EIS) for the Vickery Mine Extension Project application (HydroSimulations, 2018) predicted that the maximum water table drawdown will largely be limited to the area of the Permian outcrop adjacent to the Vickery operation.
- The Narrabri Mine is located 27 km west-northwest of the BTM Complex. Mining at the Narrabri Mine occurs within the coal seams of the Mullaley Sub-basin, which is separated from the Maules Creek sub-basin by the Boggabri Ridge. The Boggabri Ridge comprises the Boggabri Volcanics, which are characterised by very low permeability. Again, a combination of distance and lack of continuity within the coal seams means that Narrabri Mine and the BTM Complex are considered unlikely to have a cumulative impact. This conclusion is supported by modelling that predicts neither the BTM Complex nor the Narrabri Mine is expected to have any significant or extensive drawdown within the Namoi River alluvium (AGE, 2022; AGE, 2020a), which forms a significant storage of water separating the mining areas.

F6.2.1 Perimeter Model Boundaries

Boundary conditions were aligned with the conceptual hydrogeological model of the area, with groundwater flow in and out of the model largely occurring through the alluvium. Flow through the Namoi River alluvium was largely represented by General Head Boundaries (GHB) along the southern and western sides of the model, where alluvial groundwater enters and exits the model (layers 1 and 2). Groundwater levels at the Namoi River alluvium GHBs were determined based on the average groundwater levels measured in monitoring bores in proximity to the model boundary. A detailed description of this process is provided within AGE (2022), but no update is provided here as there has been no significant change since then.

The AGE (2022) model represented large sections of the northern, western and southern model perimeter boundaries with ‘no-flow’ conditions (Figure F 1). This included the areas on the eastern boundary where catchments continue, and topography and associated hydraulic gradients would allow groundwater inflow to the model from the New England Fold Belt fractured rock groundwater system. An analytical estimate of groundwater flow from the New England Fold Belt fractured rock into the model domain indicated potential inflows of approximately three megalitres per day (ML/day). The model was initially updated to represent this inflow with GHBs assigned in all model layers along the eastern model boundary adjacent to the Maules Creek and Bollol Creek alluvial plains. However, this resulted in the model failing to converge. The cause of numerical instability was attributed to the explicit representation of geology associated with the Permian coal measures sequence, where all layers are laterally discontinuous and pinch out in the west against the Boggabri volcanics. The pinching of coal measures layers in the unstructured grid laterally disconnects the Permian sequence layers from other model layers, albeit only in the horizontal direction. Vertical connections remain unaffected. The addition of the GHBs along the eastern edge of the model domain was subsequently modified to only occur in model layer 1 (Narrabri alluvium and weathered regolith), where layer 2 (Gunnedah alluvium) was present. Hydraulic heads assigned to the GHBs were set at the model cell's topographic elevation but were assumed to be approximately 2 km from the model. This simulated an effective hydraulic gradient between 0.001 and 0.003 (1:1000 to 1:333), depending on the model cell location and was factored into the initial conductance calculation for each GHB boundary cell.

2022 BTM Complex Model update

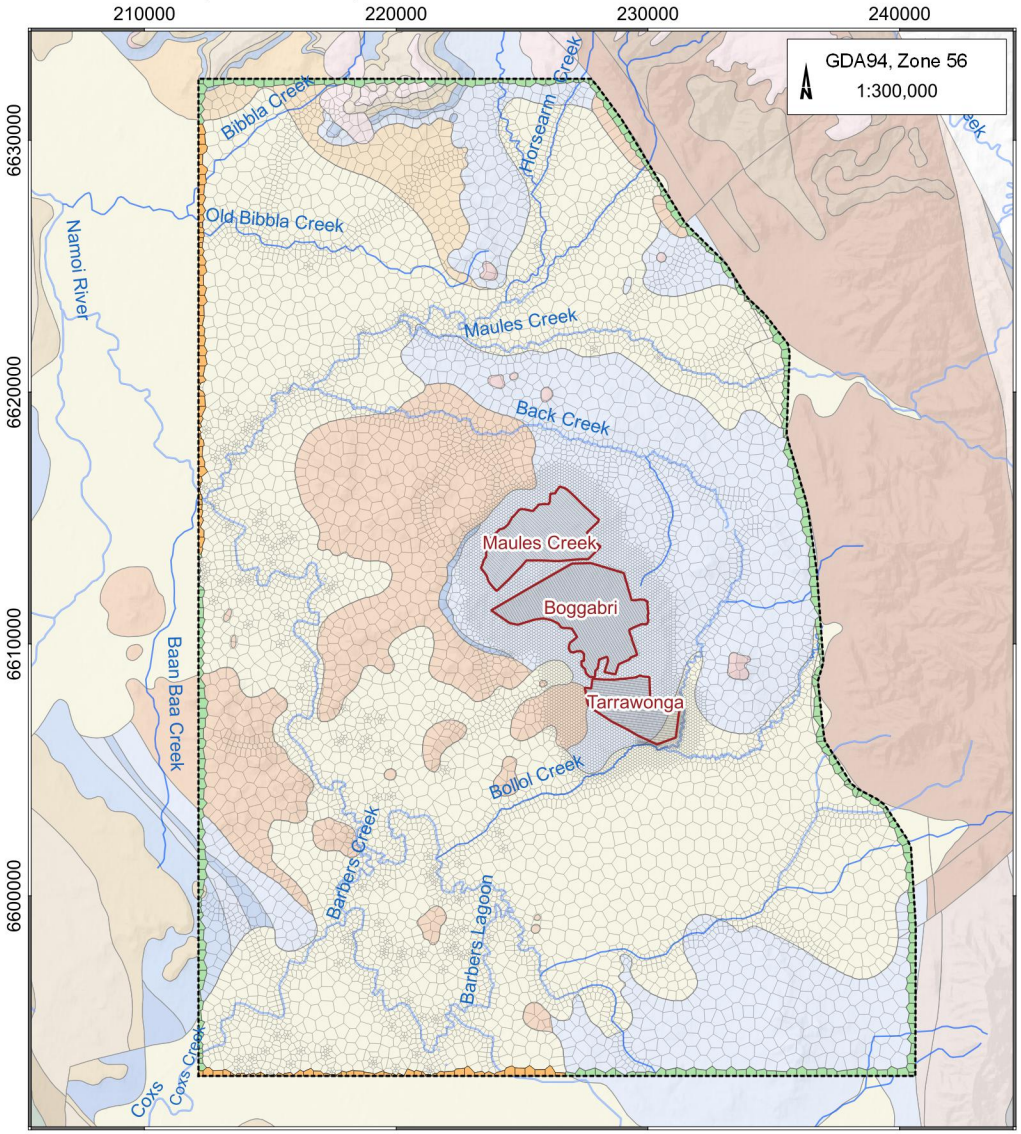

2024 BTM Complex Model update

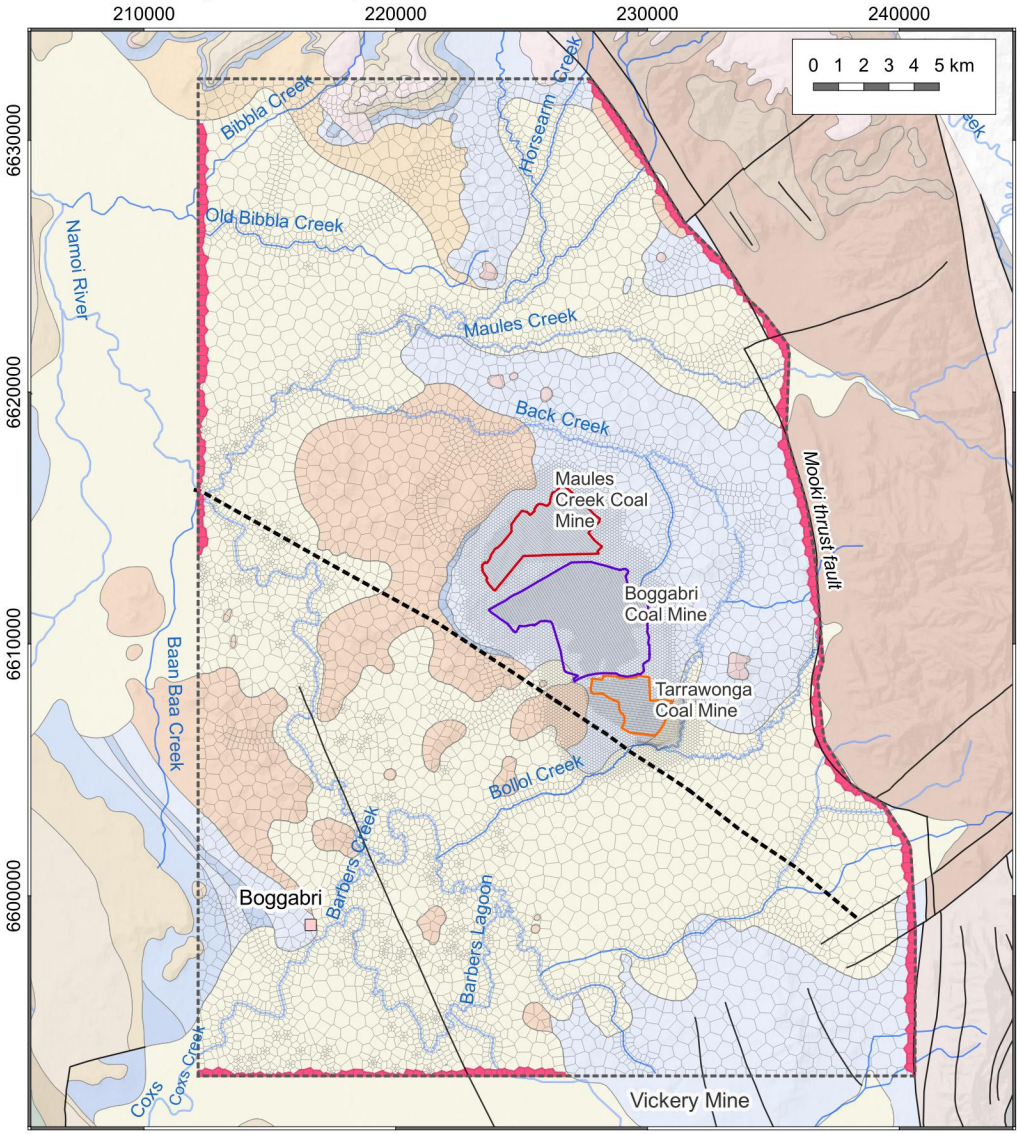

LEGEND

- MCCM Open Cut Extent
- BCM Open Cut Extent
- TCM Open Cut Extent
- BTM Complex Numerical Model Extent
- Model Grid
- GHB package (2024 model)
- GHB package (2022 model)
- No flow boundary (2022 model)
- Mine maximum open cut outlines (2022 model)
- Drainage
- Fault
- Conomos fault

Gunnedah Coalfield rock unit (1:100k)

- Qx - Quaternary Sediments
- Tv - Tertiary Volcanics
- Pmx - Maules Creek and Goonbri formations
- Plf - Leard Formation
- Pbr - Boggabri Volcanics
- Cbc - Currabubula Formation
- Crc - Rocky Creek Conglomerate

BTM Complex Groundwater Model Update 2024

AGE

Model domain and mesh

DATE
25/03/2025

FIGURE No:
F 1

©2025 Australasian Groundwater and Environmental Consultants Pty Ltd (AGE) - www.ageconsultants.com.au
Source: 1 second SRTM Derived DEM-S - © Commonwealth of Australia (Geoscience Australia) 2011.; GEODATA TOPO 250K Series 3 - © Commonwealth of Australia (Geoscience Australia) 2006.;
G:\Projects\MCJ5003.001 Maules Creek Continuation Project EIS\3_GIS\Workspaces\003_Stage 3 -EIS Report\Appendix F\F_01_MCJ5003_Model domain and mesh.qgz

F6.2.2 Grid

The model grid consisted of two types of cells: rectangular cells aligned with the primary direction of mining for each of the BTM mines and voronoi polygons for the remainder of the model area. The following cell dimensions were adopted:

- mining areas – 100 m x 50 m cells;
- adjacent to major creeks and rivers – 200 m x 200 m voronoi cells;
- buffer zone around mining area (contains most monitoring bores) – 100 m diameter voronoi cells;
- adjacent to active extraction bores – approximately 175 m diameter voronoi cells;
- adjacent to inferred Conomos Fault – approximately 450 m x 350 m voronoi cells; and
- away from areas of interest – approximately 650 m maximum diameter voronoi.

The adopted grid represents a maximum of 18,920 cells per continuous layer, as shown in Figure F 1. Further details of model layering are described in the following section. The model grid remained unchanged from that documented by AGE (2022).

F6.2.3 Model layers

Similar to the model grid, the number of model layers remained unchanged from that documented by AGE (2022). The model represents the key hydrostratigraphic units identified in the conceptual model with 34 separate layers (Table F 4) representing the alluvium, weathered rock, coal seams, interburden and volcanics basement.

Table F 4 Model layers

Layer	Geological unit	Layer	Geological unit
1	Narrabri Formation (alluvium)	18	Interburden
2	Gunnedah Formation (alluvium)	19	Interburden
3	Interburden	20	Velyama Seam / Nagero Seam
4	Interburden	21	Interburden
5	Herndale seam / Onavale Seam / Teston Seam / Thornfield Seam	22	Interburden
6	Interburden	23	Upper Northam Seam / Lower Northam Seam
7	Interburden	24	Interburden
8	Braymont Seam	25	Interburden
9	Interburden	26	Therribri A Seam / Therribri B Seam
10	Interburden	27	Interburden
11	Bollol Creek Seam	28	Interburden
12	Interburden	29	Flixton Seam/Tarrawonga Seam
13	Interburden	30	Interburden
14	Jeralong Seam	31	Interburden
15	Interburden	32	Templemore Seam
16	Interburden	33	Interburden
17	Merriown Seam	34	Boggabri volcanics

Note: model layers are unchanged to BTM Complex model update 2022 (AGE, 2022).

F6.2.4 Layer surfaces

The surfaces for the model layers were developed using a range of public-domain data sources provided by the BTM Complex. Table F 5 details the datasets used to develop the model surfaces.

Table F 5 Geological model data sources

Hydrostratigraphic layer/zone	Data source
Land surface	NSW Government 5 m DEM[a].
Base of Narrabri and Gunnedah Fm alluvial aquifer	NSW Government Upper Namoi alluvial groundwater flow model[a].
Base of regolith	CSIRO depth of regolith dataset[b].
Permian coal seams	Surfaces developed using a combination of geological model surfaces from the BTM mines[c] with the mining areas and a regional geological model of the main coal seams developed by JB Mining (2010) used outside the mining areas.
Permian non-coal interburden	No geological modelling of interburden strata has been undertaken. The surfaces were created by dividing the zone between coal seam surfaces equally and do not represent a change in lithology.
Base of Boggabri volcanics	Nominal 200 m below the top of the volcanics surface.

Notes: (a) https://elevation.fsdf.org.au.

(b) https://aclep.csiro.au/aclep/soilandlandscapegrid.

(c) Model surfaces for Boggabri, Tarrawonga and MCCM received in 2019 and 2023.

Explicit representation of the geological sequence in the model grid through deformed layering was considered necessary for history matching, as the observation dataset comprised numerous hydrographs in specific coal seams, both proximal and distant from the mines. Model layers 3 through 33, representing the Permian sequence, are confined to the Maules Creek sub-basin and laterally discontinuous, pinching out against the Boggabri volcanic basement. The layers extend from the eastern perimeter of the model to the middle of the model, where a lower layer pinches them out. Only model layer one and model layer 34 are laterally continuous, meaning that the number of layers varies from 2 to 34 depending on the location within the modelled region. Approximately half of the model consists of either 2 or 3 layers. Model layer 2 represents the Gunnedah alluvial aquifer and is laterally discontinuous, occurring only below surficial alluvial deposits.

The elevation of the coal seams within the AGE (2022) model was compared to updated geological models provided by the BTM Complex mines in 2023. This process identified that some of the elevations of the deeper coal seams within the 2022 numerical model were not aligned with the updated geological model. The elevations of these model layers were updated to better align with the updated geological model. The most significant change occurred within the footprint of the MCCM. The layers most affected were those from 29 to 34, including the Therribri and Tarrawonga seams. They were elevated on average by 30 m in the southern region of the open cut pit.

F6.2.5 Geological structures

Smaller, localised faults, which have been observed in the BTM Complex mine's open cut pits, are conceptualised as having no significant impact on the regional flow. Geologists from the BTM Complex have mapped these localised faults in each mining area. Consultation with site geologists indicated that these are primarily normal faults, with displacement generally minor, characterised by throws of less than 5 m. Whilst these faults have been identified within the active mine face, it is more challenging to identify these faults through exploration drilling and geological modelling of the wider region. Monitoring groundwater levels within coal seams at the BTM Complex and adjacent mines has generally shown declining groundwater levels adjacent to the mining areas due to depressurisation effects. This provides indirect evidence that the faults are not impeding the depressurisation and drainage of groundwater due to mining, supporting the exclusion of minor faults from the numerical model. Furthermore, minor faults are better understood close to the pits.

In contrast to the minor faults, the Conomos Fault appears to be a significant geological feature. It has an interpreted displacement of 60 m to 90 m and is immediately south of Boggabri and Tarrawonga coal mines. Given the potential for this fault to cut and offset the continuity of the coal seams to the south of the BTM Complex, it is likely to act as a barrier to groundwater flow. In the 2024 model update, however, the Conomos fault has been parameterised in a manner that allowed for assessing its potential for conduit behaviour as well (see Section F7.3.3).

The Hunter-Mooki Thrust Fault System represents the boundary between the edge of the Maules Creek sub-basin and the non-coal New England Fold Belt fractured rock. It is represented as a vertical no-flow barrier along the eastern edge of the model, spanning layers 3 to 34.

F6.2.6 Timing

An initial steady-state calibration guided the model calibration to obtain pre-mining conditions (prior to 2006). This was followed by a transient simulation for calibration, where groundwater levels and flows were matched to available measurements. Stress periods remained consistent with AGE (2022), i.e., quarterly stress periods, with the updated transient model comprising 75 quarterly stress periods from January 2006 to June 2024.

F6.3 System stresses

F6.3.1 Recharge

Recharge to groundwater systems occurs through the diffuse infiltration of rainfall into the soil profile and through localised porous creek beds during flow events. The AGE (2022) model utilised a spreadsheet-based soil moisture calculation to estimate the timing and magnitude of recharge events occurring within the model domain. The simple soil moisture balance provided estimates of when the soil profile was likely to have been fully saturated following rainfall and when subsequent deep drainage to the water table occurred. An improved recharge model was adopted for the present work, which is also based on the soil moisture balance but accounts for properties such as land use, soil type, and vegetation. This new recharge model is still a bucket model but features many buckets categorised by different combinations of properties.

F6.3.1.1 Spatially varying recharge model

A zone-based rainfall-runoff model was developed as part of the model update to improve estimates of spatially variable recharge for the groundwater model. The model was based on soil type, rainfall distribution, evapotranspiration (ET), land use, and subsurface geology, resulting in 675 distinct recharge zones. A time series of recharge rates for each zone was then converted into an input file for the groundwater model.

The recharge was calculated using a daily soil moisture balance model adapted from the Rushton model (Rushton et al., 2006; de Silva & Rushton, 2007). This model has demonstrated an accurate simulation of lysimeter results in international studies (Wilson & Lu, 2011).

Rainfall and potential evapotranspiration (PET) data for use in the recharge model were sourced from the SILO GRID database for the period 1 Jan 2005 to 31 May 2024. A total of 56 GRID point locations were used, with latitudes ranging from -30.4 to -30.75 and longitudes from 150.0 to 150.3, covering the simulated region. Figures showing the rainfall and PET grids used for the spatial recharge model are included in the main GIA report (Section 4). The model region encompasses a range of land uses, including irrigated and dryland cropping, grazing, forested areas, and mining operations. The main GIA report includes a figure illustrating the broad range of land use activities within the domain (Section 4).

The area features various soil types with differing capacities to store and infiltrate rainfall, thereby generating groundwater recharge. Figure F 2 shows the spatial distribution of soil textures in the model area. The soil textures were determined using clay, silt, and sand distributions published by NSW Department of Planning & Environment (State Government of NSW and NSW Department of Climate Change, Energy, the Environment and Water, 2012). The soil texture forms the basis for estimating the Total Available Water (TAW) and Readily Available Water (RAW) elements of the recharge model, which are described in Section F6.3.1.2.

Hydrologic soil groups (State Government of NSW and NSW Department of Climate Change, Energy, the Environment and Water, 2012) is a classification system for soils with four categories based on infiltration rate as follows:

- Category A — soils with high infiltration rates, even when thoroughly wet, and consisting chiefly of deep, well-drained to excessively drained sands or gravels. These soils have a high water transmission rate and low potential for water runoff.
- Category B — soils with moderate infiltration rates when thoroughly wet and consisting chiefly of moderately deep to deep, moderately fine to moderately coarse textures. These soils have a moderate water transmission rate.
- Category C — soils with slow infiltration rates when thoroughly wet and consisting chiefly of soils with a layer that impedes downward movement of water or soils with moderately fine to fine texture. These soils have a slow water transmission rate.
- Category D — soils with very slow infiltration rates when thoroughly wet and consisting chiefly of clay soils with a high swelling potential, soils with a permanent high water table, soils with a claypan or clay layer at or near the surface, and shallow soils over nearly impervious material. These soils have a very slow water transmission rate.

Figure F 3 shows the hydrologic soil groups in the model area. Notably, the soils in the alluvial floodplains are categorised as D, indicating very slow infiltration rates. The hydrologic soil group is used to determine the Curve Number (CN) values for the recharge model.

Finally, a limit on recharge was applied to the model based on the properties of the underlying bedrock, referred to as the geocap. This is informed by subsurface factors, such as the permeability of the aquifer, which limits the amount of water that can move from the soil to the water table. More details on the implementation of the recharge model are provided in Section F6.3.1.3. The geocap zones are shown in Figure F 4.

The rainfall, evaporation, land use, soil texture and hydrologic soil category were used to create 274 recharge zones, as illustrated in Figure F 5. Specific combinations of soil type, climate conditions, and land use characterise each recharge zone. The recharge model is then used to estimate spatially variable recharge patterns across the numerical model area.

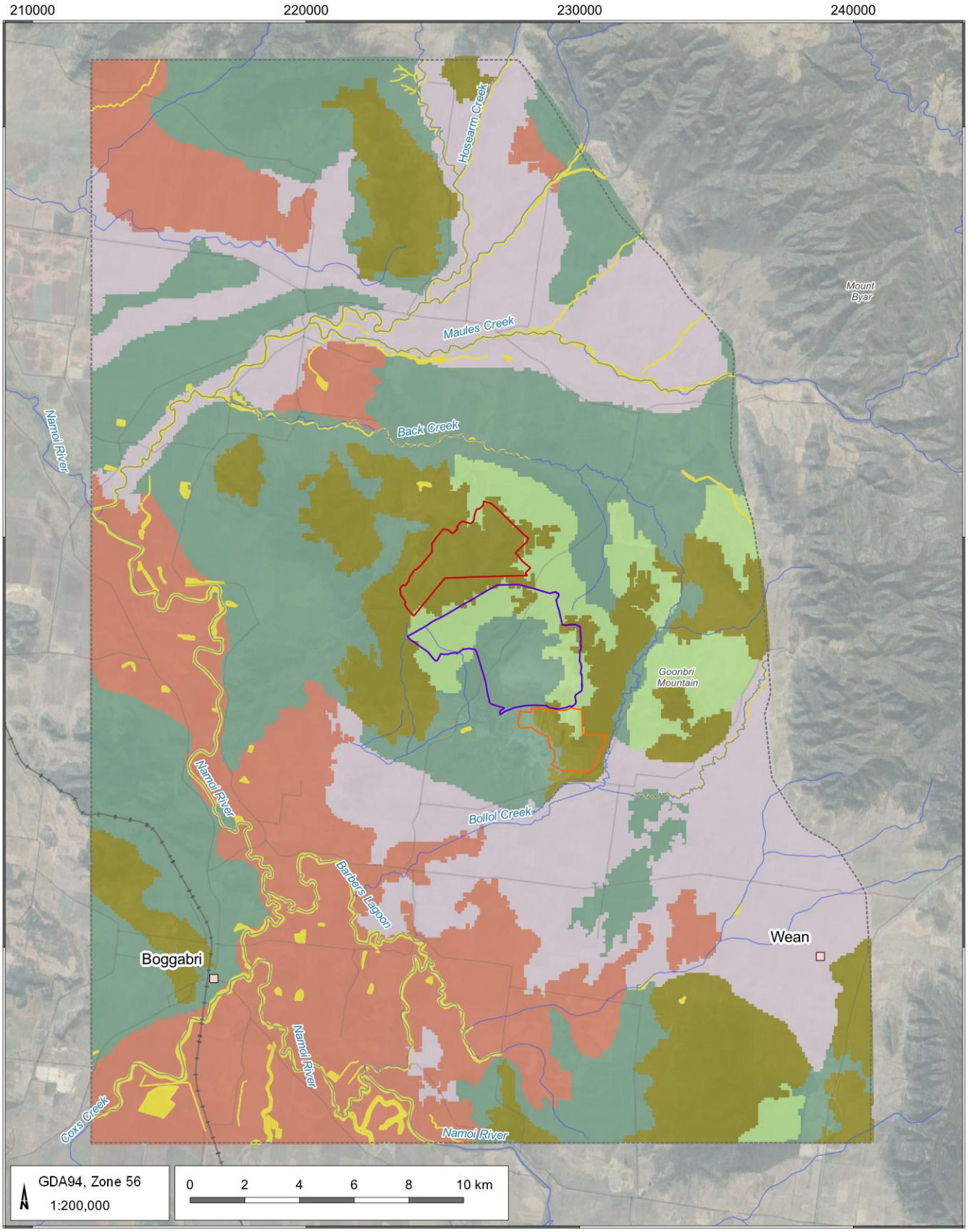

LEGEND

- Populated place
- Road
- Railway
- Drainage
- MCCM Open Cut Extent
- BCM Open Cut Extent
- TCM Open Cut Extent
- Model Extent

Soil Texture

- Clay
- Clay loam
- Loamy sand
- Sandy
- Sandy clay loam
- Sandy loam

BTM Complex Groundwater Model Update 2024

Soil texture

AGE

DATE 05/02/2025

FIGURE No: **F 2**

©2025 Australasian Groundwater and Environmental Consultants Pty Ltd (AGE) - www.ageconsultants.com.au
Source: 1 second SRTM Derived DEM-S - © Commonwealth of Australia (Geoscience Australia) 2011.; GEODATA TOPO 250K Series 3 - © Commonwealth of Australia (Geoscience Australia) 2006.;
G:\Projects\MCJ5003.001 Maules Creek Continuation Project EIS\3_GIS\Workspaces\003_Stage 3 -EIS Report\Appendix FVF_02_MCJ5003_Soil texture.qgz

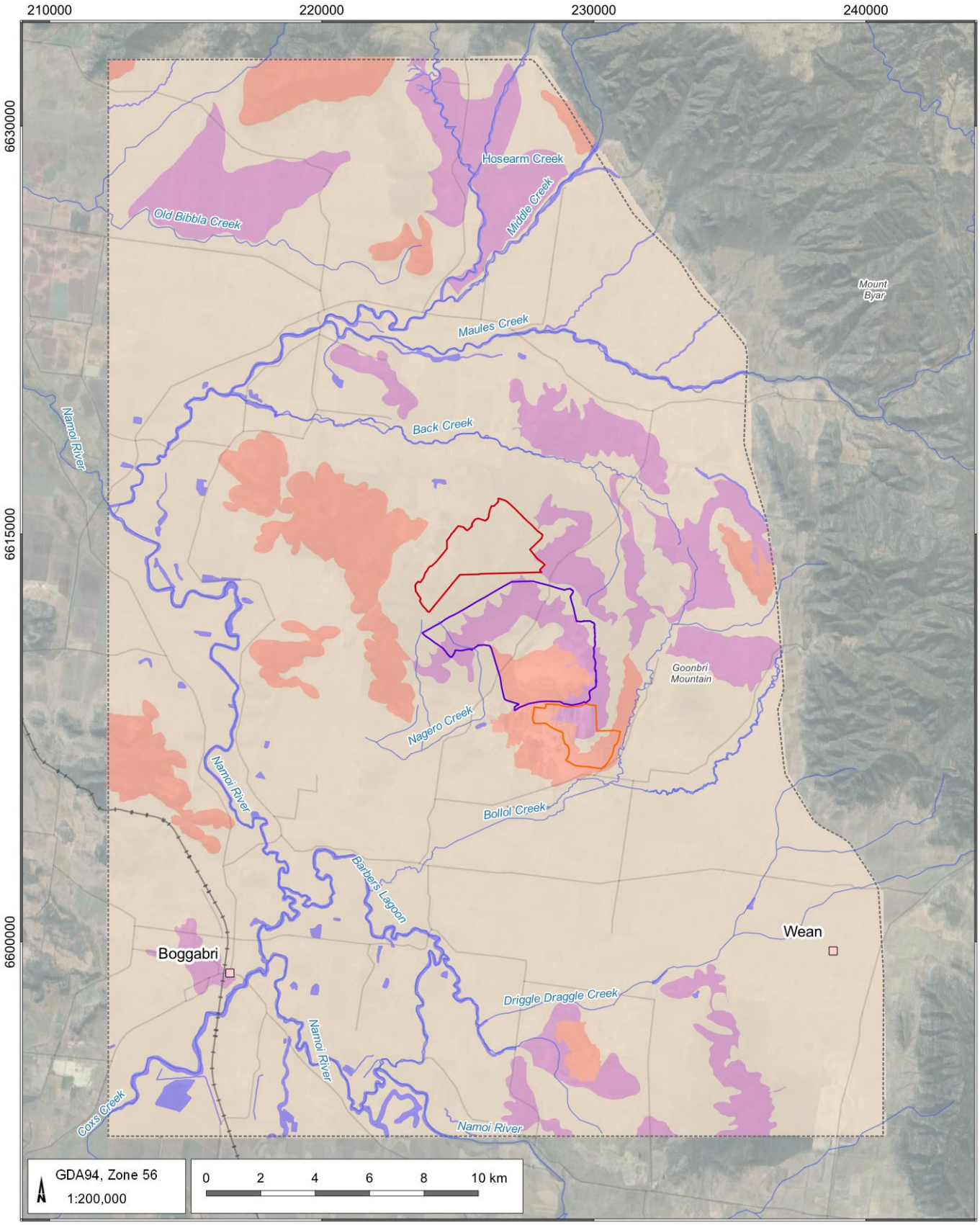

LEGEND

- Populated place
- Road
- Railway
- Drainage
- MCCM Open Cut Extent
- BCM Open Cut Extent
- TCM Open Cut Extent
- Model Extent

Hydrologic soil groups (HSG)

- A
- B
- C
- D

BTM Complex Groundwater Model Update 2024

Hydrologic soil groups

AGE

DATE 05/02/2025

FIGURE No: **F 3**

©2025 Australasian Groundwater and Environmental Consultants Pty Ltd (AGE) - www.ageconsultants.com.au
Source: 1 second SRTM Derived DEM-S - © Commonwealth of Australia (Geoscience Australia) 2011.; GEODATA TOPO 250K Series 3 - © Commonwealth of Australia (Geoscience Australia) 2006.;
G:\Projects\MCJ5003.001 Maules Creek Continuation Project EIS\3_GIS\Workspaces\003_Stage 3 -EIS Report\Appendix F\F_03_MCJ5003_Hydrologic soil groups.qgz

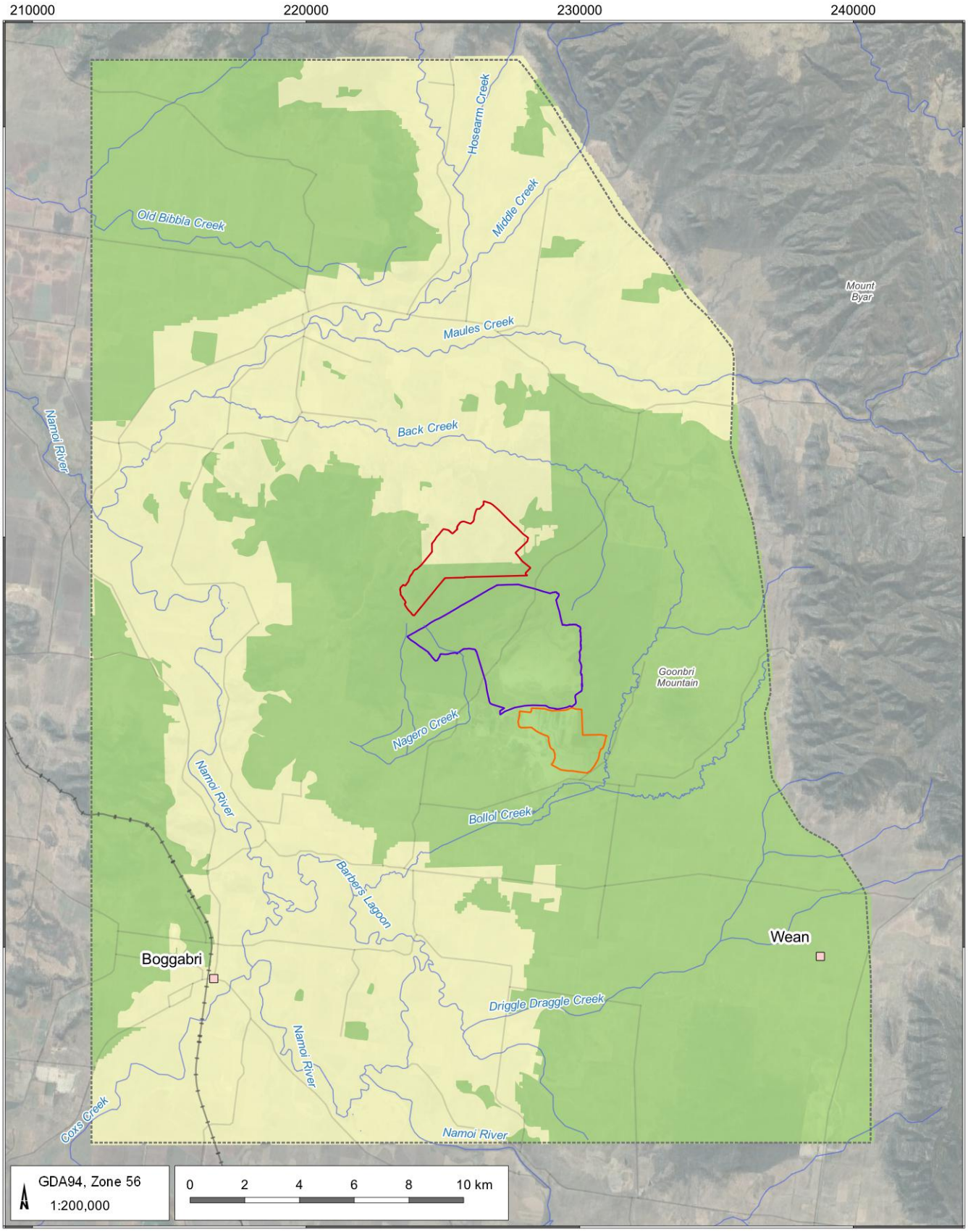

LEGEND

- Populated place
- Road
- Railway
- Drainage
- MCCM Open Cut Extent
- BCM Open Cut Extent
- TCM Open Cut Extent
- Model Extent

Geology "geocap" zones

- Regolith
- Alluvium

BTM Complex Groundwater Model Update 2024

Geology "geocap" zones

AGE

DATE 10/02/2025

FIGURE No: **F 4**

©2025 Australasian Groundwater and Environmental Consultants Pty Ltd (AGE) - www.ageconsultants.com.au
Source: 1 second SRTM Derived DEM-S - © Commonwealth of Australia (Geoscience Australia) 2011.; GEODATA TOPO 250K Series 3 - © Commonwealth of Australia (Geoscience Australia) 2006.;
G:\Projects\MCJ5003.001 Maules Creek Continuation Project EIS\3_GIS\Workspaces\003_Stage 3 -EIS Report\Appendix F\F_04_MCJ5003_Geocap zones.qgz

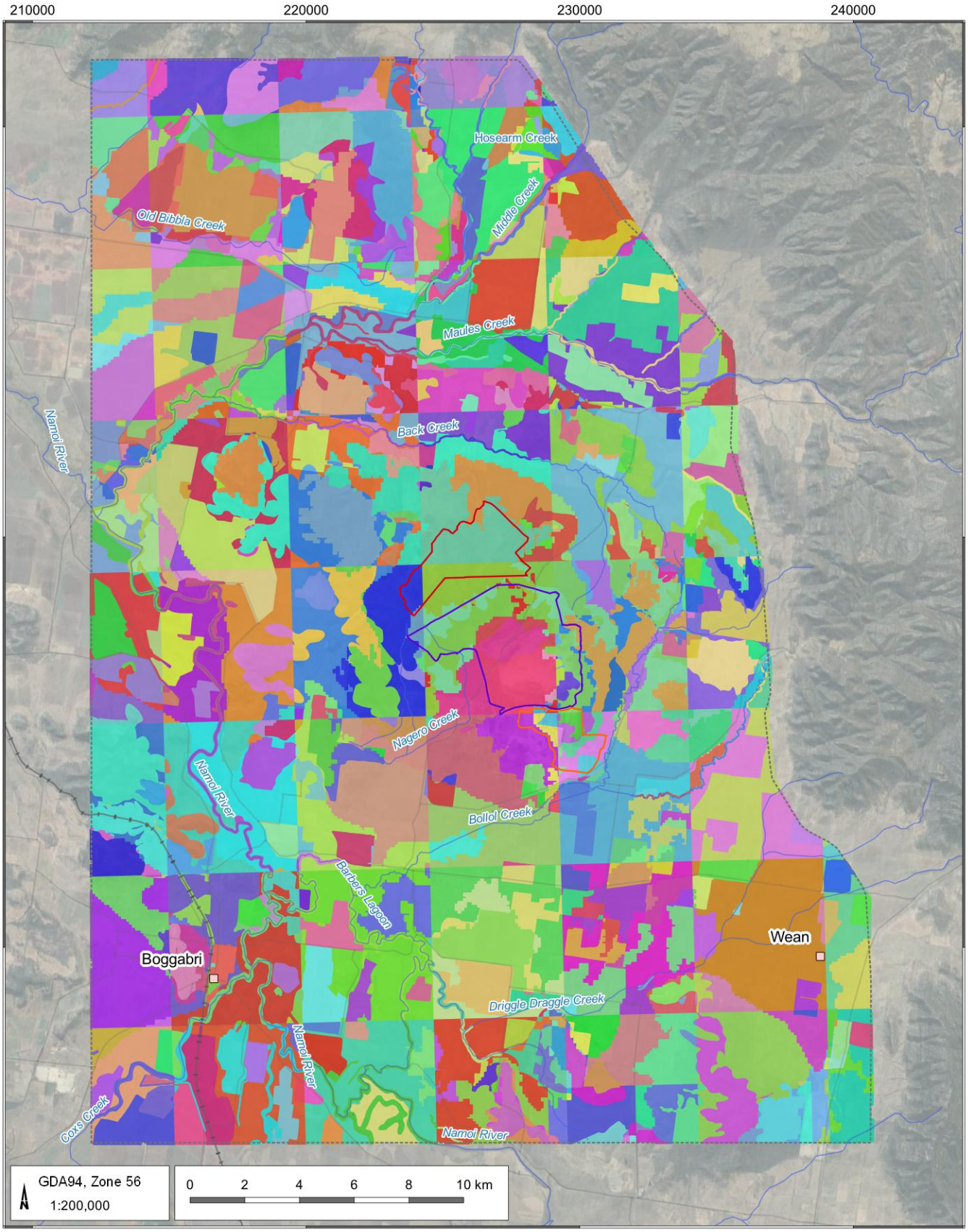

LEGEND

- Populated place
- Road
- Railway
- Drainage
- MCCM Open Cut Extent
- BCM Open Cut Extent
- TCM Open Cut Extent
- Model Extent

BTM Complex Groundwater Model Update 2024

Modelled recharge zones

AGE

DATE 05/02/2025

FIGURE No: **F 5**

©2025 Australasian Groundwater and Environmental Consultants Pty Ltd (AGE) - www.ageconsultants.com.au
Source: 1 second SRTM Derived DEM-S - © Commonwealth of Australia (Geoscience Australia) 2011.; GEODATA TOPO 250K Series 3 - © Commonwealth of Australia (Geoscience Australia) 2006.;
G:\Projects\MCJ5003.001 Maules Creek Continuation Project EIS\3_GIS\Workspaces\003_Stage 3 -EIS Report\Appendix FVF_05_MCJ5003_Modelled recharge zones.qgz

F6.3.1.2 Recharge model methodology

The recharge model utilised the algorithms provided by Rushton et al. (2006) in a two-stage process as follows:

1. **Near-surface storage:** Rainfall is first stored in the near-surface layer before infiltrating into the soil profile. Recharge only occurs when the soil profile has no moisture deficit.
2. **Soil moisture balance:** A daily soil moisture balance is calculated based on soil storage, infiltration, evapotranspiration, and moisture deficits.

The recharge model incorporates runoff, calculated using the USDA Soil Conservation Service (SCS) curve number model (Rawls, Ahuja, Brakensiek, & Shirmohammadi, 1992). The process is divided into three steps:

1. **Infiltration (In): D**aily infiltration and near-surface soil storage (SOILSTOR) are calculated based on the conditions from the previous day.
2. **Evapotranspiration (ET):** Estimated using the Penman-Monteith equation (Allen, Pereira, Raes, & Smith, 1998) and modified with depletion factors for different crops.
3. **Recharge: G**roundwater recharge is calculated when the soil moisture deficit is negative.

The model begins in winter, assuming an initial soil moisture deficit of zero, which allows for a lead-in time for calibration.

F6.3.1.3 Spatial recharge values

The key components of the recharge model are listed below:

- **Rainfall:** Rainfall is the primary input into the system. It represents the total amount of water available for surface water processes, including runoff, infiltration into the soil, and storage in surface reservoirs.
- **Surface Water Model:** The surface water model assesses how rainfall interacts with land surfaces, determining the proportion of rainfall that contributes to surface runoff, infiltration, or is stored in near-surface reservoirs. This process is influenced by land use and soil characteristics.
- **Runoff:** Runoff represents the portion of rainfall that flows over the land surface without infiltrating into the soil. It is estimated using the CN, which measures land surface characteristics, including soil type and land use. Higher CN values indicate a higher potential for runoff.
- **Soil Type:** The soil's texture determines its infiltration capacity and ability to store water. Soils with higher clay content retain more water but have lower infiltration rates, whereas sandy soils allow water to infiltrate more quickly.
- **Land Use:** The type of land use, such as agricultural land, forests, or urban developments, has a significant impact on runoff and infiltration. Urban areas with impervious surfaces tend to have higher runoff, while natural vegetation areas promote infiltration and recharge.
- **Near-Surface Storage:** This represents the temporary storage of water in the upper soil layers before it infiltrates deeper or becomes runoff. The amount of water stored near the surface depends on the rainfall, soil characteristics, and land use.
- **Readily Available Water (RAW)** and **Total Available Water (TAW):**
  - RAW is the amount of water in the soil that is easily accessible to plants before they experience moisture stress.
  - TAW represents the total amount of water the soil can hold based on its properties, influencing how much water remains in the soil after infiltration.
- **Potential Evapotranspiration (PET)** and **Actual Evapotranspiration (AET):** PET is the theoretical maximum rate at which water can evaporate from the soil and transpire from plants. AET is the actual rate, which depends on the availability of soil moisture. High AET reduces the amount of water available for recharge.
- **Soil Moisture Deficit:** The soil moisture deficit is the gap between the soil's current moisture content and its total available water capacity (TAW). A higher deficit indicates that less water is available for groundwater recharge.

- **Geological Capacity (Geo Cap):** This refers to the subsurface geological conditions that control the amount of water that can move from the soil into the groundwater. It considers factors like soil porosity and the permeability of geological formations beneath the soil profile.
- **Recharge:** The model's final output is groundwater recharge, which represents the amount of water that passes through the soil and reaches the water table. This calculation takes into account all the aforementioned factors, including rainfall, runoff, soil moisture, and geological conditions.

The flow chart in Figure F 6 illustrates the components of the rainfall-runoff model and the flow of information used to estimate groundwater recharge rates.

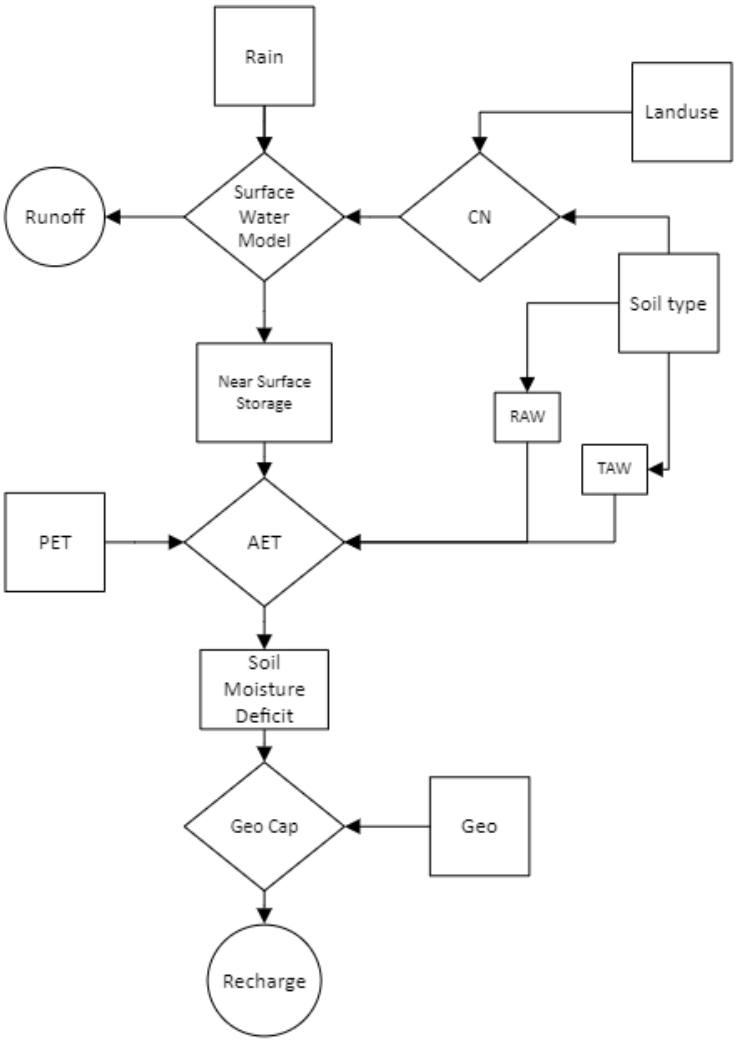

Figure F 6 Flow chart of modelled groundwater recharge rate

In summary, the recharge model represents rainfall entering the system and interacting with the land surface, either becoming runoff or infiltrating the soil. Depending on the soil type and land use, the amount of water that infiltrates will be temporarily stored in near-surface storage before being utilised by plants (AET) or contributing to groundwater recharge. The CN influences runoff, which depends on land use and soil type. The model accounts for soil moisture deficit and geological capacity to determine the amount of water that recharges the groundwater system. The estimated average annual recharge rate for each of the zones is shown in Figure F 7. The estimated volume of rainfall recharge to the model domain per calendar year is shown in Table F 6.

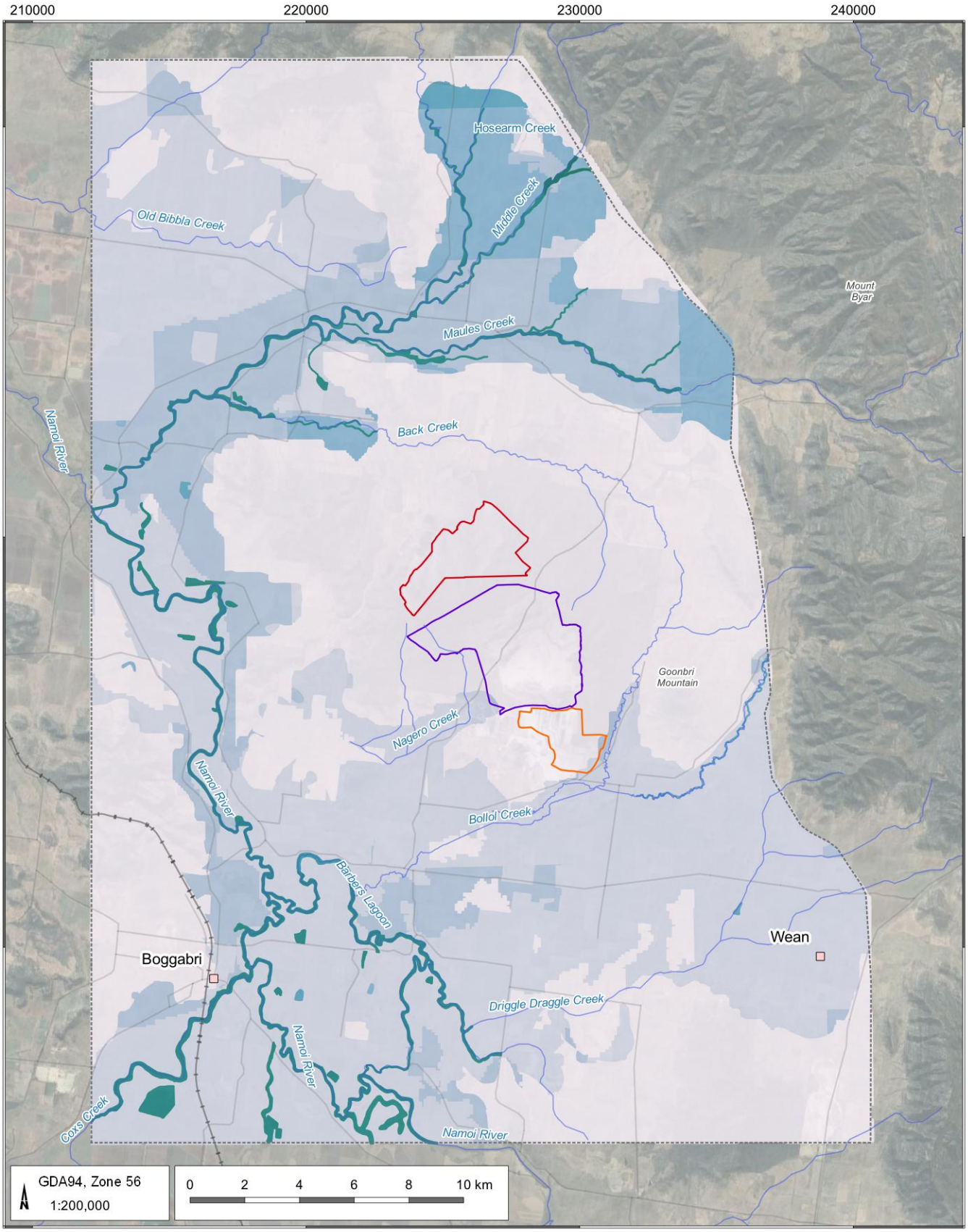

LEGEND

- Populated place
- Road
- Railway
- Drainage
- MCCM Open Cut Extent
- BCM Open Cut Extent
- TCM Open Cut Extent
- Model Extent

Recharge (mm/year)	Recharge (%rainfall)
0.6 - 10	0.1 - 1.7
10 - 20	1.7 - 3.4
20 - 30	3.4 - 5.1
30 - 40	5.1 - 6.8
40 - 50	6.8 - 8.5
50 - 60	8.5 - 10.2
60 - 70	10.2 - 11.9
70 - 76.9	11.9 - 13.0

BTM Complex Groundwater Model Update 2024

Average annual estimated recharge rates

AGE

DATE 25/03/2025

FIGURE No: F 7

©2025 Australasian Groundwater and Environmental Consultants Pty Ltd (AGE) - www.ageconsultants.com.au
Source: 1 second SRTM Derived DEM-S - © Commonwealth of Australia (Geoscience Australia) 2011.; GEODATA TOPO 250K Series 3 - © Commonwealth of Australia (Geoscience Australia) 2006.;
G:\Projects\MCJ5003.001 Maules Creek Continuation Project EIS\3_GIS\Workspaces\003_Stage 3 -EIS Report\Appendix F\F_07_MCJ5003_Average annual estimated recharge rates.qgz

Table F 6 Modelled rainfall recharge rates

Year	Estimated recharge rate (ML/Year)
2006	516
2007	2,166
2008	809
2009	26,207
2010	1,655
2011	58,184
2012	10,272
2013	17,491
2014	2,622
2015	991
2016	35,112
2017	187
2018	274
2019	20,488
2020	11,665
2021	12,771
2022	28,273
2023	63
2024	492

Pilot-point multipliers were used to adjust the recharge during calibration where necessary. Figure F 8 shows the spatial distribution of recharge in the model for the steady-state condition. This indicates the long-term mean recharge, which has increased rates along waterways. Mean rainfall for the area is approximately 590 mm/yr, with the minimum at 0.6 mm/yr and the maximum at 76.9 mm/yr, approximately 0.1% and 13.1% of annual rainfall, respectively.

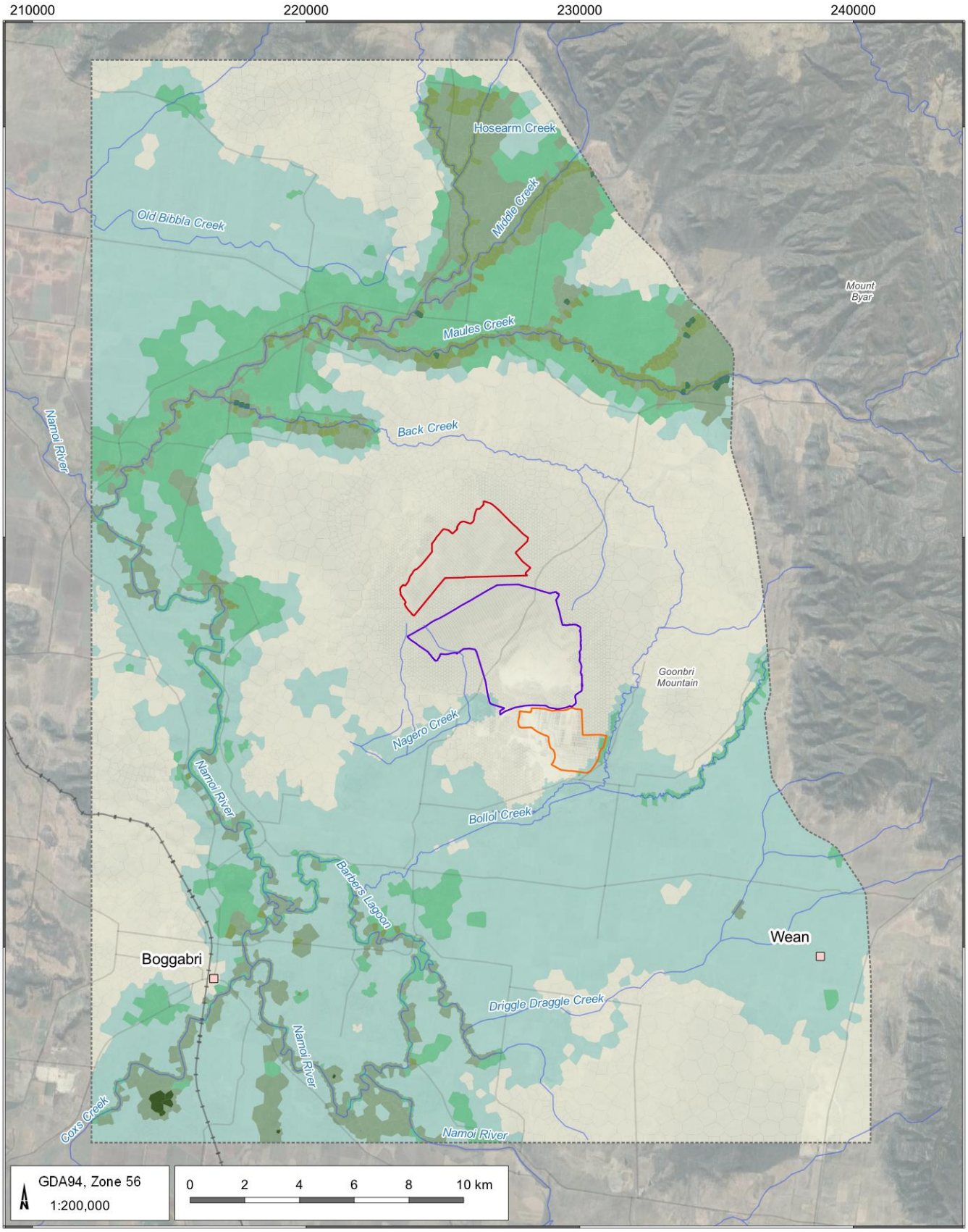

LEGEND

- Populated place
- Road
- Railway
- Drainage
- MCCM Open Cut Extent
- BCM Open Cut Extent
- TCM Open Cut Extent
- Model Extent

Recharge (mm/year)

- 0-10
- 10-20
- 20-30
- 30-40
- 40-50
- 50-60
- 60-70

BTM Complex Groundwater Model Update 2024

Rainfall recharge zones

AGE

DATE 05/02/2025

FIGURE No: **F 8**

©2025 Australasian Groundwater and Environmental Consultants Pty Ltd (AGE) - www.ageconsultants.com.au
Source: 1 second SRTM Derived DEM-S - © Commonwealth of Australia (Geoscience Australia) 2011.; GEODATA TOPO 250K Series 3 - © Commonwealth of Australia (Geoscience Australia) 2006.;
G:\Projects\MCJ5003.001 Maules Creek Continuation Project EIS\3_GIS\Workspaces\003_Stage 3 -EIS Report\Appendix F\F_08_MCJ5003_Rainfall recharge zones.qgz

F6.3.2 Surface drainage

Excluding the Namoi River, surface water features in the area are primarily ephemeral. They are conceptualised as areas of high recharge to the underlying groundwater systems during (limited) flow periods. This surface water to groundwater flux was represented in the model with enhanced recharge. To model situations where this flux could be reversed, i.e., groundwater-gaining streams, the major ephemeral creeks were represented using the MODFLOW river package (RIV) (Figure F 9). Generally, groundwater-gaining streams are only conceptualised to be present during significant recharge events where the alluvium is saturated to the extent that the water table rises to a higher elevation than the creek beds. The river cells in the model were assigned a water level equal to the bed elevation of the creek. Hence, they can only simulate the 'drainage' of water out of the aquifer where and when the groundwater levels are high enough. The bed levels for the creeks represented by RIV were based on previous observations over the area and were set by subtracting the average river depth from the topography. Based on regional observations, all creek beds were less than or equal to 1.9 m deep.

Perennial groundwater gaining surface water features are limited to sections of the Namoi River, which was represented using the MODFLOW stream (STR) package (Figure F 9), with a 30 m wide, 2 m thick sloping stream bed incised 1.9 m into the landscape. Flow in the river outside the model domain was simulated using quarterly flow observations at the upstream model boundary. The conductance for all surface water features was variable during calibration.

The previously proposed alignment of the Goonbri Creek diversion was removed from the model at the commencement of the calibration period in 2006. The water table within the model remains below the base of Goonbri Creek. Therefore, the calibration was not considered sensitive to the creek location as it does not interact with shallow groundwater.

F6.3.3 Evapotranspiration

A review of the depth of the water table was undertaken to determine if ET was a significant discharge mechanism for groundwater in the model domain. The steady-state numerical model indicated that the water table is very deep in the ridge areas and closer to the land surface in the lower-lying alluvial plains. In the area where the BTM Complex mines are situated, the water table is commonly over 50 m to 100 m below the land surface, and ET does not occur.

The alluvial plains also commonly have groundwater levels exceeding 2 m below the land surface and were considered to have limited ET, particularly considering the plains are largely cleared of deep-rooted trees and vegetation. AGE (2022) precluded the use of ET. The current model included spatially uniform ET to mitigate numerical difficulties associated with the adopted ensemble-based approach during model calibration. The extinction depth was set to 4.0 m below the surface, and the maximum evaporation rate at the surface was set at 600 mm/yr. Post-calibration checks revealed that ET was approximately one-quarter of recharge and was concentrated primarily in the southwestern and western regions of the model domain, along the Namoi River.

F6.3.4 Abstraction

Abstraction from the Namoi River alluvium irrigation bores was represented using the MODFLOW well package in the numerical model. The abstraction rates in the AGE (2022) model were updated with pumping records provided by WaterNSW for the water years 2019-20 to 2023-24. These annual totals were divided into equivalent quarterly abstractions to align with model stress period lengths. The simulated wells were located in either layer 1 or layer 2, depending on screen depth. Auto-flow reduction was used to prevent flow when heads were below the wells; however, no reductions to flow were reported in any of the simulations. Locations of private abstraction bores that are active in the model from 2006 to 2024 are shown in Figure F 10. The pumping volumes over time are shown in Figure F 11.

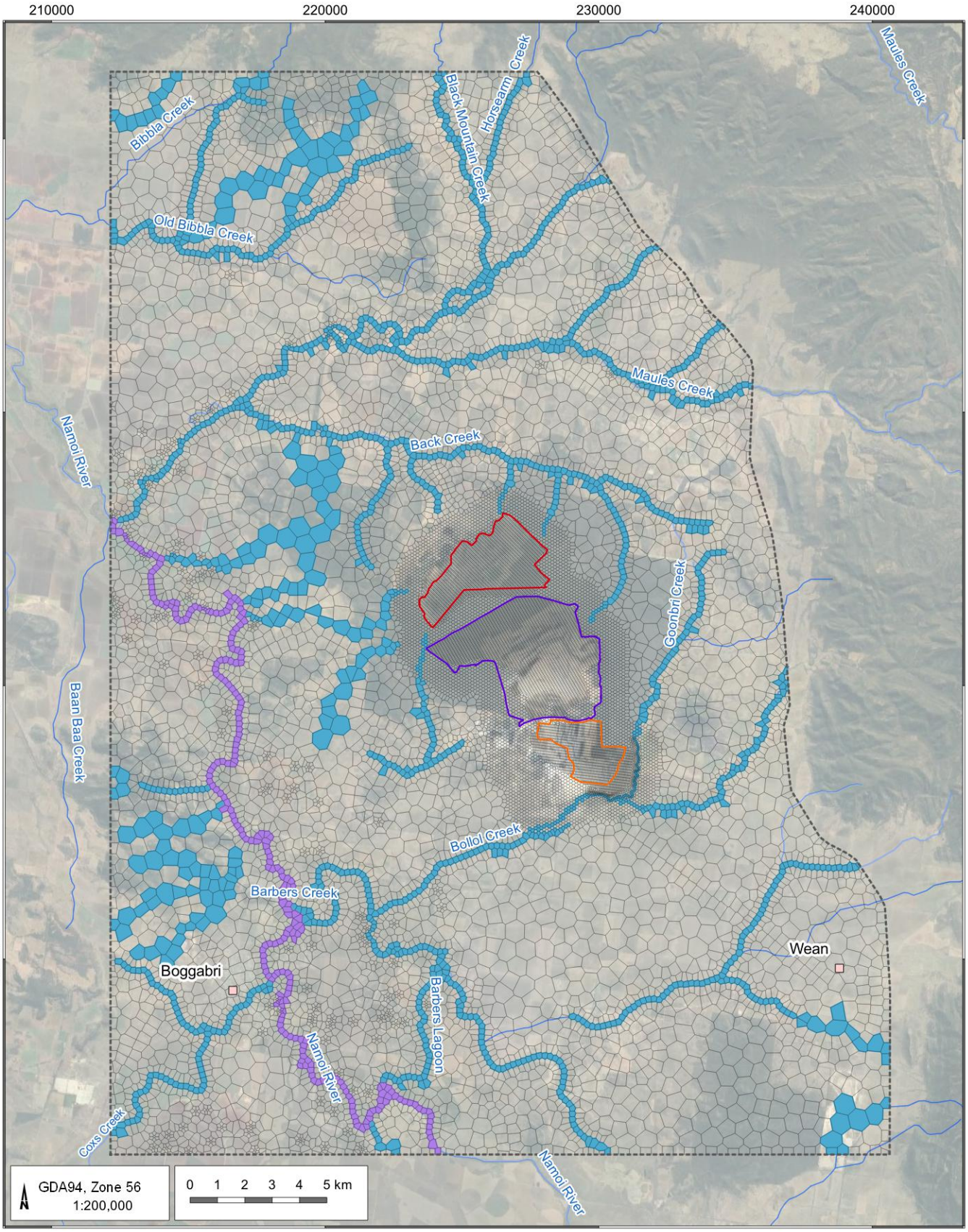

LEGEND

- Populated place
- Drainage
- MCCM Open Cut Extent
- BCM Open Cut Extent
- TCM Open Cut Extent
- Model Extent
- River package
- Stream package

BTM Complex Groundwater Model Update 2024

River and surface drainage cells

AGE

DATE 05/02/2025

FIGURE No: **F 9**

©2025 Australasian Groundwater and Environmental Consultants Pty Ltd (AGE) - www.ageconsultants.com.au
Source: LiDAR DEM © Department Finance, Services and Innovation, 2016; GEODATA TOPO 250K Series 3 - © Commonwealth of Australia (Geoscience Australia) 2006.;
G:\Projects\MCJ5003.001 Maules Creek Continuation Project EIS\3_GIS\Workspaces\003_Stage 3 -EIS Report\Appendix F\F_09_MCJ5003_River and surface drainage cells.qgz

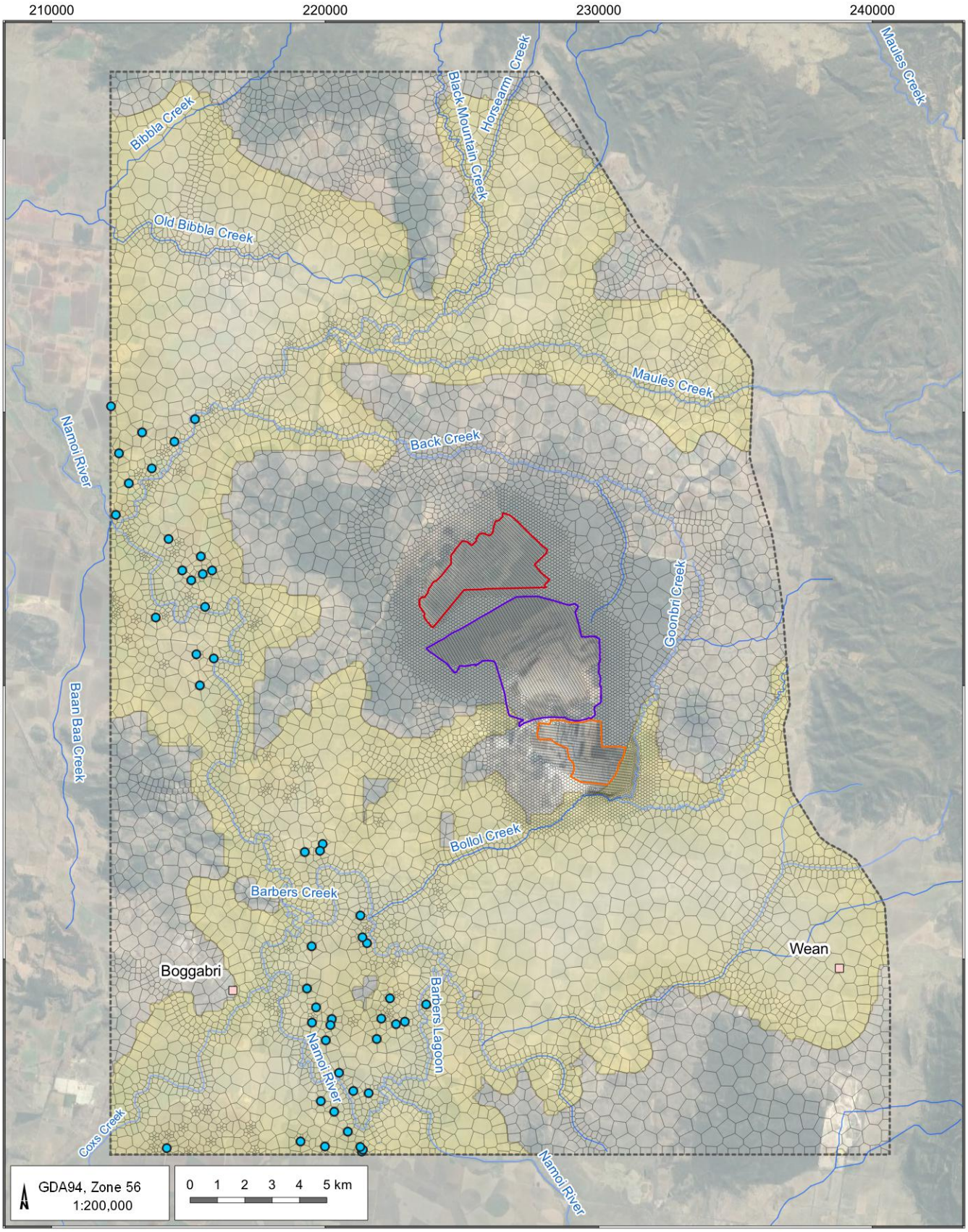

LEGEND

- Populated place
- Pumping Bores
- Drainage
- MCCM Open Cut Extent
- BCM Open Cut Extent
- TCM Open Cut Extent
- Model Extent
- Modelled Alluvium Extent

BTM Complex Groundwater Model Update 2024

Pumping bore locations

AGE

DATE 05/02/2025

FIGURE No: **F 10**

©2025 Australasian Groundwater and Environmental Consultants Pty Ltd (AGE) - www.ageconsultants.com.au
Source: LiDAR DEM © Department Finance, Services and Innovation, 2016; GEODATA TOPO 250K Series 3 - © Commonwealth of Australia (Geoscience Australia) 2006.;
G:\Projects\MCJ5003.001 Maules Creek Continuation Project EIS\3_GIS\Workspaces\003_Stage 3 -EIS Report\Appendix F\F_10_MCJ5003_Pumping bore locations.qgz

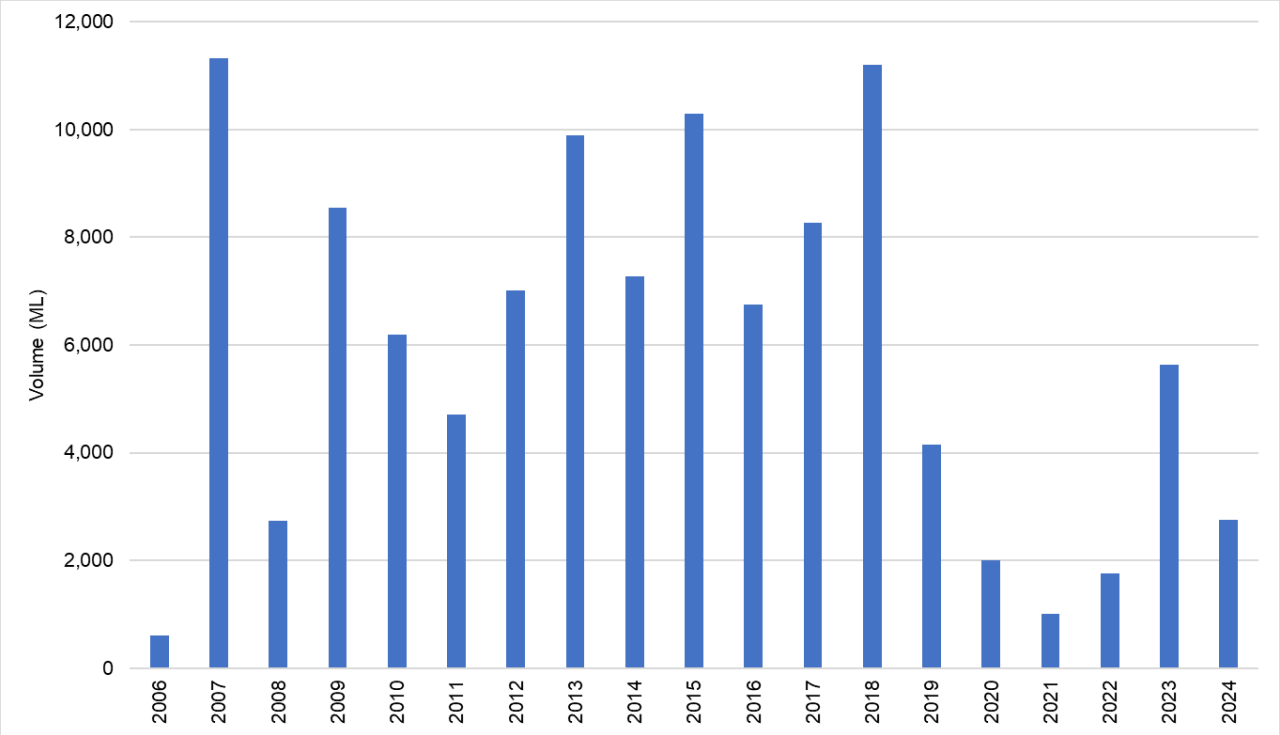

Figure F 11 Irrigation bore abstraction volumes

F6.3.5 Mining

Mining at the BTM Complex is open cut only, with no underground works. The model represents all open cut mining activities using the MODFLOW drain (DRN) package. The progression of mining over time was updated to reflect the schedules provided by the BTM Complex mines. Drain cells were applied to all intersected model cells, with reference elevations set to the floor of each cell, down to the coal seam targeted for extraction by mining. A nominally high drain conductance of 100 square metres per day (m^2/day) was applied to the drain cells to ensure the unhindered groundwater flow into the cell. The emplacement of spoils as mining progressed was not represented in the model, with the pit shells being represented as fully drained for the entire mining period until the end of calibration in June 2024. Figure F 12 shows the progression of drain cells with the model representing the approved mining over time for the calibration period (mine progression until June 2024).

The timing and location of mining represented within the numerical model contains an unavoidable element of uncertainty. Peeters and Middlemis (2023) categorise this as 'scenario uncertainty'. This is because historical mining records can be difficult to obtain or are necessarily simplified, and assumptions on the progress of mining operations, particularly older ones, are therefore required. The exact advancement of future mining operations is also uncertain. All mining operations are subject to detailed mine design, market conditions and other considerations that can alter project progression and mining rate. The historical and future mining represented within the numerical model should, therefore, be considered a guide rather than a highly accurate representation. Despite these unavoidable limitations, the model is considered to largely represent mining where it has occurred historically and is expected to occur in the future; it is only the timing and elevation of the mining that have a level of uncertainty.

The uncertainty in the location and progression of mining can affect the calibration of the model in areas where water level calibration points are situated near mining activities. In areas more distant from mining activities, the uncertainties in the historical progression of mining become less influential on the model predictions.

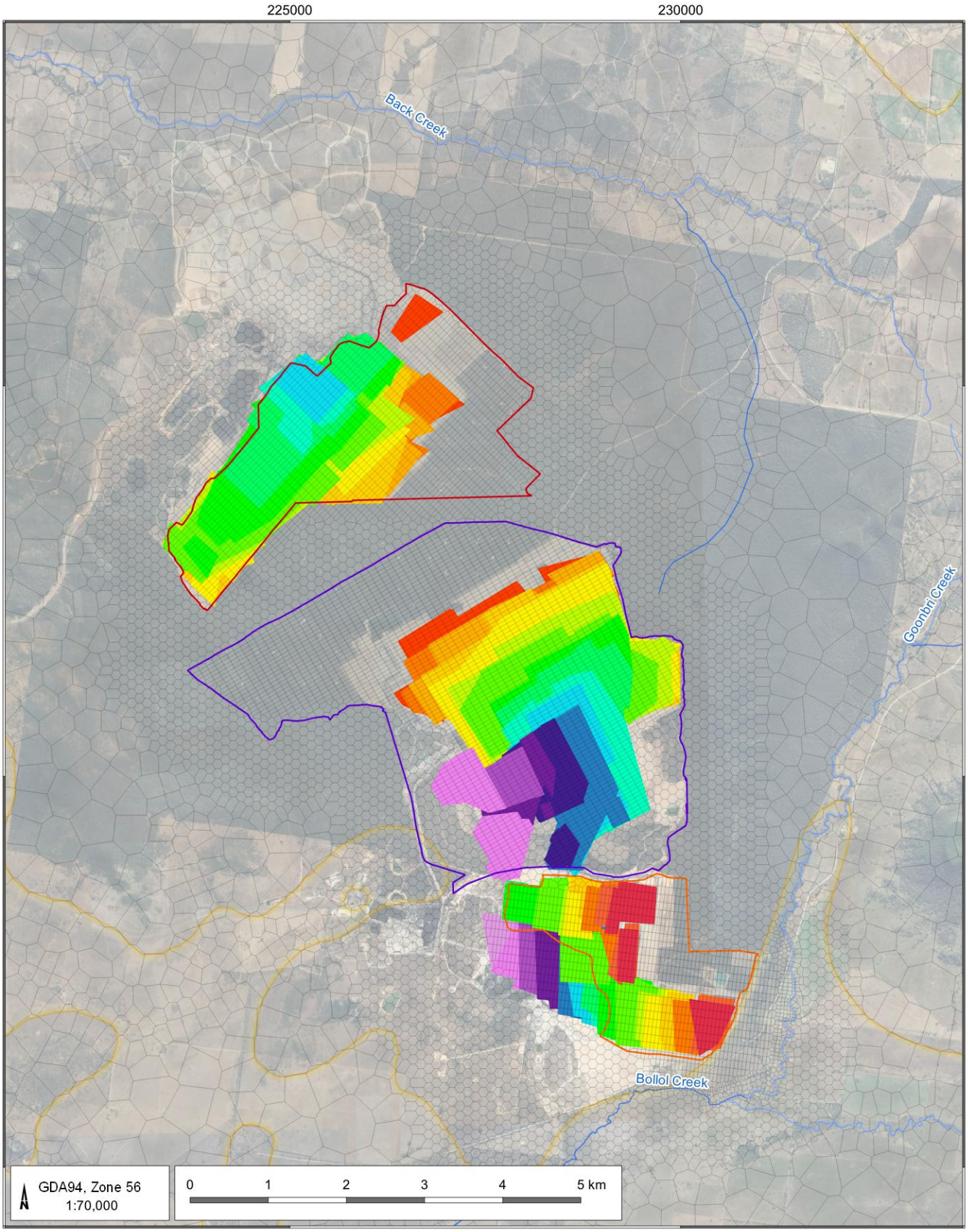

LEGEND

- Drainage
- MCCM Open Cut Extent
- BCM Open Cut Extent
- TCM Open Cut Extent
- Model Extent
- Model Grid
- Alluvial Boundary Zones

Mine Progression (Year)

2007	2016
2008	2017
2009	2018
2010	2019
2011	2020
2012	2021
2013	2022
2014	2023
2015	2024

BTM Complex Groundwater Model Update 2024

Annual mining progression – Calibration until June 2024

AGE

DATE 13/02/2025

FIGURE No: **F 12**

©2025 Australasian Groundwater and Environmental Consultants Pty Ltd (AGE) - www.ageconsultants.com.au
Source: LiDAR DEM © Department Finance, Services and Innovation, 2016; GEODATA TOPO 250K Series 3 - © Commonwealth of Australia (Geoscience Australia) 2006.;
G:\Projects\MCJ5003.001 Maules Creek Continuation Project EIS\3_GIS\Workspaces\003_Stage 3 -EIS Report\Appendix F\F_12_MCJ5003_Annual mining progression – Calibration until June 2024.qgz

F7 Model calibration

F7.1 Approach and method

The objective of the calibration process was to ensure that the model could replicate key aspects of the groundwater regime identified in the conceptual model. These key aspects of the calibration to be achieved were termed the 'success criteria' and used to guide the calibration process. The success criteria included:

- replicating the observed depressurisation trends where evident in observation data;
- reducing the spatial extent of depressurisation predicted by the AGE (2022) model compared to monitoring data, particularly at sites distant from mining along the eastern boundary of the model;
- constraining hydraulic properties and mine inflow predictions within plausible ranges; and
- replicating key climate and mining-influenced trends evident in water level monitoring data.

The AGE (2022) model was re-parameterised and recalibrated in two stages. Firstly, a steady-state model was used to reproduce groundwater levels prior to the onset of mining at the BTM Complex. The groundwater levels and parameters from the steady-state model were then used as starting conditions for a transient calibration. The transient model used for calibration was set up with quarterly (91.3 days) stress periods spanning January 2006 to June 2024.

The calibration process involved initial exploratory model runs to assess the suitability of the prior and for data conflict, followed by automated calibration using ensemble space inversion (ENSI) from the PEST_HP suite (Doherty J. , 2024). The calibration focussed on adjusting the following properties in the model:

- horizontal and vertical hydraulic conductivity;
- spatially variable recharge;
- storage properties - specific yield and specific storage;
- head-dependent flux boundary conductance; and
- conduit or barrier behaviour of the Conomos Fault.

The use of ENSI includes preferred value regularisation and targets the minimum error variance parameter set of the inverse problem. The parameter set from the AGE (2022) model provided the preferred values for aquifer properties, recharge, and boundary conductance. Parameters were configured as multipliers of the preferred values, meaning that the probability distributions for model parameters in the prior were centred on AGE (2022) calibration. An ensemble of 275 models was used, comprising nine realisation groups. The number of optimisation iterations was limited to six. Two-point derivatives were used from optimisation three onwards.

After model calibration, the model parameters were manually checked to ensure consistency with the conceptual understanding of the area.

F7.2 Parameterisation

Several parameterisation devices were used during calibration. These include pilot points for aquifer properties and recharge, seglists for river, stream and general head boundaries, and a structural overlay for the Conomos Fault.

Pilot points (Figure F 13) were implemented using PLPROC, with the same distribution of points used in each layer, noting that not all layers are laterally continuous. Points falling outside of discontinuous layers were removed so that only layer 1 and layer 34 included a full complement of points. Locations were selected so that at least one pilot point would be between observation locations, irrespective of the model layer. The points were configured as multipliers of the existing property fields with the bounds on multipliers presented in Table F 7.

Table F 7 Multiplier parameters for spatially distributed properties

Pilot point property	Number of parameters	Initial value	Lower bound	Upper bound
Kx	4200	1.0	0.01	100.0
Kz	4200	1.0	0.01	100.0
Ss	4200	1.0	0.01	100.0
Sy	4200	1.0	0.1	3.0
Rch	22875*	1.0	0.3	3.0

Note: * 305 per stress period.

In addition to the multipliers, absolute value thresholds associated with hydrogeological units were also enforced through PLPROC. These considered both maximum and minimum values for horizontal hydraulic conductivity (Kx), vertical hydraulic conductivity (Kz), specific storage (Ss) and specific yield (Sy). Limits on the ratios of vertical to horizontal hydraulic conductivity were also included. These are presented in Table F 8. The hydrogeological units identified in the modelled area are informed by field-derived values from New South Wales and Queensland (QLD) coal fields.

Table F 8 Absolute value thresholds for aquifer properties

Unit	Kx min (m/d)	Kx max (m/d)	Kz min (m/d)	Kz max (m/d)	Kz/Kx (--)	Ss min (1/m)	Ss max (1/m)	Sy min (--)	Sy max (--)
Alluvium	1.0E-5	1.0E+2	1.0E-5	1.0E+1	< 0.5	-	-	1.0E-2	3.0E-1
Regolith	1.0E-5	1.0E+1	1.0E-5	1.0E+0	< 0.5	-	-	1.0E-2	3.0E-1
Tertiary	1.0E-5	1.0E+2	1.0E-5	1.0E+1	< 1.0	1.0E-6	1.0E-4	1.0E-4	2.0E-1
Interburden	8.6E-6	1.0E-2	1.0E-8	5.0E-3	< 0.5	7.0E-7	1.0E-4	1.0E-4	6.0E-2
Coal seam	8.6E-6	1.0E-1	8.6E-6	1.0E-1	< 1.0	2.0E-6	1.0E-4	1.0E-4	5.0E-2
Volcanic	1.0E-7	1.0E+0	1.0E-7	1.0E-1	< 1.0	1.0E-7	1.0E-4	1.0E-4	1.0E-1

The maximum value allowed for recharge in a cell during any stress period was 70 mm/yr, which was only possible in a few locations along the Namoi and the ephemeral creeks, representing recharge from a major flow event.

Spatial correlation between pilot point properties of the prior were constrained with covariance matrices. These were developed using MKPPSTAT and PPCOV_SVA from the PEST groundwater utilities suite. The correlation was assumed to be in two dimensions only. The estimated values for pilot points were interpolated across the model domain in each layer using ordinary kriging through PLPROC (Watermark Numerical Computing, 2023). Horizontal and vertical conductivity were then adjusted, and the absolute values were capped to ensure maximum and minimum values did not exceed appropriate ranges for each unit outlined in Table F 8.

Seglist parameters (Figure F 14) were configured for the river, stream, and general head boundary conditions. Here, a multiplier estimated at each vertex and linearly interpolated along the segment was used to vary conductance by two orders of magnitude during calibration.

The structural overlay (Figure F 15) was configured through the model grid with Kx and Kz properties estimated from preferred values of $1.0x10^{-5}$ metres per day (m/d) and $1.0x10^{-6}$ m/d, respectively (barrier). Note that these values are assigned to the vertices of the overlay and then calibrated. This means that aquifer properties along the fault can be variable along its length during calibration. The upper bounds for the same properties were 1.0 m/d and 0.1 m/d (conduit). The overlay was configured to have no impact on layer 1 and layer 2 – representing the alluvium and weathered regolith. Sliders were also included to allow the strike of the fault to shift by moving segment vertices within 250 m to the left or right, perpendicular to the fault.

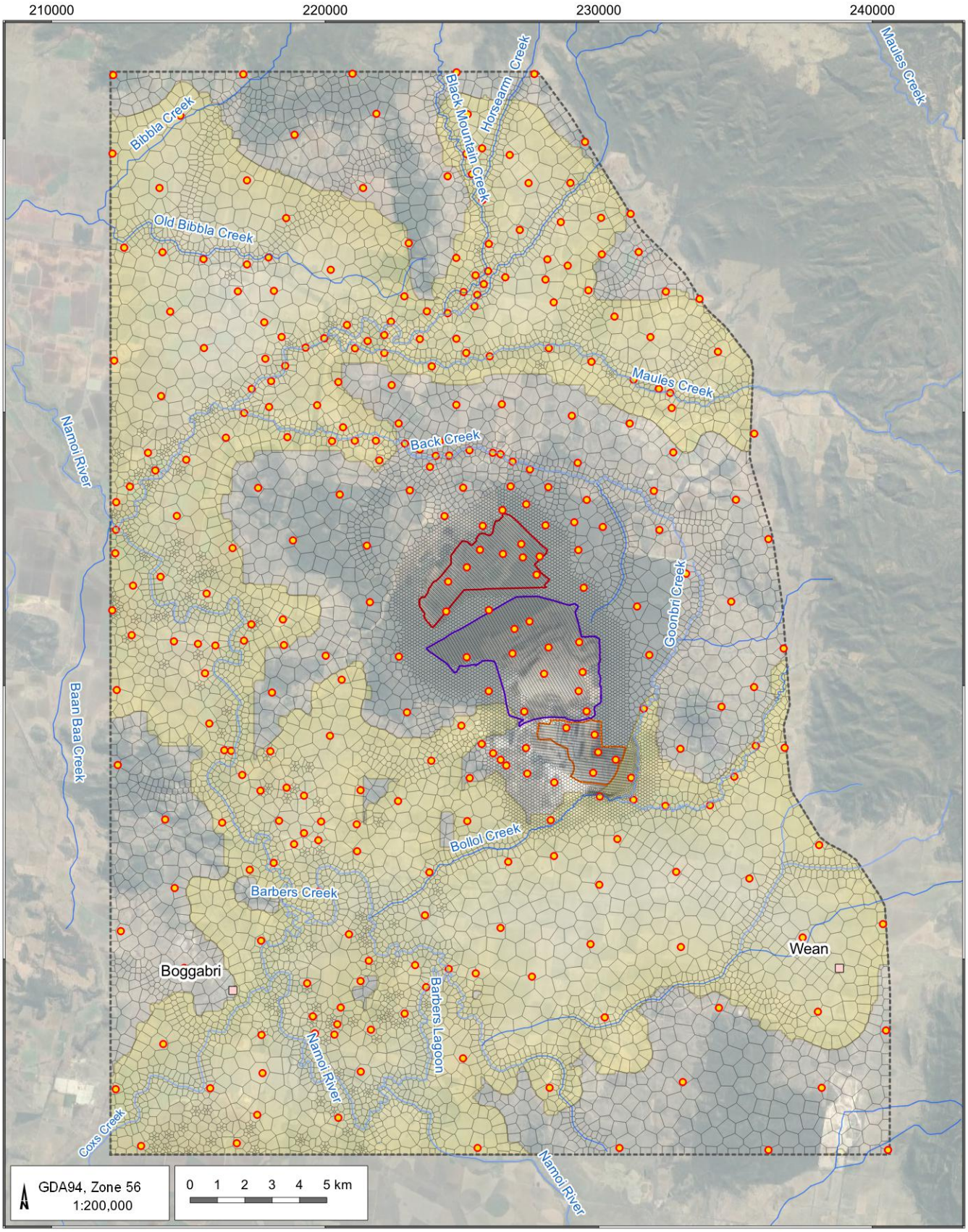

LEGEND

- Populated place
- Pilot Point Locations
- Drainage
- MCCM Open Cut Extent
- BCM Open Cut Extent
- TCM Open Cut Extent
- Model Extent
- Model Grid
- Modelled Alluvium Extent

BTM Complex Groundwater Model Update 2024

Pilot point locations

AGE

DATE 10/02/2025

FIGURE No: **F 13**

©2025 Australasian Groundwater and Environmental Consultants Pty Ltd (AGE) - www.ageconsultants.com.au
Source: LiDAR DEM © Department Finance, Services and Innovation, 2016; GEODATA TOPO 250K Series 3 - © Commonwealth of Australia (Geoscience Australia) 2006.;
G:\Projects\MCJ5003.001 Maules Creek Continuation Project EIS\3_GIS\Workspaces\003_Stage 3 -EIS Report\Appendix F\F_13_MCJ5003_Pilot point locations.qgz

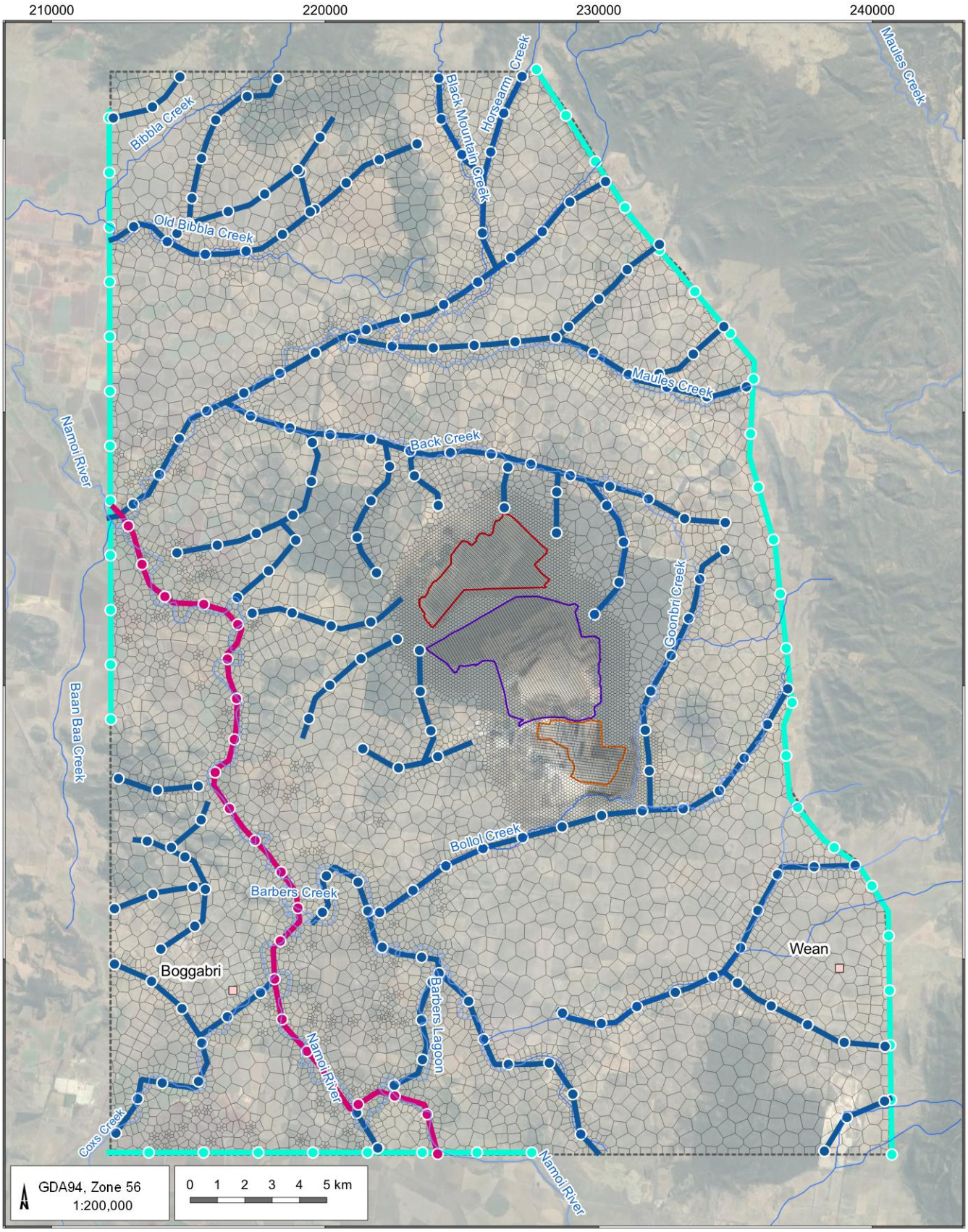

LEGEND

- Populated place
- Drainage
- MCCM Open Cut Extent
- BCM Open Cut Extent
- TCM Open Cut Extent
- Model Extent

Parameters List

- Stream pilot points
- Stream segment
- River pilot points
- River segment
- GHB pilot points
- GHB segment

BTM Complex Groundwater Model Update 2024

Segment parameters for boundary conditions

AGE

DATE 10/02/2025

FIGURE No: **F 14**

©2025 Australasian Groundwater and Environmental Consultants Pty Ltd (AGE) - www.ageconsultants.com.au
Source: LiDAR DEM © Department Finance, Services and Innovation, 2016; GEODATA TOPO 250K Series 3 - © Commonwealth of Australia (Geoscience Australia) 2006.;
G:\Projects\MCJ5003.001 Maules Creek Continuation Project EIS\3_GIS\Workspaces\003_Stage 3 -EIS Report\Appendix F\F_14_MCJ5003_Segment parameters for boundary conditions.qgz

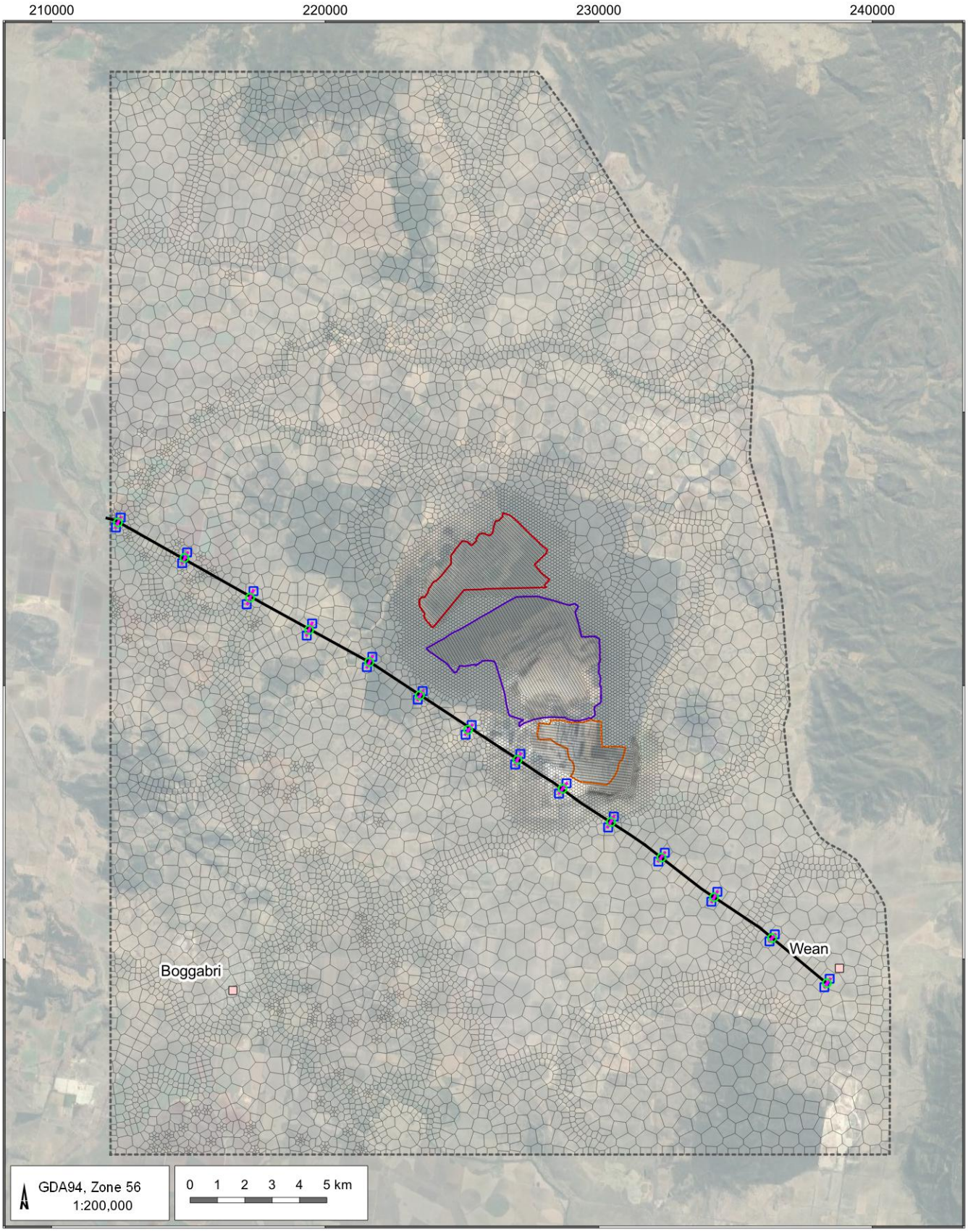

LEGEND

- Populated place
- MCCM Open Cut Extent
- BCM Open Cut Extent
- TCM Open Cut Extent
- Model Extent

Structure Overlay

- Conomos vertices
- Conomos slider lines
- Conomos fault plane
- Conomos slider vertices

BTM Complex Groundwater Model Update 2024

Structural overlay (vertices and sliders) used for the Conomos Fault

AGE

DATE 10/02/2025

FIGURE No: **F 15**

©2025 Australasian Groundwater and Environmental Consultants Pty Ltd (AGE) - www.ageconsultants.com.au
Source: LiDAR DEM © Department Finance, Services and Innovation, 2016; GEODATA TOPO 250K Series 3 - © Commonwealth of Australia (Geoscience Australia) 2006.;
G:\Projects\MCJ5003.001 Maules Creek Continuation Project EIS\3_GIS\Workspaces\003_Stage 3 -EIS Report\Appendix F\F_15_MCJ5003_Structural overlay (vertices and sliders) used for the Conomos Fault.qgz

F7.3 Calibration targets

The model domain contains a significant network of monitoring bores and water level datasets. The water level responses recorded in the monitoring bores vary depending on a range of factors, including geology, hydraulic properties, location, climatic conditions, and mining activities. The water levels recorded in the monitoring bores indicate heterogeneous hydraulic properties and recharge rates.

A total of 247 monitoring points were used to calibrate the model, comprising:

- 155 monitoring points from the BTM Complex monitoring network, which included bores and Vibrating Wire Piezometers (VWPs) that screen the alluvium and Permian coal measures; and
- 92 NSW Government monitoring bores installed primarily within the Quaternary alluvium.

The calibration dataset comprised 24258 observations during the period 2006-2024. These comprised absolute hydraulic heads and temporal head differences, with approximately half of the observations in the different alluvial zones surrounding the complex (layer 1 and layer 2 of the numerical model). The observations in the Permian were primarily from nested VWPs proximal to the mines, specifically targeting the Braymont, Merriown, Tarrawonga and Therribri coal seams. In addition, an inequality constraint was applied to mine inflow rates for the entire BTM Complex, with an upper limit of 5.0 GL/yr (approximately three times the estimated value from inflow data). This represents the only flux target formally part of the calibration process.

Peeters & Middlemis (2023) suggest groundwater assessments consider the uncertainty around measurements used during the modelling process. The groundwater levels within the monitoring network are measured manually with electronic water level dippers, and the water level is converted to an elevation based on surveyed levels at the measurement point, which is usually the top of the bore casing. Modern electronic water level dippers are expected to be accurate to within ±1 cm, and the measurement point elevation is also expected to be accurate to within ±1 cm to 10 cm, depending on the surveying method. Therefore, the measurement of water levels within the monitoring network is considered unlikely to have introduced any significant uncertainty to the model predictions. VWPs, in contrast, measure pore pressure, which is converted to a potentiometric surface based on the elevation of the VWP sensor. The VWPs are sealed with cement grout within the boreholes and, therefore, cannot be validated or the data loggers checked for instrument drift.

Therefore, the measurement error for the VWPs is considered potentially higher than that for the monitoring bores and possibly in the range of ±5 m to 10 m. Despite the potential for larger measurement errors in the VWP data, when used with caution, it remains a useful additional dataset for understanding the groundwater regime and guiding the calibration of the numerical model, provided that the observed pressure changes are considered conceptually sound. Absolute hydraulic heads were weighted less than temporal differences to focus on matching depressurisation trends. Weights were balanced so that the absolute hydraulic heads contributed approximately a third of the starting total objective function during calibration compared with two-thirds for the temporal differences.

Figure F 16 shows the locations of the observation bores and VWPs used in the calibration process. For model calibration purposes, the observation bore water level records were weighted as follows:

- anomalous results were removed;
- datalogger data were processed with a 90-day moving average to be consistent with the resolution of stresses simulated in the model and then resampled quarterly;
- the absolute hydraulic head dataset was processed to extract a temporal difference hydraulic head observation dataset;
- datapoints for absolute heads at each location were weighted according to the formula: weight of datapoint = 1/ $\sqrt{}$ (number of points for that site); and
- datapoints for temporal differences were weighted 10 times greater than their absolute counterparts.

Using this method, bores with longer records have a lower weighting per data point but a higher overall weighting in the combined dataset, and more attention is paid to fitting trends than absolutes.

The pilot points (Figure F 13) were situated where it was clear from water level monitoring data that heterogeneity in hydraulic properties and/or recharge may influence water level observations and would be required in the model to provide similar predictions.

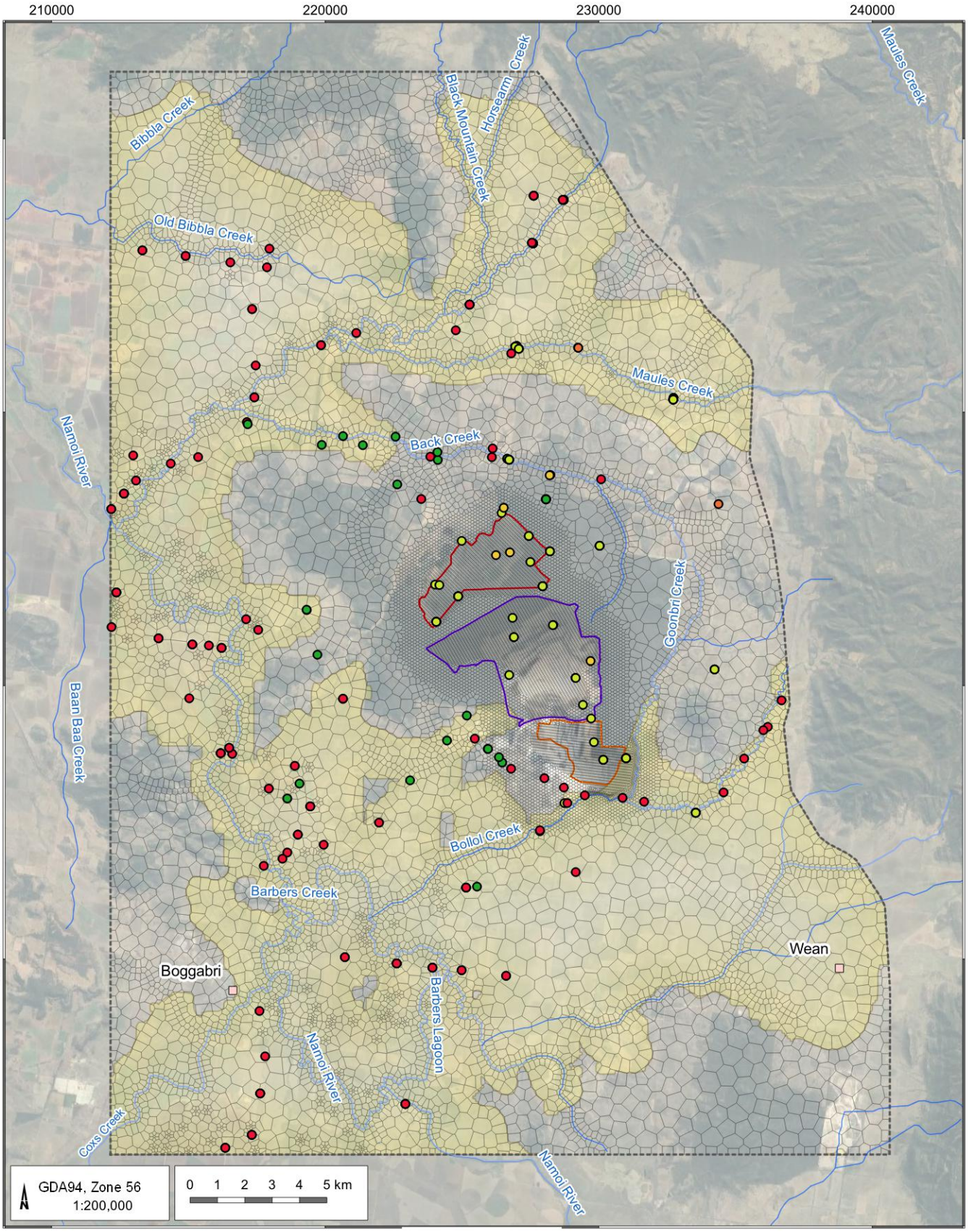

LEGEND

- Populated place
- Drainage
- MCCM Open Cut Extent
- BCM Open Cut Extent
- TCM Open Cut Extent
- Model Extent
- Model Grid
- Modelled Alluvium Extent

Observation layers

- 1 - 2
- 3 - 5
- 6 - 10
- 11 - 30
- 31 - 34

BTM Complex Groundwater Model Update 2024

Observation layers used for calibration

AGE

DATE 26/03/2025

FIGURE No: **F 16**

©2025 Australasian Groundwater and Environmental Consultants Pty Ltd (AGE) - www.ageconsultants.com.au
Source: LiDAR DEM © Department Finance, Services and Innovation, 2016; GEODATA TOPO 250K Series 3 - © Commonwealth of Australia (Geoscience Australia) 2006.;
G:\Projects\MCJ5003.001 Maules Creek Continuation Project EIS\3_GIS\Workspaces\003_Stage 3 -EIS Report\Appendix F\F_16_MCJ5003_Observation layers used for calibration.qgz

F7.3.1 Water level history matching

Figure F 17 presents the observed and modelled groundwater levels determined from the calibration in a scattergram.

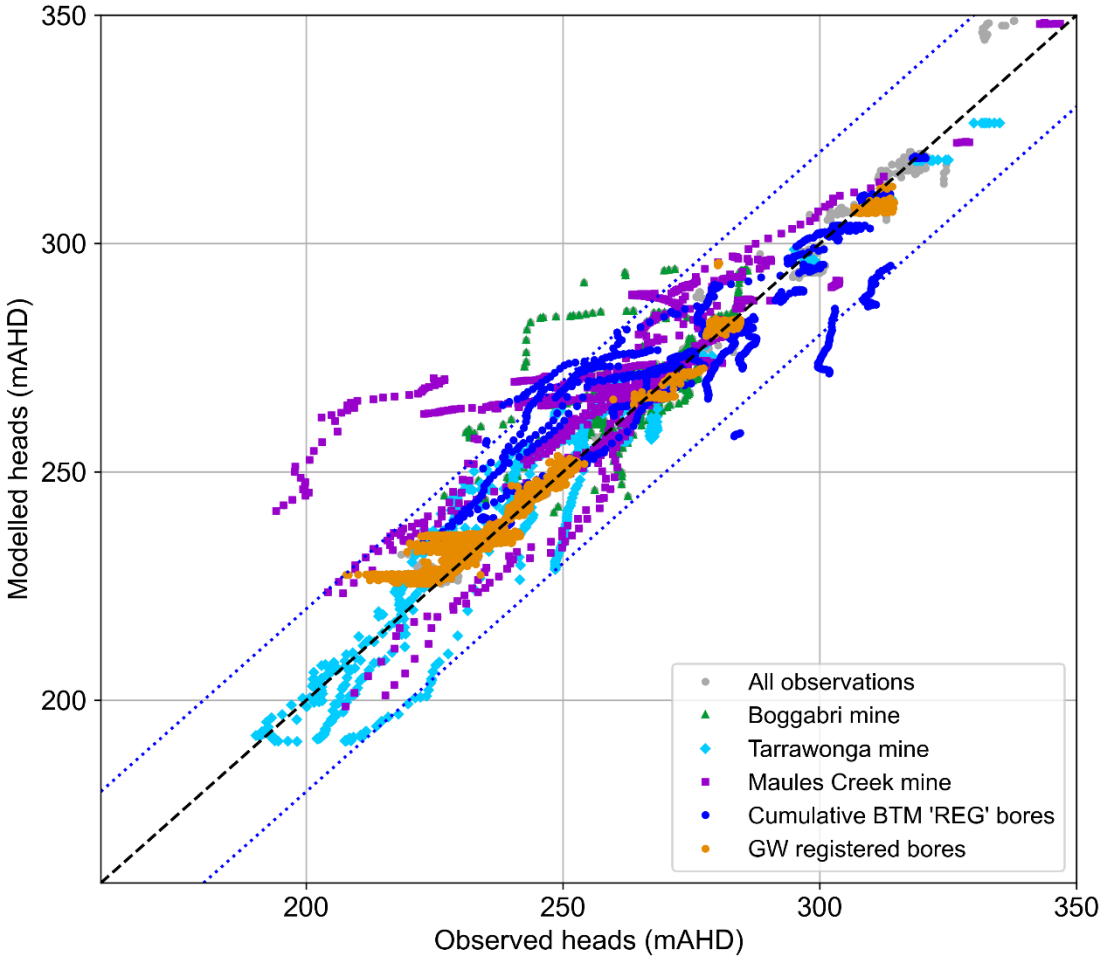

Figure F 17 Transient calibration – modelled vs observed groundwater levels

The root mean square (RMS) error calculated for the calibrated model was 6.6 m. The total measured head change across the model domain was 156.52 m, with a standardised root mean square (SRMS) of 4.2%, which can be considered a good match for the modelled system type. Overall, the model reasonably reproduces the trends and absolute hydraulic heads in the surficial aquifers, evidenced by location hydrographs in Section F13. This is acceptable because the boundaries feature static hydraulic heads and are distant enough from the QoIs to have minimal influence. Absolute hydraulic heads, and in many cases, the hydraulic trends, are not as well matched in the Permian sequence. However, it should be acknowledged that both the observation data for the coal seams (mostly VWP) and the representation of the coal/interburden sequence in the model include a large amount of uncertainty.

Three bores have very poor fits, over-shooting the measured observations. Two are RB series (RB04-V2 and RB05-V4) and the other is IB series (IBC2114). In all cases, the model cells where the simulated observations are extracted occur close to a pinch out in the model grid. Lateral discontinuity in the coal seams as they are represented in the model are problematic for the automated calibration process, which relies on interpolation of property fields between pilot-point locations.

The approximate error associated with VWP data has already been discussed in Section F7.3 above. The structural error incurred from the explicit representation of the coal seam and interburden units may be very large. The model assumes that coal seams exist where point data is available to inform them. Seams are also assumed not to exist if their thickness is less than 0.5 m. Interpolation between points and extrapolation outside the convex hull of those points governs the continuity and thickness of the coal seam layers. The density of drill logs used to inform coal seam elevation and thickness is greatest near the mines but reduces significantly further from them. Consequently, there is an increasing potential for error in the elevations and thickness of coal seams with distance from the mines.

Hydrographs showing the measured and simulated hydraulic heads are in Section F13. The hydrograph plot observations are the following:

- The hydrographs indicate that the model can replicate declining pressure trends, as observed via VWPs, in most locations. It is also capable of replicating some of the head separations that occur throughout the Permian strata, particularly in areas adjacent to the BTM mines, where depressurisation enhances the vertical gradients within the Permian strata (e.g., RB-series, REG-series).
- A notable recharge event in mid-to-late 2016, evident in the monitoring data, is not reproduced at the same scale in many of the monitoring bores installed within the Permian strata around the mines. The reasons for this are related to the starting property fields adopted from AGE (2022) and the absolute limits placed on layers designated as interburden combined with constraints on the ratios between vertical and horizontal hydraulic conductivity. These all act to inhibit short-term stress responses from propagating vertically through the Permian sequence.
- REG01 and REG10 series of VWP data, as well as the GW967138 monitoring bore, monitor coal seams between the MCCM and the Maules Creek alluvium in the Permian. REG10 is closer to MCCM and exhibits depressurisation in the deeper seams, which the model can simulate, albeit to a lesser extent than what is observed. REG01 is a multilevel VWP site adjacent to Maules Creek and NSW Government monitoring bore GW967138. The monitoring bore has two sensors at different depths, both located in the second layer of the model; consequently, the simulated hydrographs are the same. The model simulates the higher groundwater level observed within the alluvial aquifer and a lower pressure within the underlying Permian bedrock, indicating a downgradient from the alluvium to the underlying bedrock. At REG01, the different pressures observed within the Permian VWP sensors are not well replicated by the model.
- The groundwater series within the alluvial aquifer west of the BTM Complex consists mainly of government monitoring bores. The model replicates the absolute levels well within the alluvial aquifer. Trends in the groundwater series of monitoring bores are generally not influenced by mining, as evidenced by the absence of depressurisation trends; however, they do show the influence of climatic conditions, as reflected in recharge responses in their respective hydrographs (e.g., GW036185). In addition to recharge events, responses to groundwater abstraction from private irrigation bores can also be observed in some hydrographs (e.g., GW030471). Climatic trends influence groundwater levels within the model, sometimes more significantly than observed within the monitoring data.

F7.3.2 Water table and potentiometric surface

The simulated water table, along with measured groundwater levels in monitoring bores in June 2024, is shown in Figure F 18. The water table shows the dominant east-to-west flow direction within the model domain, which is influenced by the topography and alignment of the Maules Creek and Bollol Creek alluvial aquifers. At the western boundary of the model, the dominant flow direction turns north, following the alignment and flow of the Namoi River. The active mining areas within the BTM Complex area are evident in the water table as areas of locally lowered water levels with inward hydraulic gradients.

Figure F 19 shows the simulated potentiometric surface within the Merriown Seam in June 2024. The figure shows that flow directions are more strongly influenced by the active mining areas relative to the water table. The Merriown Seam potentiometric surface is generally lower than the water table, indicating a vertical gradient from the alluvium downwards into the underlying coal measures. Mining-induced depressurisation within the area is also evident in Figure F 19.

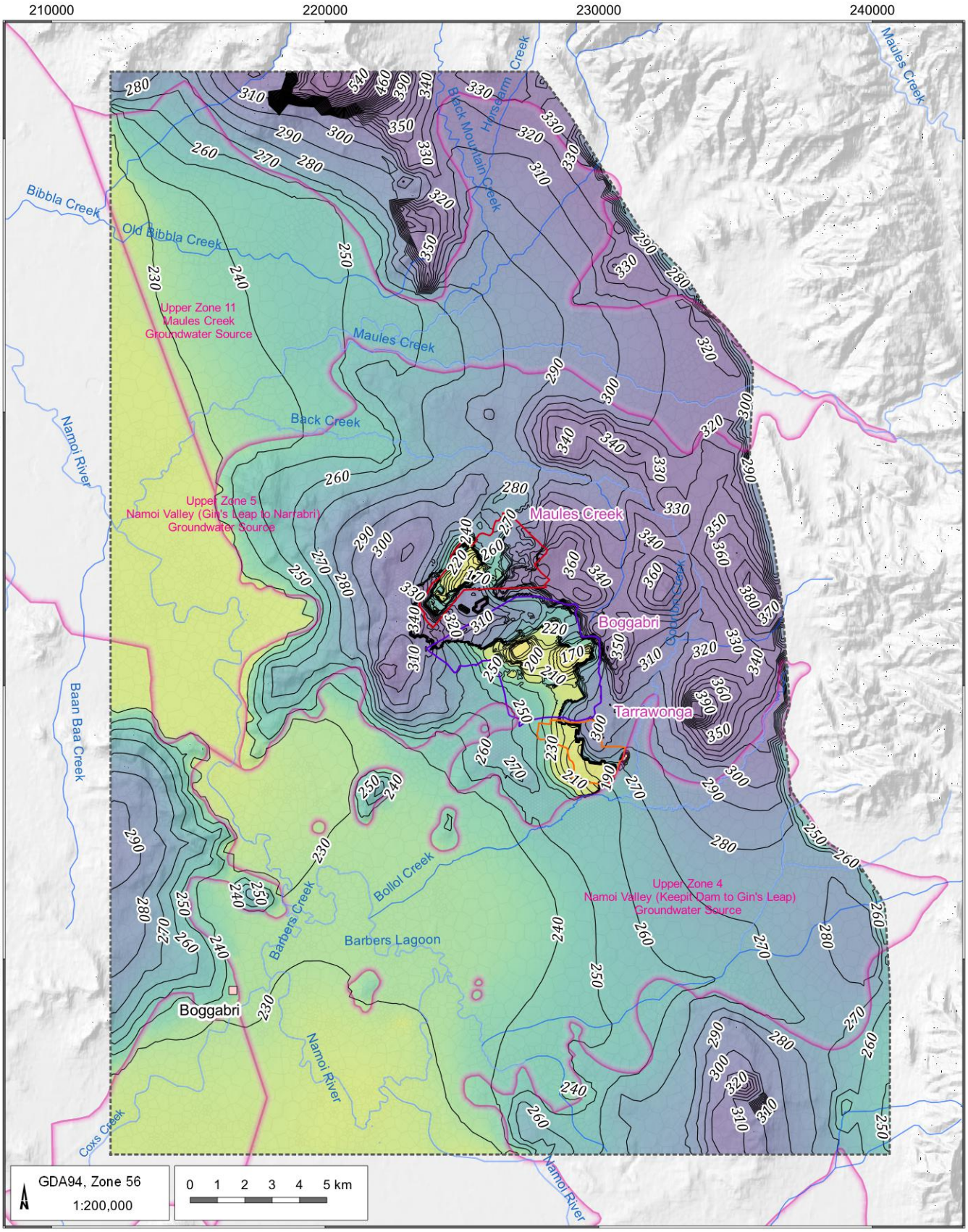

LEGEND

- Populated place
- Drainage
- Contour line
- MCCM Open Cut Extent
- BCM Open Cut Extent
- TCM Open Cut Extent
- Model Extent
- Model Grid
- Alluvial boundary zones

Simulated water table (mAHD)

- 147
- 228
- 230
- 235
- 245
- 260
- 270
- 280
- 300
- 320
- 576

BTM Complex Groundwater Model Update 2024

Simulated water table 2024

AGE

DATE 10/02/2025

FIGURE No: **F 18**

©2025 Australasian Groundwater and Environmental Consultants Pty Ltd (AGE) - www.ageconsultants.com.au
Source: LiDAR DEM © Department Finance, Services and Innovation, 2016; GEODATA TOPO 250K Series 3 - © Commonwealth of Australia (Geoscience Australia) 2006.;
G:\Projects\MCJ5003.001 Maules Creek Continuation Project EIS\3_GIS\Workspaces\003_Stage 3 -EIS Report\Appendix F\F_18_MCJ5003_Simulated water table 2024_v2.qgz

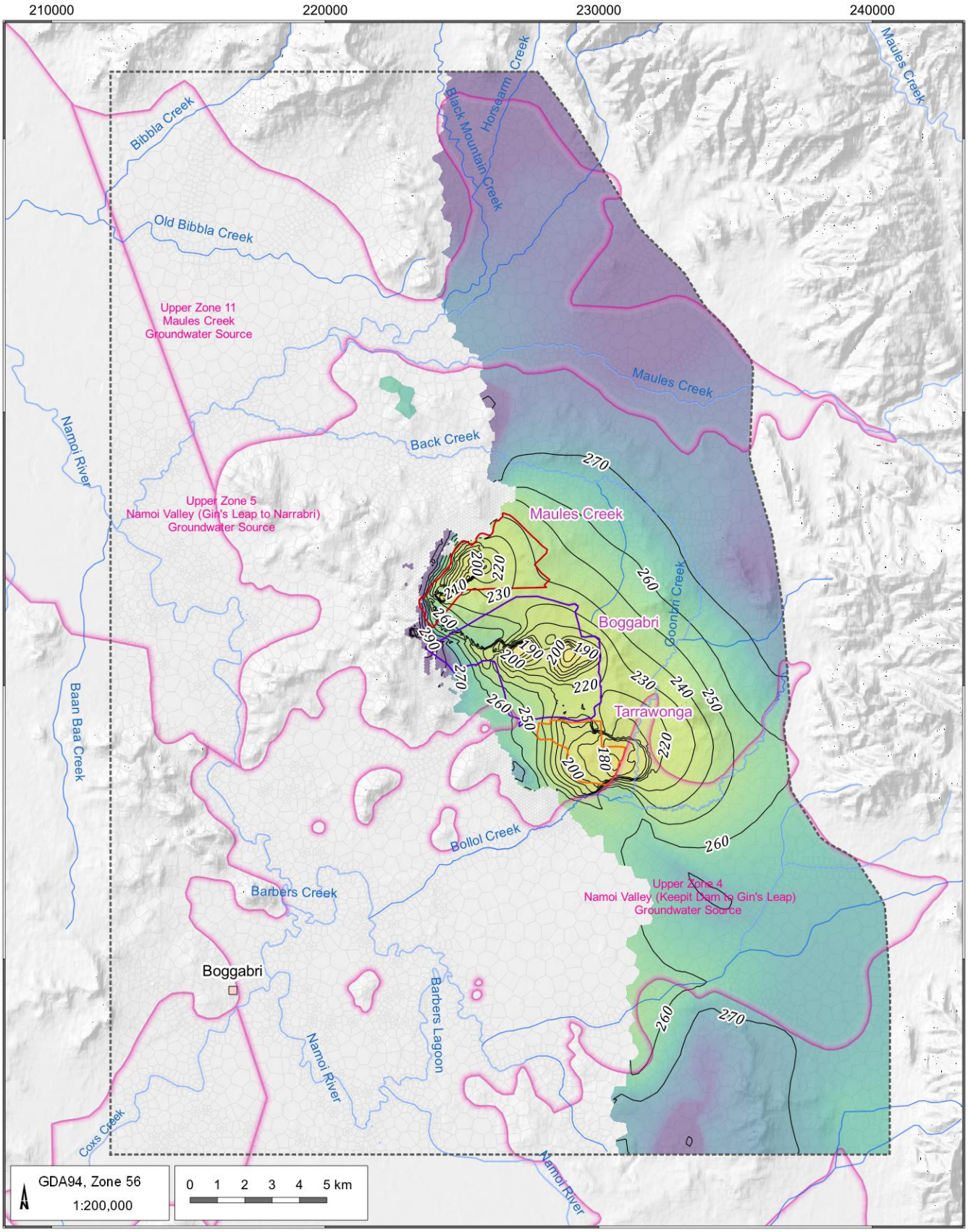

LEGEND

- Populated place
- Drainage
- Contour line
- MCCM Open Cut Extent
- BCM Open Cut Extent
- TCM Open Cut Extent
- Model Extent
- Model Grid
- Alluvial boundary zones

Simulated water table (mAHD)

- 147
- 228
- 230
- 235
- 245
- 260
- 270
- 280
- 300
- 320
- 576

BTM Complex Groundwater Model Update 2024

Simulated potentiometric surface – Merriown Seam 2024

AGE

DATE 10/02/2025

FIGURE No: **F 19**

©2025 Australasian Groundwater and Environmental Consultants Pty Ltd (AGE) - www.ageconsultants.com.au
Source: LiDAR DEM © Department Finance, Services and Innovation, 2016; GEODATA TOPO 250K Series 3 - © Commonwealth of Australia (Geoscience Australia) 2006.;
G:\Projects\MCJ5003.001 Maules Creek Continuation Project EIS\3_GIS\Workspaces\003_Stage 3 -EIS Report\Appendix F\F_18_MCJ5003_Simulated water table 2024_v2.qgz

F7.3.3 Hydraulic parameters

The hydraulic parameter ranges adopted for each model layer were guided by the field measurements described in the model update report 2022 (AGE, 2022). Where data was absent, experience with similar hydrogeological settings was used to guide parameter ranges.

The calibration was commenced using hydraulic conductivity values for the model layers adopted in the AGE (2022) model version. A function representing hydraulic conductivity that reduces with depth below the surface in the AGE (2022) model was removed to allow the calibration process more flexibility in matching observed water levels. Absolute thresholds on properties were enforced during calibration. The calibrated property fields for each model layer are presented in Figure F 20 to Figure F 53. In addition to aquifer properties, the plots also show the discontinuity of the Permian sequence as represented in the model. Only model layer 1 and model layer 34, representing the Narrabri alluvium and the Boggabri volcanics, are laterally continuous.

Layer 1 shows a distinct difference in hydraulic conductivity, where alluvium is observed, and weathered regolith from outcropping Permian or volcanic units is present. This is in keeping with the system conceptual model, which states that most groundwater flux occurs through the alluvium. Layer 2 represents the deeper alluvium (Gunnedah), which is only present beneath the observed surficial alluvium and absent beneath the weathered regolith. Here, hydraulic properties reflect an alluvial system, albeit with reduced hydraulic conductivity in the southeast. Two layers of interburden follow the Permian sequence, then a coal seam, repeating until reaching layer 34, which represents the basement volcanics. The properties of the interburden layers are characterised by low storage and reduced hydraulic conductivity, which contrasts with some of the coal seams, which show slightly elevated confined storage and noticeably elevated hydraulic conductivity.

The preferred hydraulic properties were those used in AGE (2022) and are summarised in Table F 9. These hydraulic properties are the initial values used as the mean of the prior probability distribution for the model and were then adjusted using pilot points during the calibration process. The final hydraulic property values determined from the calibration process are presented on the maps shown in Figure F 20 to Figure F 53. These maps illustrate the spatial variability in calibrated hydraulic properties, including horizontal and vertical hydraulic conductivity, specific storage, and specific yield, for the model with the minimum error variance, which is the outcome of the transient calibration.

The effects of the calibrated Conomos fault are also expressed through the aquifer hydraulic parameters where, for the most part, the structural overlay shows barrier behaviour in the lower coal seam layers (e.g. Merriown–layer 17 and Nagero–layer 20) and the volcanics. Because the effect of the fault on aquifer properties is projected through the grid, it does have the potential to increase the hydraulic conductivity of interburden layers along its length. Note that lateral flow through the interburden is negligible compared to the coal seams due to the low hydraulic conductivity values employed.

Table F 9 Pre-calibrated base hydraulic properties used in the numerical groundwater model

Model layer	Lithology	Kh (m/day)			Kv (m/day)	Sy (--)	Ss (1/m)
		Base value	cap max	cap min			
1	Alluvium - Narrabri Fm	10	-	-	Kh x 0.5	0.008	2.3E-7
1	Regolith	0.032	-	-	Kh x 0.12	0.004	2.2E-7
2	Alluvium - Gunnedah Fm	4.74	-	-	Kh x 0.54	0.25	2.3E-7
3	Interburden	2500 x (depth ^ -2.7)	1.0E-2	1.0E-5	Kh x 0.037	0.0007	1.0E-6
4	Interburden	1500 x (depth ^ -3.7)	1.0E-2	1.0E-5	Kh x 0.02	0.0009	1.0E-6
5	Seam Herndale, Onavale, Teston, Thornfield	0.005	-	-	Kh x 0.01	0.05	9.1E-6
6	Interburden	2500 x (depth ^ -3.7)	1.0E-2	1.0E-5	Kh x 0.01	0.0007	1.0E-6
7	Interburden	1500 x (depth ^ -2.7)	1.0E-2	1.0E-5	Kh x 0.03	0.0007	1.0E-6
8	Seam Braymont	0.63	-	-	Kh x 0.3	0.05	1.3E-5
9	Interburden	2500 x (depth ^ -3.7)	1.0E-2	1.0E-5	Kh x 0.0009	0.0007	1.0E-6
10	Interburden	2500 x (depth ^ -2.3)	1.0E-2	1.0E-5	Kh x 0.08	0.0007	1.0E-6
11	Seam Bollol Ck	0.13	-	-	Kh x 0.08	0.05	9.2E-6
12	Interburden	1500 x (depth ^ -3.7)	1.0E-2	1.0E-5	Kh x 0.1	0.0009	1.0E-6
13	Interburden	1500 x (depth ^ -3.7)	1.0E-2	1.0E-5	Kh x 0.001	0.0009	2.3E-7
14	Seam Jeralong	0.14	-	-	Kh x 0.08	0.05	1.0E-5
15	Interburden	1500 x (depth ^ -3)	1.0E-2	1.0E-5	Kh x 0.001	0.0007	1.0E-6
16	Interburden	2500 x (depth ^ -2.3)	1.0E-2	1.0E-5	Kh x 0.0004	0.0007	1.0E-6
17	Seam Merriown	0.29	-	-	Kh x 0.55	0.01	3.0E-6
18	Interburden	2500 x (depth ^ -2.3)	1.0E-2	1.0E-5	Kh x 0.0002	0.0009	2.3E-7
19	Interburden	2500 x (depth ^ -2.3)	1.0E-2	1.0E-5	Kh x 0.1	0.0009	3.1E-7

Model layer	Lithology	Kh (m/day)			Kv (m/day)	Sy (--)	Ss (1/m)
		Base value	cap max	cap min			
20	Seams Velyama, Nagero	0.313	-	-	Kh x 0.115	0.01	1.3E-5
21	Interburden	2500 x (depth ^ -2.3)	1.0E-2	1.0E-5	Kh x 0.052	0.0007	2.3E-7
22	Interburden	2500 x (depth ^ -2.3)	1.0E-2	1.0E-5	Kh x 0.1	0.0007	2.3E-7
23	Seams Upper Northam, Lower Northam	0.025	-	-	Kh x 0.3	0.01	1.14E-5
24	Interburden	2500 x (depth ^ -2.3)	1.0E-2	1.0E-5	Kh x 0.001	0.0009	2.3E-7
25	Interburden	1500 x (depth ^ -2.3)	1.0E-2	1.0E-5	Kh x 0.05	0.0009	2.3E-7
26	Seams Therribri A, Therribri B	0.086	-	-	Kh x 0.024	0.01	8.0E-6
27	Interburden	1502 x (depth ^ -2.3)	1.0E-2	1.0E-5	Kh x 0.013	0.0007	2.3E-7
28	Interburden	2500 x (depth ^ -3.7)	1.0E-2	1.0E-5	Kh x 0.003	0.0009	2.3E-7
29	Seams Flixton, Tarrawonga	0.036	-	-	Kh x 0.043	0.01	8.3E-6
30	Interburden	2119 x (depth ^ -3.7)	1.0E-2	1.0E-5	Kh x 0.028	0.0007	2.3E-7
31	Interburden	2016 x (depth ^ -3.7)	1.0E-2	1.0E-5	Kh x 0.003	0.0009	2.3E-7
32	Seam Templemore	0.052	-	-	Kh x 0.027	0.01	1.3E-5
33	Interburden	1500 x (depth ^ -3.7)	1.0E-2	1.0E-5	Kh x 0.007	0.0009	5.7E-7
34	Volcanics	0.001	-	-	Kh x 0.548	0.0009	2.2E-7

Notes: * Specific storage values for layer 1 are included for completeness because convertible model layers are adopted but this parameter has no effect on the model. Specific yield is only relevant to unconfined and temporarily dewatered model cells.

***** depth: For the Kh calculation, depth of the cell in metres from the ground level. For the numerical groundwater model, the depth of a given cell is measured between the cell centre and the top of layer 01 in the vertical column of cells.

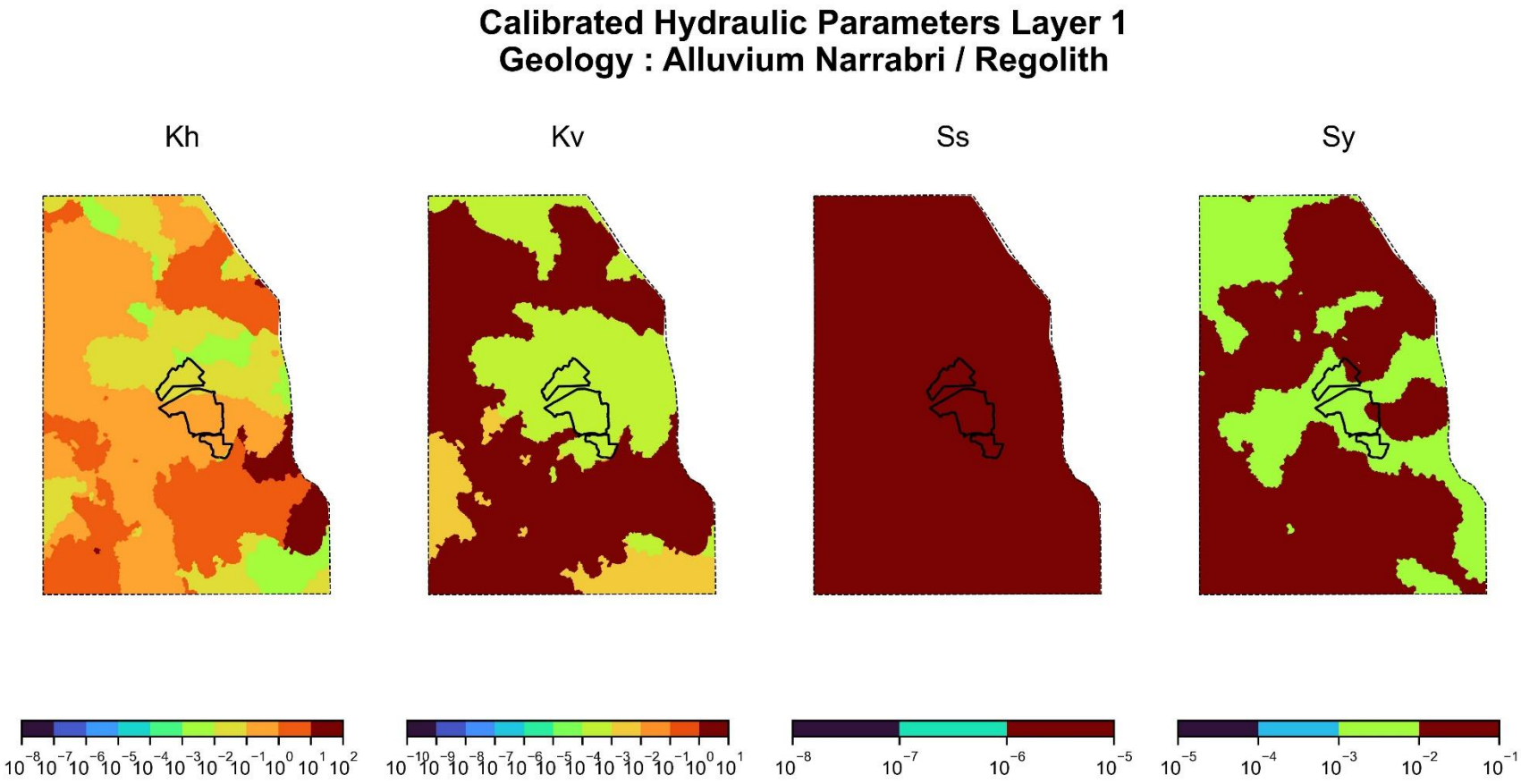

Note: Kh and Kv are in m/day.

Figure F 20 Calibrated hydraulic parameters - layer 1

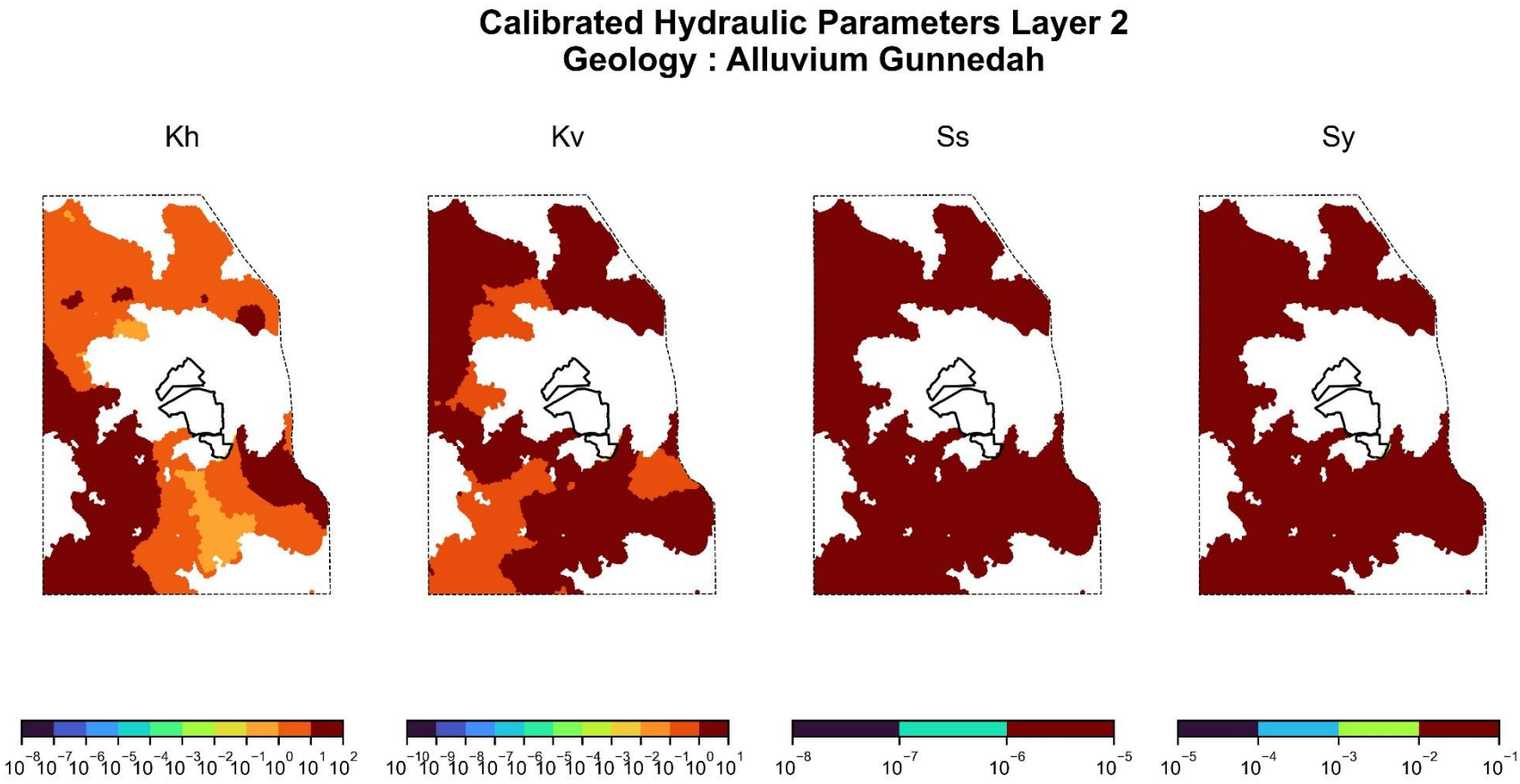

Note: Kh and Kv are in m/day.

Figure F 21 Calibrated hydraulic parameters - layer 2

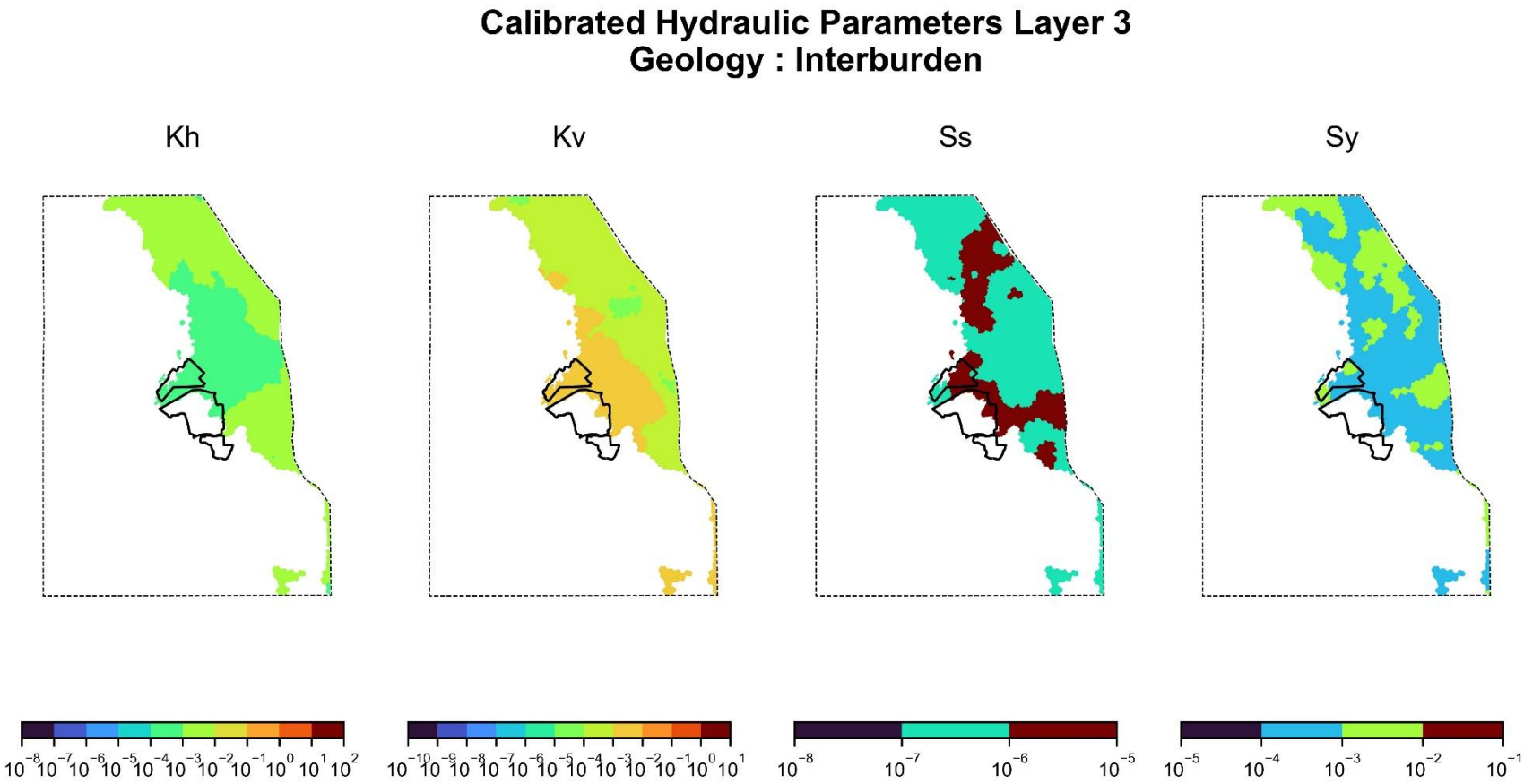

Note: Kh and Kv are in m/day.

Figure F 22 Calibrated hydraulic parameters - layer 3

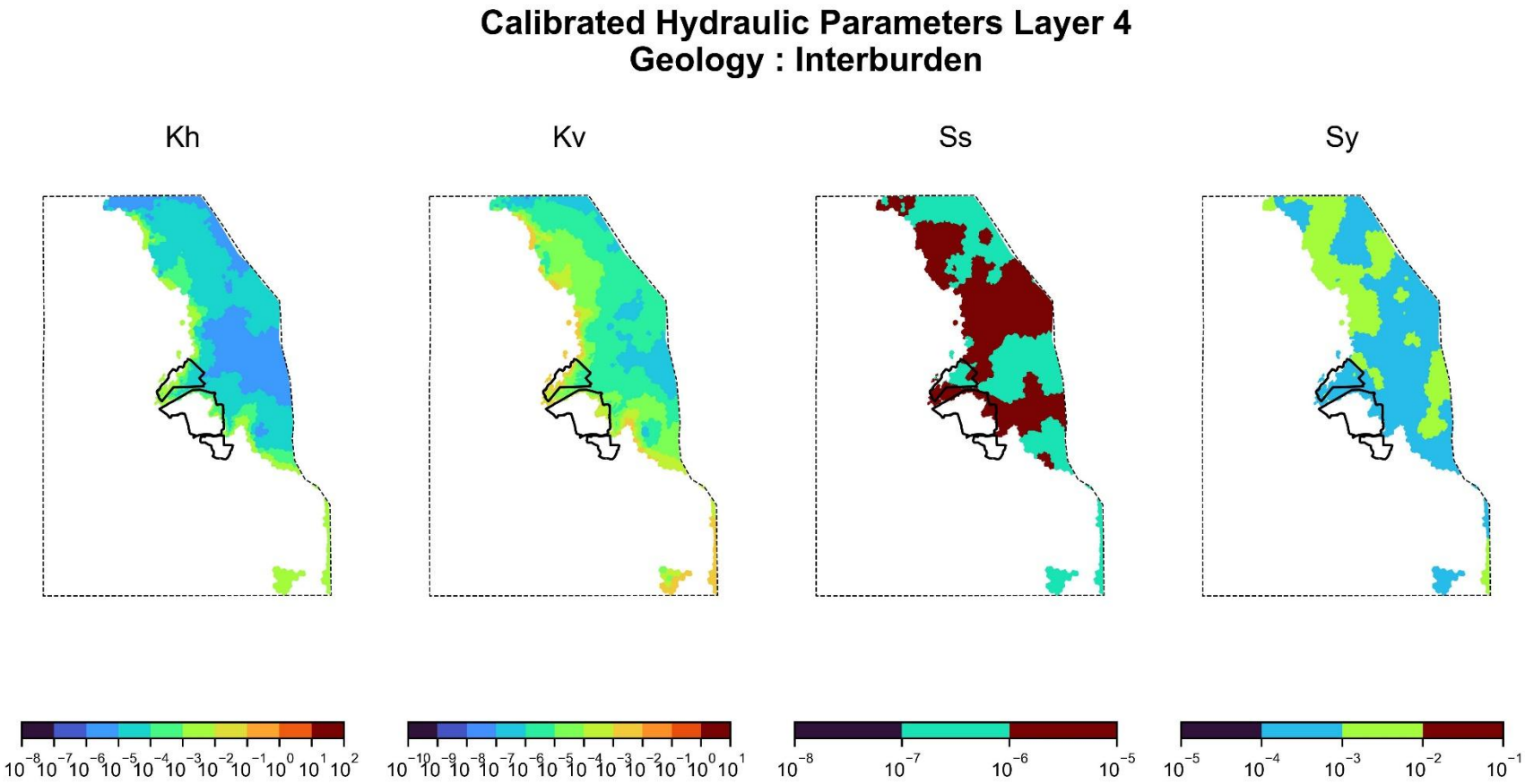

Note: Kh and Kv are in m/day.

Figure F 23 Calibrated hydraulic parameters - layer 4

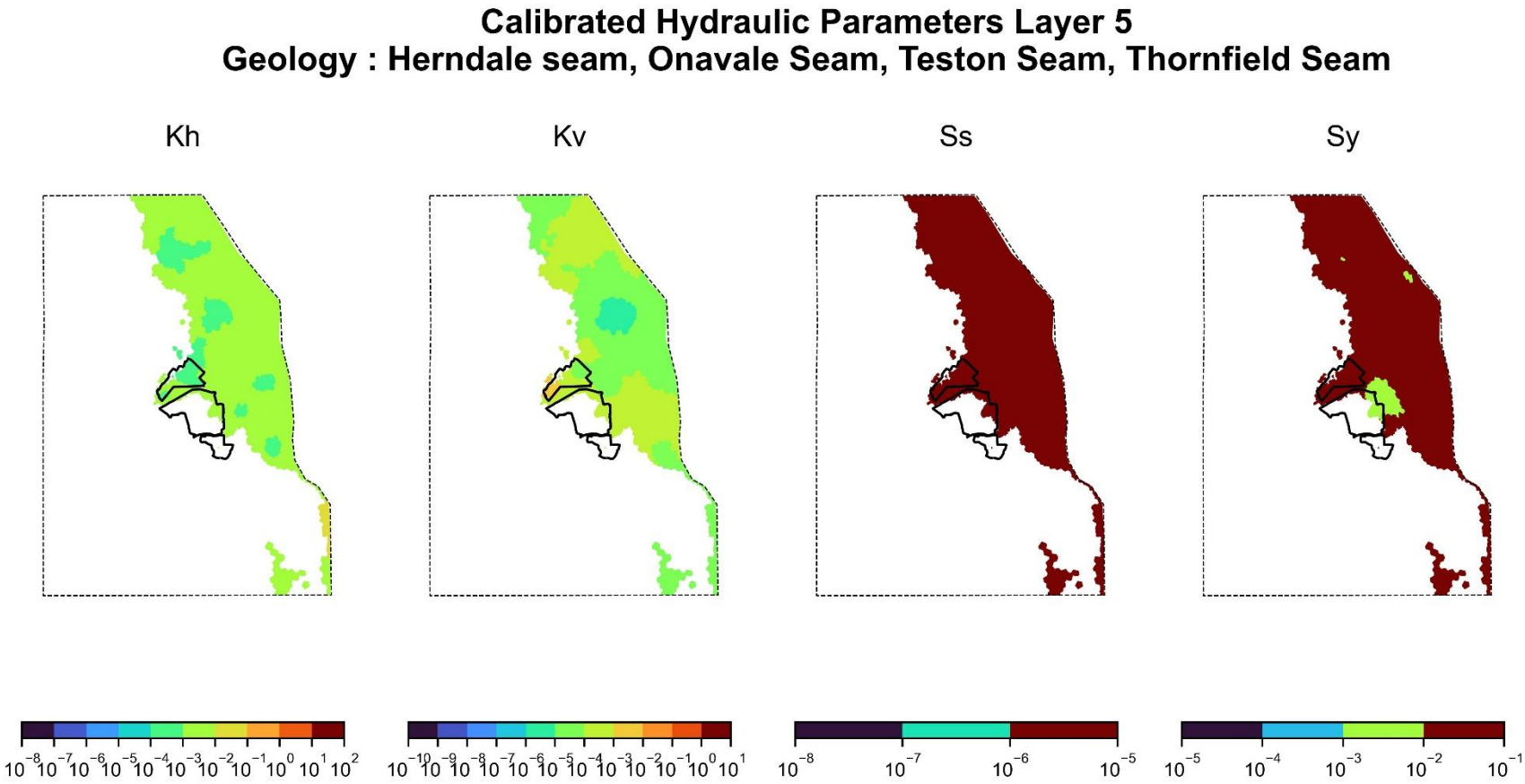

Note: Kh and Kv are in m/day.

Figure F 24 Calibrated hydraulic parameters - layer 5

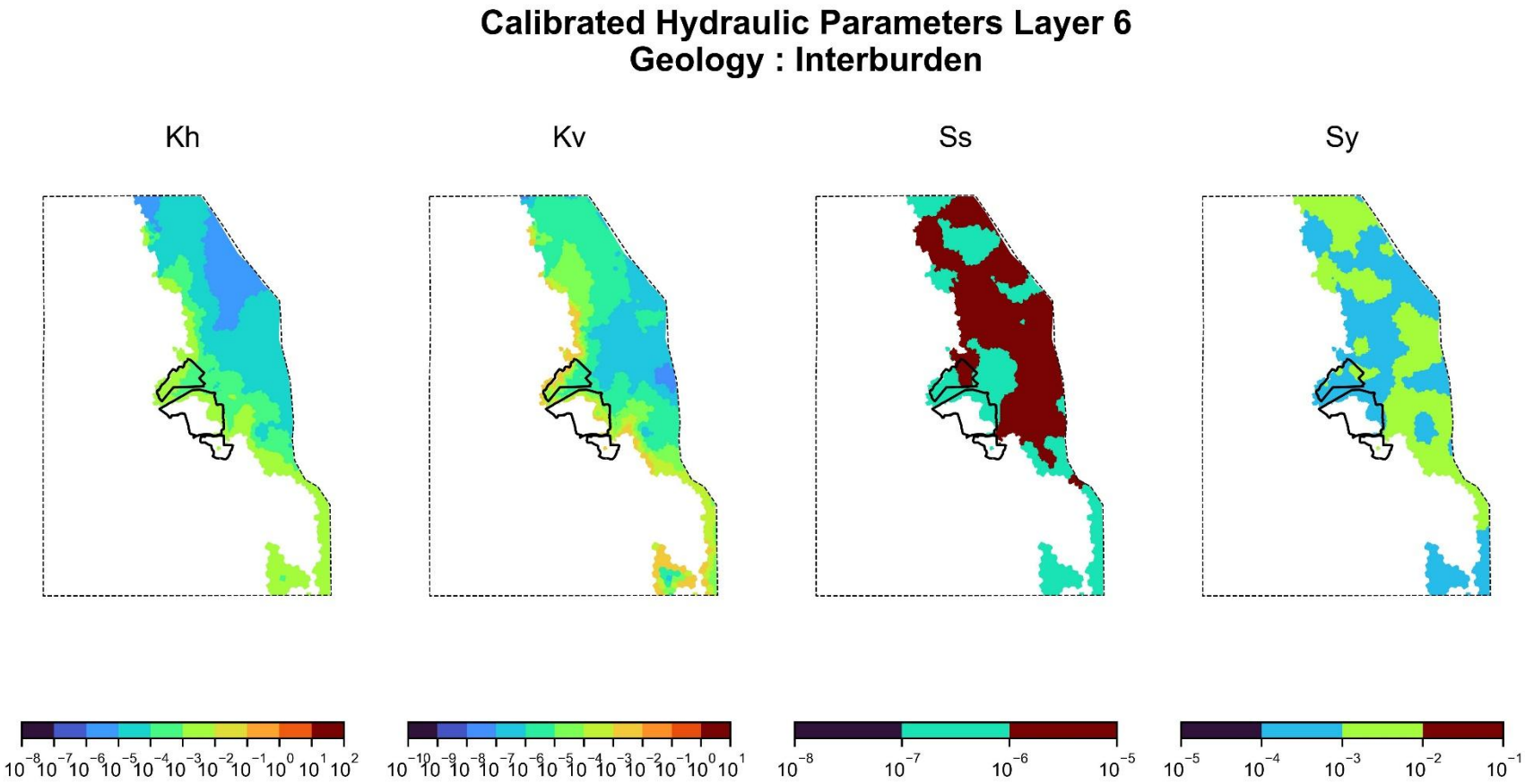

Note: Kh and Kv are in m/day.

Figure F 25 Calibrated hydraulic parameters - layer 6

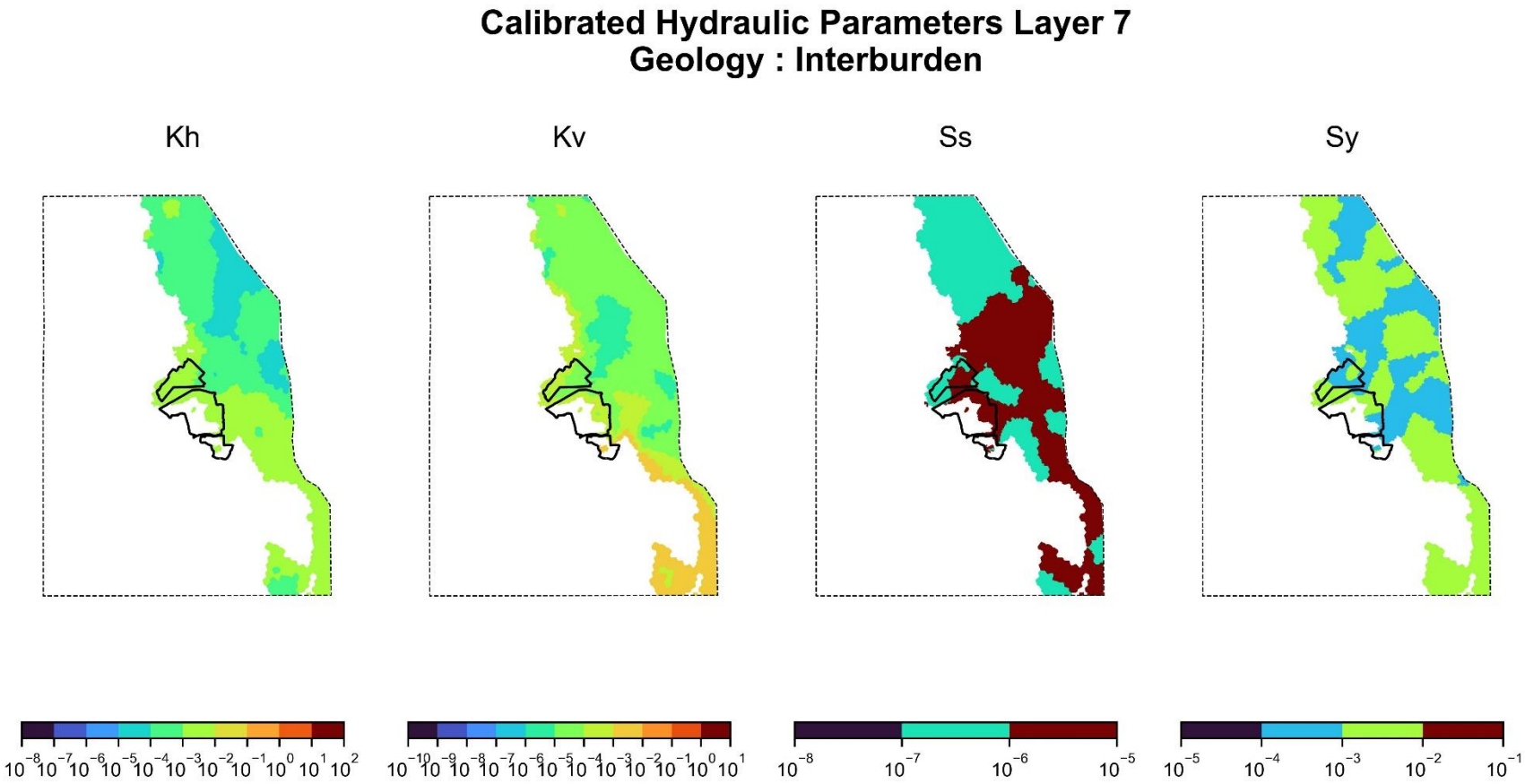

Note: Kh and Kv are in m/day.

Figure F 26 Calibrated hydraulic parameters - layer 7

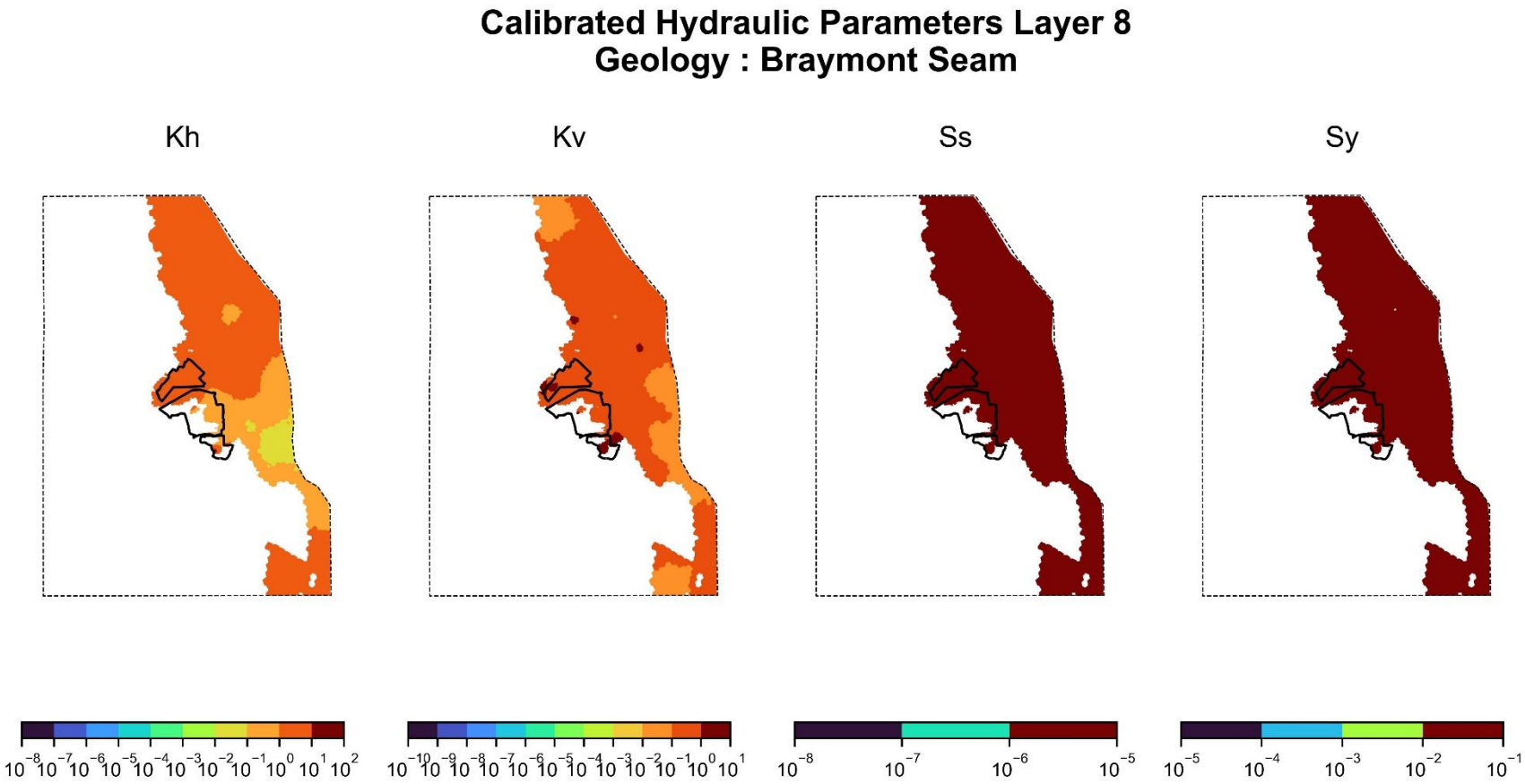

Note: Kh and Kv are in m/day.

Figure F 27 Calibrated hydraulic parameters - layer 8

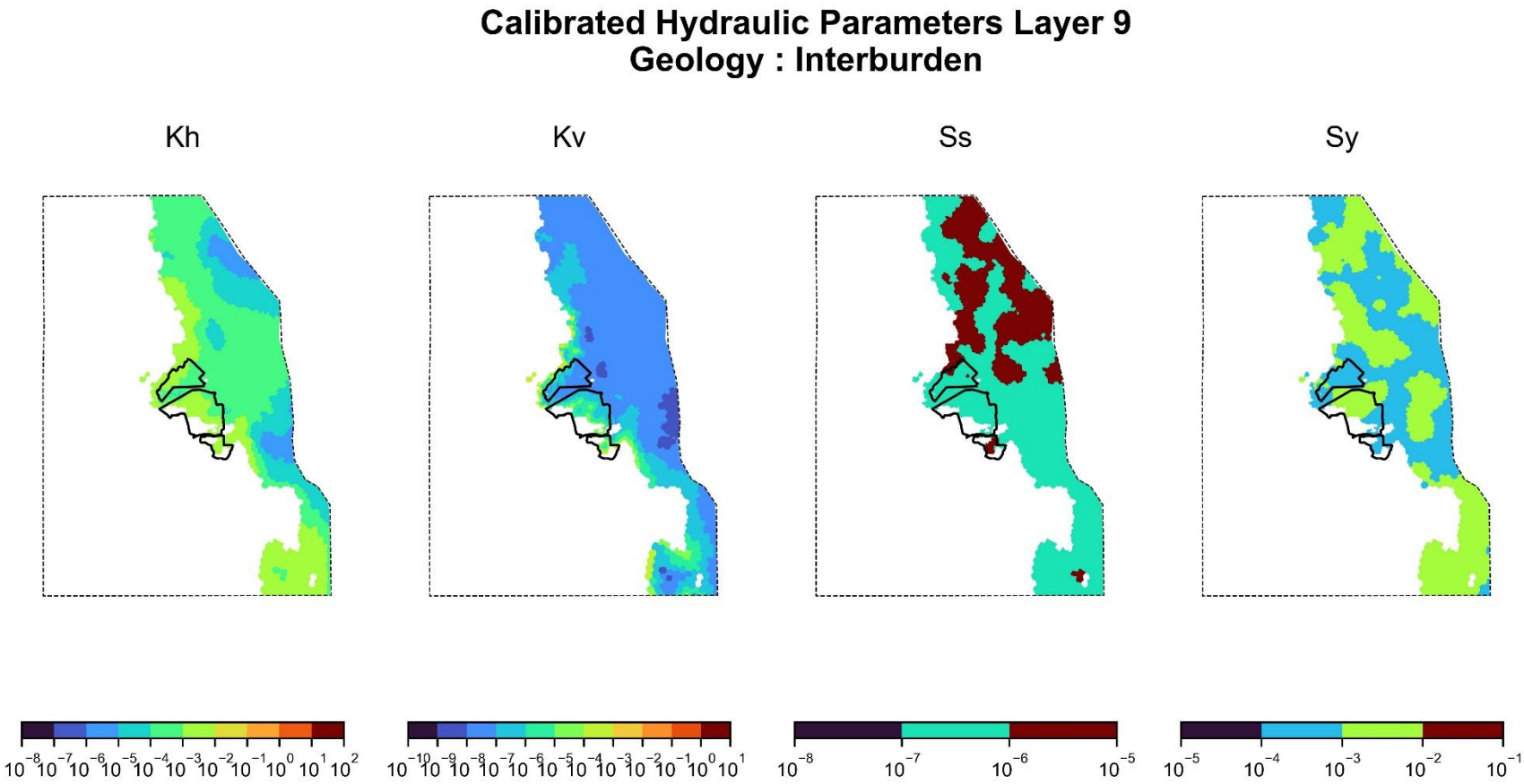

Note: Kh and Kv are in m/day.

Figure F 28 Calibrated hydraulic parameters - layer 9

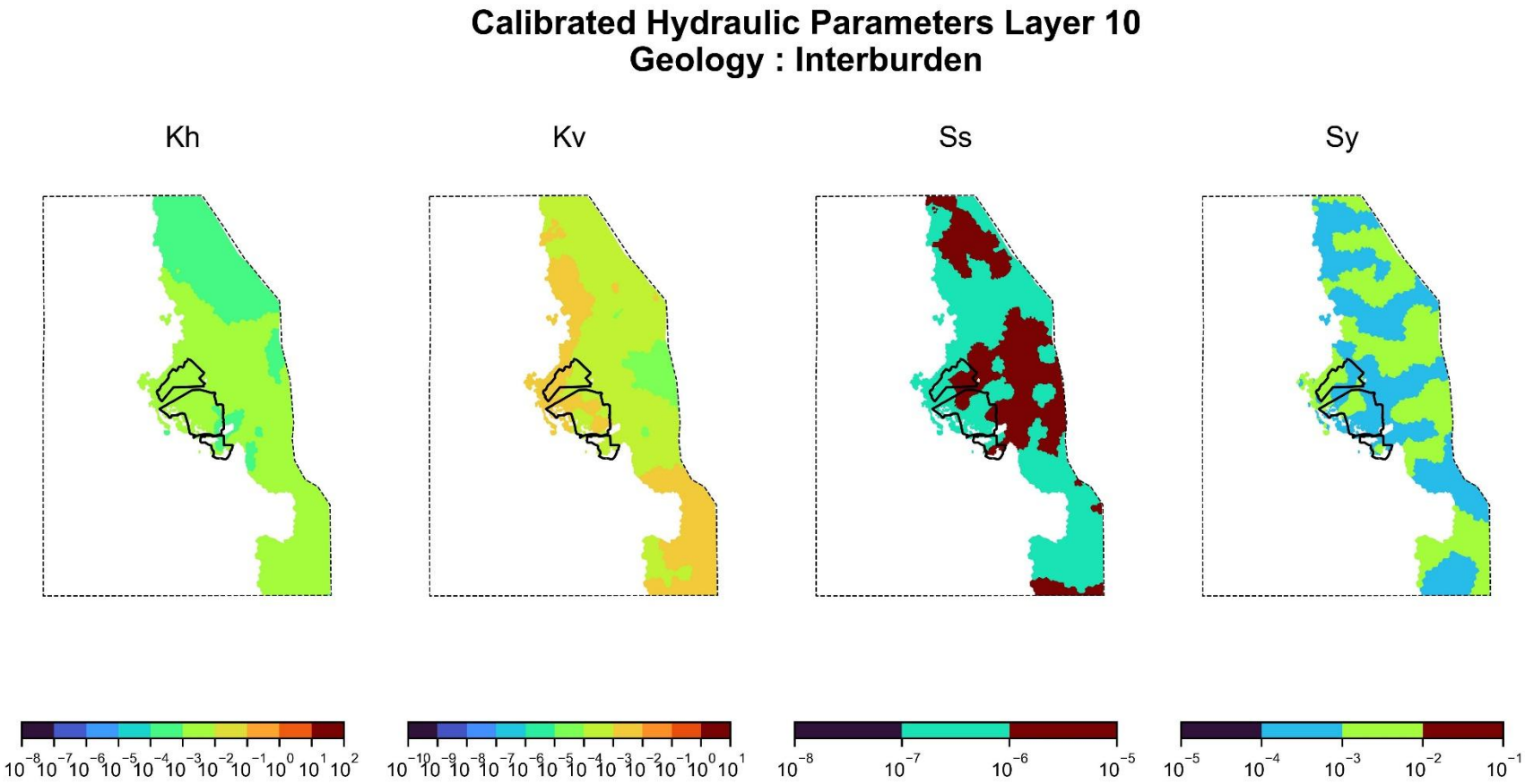

Note: Kh and Kv are in m/day.

Figure F 29 Calibrated hydraulic parameters - layer 10

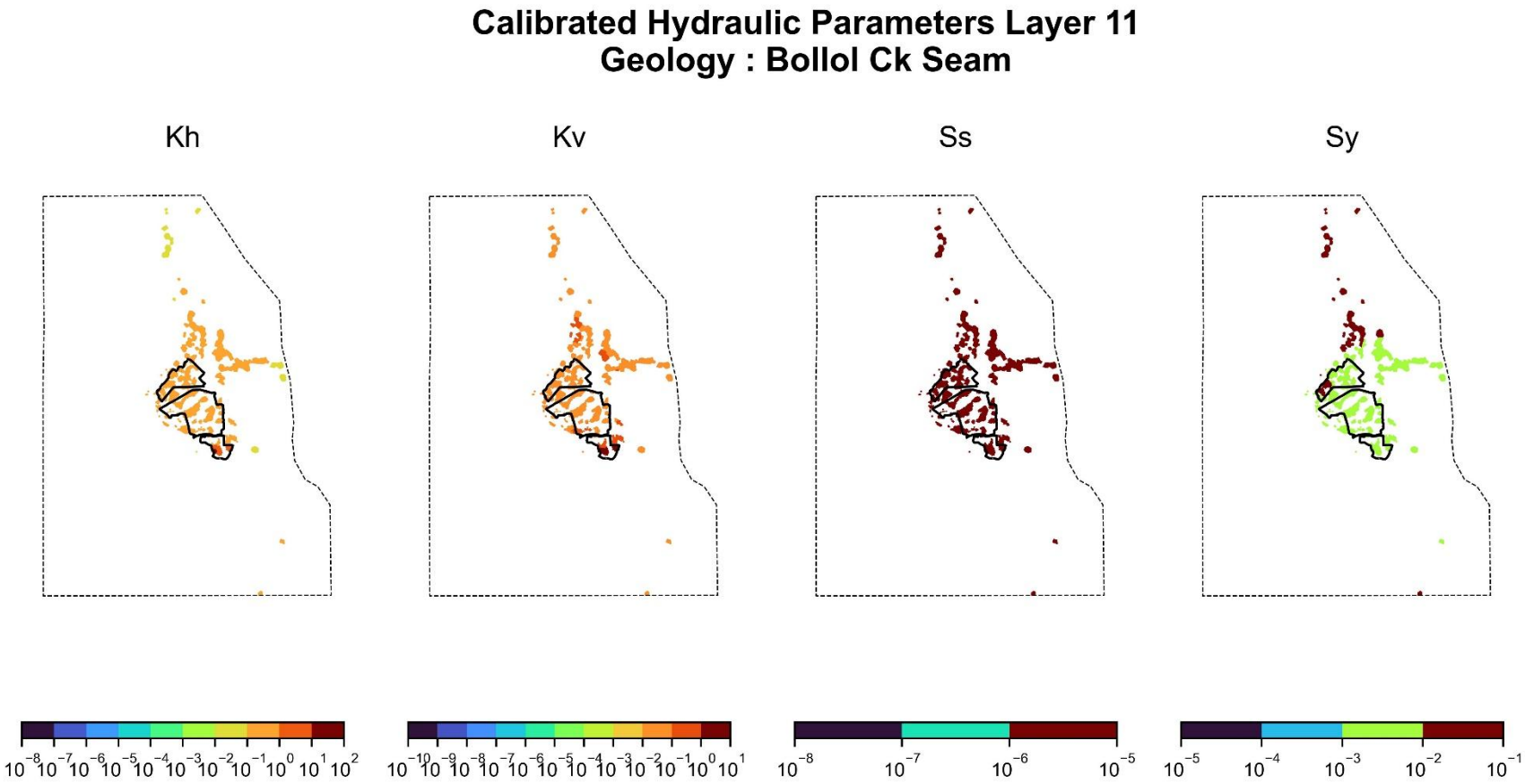

Note: Kh and Kv are in m/day.

Figure F 30 Calibrated hydraulic parameters - layer 11

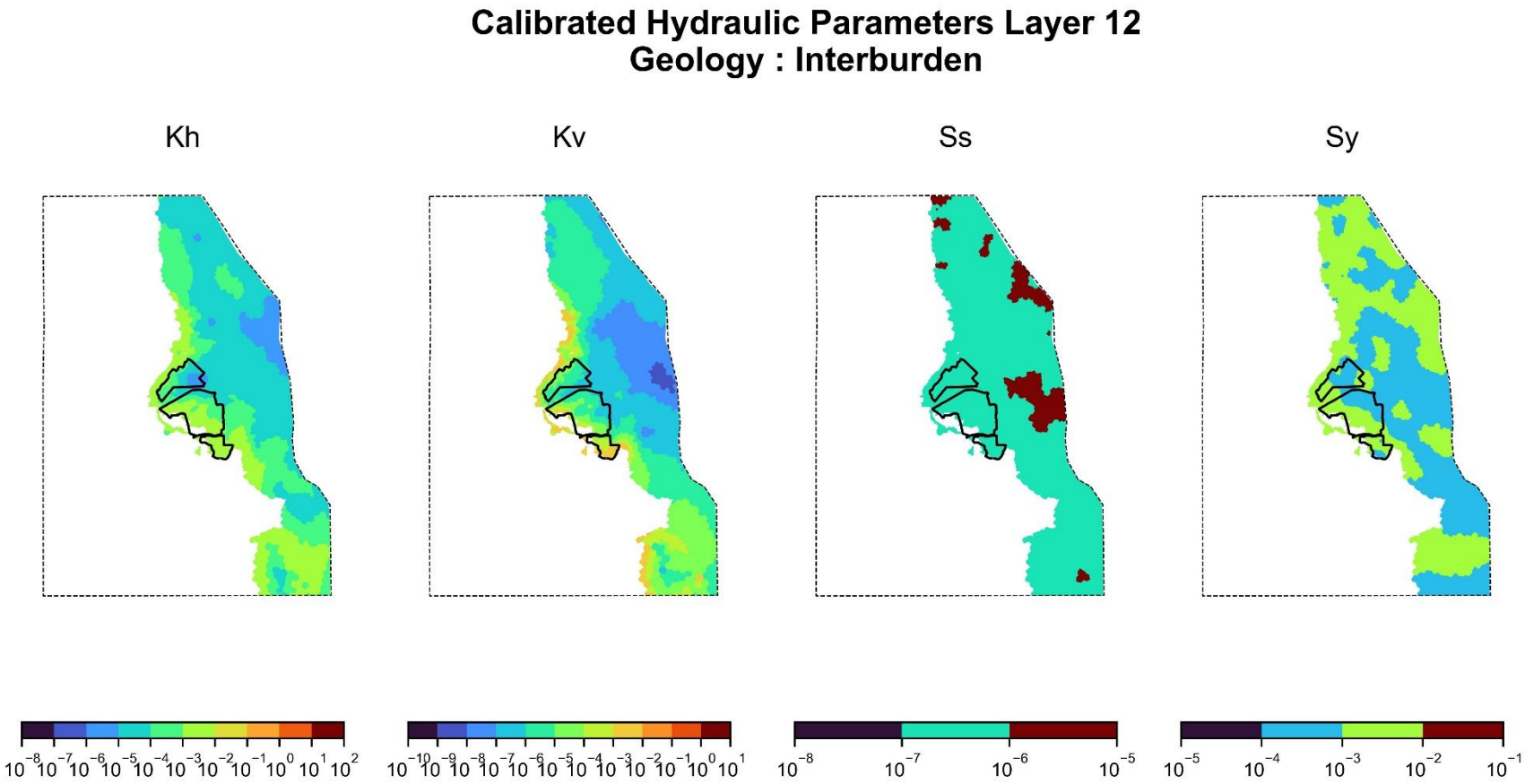

Note: Kh and Kv are in m/day.

Figure F 31 Calibrated hydraulic parameters - layer 12

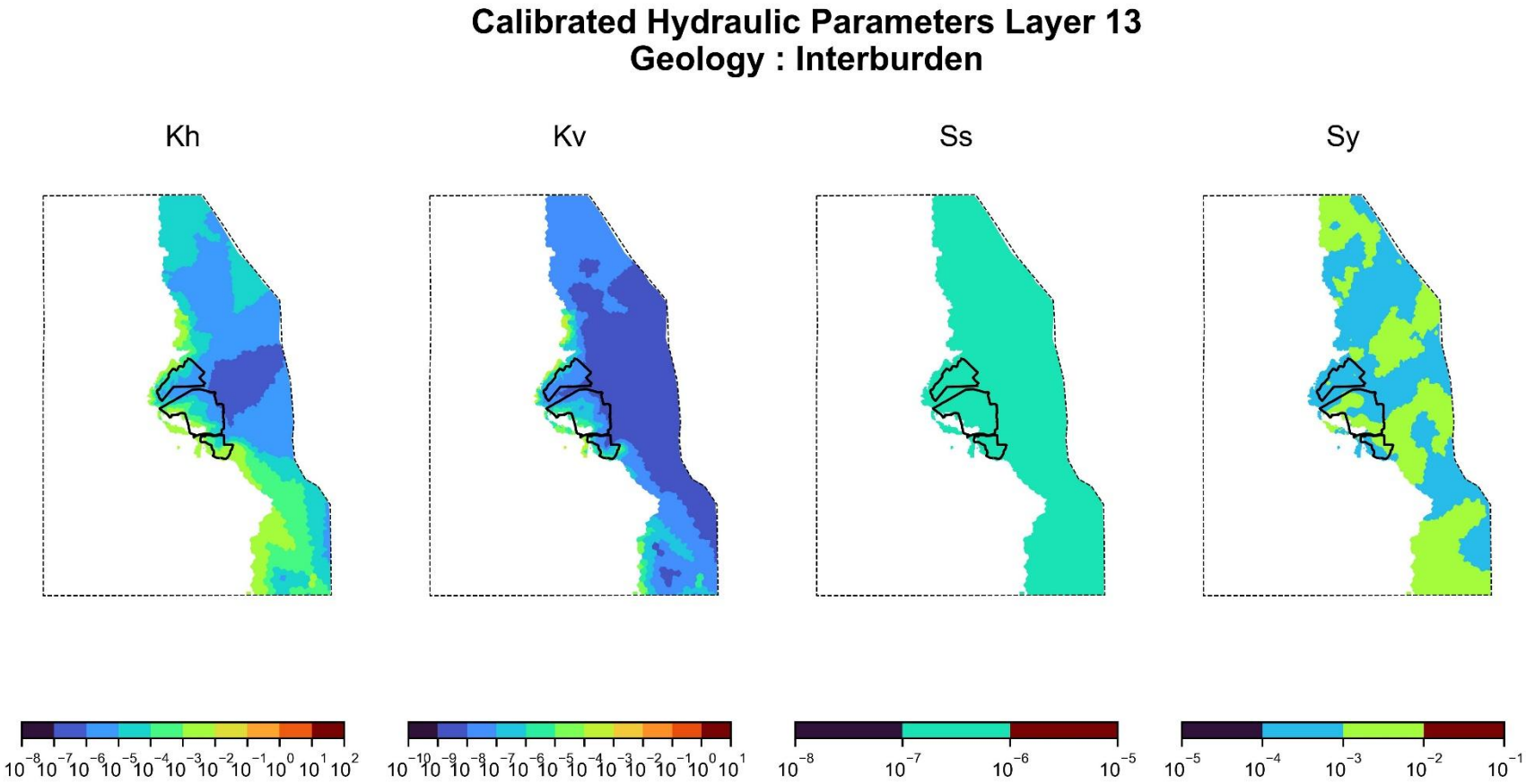

Note: Kh and Kv are in m/day.

Figure F 32 Calibrated hydraulic parameters - layer 13

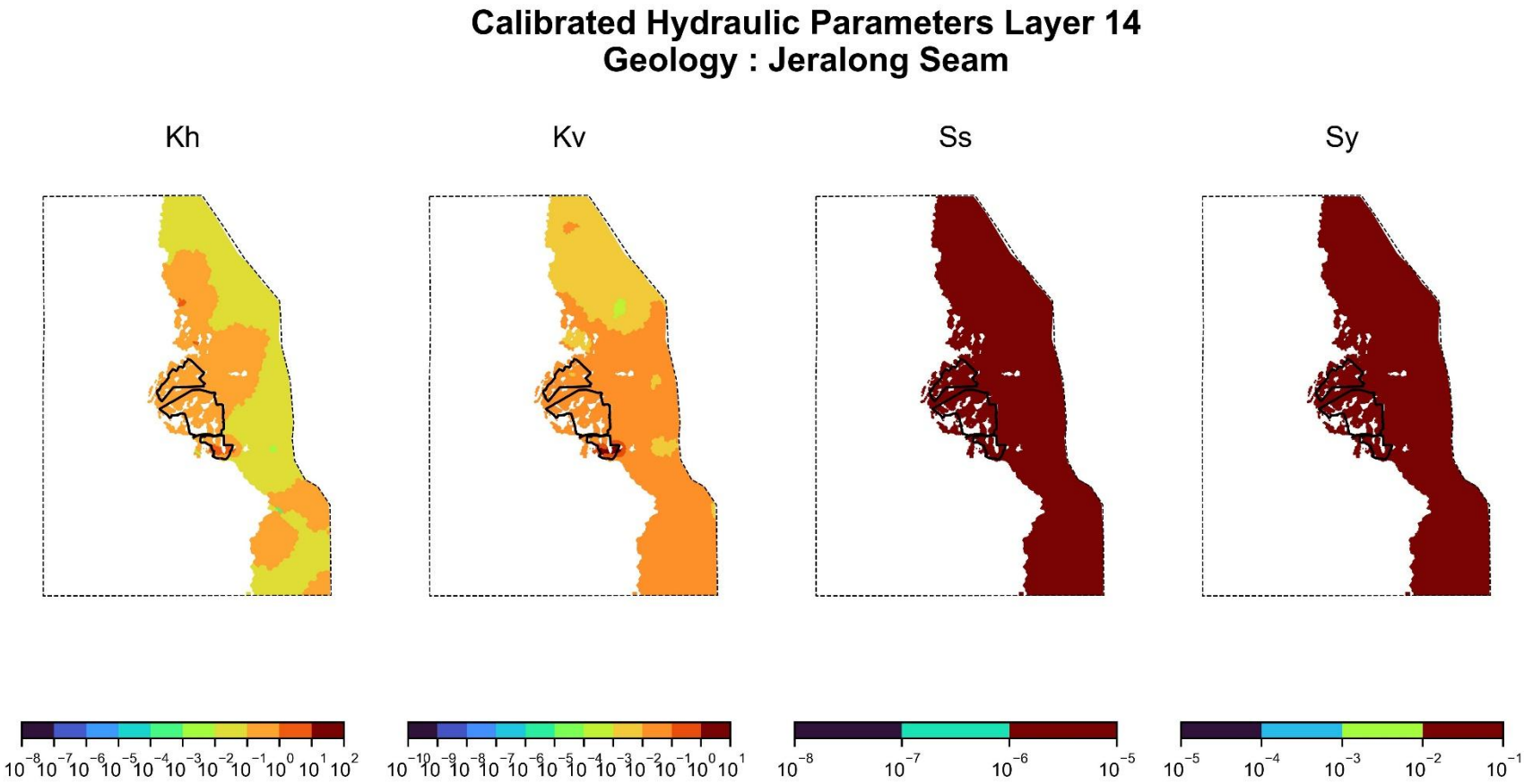

Note: Kh and Kv are in m/day.

Figure F 33 Calibrated hydraulic parameters - layer 14

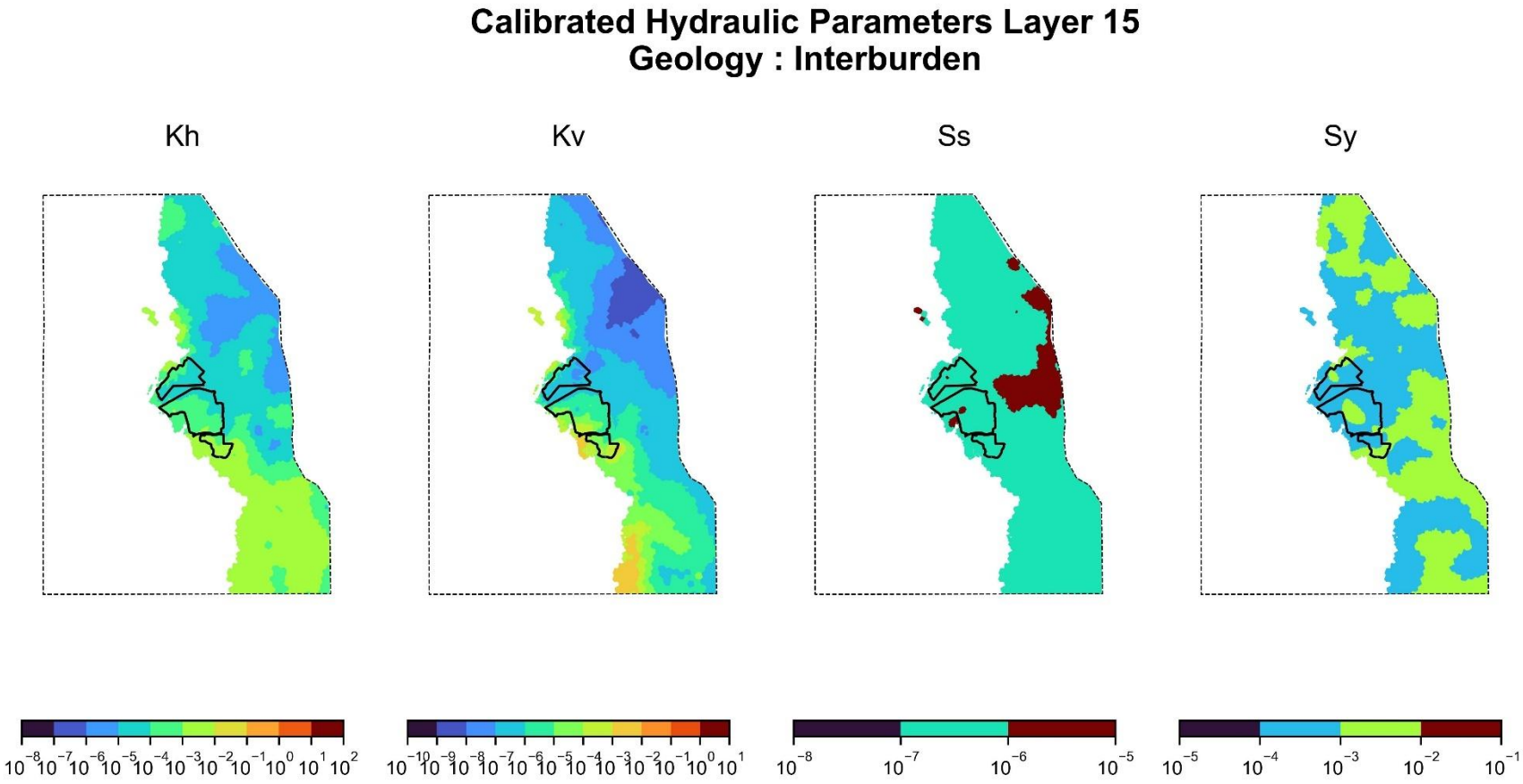

Note: Kh and Kv are in m/day.

Figure F 34 Calibrated hydraulic parameters - layer 15

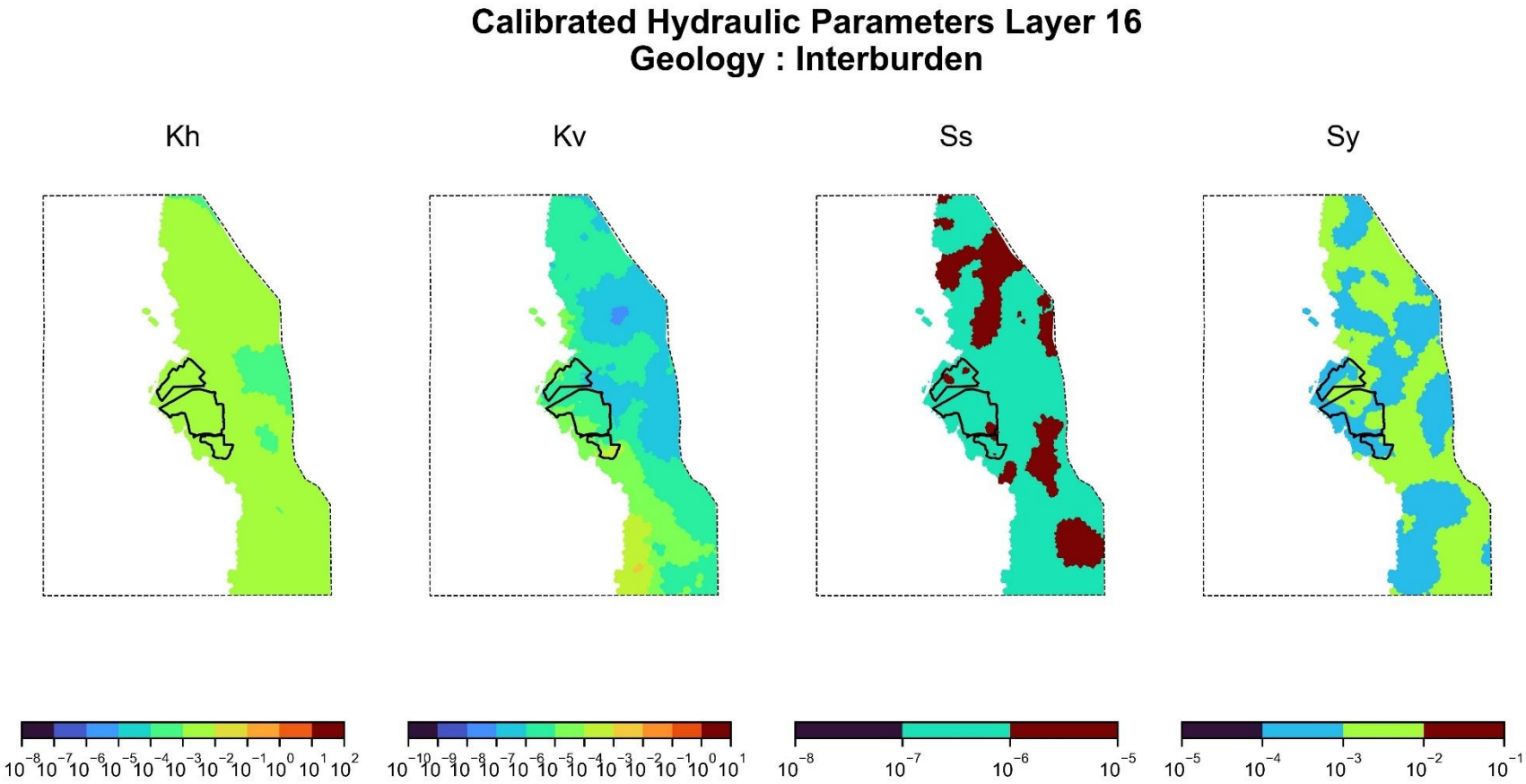

Note: Kh and Kv are in m/day.

Figure F 35 Calibrated hydraulic parameters - layer 16

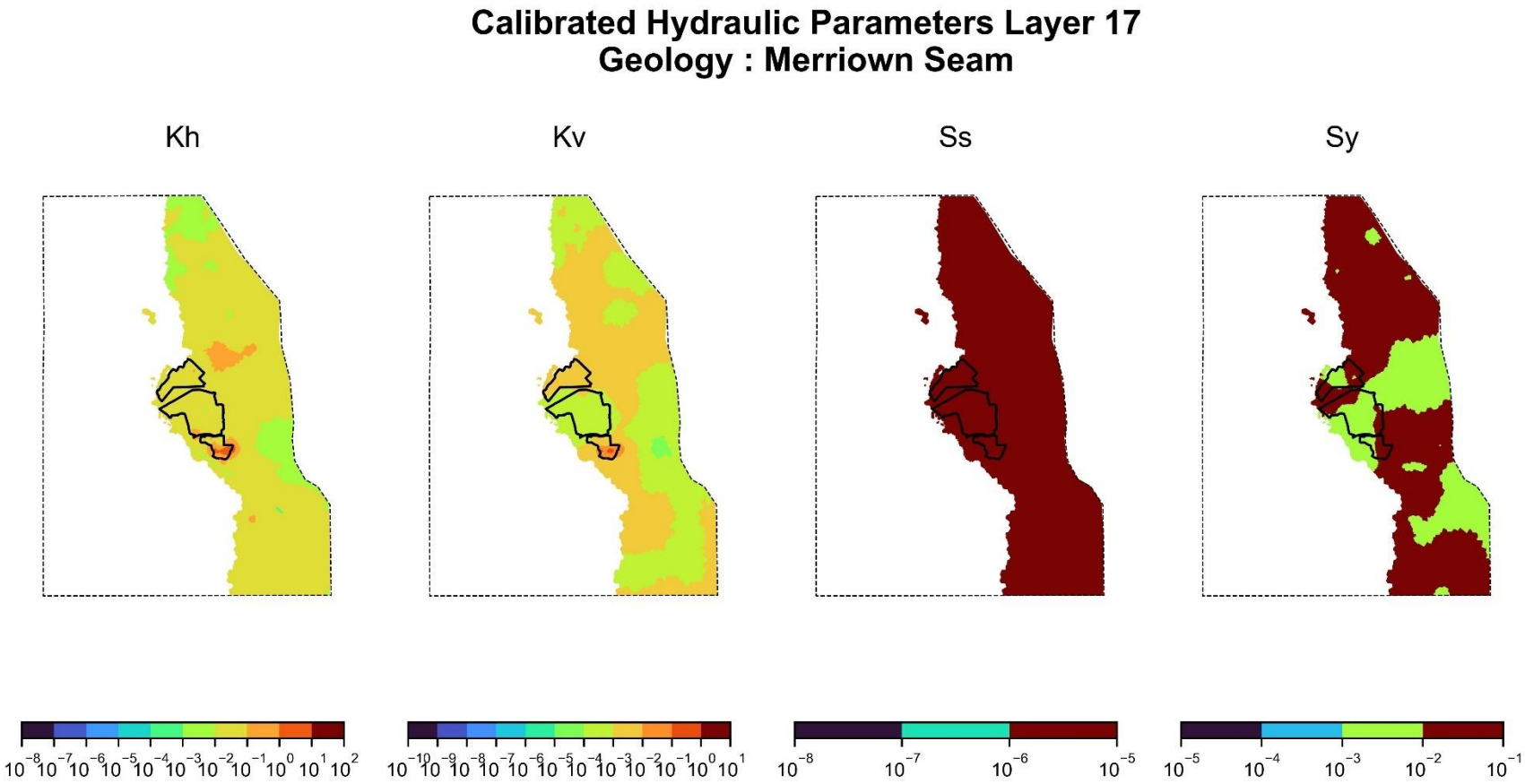

Note: Kh and Kv are in m/day.

Figure F 36 Calibrated hydraulic parameters - layer 17

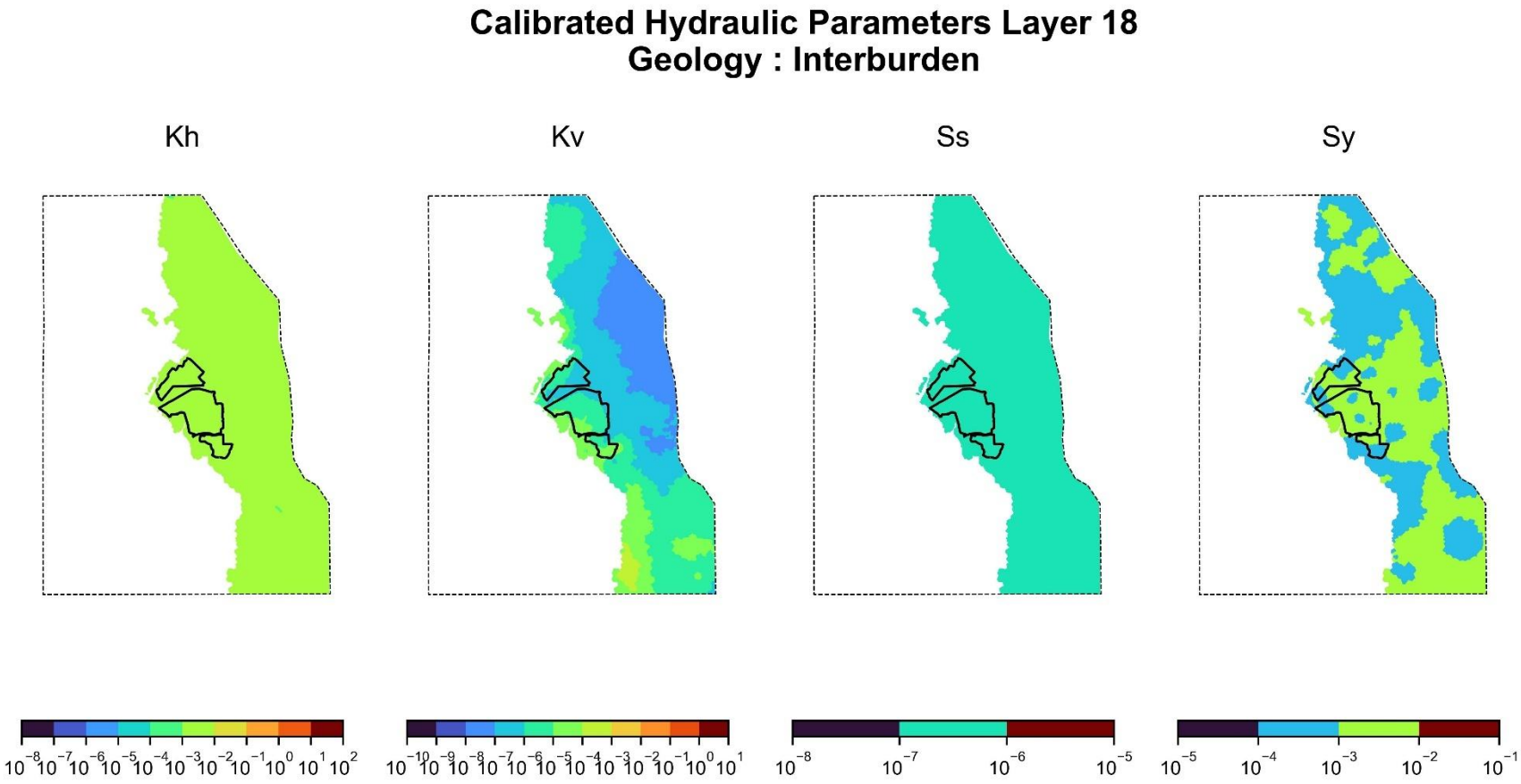

Note: Kh and Kv are in m/day.

Figure F 37 Calibrated hydraulic parameters - layer 18

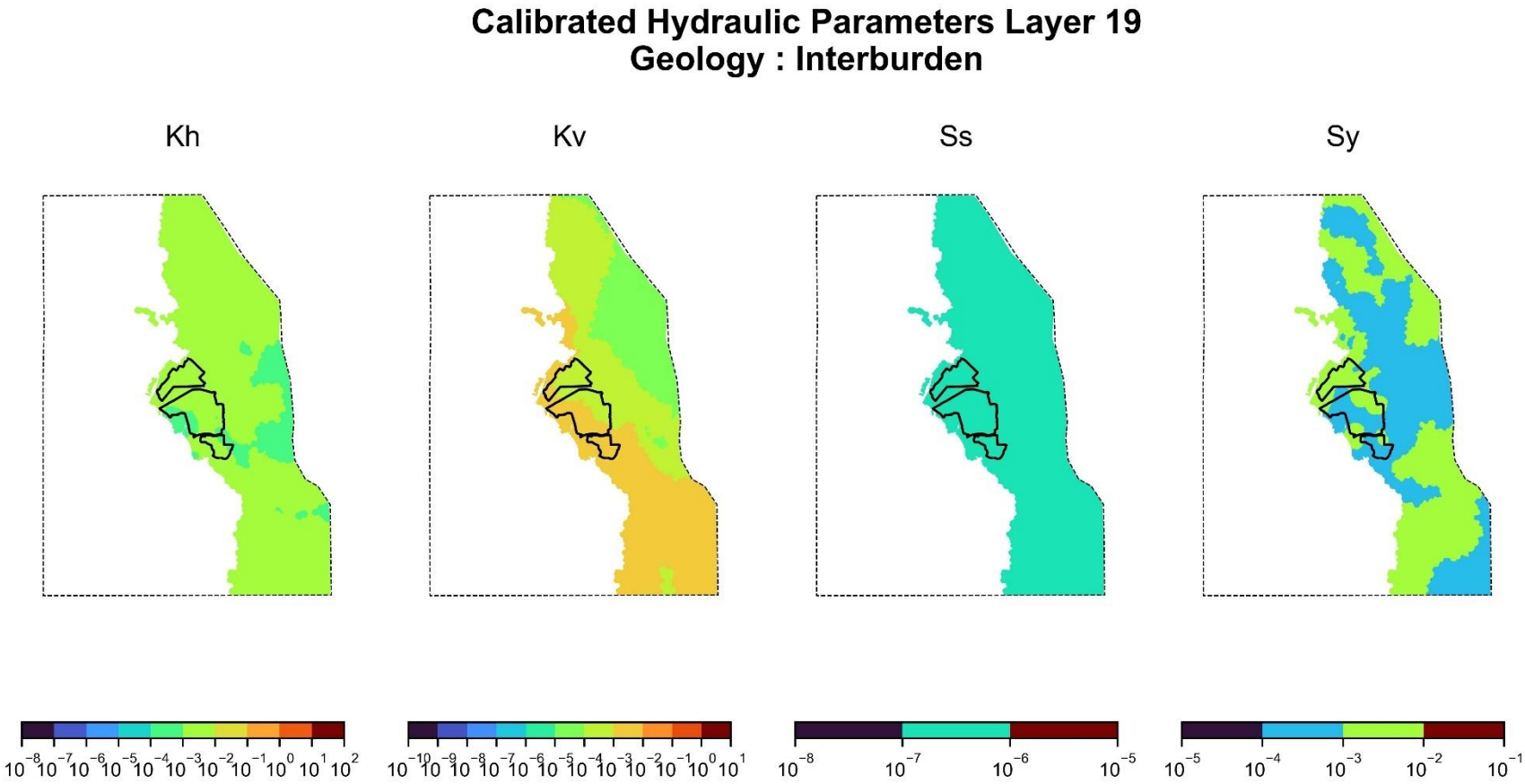

Note: Kh and Kv are in m/day.

Figure F 38 Calibrated hydraulic parameters - layer 19

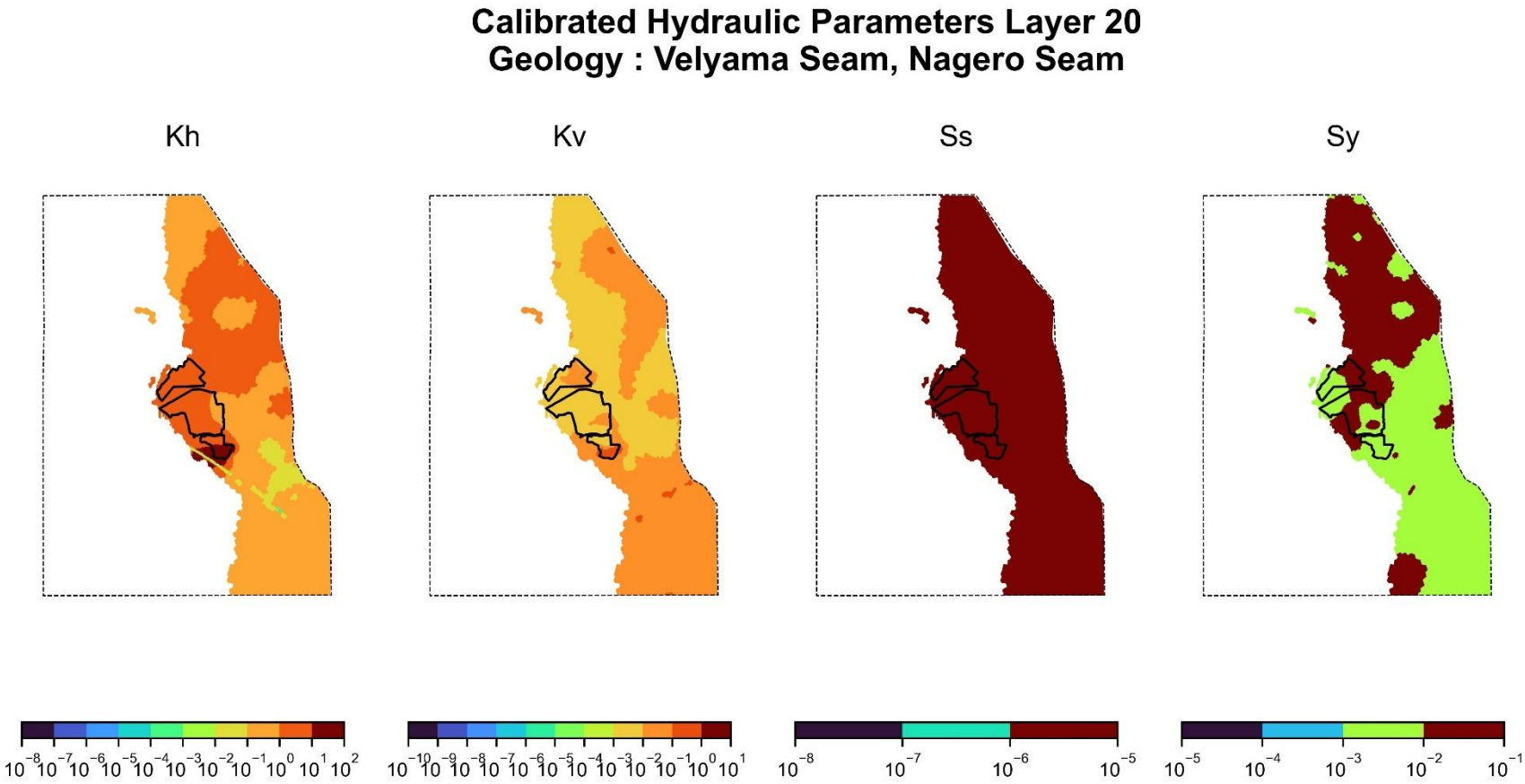

Note: Kh and Kv are in m/day.

Figure F 39 Calibrated hydraulic parameters - layer 20

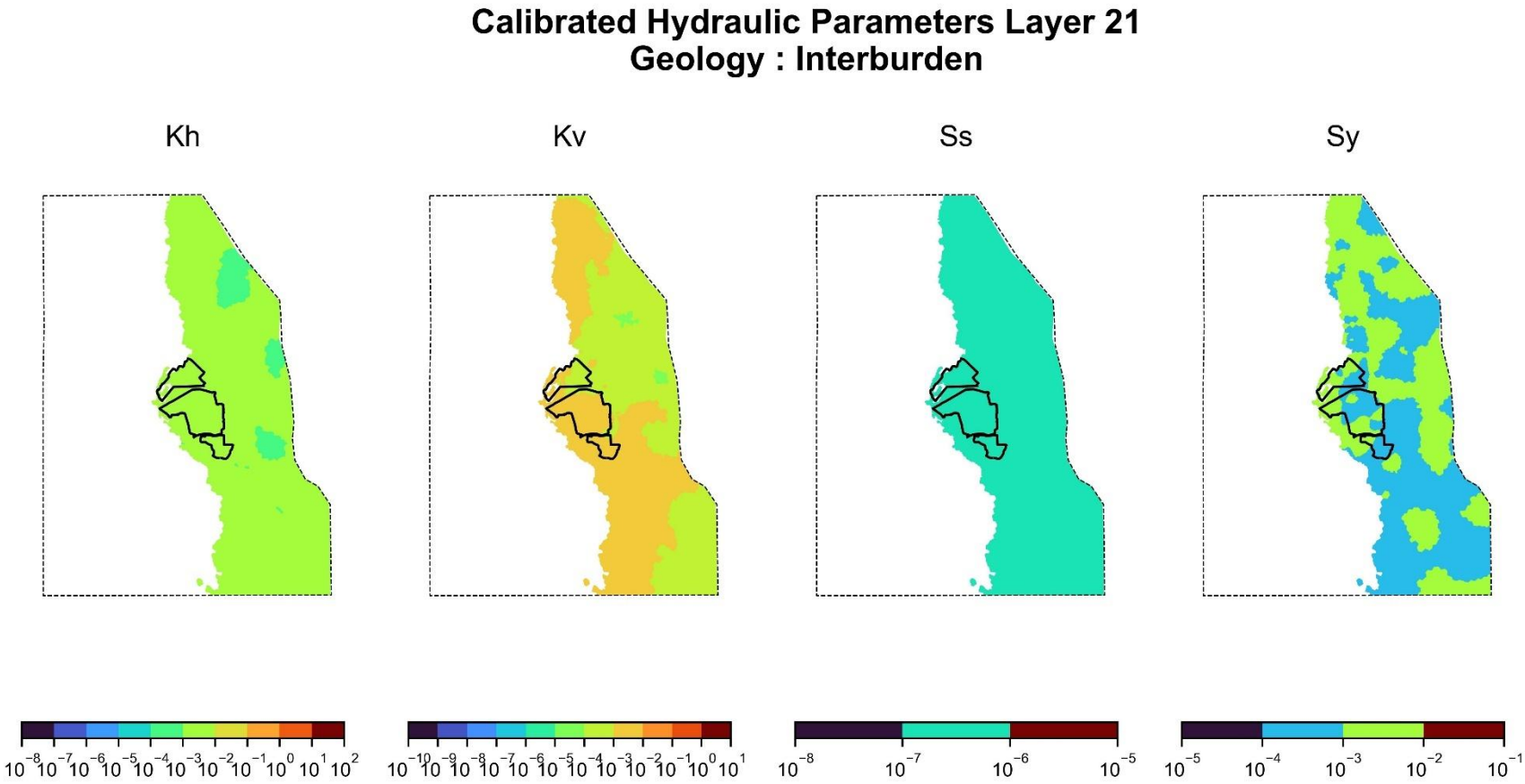

Note: Kh and Kv are in m/day.

Figure F 40 Calibrated hydraulic parameters - layer 21

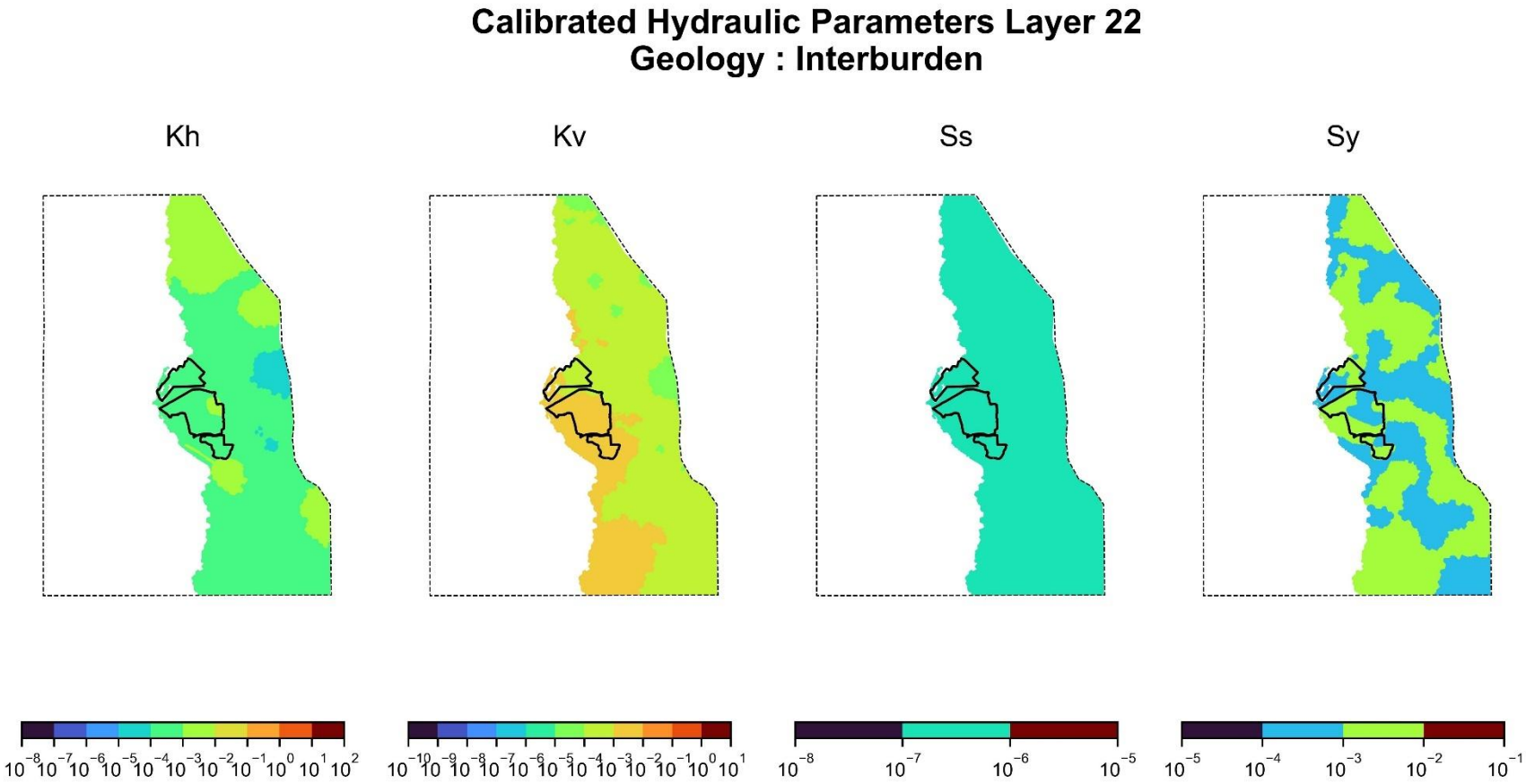

Note: Kh and Kv are in m/day.

Figure F 41 Calibrated hydraulic parameters - layer 22

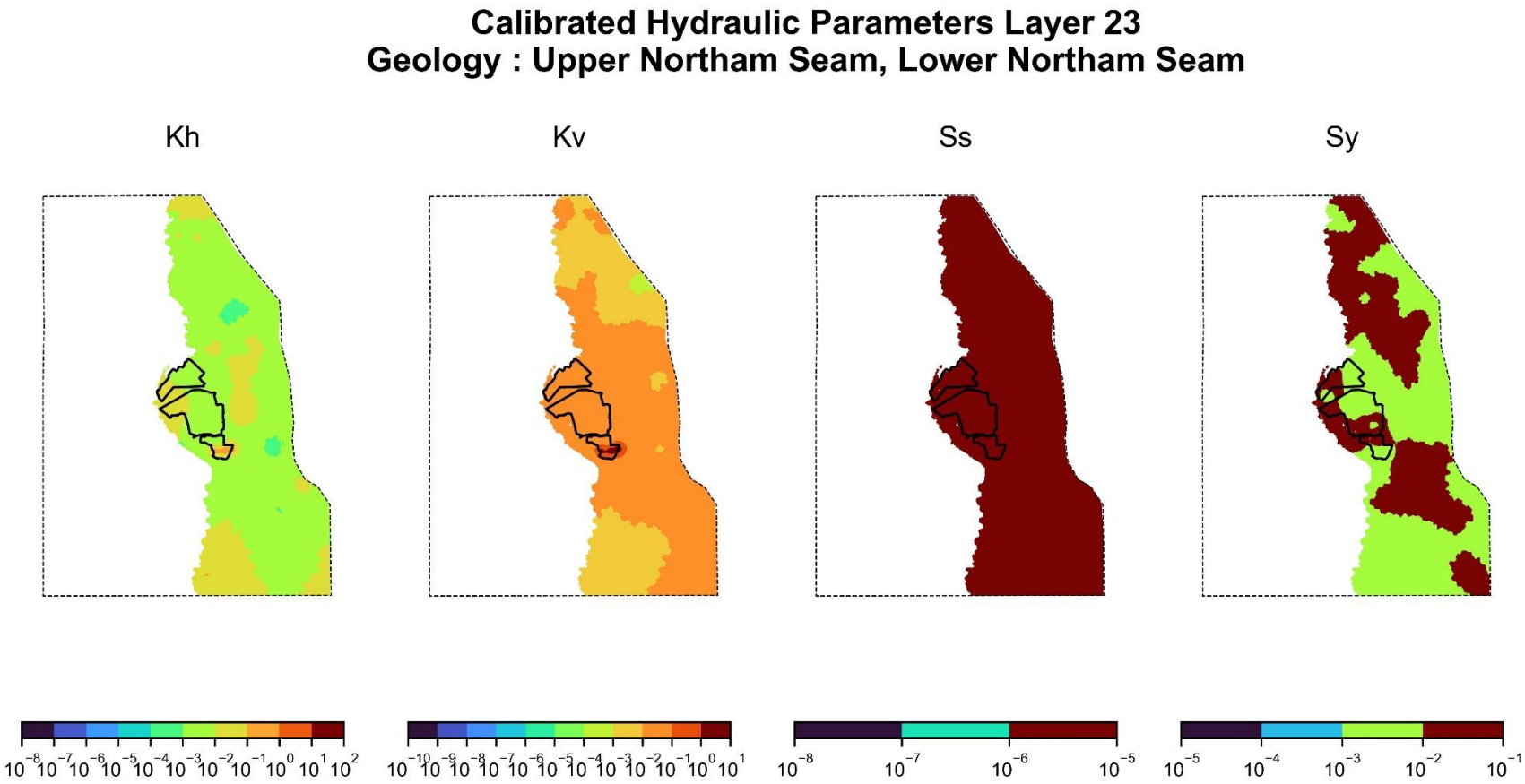

Note: Kh and Kv are in m/day.

Figure F 42 Calibrated hydraulic parameters - layer 23

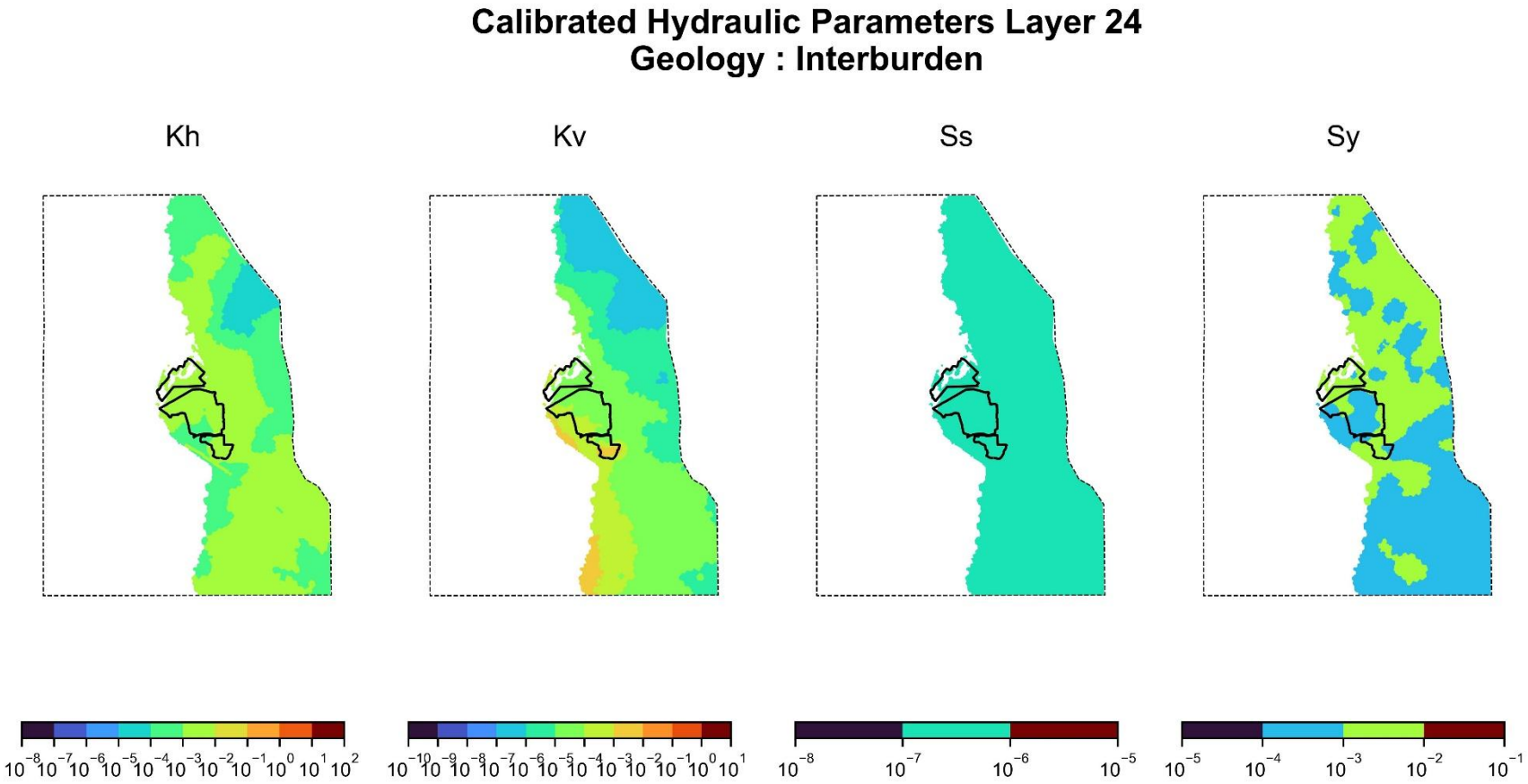

Note: Kh and Kv are in m/day.

Figure F 43 Calibrated hydraulic parameters - layer 24

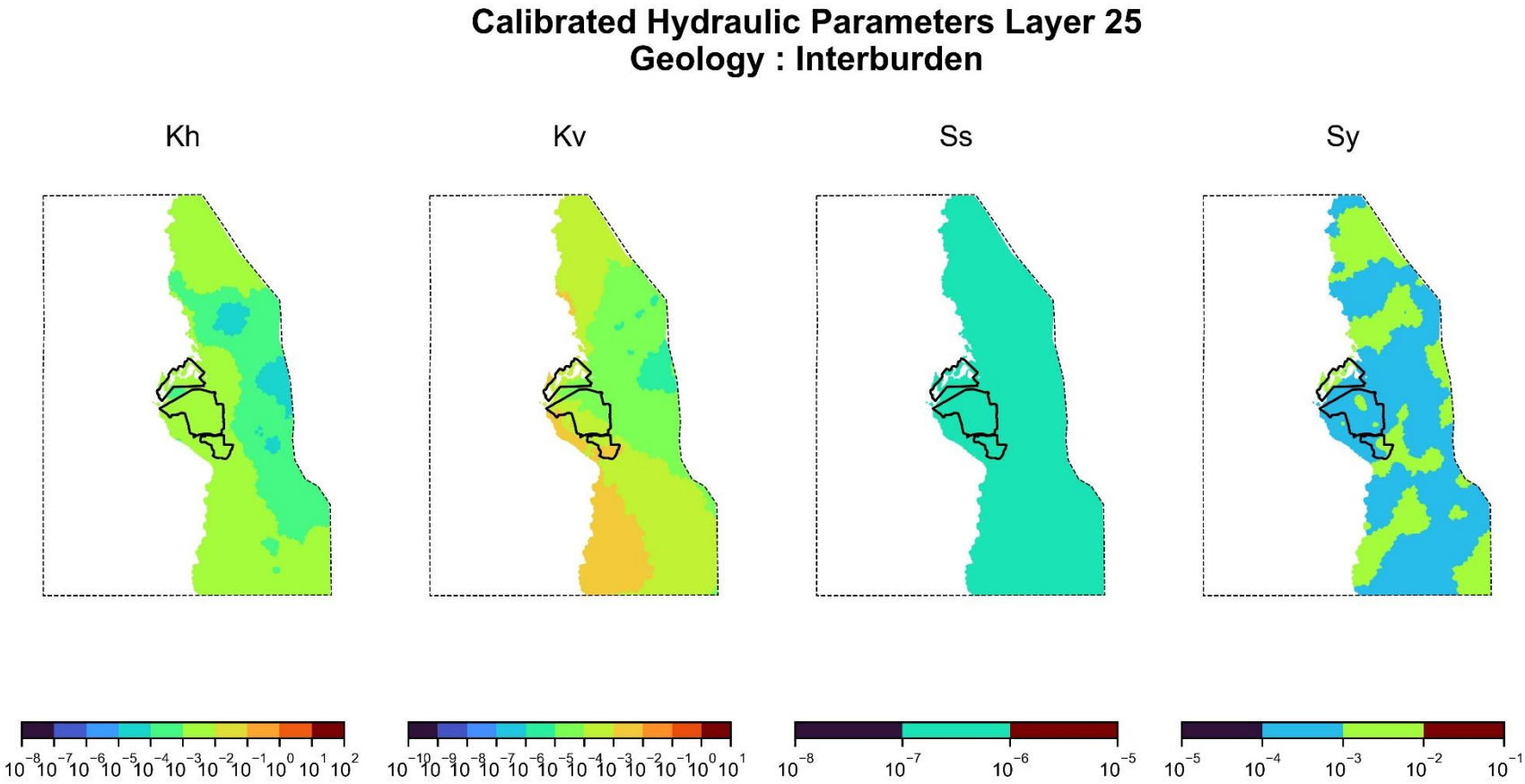

Note: Kh and Kv are in m/day.

Figure F 44 Calibrated hydraulic parameters - layer 25

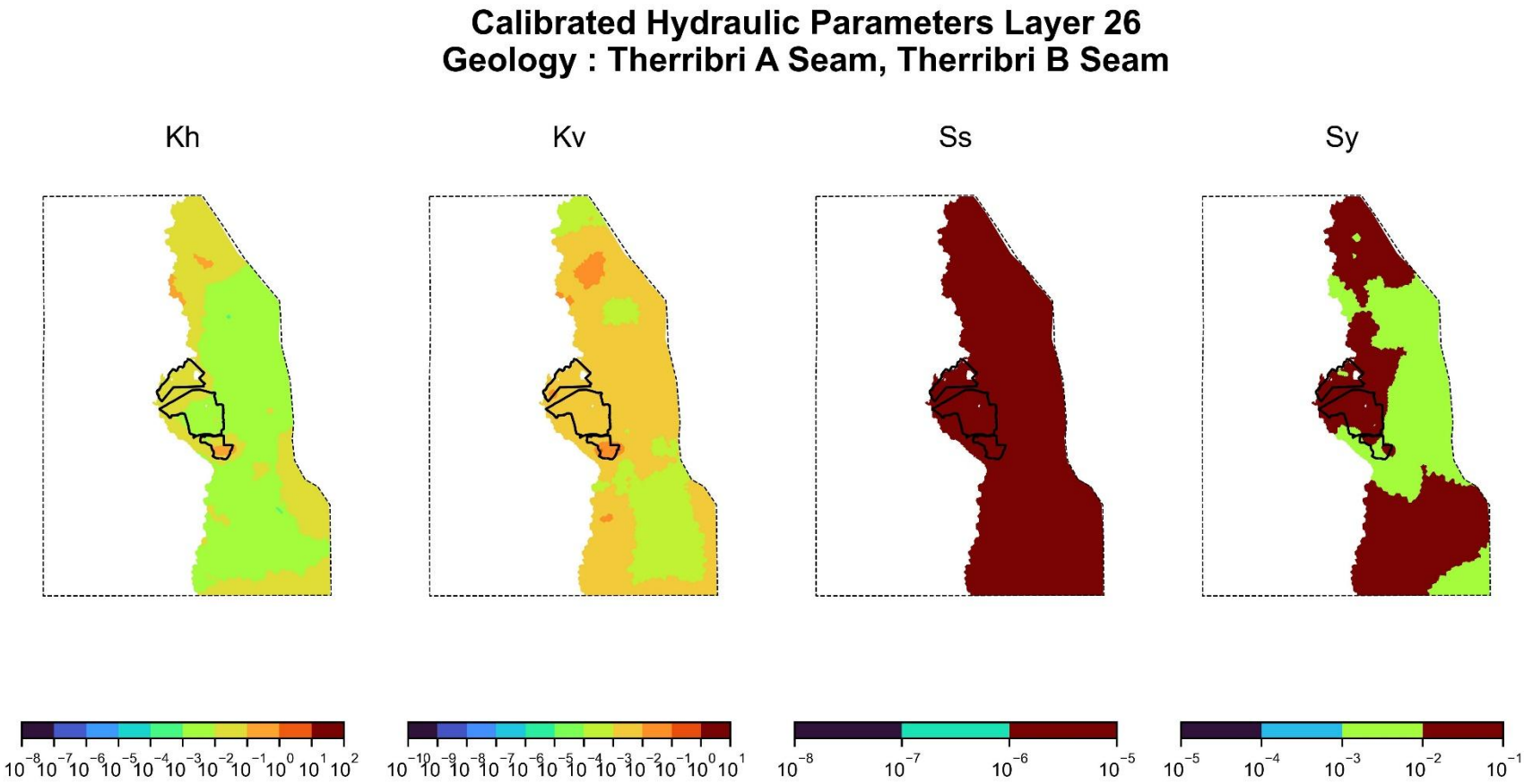

Note: Kh and Kv are in m/day.

Figure F 45 Calibrated hydraulic parameters - layer 26

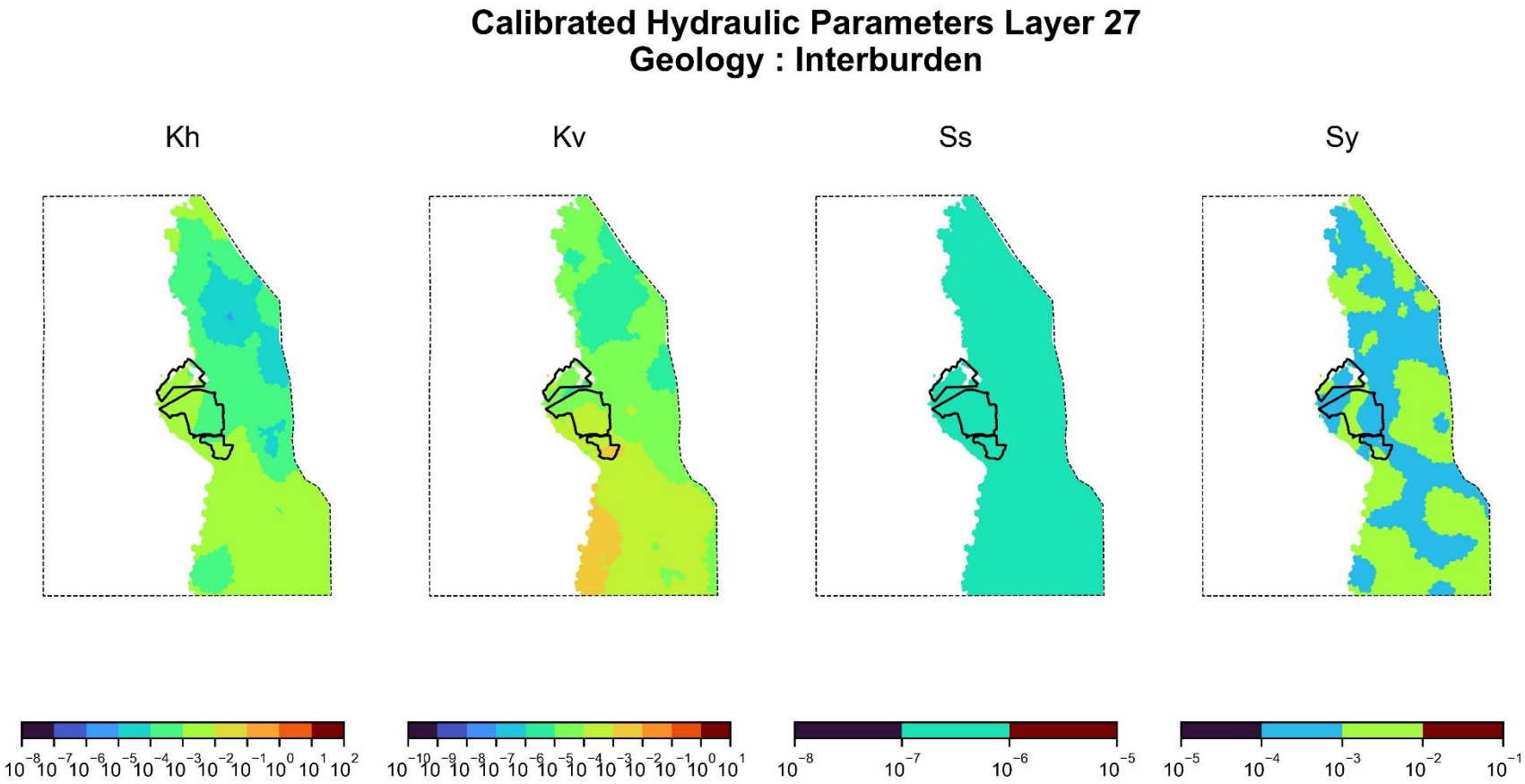

Note: Kh and Kv are in m/day.

Figure F 46 Calibrated hydraulic parameters - layer 27

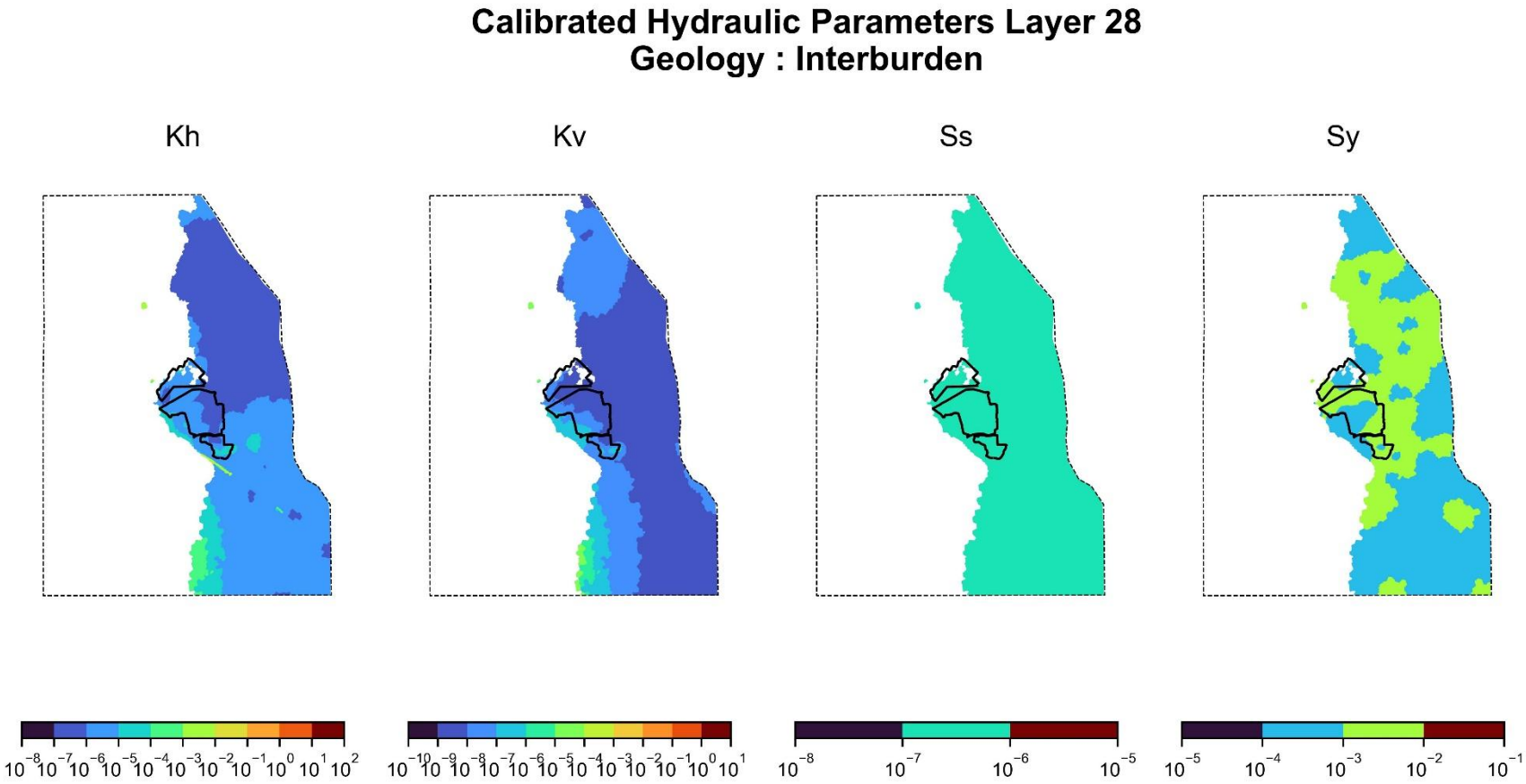

Note: Kh and Kv are in m/day.

Figure F 47 Calibrated hydraulic parameters - layer 28

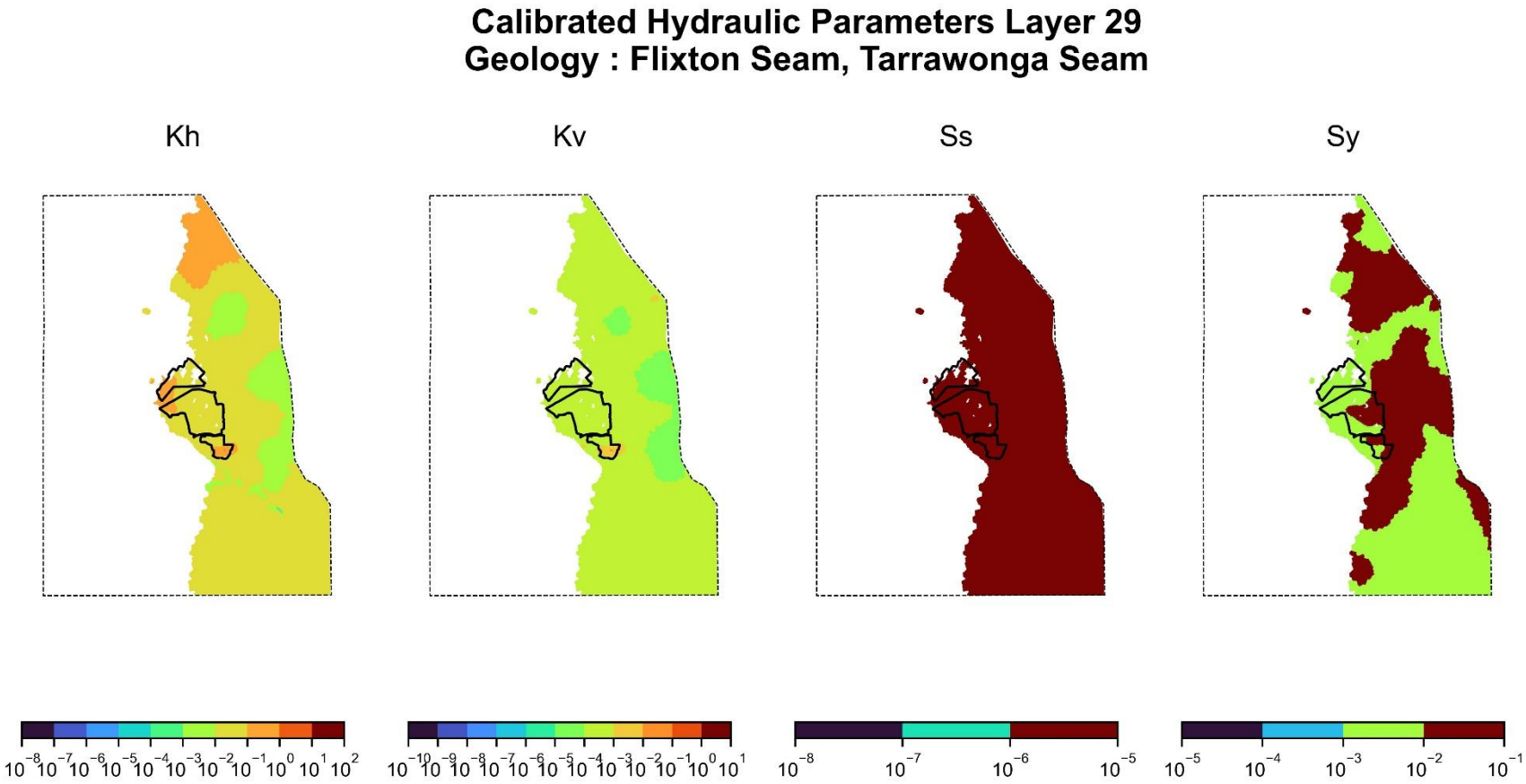

Note: Kh and Kv are in m/day.

Figure F 48 Calibrated hydraulic parameters - layer 29

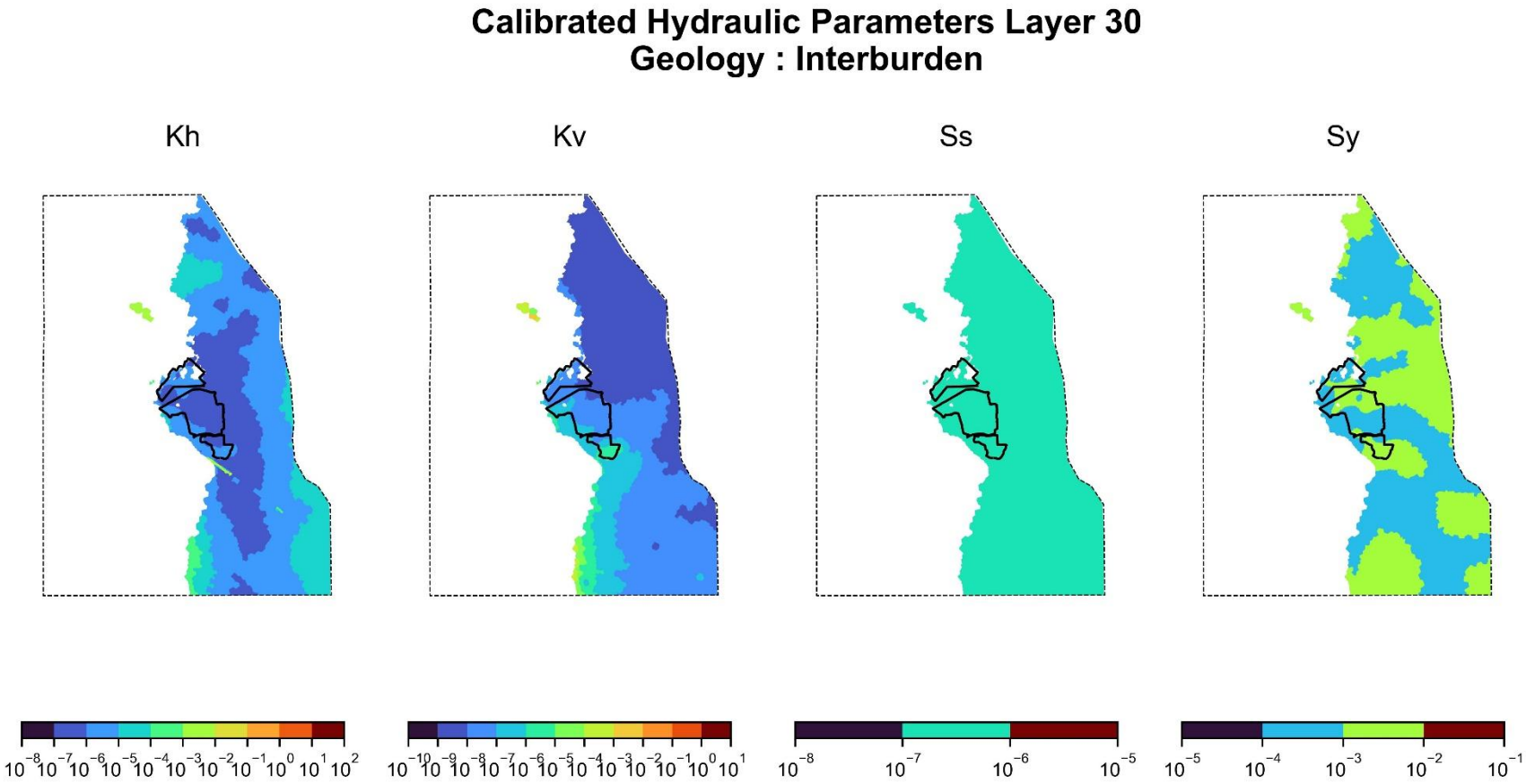

Note: Kh and Kv are in m/day.

Figure F 49 Calibrated hydraulic parameters - layer 30

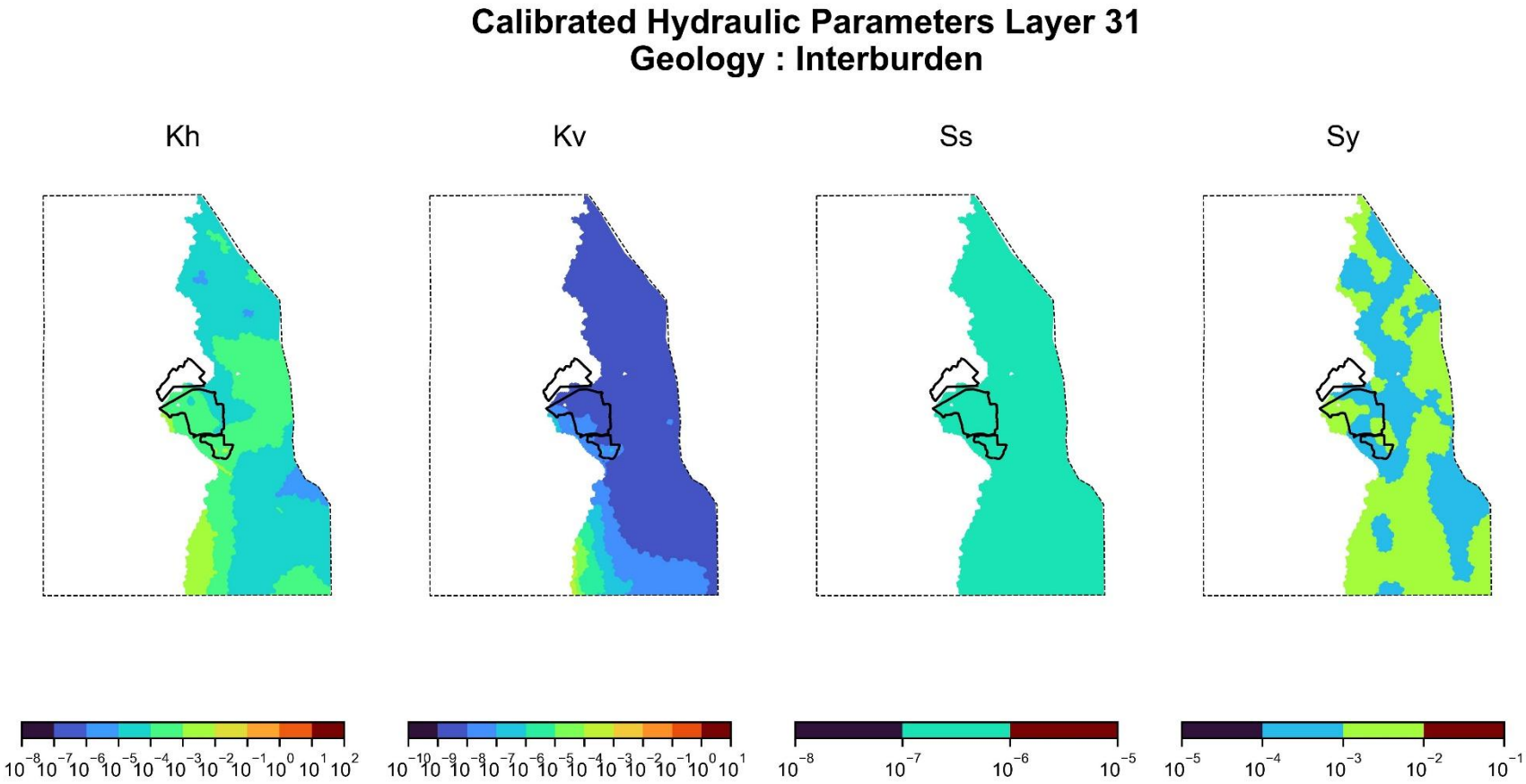

Note: Kh and Kv are in m/day.

Figure F 50 Calibrated hydraulic parameters - layer 31

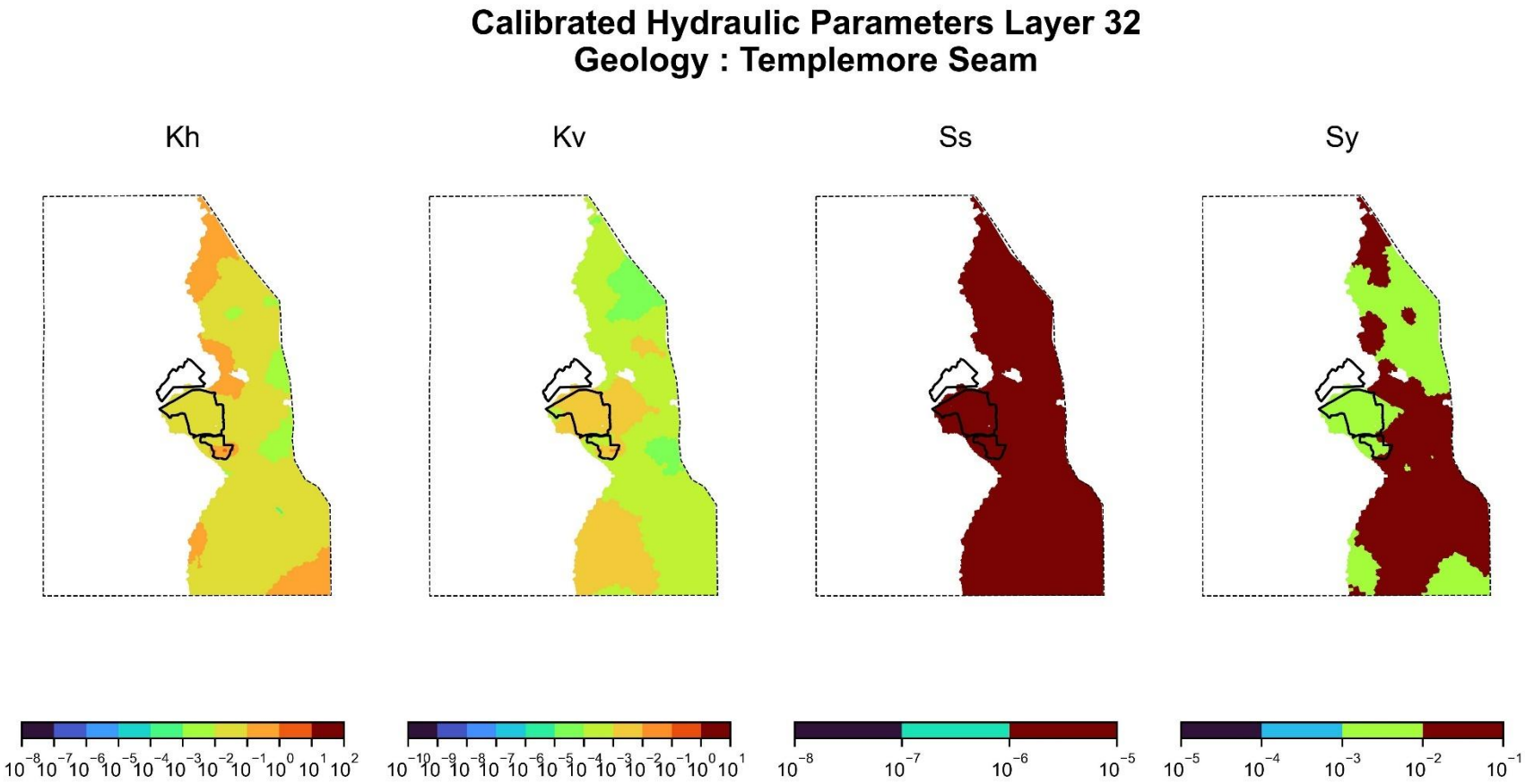

Note: Kh and Kv are in m/day.

Figure F 51 Calibrated hydraulic parameters - layer 32

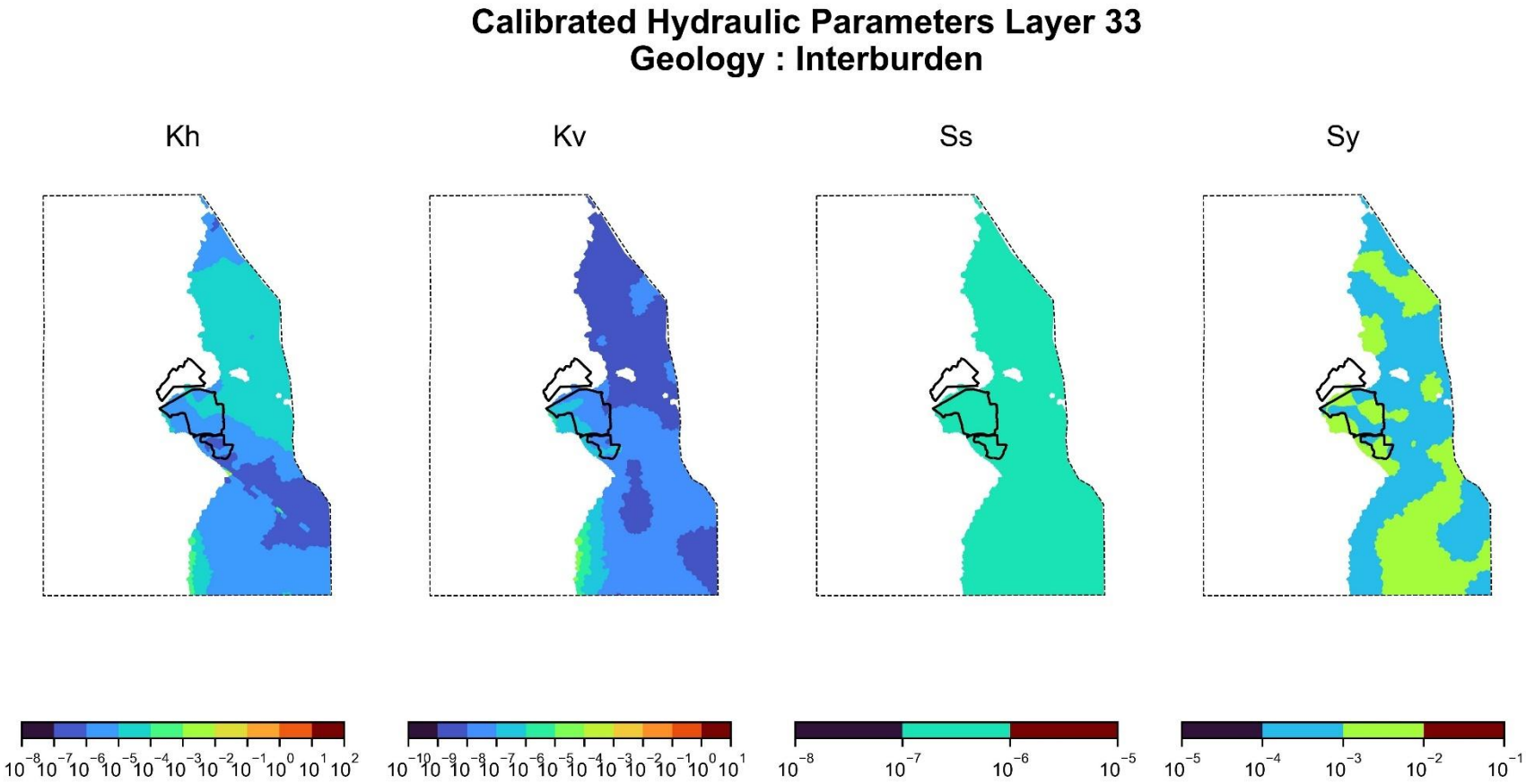

Note: Kh and Kv are in m/day.

Figure F 52 Calibrated hydraulic parameters - layer 33

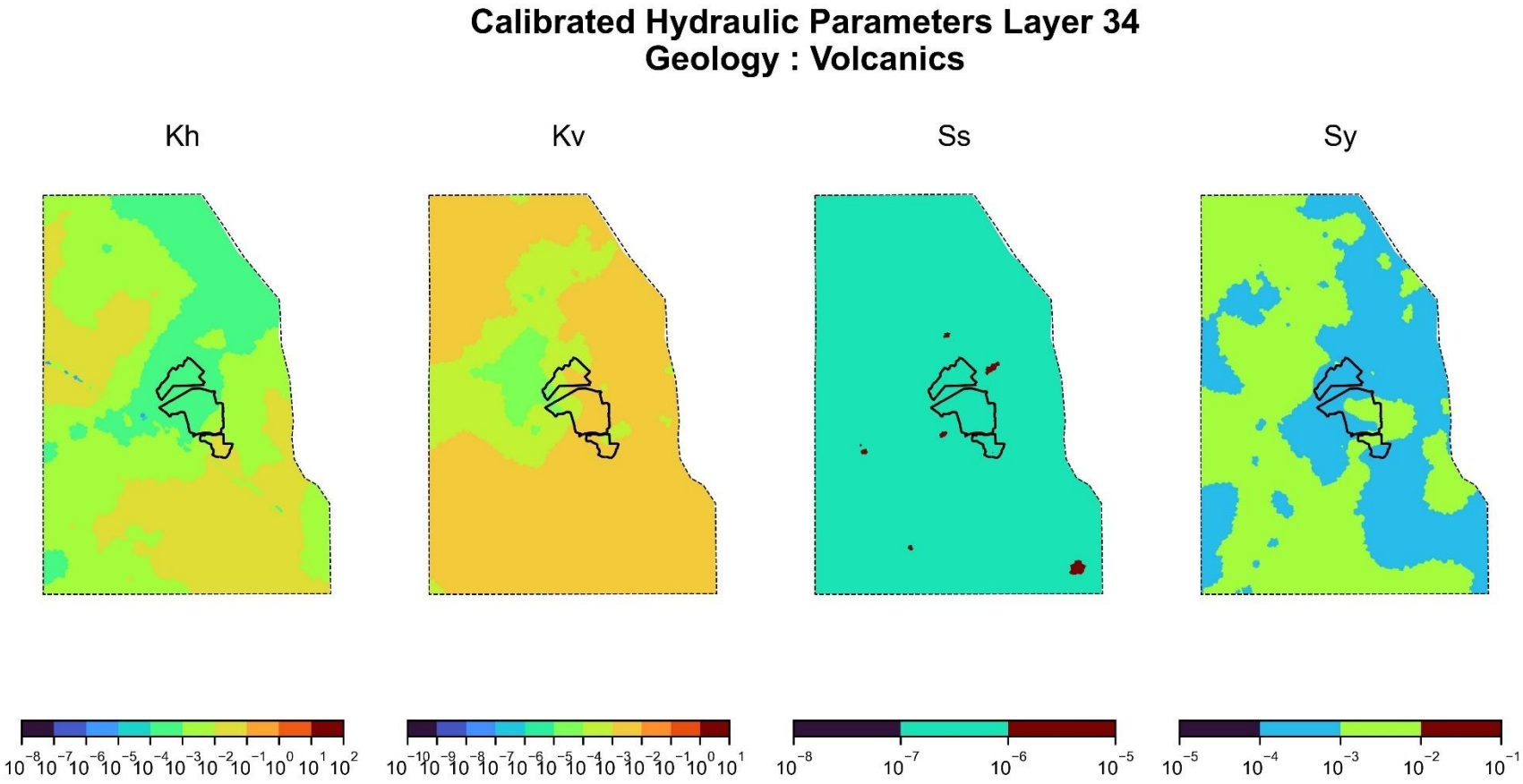

Note: Kh and Kv are in m/day.

Figure F 53 Calibrated hydraulic parameters - layer 34

F7.3.4 Water budget

The mass balance error, which is the difference between the calculated model inflows and outflows at the completion of the steady-state calibration, was 0.0%. The maximum percent discrepancy at any time step in the transient simulation was 0.05%. This value indicates that the model is stable and achieves an accurate numerical solution. This maximum error is within acceptable limits for adequate numerical convergence (<2%: Australian Groundwater Modelling Guidelines [Barnett et. al., 2012]).

Table F 10 shows the water budget for the steady-state (pre-mining) model and the averages from the transient model from 2006 to 2024.

Table F 10 Calibration stage water budget (ML/day)

Parameter	Steady-state model			Transient model average		
	in	out	in - out	In	out	in - out
Storage	0	0	0	29.84	28.14	1.70
Recharge	30.80	0	30.80	35.27	0	35.27
ET	0	6.92	-6.92	0	7.82	-7.82
River	0	2.12	-2.12	0	1.30	-1.30
Stream	13.31	11.91	1.40	8.96	8.34	0.62
General head boundary	83.61	106.78	-23.17	90.42	99.42	-9.00
Wells	0	0	0	0	16.86	-16.86
Drains	0	0	0	0	2.62	-2.62
Total	**127.72**	**127.73**	**-0.01**	**164.49**	**164.5**	**-0.01**

The steady-state water budget indicates that recharge to the groundwater system within the model averages 30.8 ML/day, with approximately 0.72 ML/day being discharged via surface drainage. Regional through flow from the general head boundary contributes 65% of the total input to the groundwater model.

The transient model water budget deviates from steady-state conditions due to mining within the model domain and a generally wetter-than-average period. Mine dewatering, represented by drain cells, indicates regional dewatering intercepts 2.62 ML/day on average, indirectly reducing stream baseflow and increasing inflows from the general head boundaries. Recharge from rainfall and river leakage increases vary within the transient model due to the use of actual climatic data during the transient calibration period from 2006 to 2024.

The calibrated model water budget represents the optimal balance that PEST arrived at, using groundwater levels and inflow as targets. These volume estimates are inherently uncertain as the majority of the budget components are not directly measurable in the field across the model domain and, thus, are not target datasets for the calibration process.

F7.3.5 Mine inflow verification

Figure F 54 shows the simulated groundwater inflow to the drain cells representing the BTM Complex open cut mining areas.

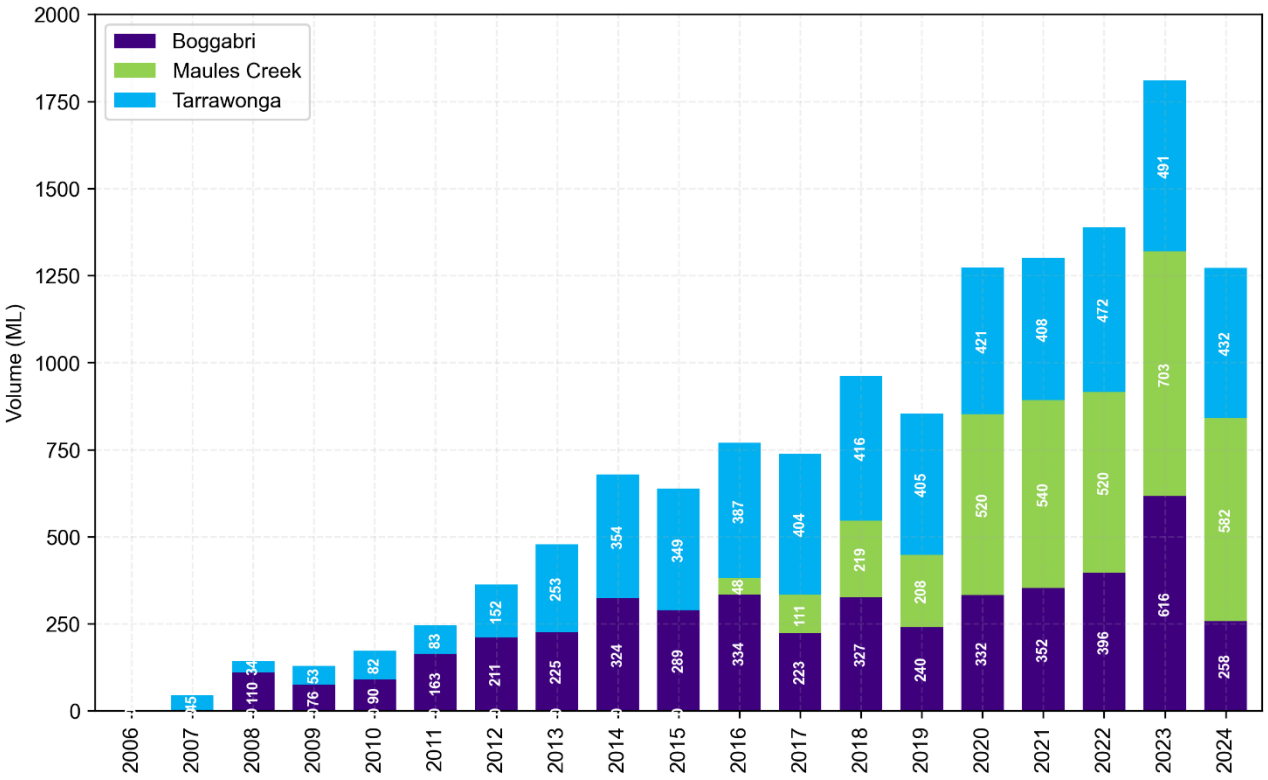

Figure F 54 Simulated inflow to mining areas (2006 to 2024)

Quantifying groundwater inflow to open cut mining areas can be challenging as groundwater seepage within pits mixes with rainfall runoff, and water pumped into mining areas for dust suppression, masking the source of the pumped water. Moreover, measuring seepage expressed directly from the faces within the pit is presently not feasible. A standard method for estimating groundwater inflow to mining areas involves using a water balance model to compare water inputs and outputs in open cut pits. When more water is pumped out than that entering pits by pumping and rainfall, it can indicate groundwater inflows. This method estimates 'pumpable' groundwater seepage to the mining areas but does not account for groundwater that evaporates from the pit face or is bound as moisture with coal and spoil. In contrast, groundwater models estimate the total volume of groundwater removed from the groundwater regime, including groundwater that evaporates from the pit or is bound in spoil and coal materials. Although methods are not directly comparable due to differing underlying assumptions, comparing these estimates is helpful for constraining groundwater modelling predictions.

Estimates of groundwater inflow from water balance models were used to guide the calibration process by means of an inequality constraint for total inflow not exceeding 5.0 GL/yr. Figure F 55 shows the model prediction of groundwater inflow for the MCCM compared with estimates of groundwater inflow from the site water balance model. Figure F 56 and Figure F 57 shows the same predictions for BCM and TCM, respectively. There is a notable discrepancy between the inflows reported in the annual review for Tarrawonga and those from the numerical model, which contrasts with AGE (2022), where the values were more closely aligned. The difference is primarily related to removing the hydraulic barrier, which represents the Conomos Fault, from the Gunnedah alluvium.

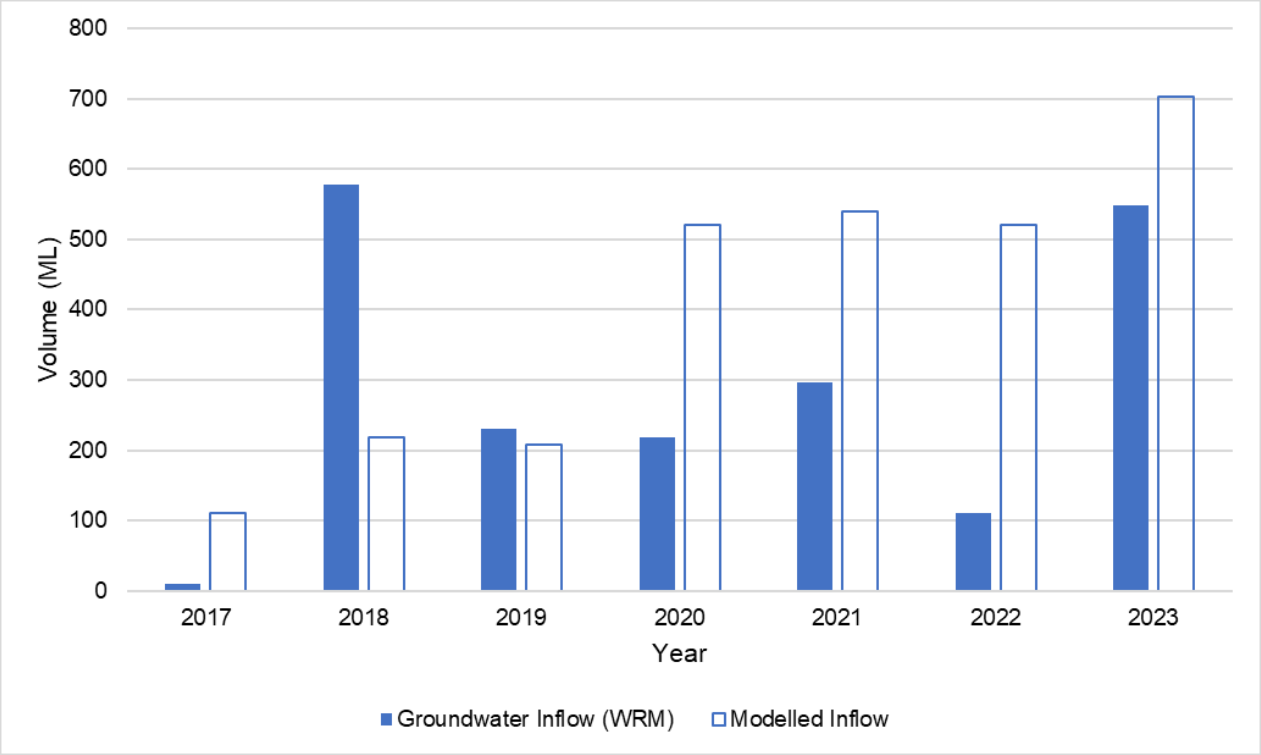

Figure F 55 Simulated inflow to mining areas - MCCM

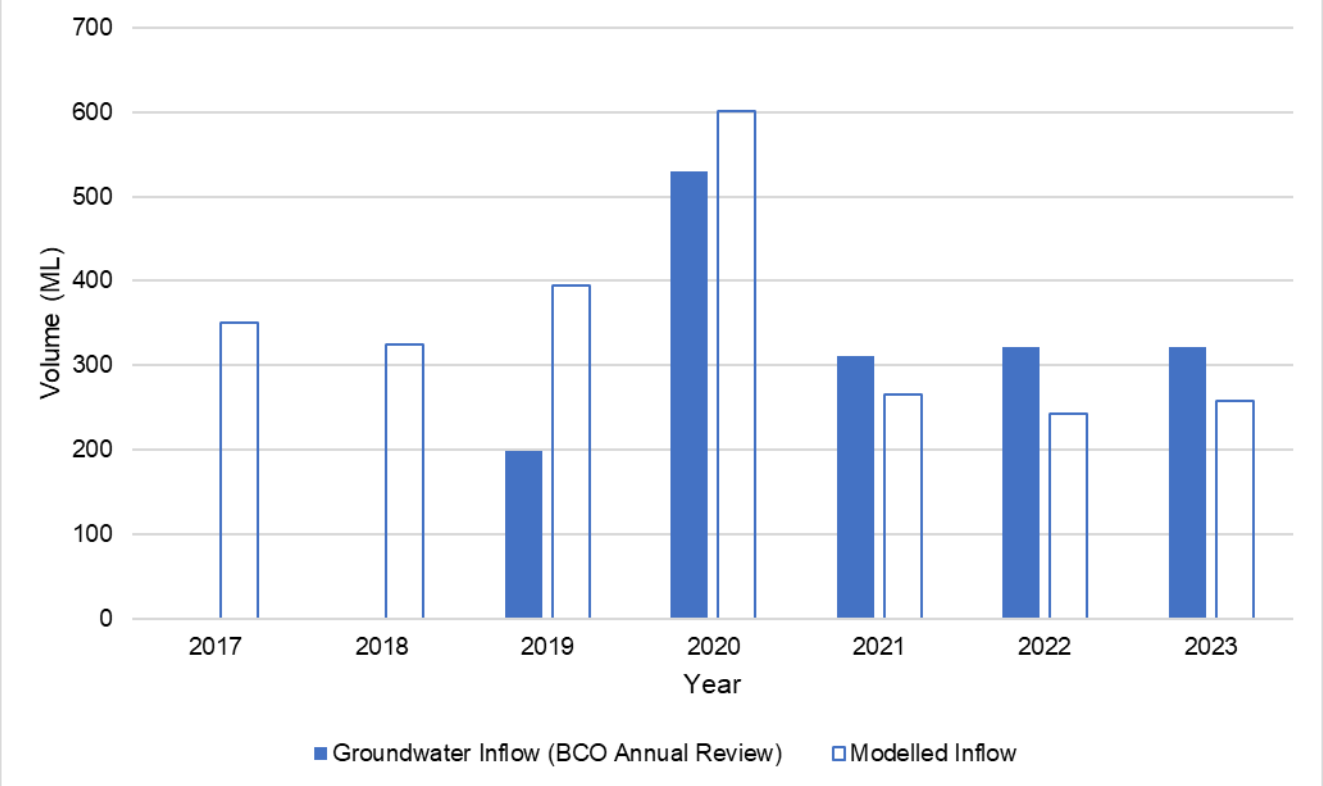

Note: groundwater inflow from the annual review was not available for reporting periods 2017 and 2018.

Figure F 56 Simulated inflow to mining areas - Boggabri Coal Mine

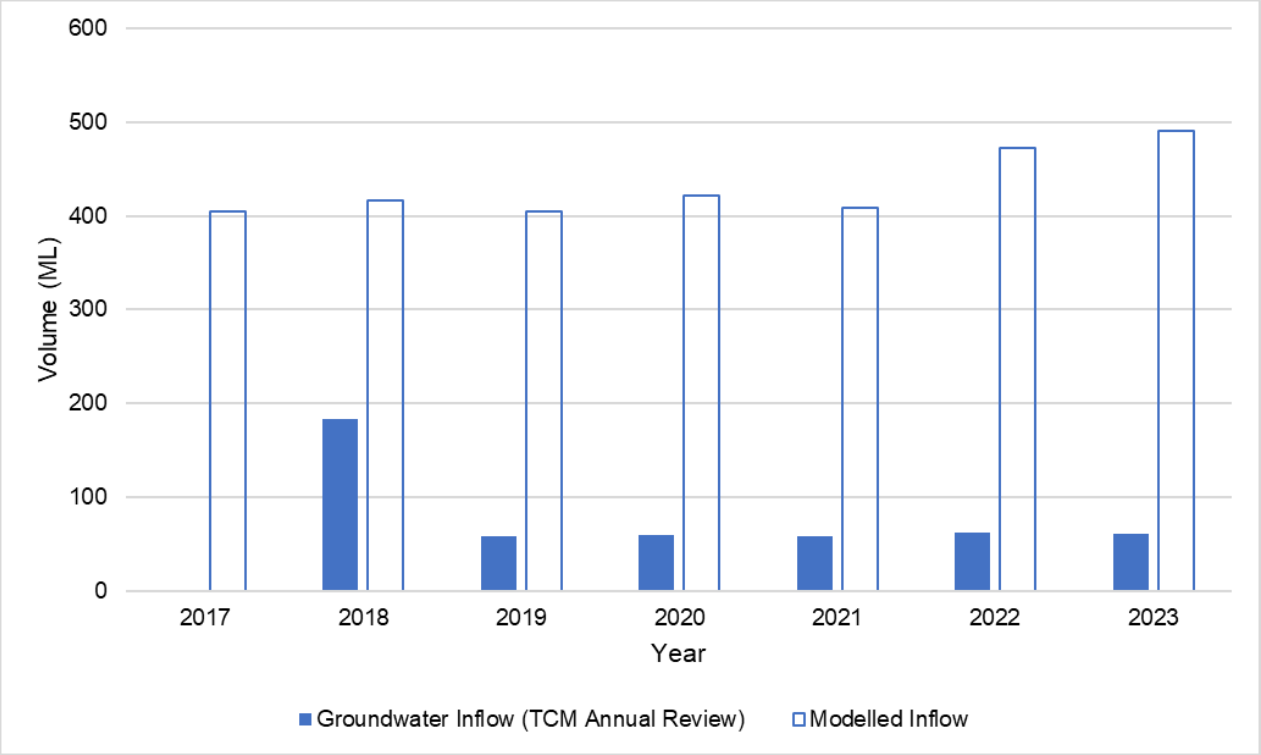

Figure F 57 Simulated inflow to mining areas – Tarrawonga Coal Mine

F8 Predictions

The calibrated model was used to undertake future predictions to assess the following:

- cumulative impact of approved mining at the BTM Complex as required by the conditions of consent for the BTM mines;
- cumulative impact of proposed mining at MCCM and BCM; and
- individual impact of proposed mining at MCCM and BCM.

This appendix describes the cumulative impacts of the approved and proposed mining at the BTM Complex. The main report describes the predicted impacts of the proposed mining during the operations and closure phases.

F8.1 Model scenarios and setup

Fifteen scenarios were developed to assess the cumulative impacts of the BTM Complex and the individual impacts of the approved and proposed mining projects at each mine. Table F 11 summarises the mining represented in all the scenarios used to determine the cumulative and individual impacts.

The cumulative impacts were assessed by determining the differences in groundwater levels and fluxes between a model scenario representing all mining within the BTM Complex and a 'null scenario' that excluded mining. For example, the difference in groundwater level between Scenario 1 and Scenario 2 was used to assess the cumulative drawdown generated by all approved mining. The differences between Scenario 6 and Scenario 1 provided an assessment of the cumulative impact of proposed future mining projects at MCCM and BCM.

The contribution of individual mining operations within the complex to the cumulative impact was determined by calculating the difference between a scenario that included all approved and proposed mining in the BTM Complex and a second scenario that excluded mining at the subject mine.

Table F 11 Mining activities represented in predictive scenarios

Scenario	MCCM approved	MCCM Continuation Project	BCM approved	BCM MOD10	TCM	Description
1						Null
2	X		X		X	All cumulative approved
3			X		X	All cumulative approved - ex MCCM
4	X				X	All cumulative approved - ex BCM
5	X		X			All cumulative approved - ex TCM
6		X		X	X	all cumulative proposed
7				X	X	all cumulative proposed - ex MCCM
8		X			X	all cumulative proposed - ex BCM
9		X		X		all cumulative proposed - ex TCM
10		X				proposed MCCM only
11				X		proposed BCM only
12					X	approved TCM only
13	X					approved MCCM only
14			X			approved BCM only
15	X			X	X	Cumulative approved (MCCM, TCM) and proposed BCM

The model scenarios were created by extending the model time to the end of approved or proposed mining and then for 200 years after mine closure to assess the recovery equilibrium of the groundwater regime.

The predictive models were set up with quarterly stress periods of 91.3 days, representing the period from January 2025 to December 2044. December 2044 marked the end-of-operations period when the last BTM mines were proposed to cease operation. An additional 200 years were added to each model simulation from 2045, with the model simulating recovery until 2245. This was considered reasonable, given the ever-increasing epistemic uncertainty in system drivers, as well as unquantifiable aleatoric uncertainty further into the future.

Each mine within the BTM Complex provided future mining schedules, which were processed to align with the quarterly stress periods. As required in each scenario, the drain cells were set to the base of the lowest coal seam approved or proposed for mining.

The previously planned low permeability barrier, adjacent to the Tarrawonga Mine, featured in the original model design, was removed for the current model update. The barrier was installed through model layers 1 and 2 (alluvium) and assigned a hydraulic conductivity of $1x10^{-10}$ m/day. Moreover, the simulation of the Conomos Fault as a hydraulic flow barrier (HFB) in AGE (2022) affected the Gunnedah alluvium in layer 2, thereby reducing the potential for inflows. This was corrected so that the representation of the fault affected only the Permian and volcanic layers. Both changes contributed to increased mine inflows and indirect take estimates from the alluvial zones south of TCM.

F8.2 Operations stage setup

Operations at the BTM Complex are limited to open cut methods and do not involve underground mining. As discussed in Section F6.3.5, the model represents open cut mining activities using the MODFLOW drain (DRN) package. The progression of future mining from 2025 to 2045 was updated to reflect the schedules provided by the BTM Complex mines. Drain cells were applied to all intersected model cells, with reference elevations set to the floor of each cell, down to the coal seam targeted for extraction by mining. The original model design (model update 2022) did not allow for the effects of spoil emplacement while mining progressed. Instead, pit shells were represented as fully drained for the entire mining period of all mines. That is, all mines in the BTM Complex transitioned to closure simultaneously. The model update predictions account for spoil emplacement within the open cut pits and the different closure timings for each operation. Figure F 58 and Figure F 59 show the progression of drain cells within the model representing the future approved and proposed mining.

Time-variant model packages unrelated to mining were extended from the end of calibration to the end of the simulation using mean values (RCH, STR, WEL). The other head-dependent boundary packages (RIV and GHB) were extended using the same values obtained during calibration. Drains used to simulate mining were deactivated according to mine and closure plans. Where drains were deactivated, either spoil or void properties were assigned. Voids evolving to pit lakes are included in closure plans for TCM and MCCM. The time-variant materials (TVM) package in MFUSG was used to convert the host aquifer properties to approximate void behaviour (Kh and Kv = 1000 m/d, Sy = 0.99) or nominal spoil properties (Kh and Kv = 0.3 m/d, Sy = 0.3). Areas designated as spoil also included enhanced recharge at 2% of mean annual rainfall. The evapotranspiration surface was also modified to reflect the final landforms at each mine, with extinction depths set to 2 m. It is noteworthy that in the previous version of the BTM-complex model, all mines were simulated to be open until the last mine in the complex reached closure. The current model has mines transitioning to closure in accordance with their individual mine plans.

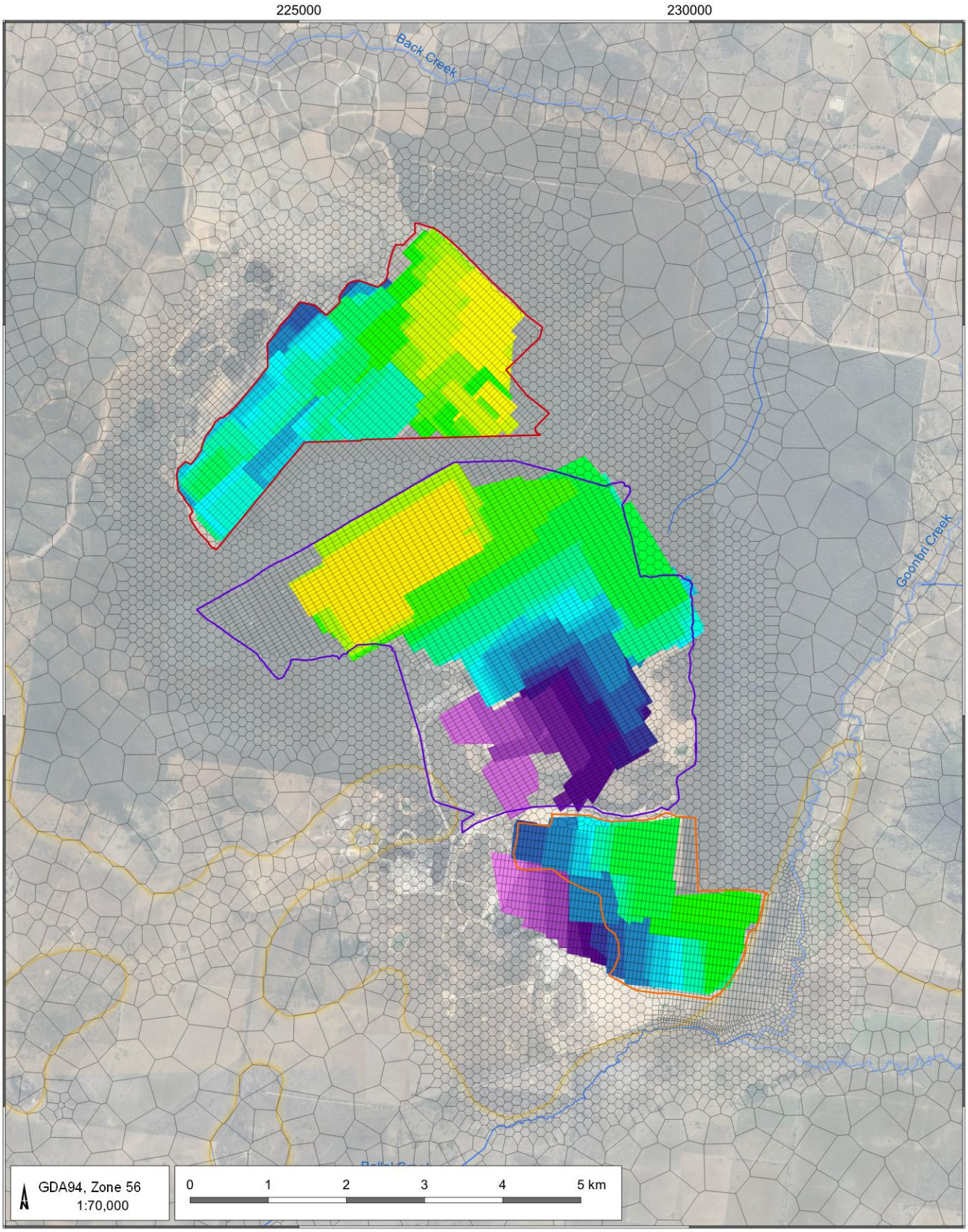

LEGEND

- Drainage
- MCCM Open Cut Extent
- BCM Open Cut Extent
- TCM Open Cut Extent
- Model grid
- Alluvial boundary zones

Mine progression (Year)

2007	2017	2027
2008	2018	2028
2009	2019	2029
2010	2020	2030
2011	2021	2031
2012	2022	2032
2013	2023	2033
2014	2024	2034
2015	2025	
2016	2026	

BTM Complex Groundwater Model Update 2024

Annual mining progression for predictions - approved mining (scenario 2)

AGE

DATE 25/03/2025

FIGURE No: **F 58**

©2025 Australasian Groundwater and Environmental Consultants Pty Ltd (AGE) - www.ageconsultants.com.au
Source: LiDAR DEM © Department Finance, Services and Innovation, 2016; GEODATA TOPO 250K Series 3 - © Commonwealth of Australia (Geoscience Australia) 2006.;
G:\Projects\MCJ5003.001 Maules Creek Continuation Project EIS\3_GIS\Workspaces\003_Stage 3 -EIS Report\Appendix F\F_58_MCJ5003_Annual mining progression for predictions - approved mining (scenario 2).qgz

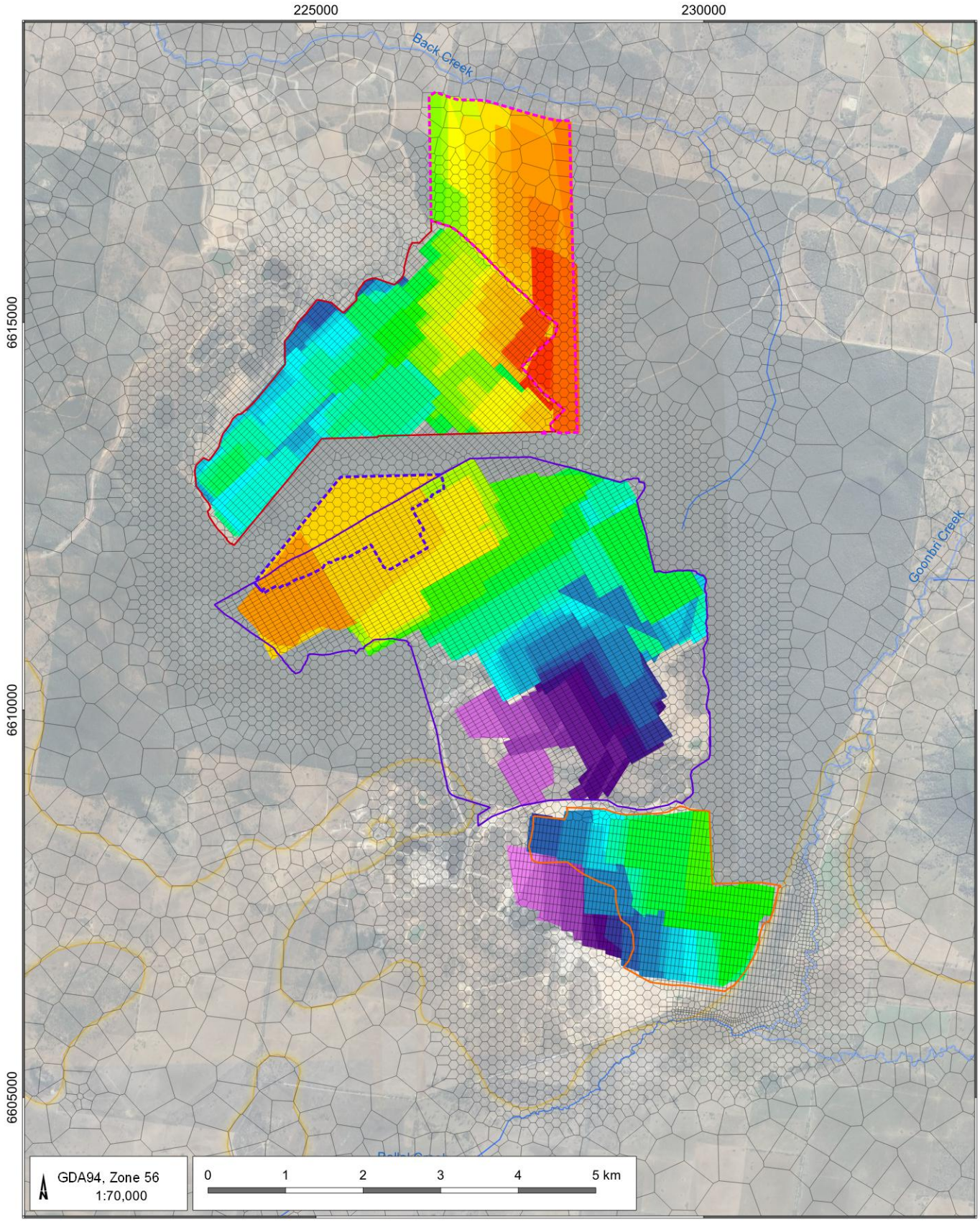

LEGEND

- Drainage
- MCCM Open Cut Extent
- MCCM Continuation Project
- BCM Open Cut Extent
- BCM Modification Mining Area
- TCM Open Cut Extent
- Model grid
- Alluvial boundary zones

Mine progression (Year)

2007	2017	2027	2037
2008	2018	2028	2038
2009	2019	2029	2039
2010	2020	2030	2040
2011	2021	2031	2041
2012	2022	2032	2042
2013	2023	2033	2043
2014	2024	2034	2044
2015	2025	2035	
2016	2026	2036	

BTM Complex Groundwater Model Update 2024

Annual mining progression for predictions – proposed mining (MCCM Continuation Project and BCO MOD 10 - scenario 6)

AGE

DATE 13/02/2025

FIGURE No: **F 59**

©2025 Australasian Groundwater and Environmental Consultants Pty Ltd (AGE) - www.ageconsultants.com.au
Source: LiDAR DEM © Department Finance, Services and Innovation, 2016; GEODATA TOPO 250K Series 3 - © Commonwealth of Australia (Geoscience Australia) 2006.;
G:\Projects\MCJ5003.001 Maules Creek Continuation Project EIS\3_GIS\Workspaces\003_Stage 3 -EIS Report\Appendix F\F_59_MCJ5003_Annual mining progression for predictions – proposed mining (MCCM Continuation Project and BCO MOD 10 - scenario 6).qgz

F8.3 Post closure setup

Each of the BTM mines will be gradually backfilled with mine spoil over the course of mining. Following closure, residual voids will remain at the final operating face at each of the mines except BCM. BCM will be fully backfilled with a landform surface designed to remain largely above the water table. Residual voids will remain at MCCM and TCM. Figure F 60 shows the approved and proposed final voids at the BTM Complex mines.

Following the cessation of mining, a lake will form within each residual void. The rate of water level rise within the lake and the equilibrium water level will be determined by the inputs to the lake, which are comprised of rainfall on the lake surface, rainfall runoff from the surrounding catchment, groundwater inflow through spoils and undisturbed geological units, and loss of water from the lake surface via evaporation.

The groundwater flow model does not represent rainfall runoff and does not have cell and layer refinement to represent each final void's morphology in detail. Therefore, predictions from a separate water balance model provided by each mine's surface water consultants were used to provide inputs to the groundwater model. The process to determine the final void water level recovery was as follows:

- Model cells in the area designated as the void spill were configured to have fixed head boundaries. The model then executed successive steady-state simulations with fixed head boundaries stepping down to the base of the proposed void in 10.0 m increments for each simulation. Inflows were recorded and provided to a surface water modelling team as input for a pit lake water balance model.
- The resulting pit lake stage time series was then incorporated into the groundwater model prediction simulations, with updated inflows recorded and provided to the surface water modelling team.
- This process was repeated until convergence was achieved between the model-simulated inflows and the surface water pit lake stage time series.

It should be noted that the pit lake water balance model and the groundwater flow models simulate the recovery of water levels and the long-term equilibrium within the residual voids of the BTM Complex. While there is some sharing of predictions between the models, it should not be expected that the outcome is an absolute for future pit lake stage prediction. This is because the models use differing methodologies, and both have their strengths, weaknesses and applications. In this case, the models provide semi-independent converging (to a similar value) estimates of water levels within the residual voids and provide information that can be used to assess long-term risks to the surface water and groundwater regimes. Both models rely on numerous assumptions, and their respective uncertainties are compounded as a result. Four iterations were required between the groundwater and surface water models to ensure that inflows were approximately aligned.

Scenario 2 (approved)

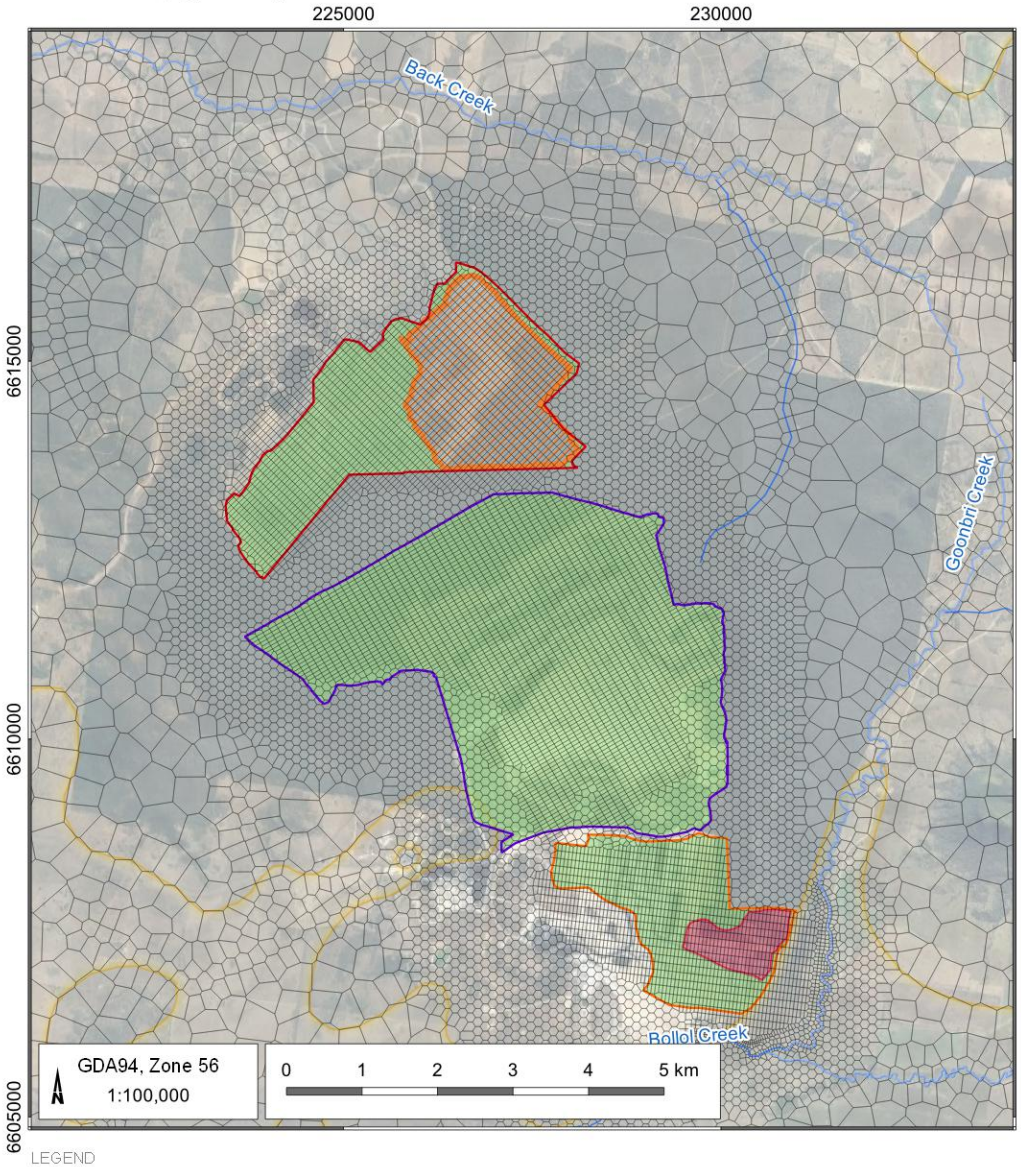

Scenario 6 (proposed)

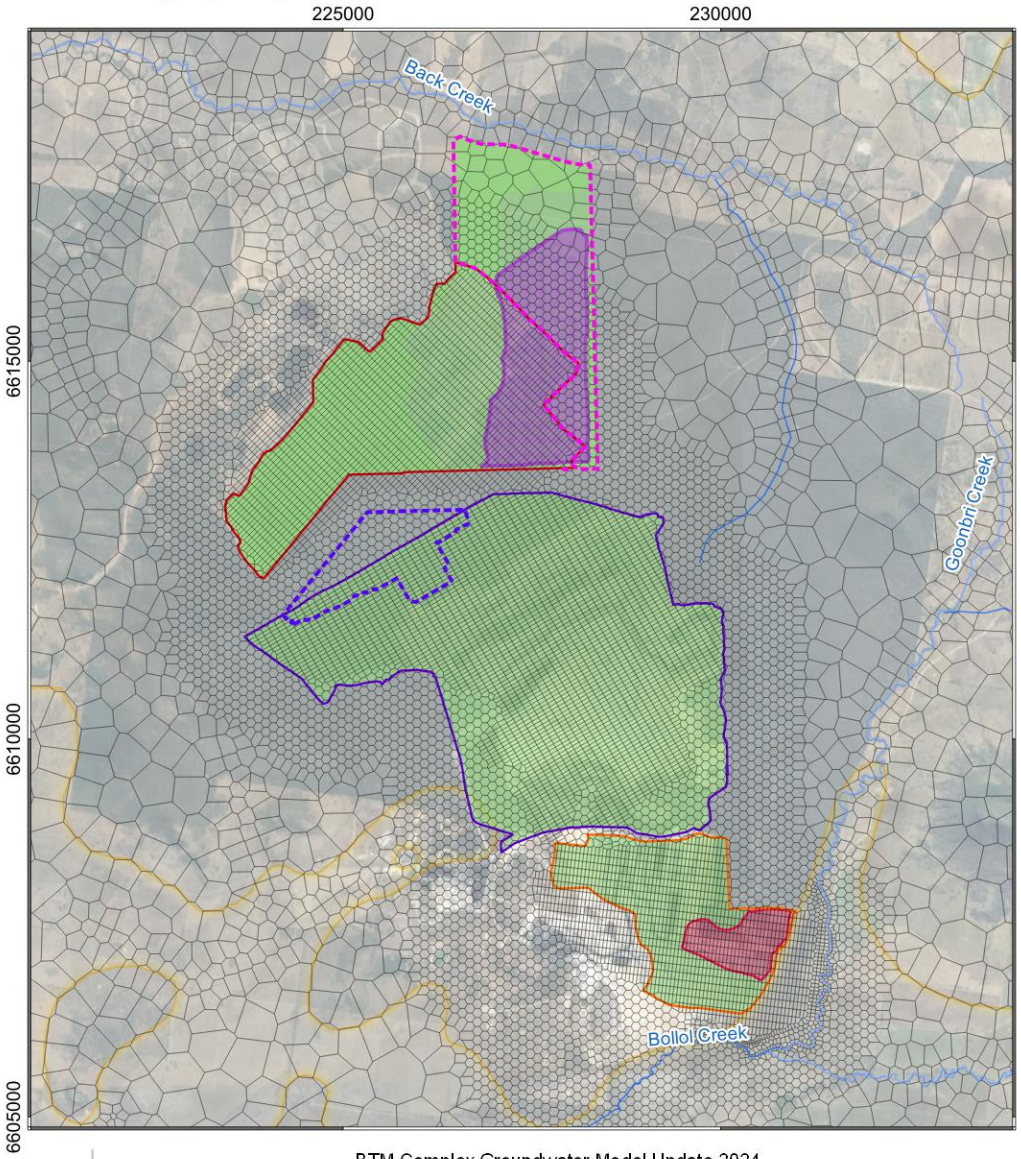

LEGEND

- Drainage
- MCCM Open Cut Extent
- BCM Open Cut Extent
- TCM Open Cut Extent
- MCCM Continuation Project
- BCM Modification Mining Area
- Model Grid
- Alluvial Boundary Zones
- MCCM approved void
- TCM approved void
- MCCM proposed void
- Backfill

BTM Complex Groundwater Model Update 2024

AGE

BTM Complex - approved and proposed mining - End of Mining (EOM)

DATE
26/03/2025

FIGURE No:
F 60

©2025 Australasian Groundwater and Environmental Consultants Pty Ltd (AGE) - www.ageconsultants.com.au
Source: 1 second SRTM Derived DEM-S - © Commonwealth of Australia (Geoscience Australia) 2011.; GEODATA TOPO 250K Series 3 - © Commonwealth of Australia (Geoscience Australia) 2006.;
G:\Projects\MCJ5003.001 Maules Creek Continuation Project EIS\3_GIS\Workspaces\003_Stage 3 -EIS Report\Appendix F\F_60_MCJ5003_BTM Complex – approved and proposed mining – End Of Mining (EOM).qgz

F8.4 Water budgets

Figure F 61 and Figure F 62 show the water budget for approved and proposed cumulative mining scenarios. Positive values indicate water entering the model, and negative numbers represent water leaving the model.

Table F 12 and Table F 13 summarise the average water budget fluxes for the same scenarios. They show that the predicted flows to the drain cells in the model are a relatively small component of the water budget at the scale of the regional model.

The cumulative mass balance error after the predictive run was 0.0%. The maximum percent discrepancy for individual time steps within the transient model run is 0.01%. This maximum error falls within the acceptable limits recommended for adequate numerical convergence (<2%, as per the Australian Modelling Guidelines – Barnett et al., 2012).

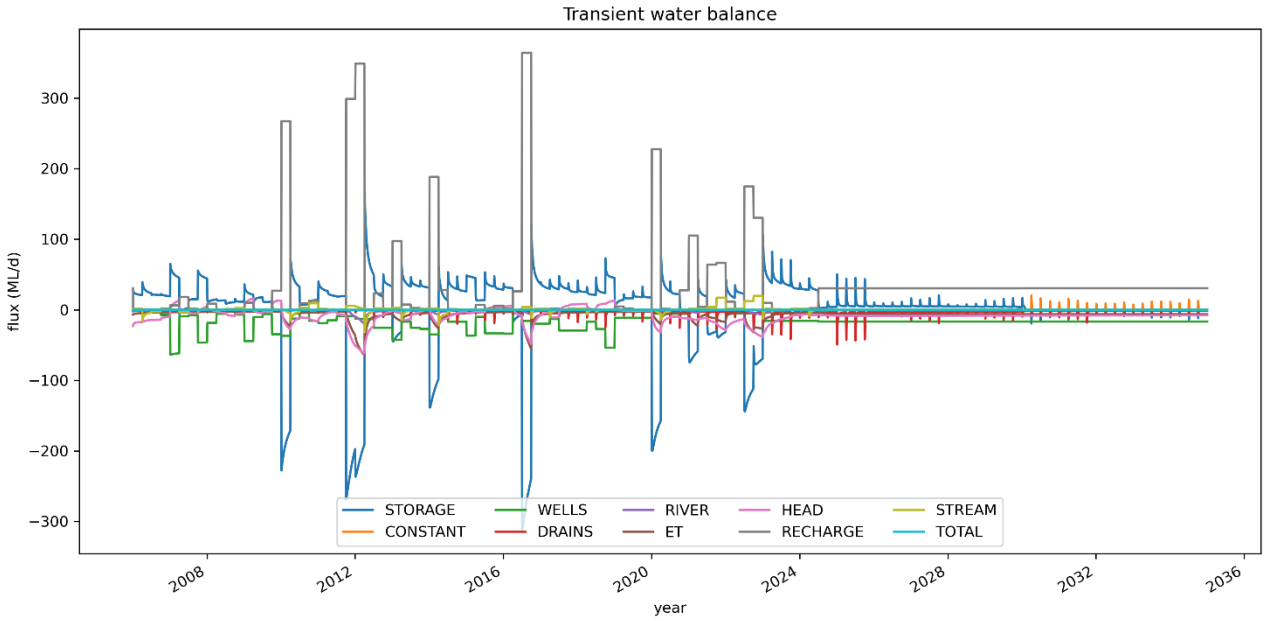

Figure F 61 Predictive model water budget - Scenario 2 (cumulative approved)

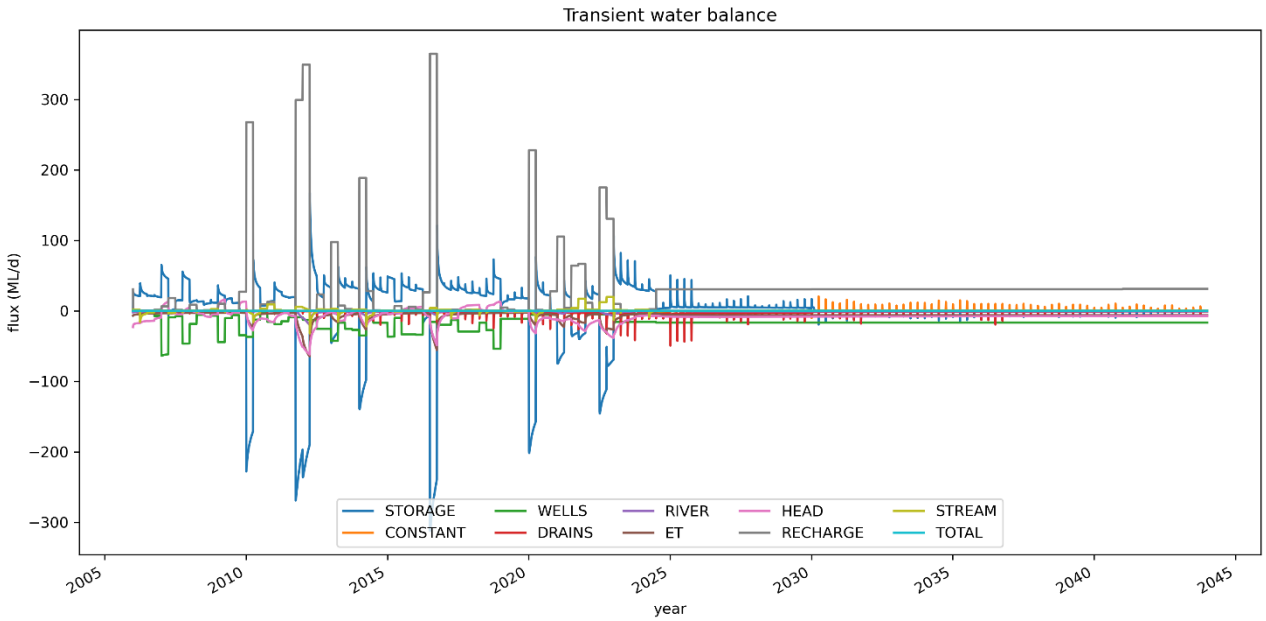

Figure F 62 Predictive model water budget - Scenario 6 (cumulative proposed)

Table F 12 Predictive transient model water budget averages – cumulative approved (Scenario 2)

Parameter	Input (ML/day)			Output (ML/day)		
	minimum	average	maximum	minimum	average	maximum
Storage	0	28	202	0	24	307
Recharge	0	32	364	-	-	-
River	-	-	-	0	1	20
Stream	2	9	22	0	9	44
General Head boundary	76	89	108	88	98	138
Wells	-	-	-	0	17	64
Drains	-	-	-	0	2	49
Evapotranspiration	-	-	-	2	6	65
Fixed head (pit lakes)	0	3	30	0	0.3	30
MODEL TOTAL IN/OUT*	**111**	**158**	**726**	**111**	**157**	**727**

*** Note:** It should be noted that model total in/out row represents the values reported by the model during the water balance calculations, and they might not coincide with the sum of individual rows in this table.

Table F 13 Predictive model water budget averages – cumulative proposed (Scenario 6)

Parameter	Input (ML/day)			Output (ML/day)		
	minimum	average	maximum	minimum	average	maximum
Storage	0	15	203	0	15	307
Recharge	0	32	364	-	-	-
River	-	-	-	0	1	20
Stream	2	9	22	0	9	43
General Head boundary	76	89	108	88	98	138
Wells	-	-	-	0	17	64
Drains	-	-	-	0	3	49
Evapotranspiration	-	-	-	2	6	65
Fixed head (pit lakes)	0	3	30	0	0.3	30
MODEL TOTAL IN/OUT*	**111**	**150**	**727**	**112**	**159**	**727**

*** Note:** Model total in /out row represent the values reported by the model during the water balance calculations, and they might not coincide with the sum of individual rows in this table.

F8.5 Water levels

F8.5.1 Water table

The simulated water table for the approved and proposed cumulative scenarios is shown in Figure F 63 and Figure F 64, respectively.

Outside the mining footprint, the water table remains similar to that of the AGE (2022) simulation, with a dominant east-to-west flow direction aligned with the Maules Creek and Bollol Creek alluvial aquifers and northward flow following the alignment of the Namoi River. The active mining areas within the BTM Complex area are evident in the water table as areas of locally lowered water levels with inward hydraulic gradients.

F8.5.2 Merriown Seam

Figure F 65 and Figure F 66 shows the simulated potentiometric surface within the Merriown Seam at the end of mining. Similar to the AGE (2022) predictions, the figures show a flatter hydraulic gradient and lower water levels than is predicted for the water table, indicating a downward vertical gradient. The flow directions remain strongly influenced by the active mining areas, with flow from the north and south along the strike of the coal seams towards the mining areas. An extensive drawdown within the Merriown coal seam is evident, as all mining projects have been approved to target this coal seam. There is a notable increase in the east-west affected area between the two scenarios.

F8.5.3 Boggabri Volcanics

There is a notable difference in the Boggabri Volcanics hydraulic heads between Scenario 2 (Figure F 67) and Scenario 6 (Figure F 68) where the area with hydraulic heads at 230 m AHD is more pronounced across the entire footprint of the BTM Complex. This can be attributed to the extended mining periods for both BCM and MCCM. There is little change in the extent of reduced heads in the north-south direction, but there is a clear increase in the east-west affected area between the two scenarios.

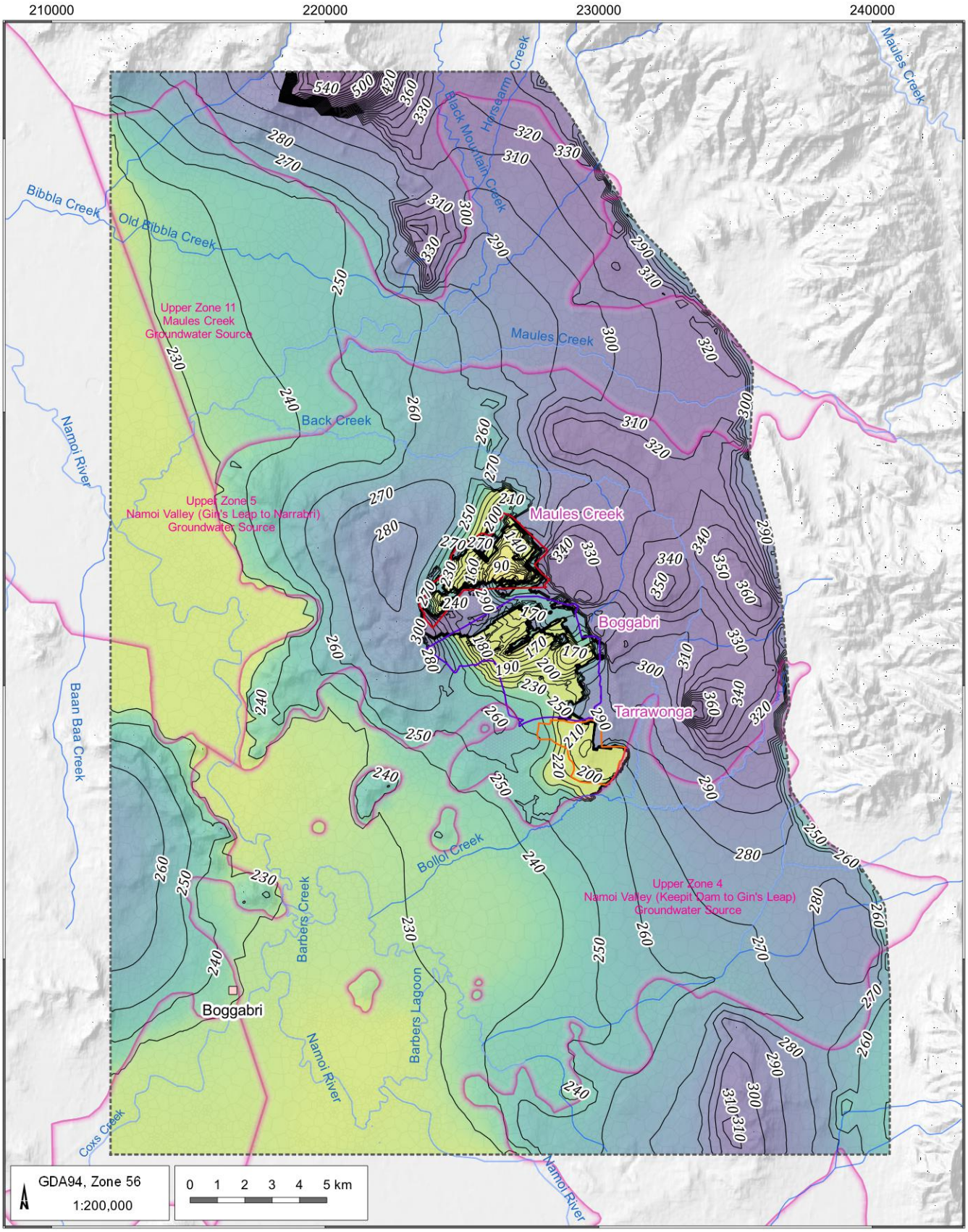

LEGEND

- Populated place
- Drainage
- Contour line
- MCCM Open Cut Extent
- BCM Open Cut Extent
- TCM Open Cut Extent
- Model Extent
- Model Grid
- Alluvial boundary zones

Water Table (mAHD)

- 26
- 230
- 240
- 250
- 260
- 270
- 290
- 310
- 550

BTM Complex Groundwater Model Update 2024

Predicted water table end of mining – approved cumulative scenario (Scenario 2)

AGE

DATE 10/02/2025

FIGURE No: **F 63**

©2025 Australasian Groundwater and Environmental Consultants Pty Ltd (AGE) - www.ageconsultants.com.au
Source: LiDAR DEM © Department Finance, Services and Innovation, 2016; GEODATA TOPO 250K Series 3 - © Commonwealth of Australia (Geoscience Australia) 2006.;
G:\Projects\MCJ5003.001 Maules Creek Continuation Project EIS\3_GIS\Workspaces\003_Stage 3 -EIS Report\Appendix F\F_63_MCJ5003_Predicted water table end of mining – approved cumulative scenario (Scenario 2).qgz

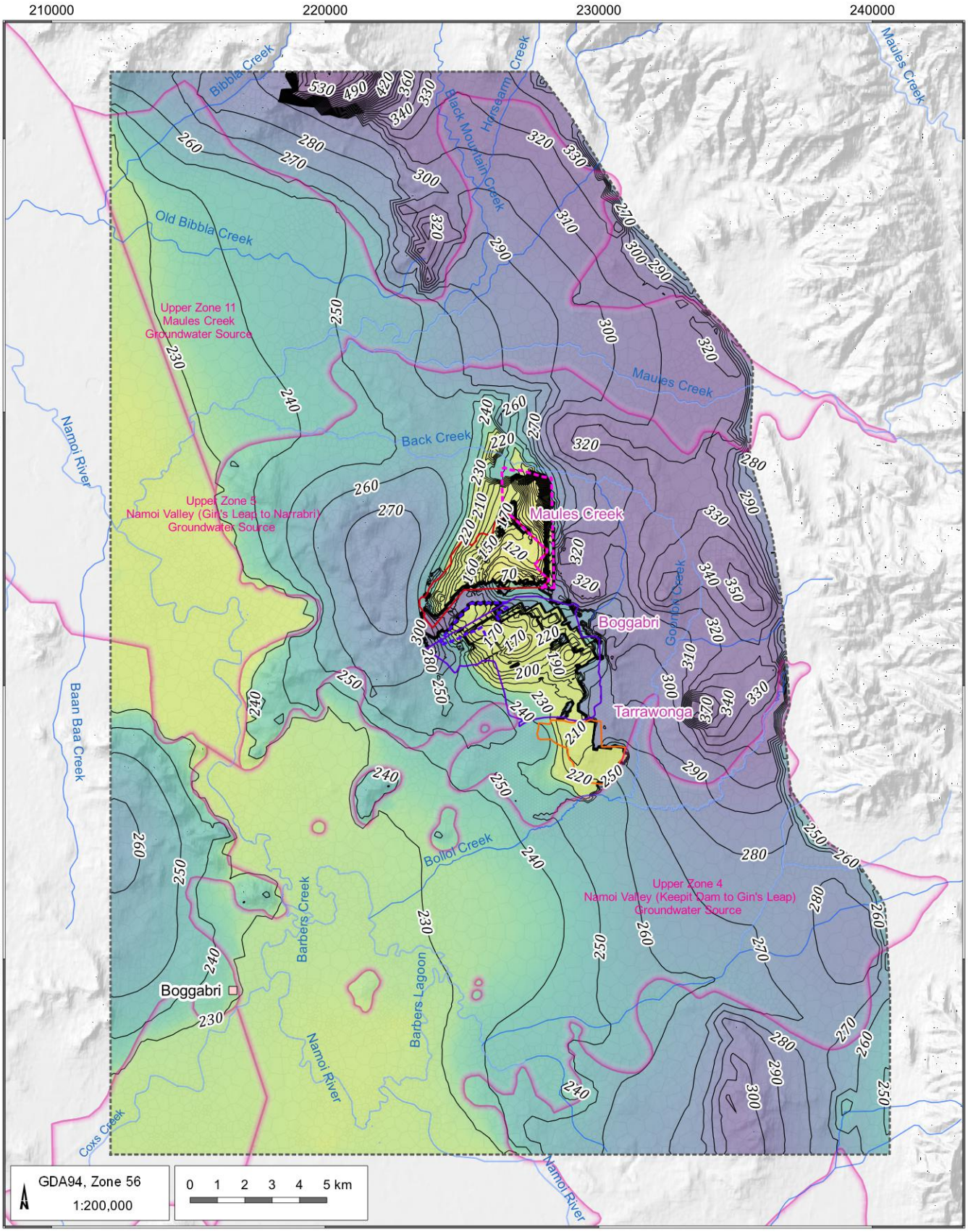

LEGEND

- Populated place
- Drainage
- Contour line
- MCCM Open Cut Extent
- MCCM Continuation Project
- BCM Open Cut Extent
- BCM Modification Mining Area
- TCM Open Cut Extent
- Model Extent
- Model Grid
- Alluvial boundary zones

Water Table (mAHD)

- 26
- 230
- 240
- 250
- 260
- 270
- 290
- 310
- 550

BTM Complex Groundwater Model Update 2024

Predicted water table end of mining – proposed cumulative scenario (Scenario 6)

AGE

DATE 10/02/2025

FIGURE No: **F 64**

©2025 Australasian Groundwater and Environmental Consultants Pty Ltd (AGE) - www.ageconsultants.com.au

Source: LiDAR DEM © Department Finance, Services and Innovation, 2016; GEODATA TOPO 250K Series 3 - © Commonwealth of Australia (Geoscience Australia) 2006.;
G:\Projects\MCJ5003.001 Maules Creek Continuation Project EIS\3_GIS\Workspaces\003_Stage 3 -EIS Report\Appendix F\F_63_MCJ5003_Predicted water table end of mining – approved cumulative scenario (Scenario 2).qgz

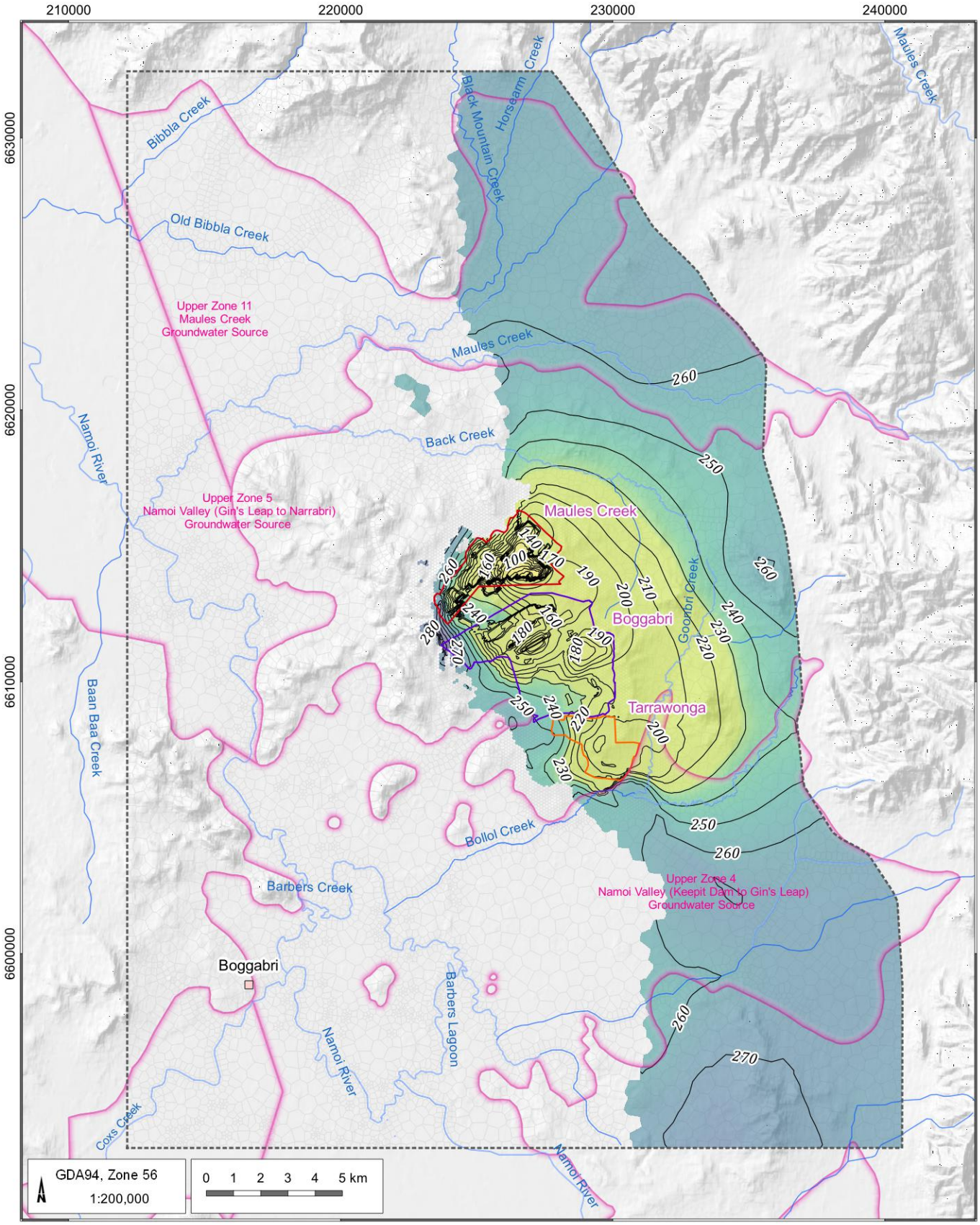

LEGEND

- Populated place
- Drainage
- Contour line
- MCCM Open Cut Extent
- BCM Open Cut Extent
- TCM Open Cut Extent
- Model Extent
- Model Grid
- Alluvial boundary zones

Water Table (mAHD)

- 26
- 230
- 240
- 250
- 260
- 270
- 290
- 310
- 550

BTM Complex Groundwater Model Update 2024

Predicted potentiometric surface end of mining Merriown seam – approved cumulative scenario (Scenario 2)

AGE

DATE 10/02/2025

FIGURE No: **F 65**

©2025 Australasian Groundwater and Environmental Consultants Pty Ltd (AGE) - www.ageconsultants.com.au
Source: LiDAR DEM © Department Finance, Services and Innovation, 2016; GEODATA TOPO 250K Series 3 - © Commonwealth of Australia (Geoscience Australia) 2006.;
G:\Projects\MCJ5003.001 Maules Creek Continuation Project EIS\3_GIS\Workspaces\003_Stage 3 -EIS Report\Appendix F\F_63_MCJ5003_Predicted water table end of mining – approved cumulative scenario (Scenario 2).qgz

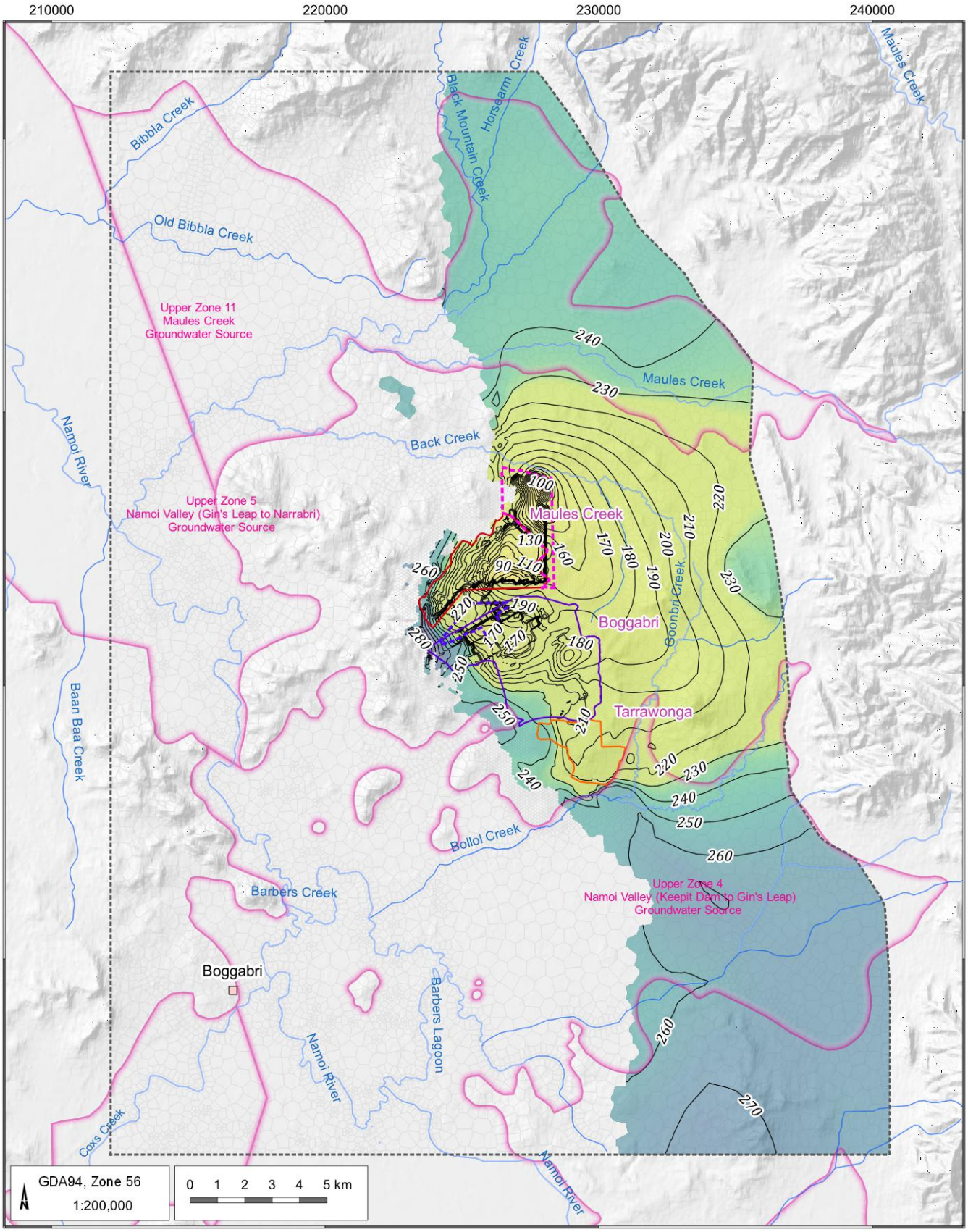

LEGEND

- Populated place
- Drainage
- Contour line
- MCCM Open Cut Extent
- MCCM Continuation Project
- BCM Open Cut Extent
- BCM Modification Mining Area
- TCM Open Cut Extent
- Model Extent
- Model Grid
- Alluvial boundary zones

Water Table (mAHD)

- 26
- 230
- 240
- 250
- 260
- 270
- 290
- 310
- 550

BTM Complex Groundwater Model Update 2024

Predicted potentiometric surface end of mining Merriown seam – proposed cumulative scenario (Scenario 6)

AGE

DATE 10/02/2025

FIGURE No: **F 66**

©2025 Australasian Groundwater and Environmental Consultants Pty Ltd (AGE) - www.ageconsultants.com.au
Source: LiDAR DEM © Department Finance, Services and Innovation, 2016; GEODATA TOPO 250K Series 3 - © Commonwealth of Australia (Geoscience Australia) 2006.;
G:\Projects\MCJ5003.001 Maules Creek Continuation Project EIS\3_GIS\Workspaces\003_Stage 3 -EIS Report\Appendix F\F_63_MCJ5003_Predicted water table end of mining – approved cumulative scenario (Scenario 2).qgz

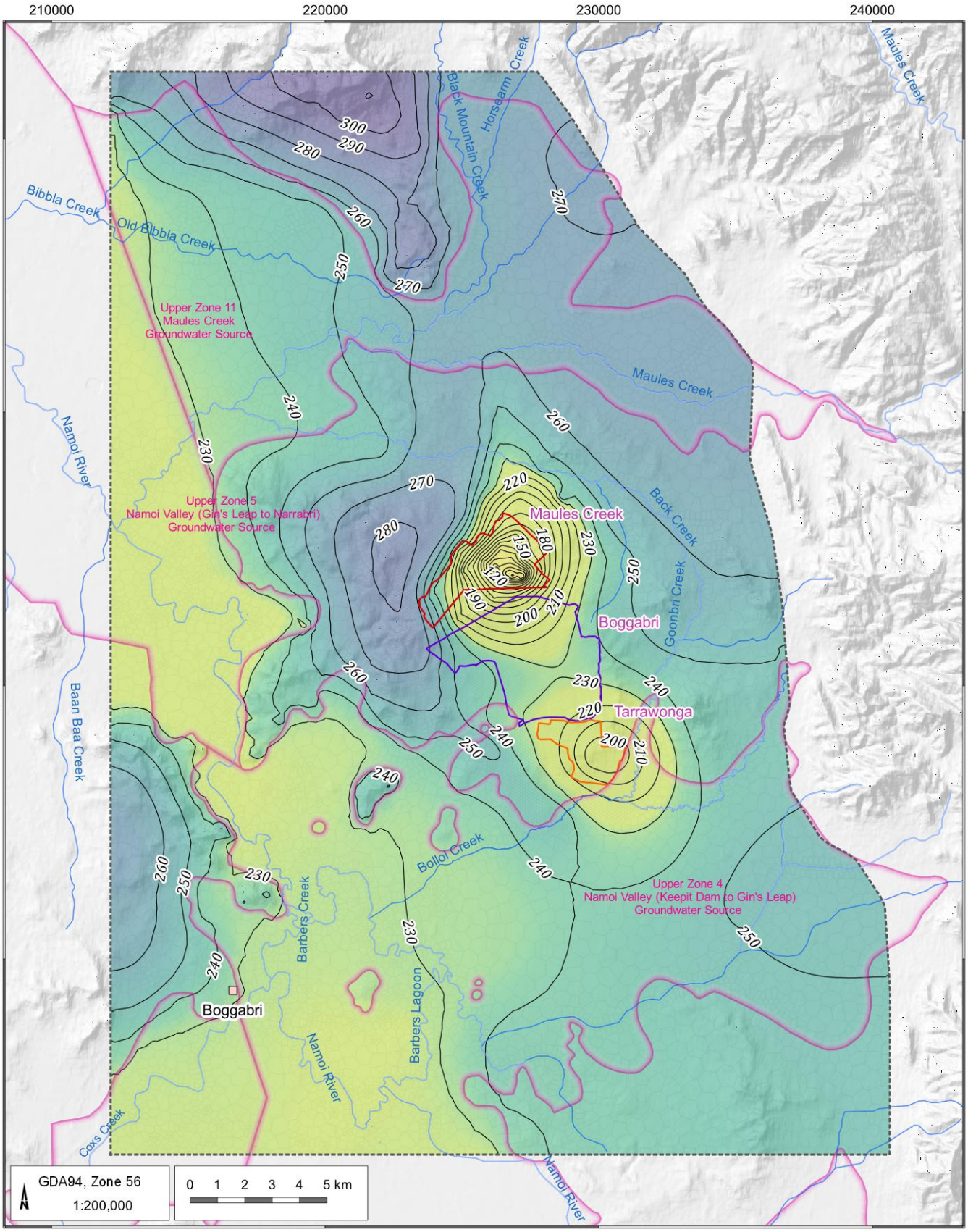

LEGEND

- Populated place
- Drainage
- Contour line
- MCCM Open Cut Extent
- BCM Open Cut Extent
- TCM Open Cut Extent
- Model Extent
- Model Grid
- Alluvial boundary zones

Water Table (mAHD)

- 26
- 230
- 240
- 250
- 260
- 270
- 290
- 310
- 550

BTM Complex Groundwater Model Update 2024

Predicted potentiometric surface end of mining Boggabri volcanics – approved cumulative scenario (Scenario 2)

AGE

DATE 10/02/2025

FIGURE No: **F 67**

©2025 Australasian Groundwater and Environmental Consultants Pty Ltd (AGE) - www.ageconsultants.com.au
Source: LiDAR DEM © Department Finance, Services and Innovation, 2016; GEODATA TOPO 250K Series 3 - © Commonwealth of Australia (Geoscience Australia) 2006.;
G:\Projects\MCJ5003.001 Maules Creek Continuation Project EIS\3_GIS\Workspaces\003_Stage 3 -EIS Report\Appendix F\F_63_MCJ5003_Predicted water table end of mining – approved cumulative scenario (Scenario 2).qgz

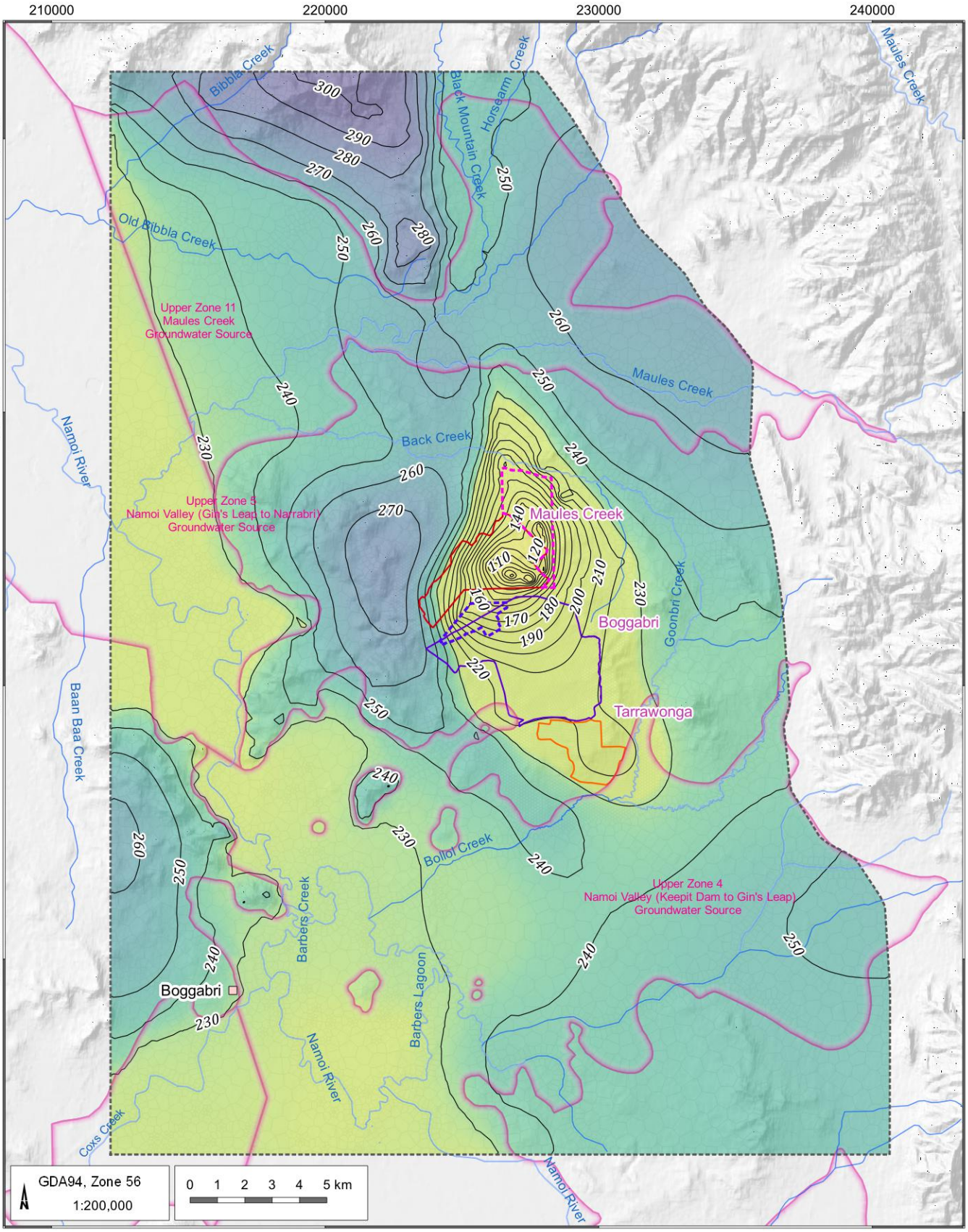

LEGEND

- Populated place
- Drainage
- Contour line
- MCCM Open Cut Extent
- MCCM Continuation Project
- BCM Open Cut Extent
- BCM Modification Mining Area
- TCM Open Cut Extent
- Model Extent
- Model Grid
- Alluvial boundary zones

Water Table (mAHD)

- 26
- 230
- 240
- 250
- 260
- 270
- 290
- 310
- 550

BTM Complex Groundwater Model Update 2024

Predicted potentiometric surface end of mining Boggabri volcanics – proposed cumulative scenario (Scenario 6)

AGE

DATE 28/02/2025

FIGURE No: **F 68**

©2025 Australasian Groundwater and Environmental Consultants Pty Ltd (AGE) - www.ageconsultants.com.au

Source: LiDAR DEM © Department Finance, Services and Innovation, 2016; GEODATA TOPO 250K Series 3 - © Commonwealth of Australia (Geoscience Australia) 2006.;
G:\Projects\MCJ5003.001 Maules Creek Continuation Project EIS\3_GIS\Workspaces\003_Stage 3 -EIS Report\Appendix F\F_63_MCJ5003_Predicted water table end of mining – approved cumulative scenario (Scenario 2).qgz

F8.6 Drawdown

The updated model was used to simulate drawdown at the end of mining for both the approved scenario (Scenario 2) and the proposed scenario (Scenario 6). Figure F 69 to Figure F 71 show the cumulative drawdown for the following model layers at the end of mining:

- layer 1: Alluvium/regolith;
- layer 17: Merriown seam; and
- layer 34: Boggabri volcanics.

The figures compare the cumulative drawdown predicted by the previous iteration of the BTM Complex model (AGE 2022) with the predictions of the updated model (scenarios 2 and 6). The figures show that the AGE (2022) model predicted that the drawdown zone within the Merriown seam would expand over time and reach the model boundaries by 2036. This was considered a conservative overestimate of the drawdown. The updated model predicts reduced drawdown propagation to the east through the coal seams relative to that of AGE (2022); where evidence of depressurisation has not been observed in monitoring points that are more distant from the mining areas (e.g., REG07, REG09).

The influence of the Conomos Fault is evident in the shape of the predicted drawdown within the coal seams and Boggabri volcanics basement in the previous BTM model (AGE, 2022). The model previously predicted that the Conomos Fault retarded the magnitude of the drawdown to the south of the fault. In the previous version of the model (AGE, 2022), this was implemented explicitly via an HFB with the same effect in all layers except layer 1. The updated model shows that the calibrated fault is less restrictive in all the layers.

When interpreting the predicted drawdown, it is important to note that other faults are known to exist to the north and south of the BTM Complex; however, they are not represented within the numerical model. Depressurisation and drawdown within the coal seams may not propagate beyond the faults that offset and terminate the coal seams against lower permeability interburden. This is potentially already evident in the lack of drawdown observed to the east in the observation network (e.g., REG07, REG09).

Whilst the drawdown is predicted to be extensive within the coal seams, it does not result in a large and widespread drawdown propagating upwards and into the Namoi Valley alluvium. The drawdown is largely confined to the alluvial areas immediately adjacent to the active mining operations at BCM and TCM. The nature of this prediction remains consistent between the former BTM Complex model and this updated version.

The model predicts that drawdown within the alluvial groundwater systems is between 1 m and 2 m in part of the Bollol Creek alluvium, south of the BTM Complex, for the cumulative proposed mines scenario at the end of operations. The model also predicts less than 1 m of drawdown within the Maules Creek alluvium to the north. The relatively high storage and high recharge characteristics of the Maules Creek alluvial aquifer mean that any losses occurring through the base of the aquifer to the low-permeability bedrock are a small portion of the total system water budget and, therefore, are readily buffered. This small amount of drawdown would not likely be discernible from climatically induced fluctuations in groundwater levels (recharge-discharge cycles) observed in monitoring bores.

The model does not predict any groundwater drawdown within the alluvium in the vicinity of the Namoi River.

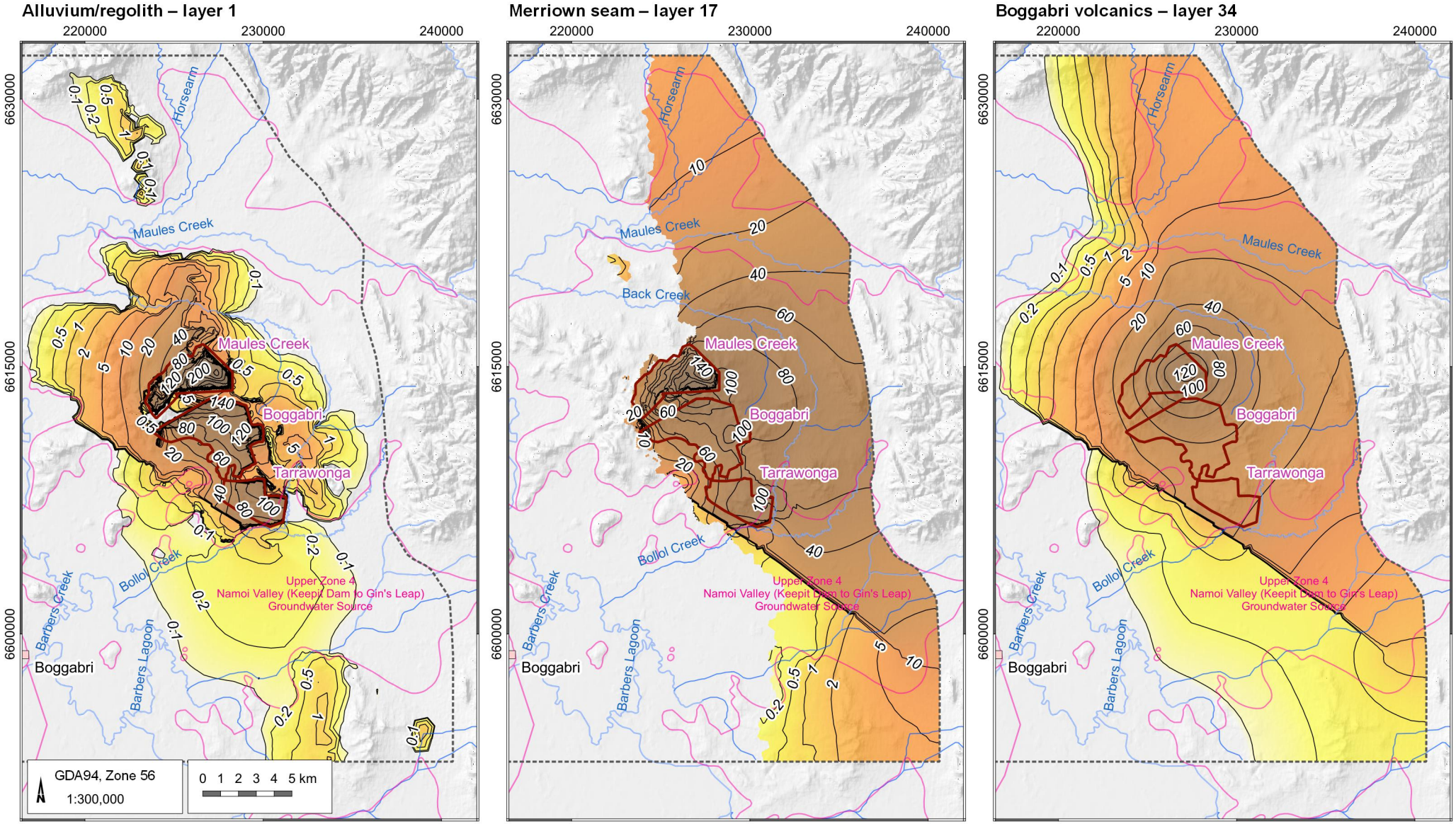

LEGEND

- Populated place
- Drainage
- Contour line
- Model extent
- Mine outline
- Alluvial boundary zones

Drawdown (m)

0	2	100
0.1	5	200
0.2	10	500
0.5	20	
1	50	

BTM Complex Groundwater Model Update 2024

Predicted drawdown at end of 2036 (AGE, 2022)

DATE
10/02/2025

FIGURE No:
F 69

©2025 Australasian Groundwater and Environmental Consultants Pty Ltd (AGE) - www.ageconsultants.com.au
Source: 1 second SRTM Derived DEM-S - © Commonwealth of Australia (Geoscience Australia) 2011.; GEODATA TOPO 250K Series 3 - © Commonwealth of Australia (Geoscience Australia) 2006.;
G:\Projects\MCJ5003.001 Maules Creek Continuation Project EIS\3_GIS\Workspaces\003_Stage 3 -EIS Report\Appendix F\F_69_MCJ5003_Predicted drawdown at end of 2036 (AGE, 2022).qgz

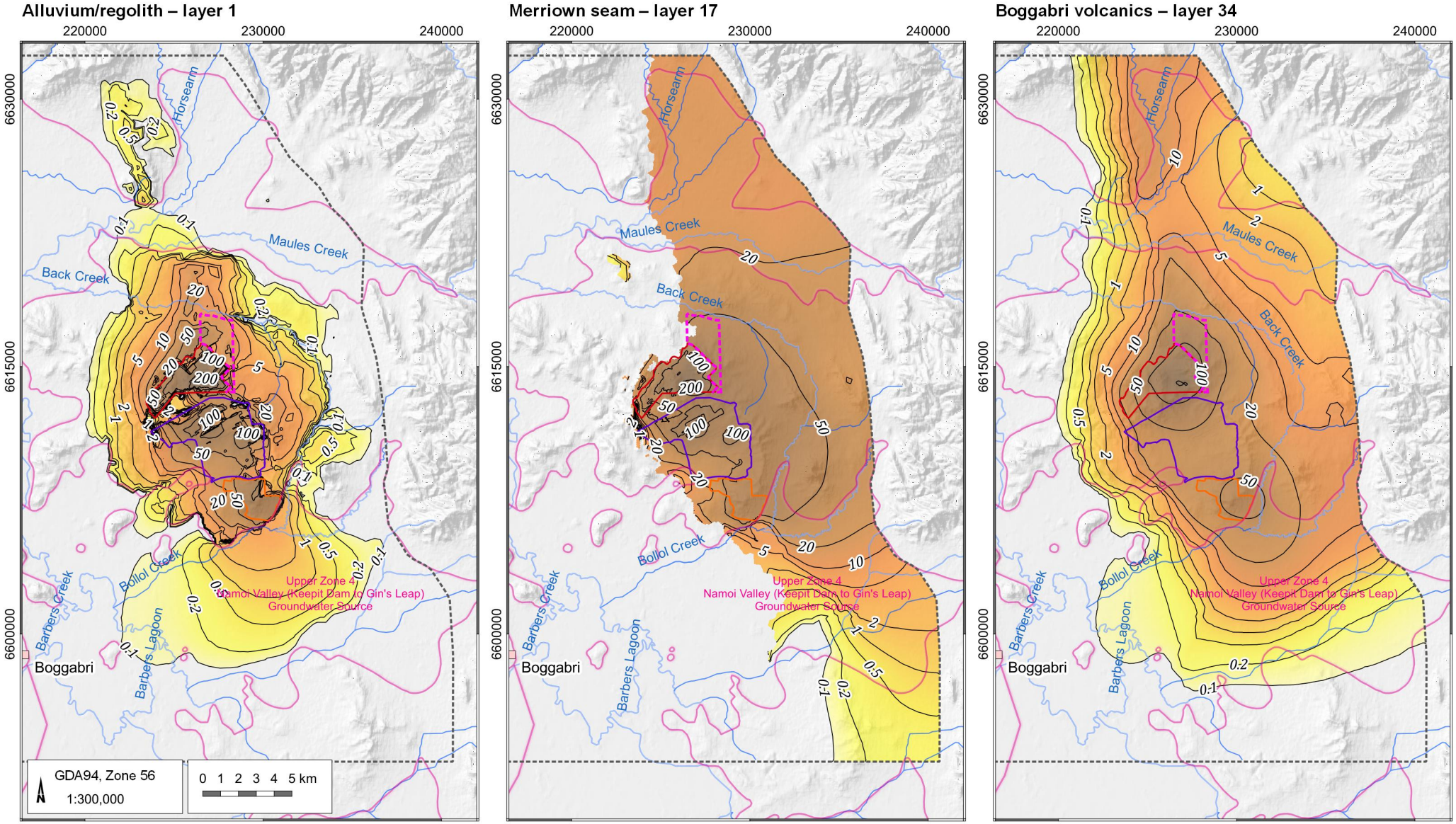

LEGEND

- Populated place
- Drainage
- Contour line
- MCCM Open Cut Extent
- BCM Open Cut Extent
- TCM Open Cut Extent
- Model extent
- Alluvial boundary zones

Drawdown (m)

0, 0.1, 0.2, 0.5, 1, 2, 5, 10, 20, 50

AGE

BTM Complex Groundwater Model Update 2024

Predicted drawdown at end of mining (2036) for cumulative approved mining (Scenario 2)

DATE
25/03/2025

FIGURE No:
F 70

©2025 Australasian Groundwater and Environmental Consultants Pty Ltd (AGE) - www.ageconsultants.com.au
Source: 1 second SRTM Derived DEM-S - © Commonwealth of Australia (Geoscience Australia) 2011.; GEODATA TOPO 250K Series 3 - © Commonwealth of Australia (Geoscience Australia) 2006.;
G:\Projects\MCJ5003.001 Maules Creek Continuation Project EIS\3_GIS\Workspaces\003_Stage 3 -EIS Report\Appendix F\F_70_MCJ5003_Predicted drawdown at end of mining (2034) for cumulative approved mining (Scenario 2).qgz

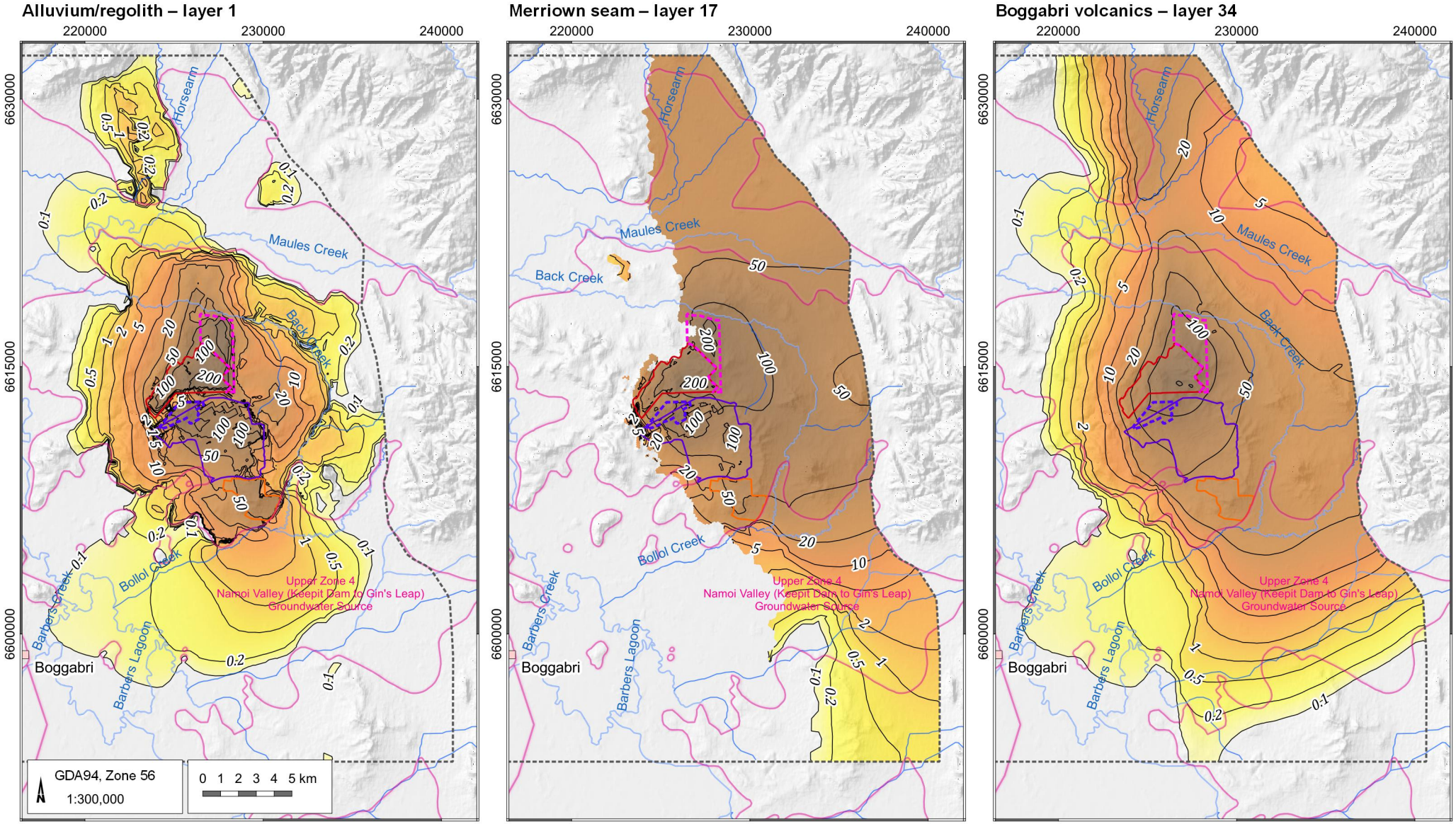

LEGEND

- Populated place
- Drainage
- Contour line
- MCCM Open Cut Extent
- MCCM Continuation Project
- BCM Open Cut Extent
- BCM Modification Mining Area
- TCM Open Cut Extent
- Model extent
- Alluvial boundary zones

Drawdown (m)

0, 0.1, 0.2, 0.5, 1, 2, 5, 10, 20, 50

BTM Complex Groundwater Model Update 2024

Predicted drawdown at end of mining (2044) for cumulative proposed mining (Scenario 6)

DATE
12/02/2025

FIGURE No:
F 71

©2025 Australasian Groundwater and Environmental Consultants Pty Ltd (AGE) - www.ageconsultants.com.au
Source: 1 second SRTM Derived DEM-S - © Commonwealth of Australia (Geoscience Australia) 2011.; GEODATA TOPO 250K Series 3 - © Commonwealth of Australia (Geoscience Australia) 2006.;
G:\Projects\MCJ5003.001 Maules Creek Continuation Project EIS\3_GIS\Workspaces\003_Stage 3 -EIS Report\Appendix F\F_70_MCJ5003_Predicted drawdown at end of mining (2034) for cumulative approved mining (Scenario 2).qgz

F8.7 Mine inflow

The AIP requires accounting for all groundwater taken directly or indirectly from groundwater systems. Groundwater intercepted from the BTM Complex is considered a direct take from the Permian groundwater system. The discussion below refers to the volume of groundwater intercepted by mining from the Permian groundwater systems. This includes groundwater that cannot be pumped because it evaporates, groundwater bound to coal/spoils, and groundwater that flows into sumps for pumping.

Figure F 72 to Figure F 74 show the estimated annual volume of groundwater directly intercepted by mining at the BTM Complex within each mining area for the previous model (AGE, 2022) and the updated model approved and proposed scenarios for the entire operation time. Observations are the following:

- Figure F 72 shows that the previous model predicted the volume of groundwater intercepted by the BTM Complex would gradually rise as the footprint of mining grows, peaking at around 1,660 ML/year by 2023/2024. After this time, the model predicts the volume of groundwater directly intercepted by the open cut mines gradually falls as the coal seams become dewatered and depressurised by the cumulative impacts of the three mines, resulting in gentler hydraulic gradients and less mine inflow.
- The overall behaviour of the mine inflow time series for the approved and proposed mining operation in the BTM Complex remains similar to that obtained from the previous model (AGE, 2022). Mine inflows resulting from the cumulative approved and proposed peaked in 2023 at 1,810 ML/year (Figure F 73 and Figure F 74). A secondary peak is observed in 2025, but the overall decreasing trend in mine inflows for the cumulative approve scenario is preserved.

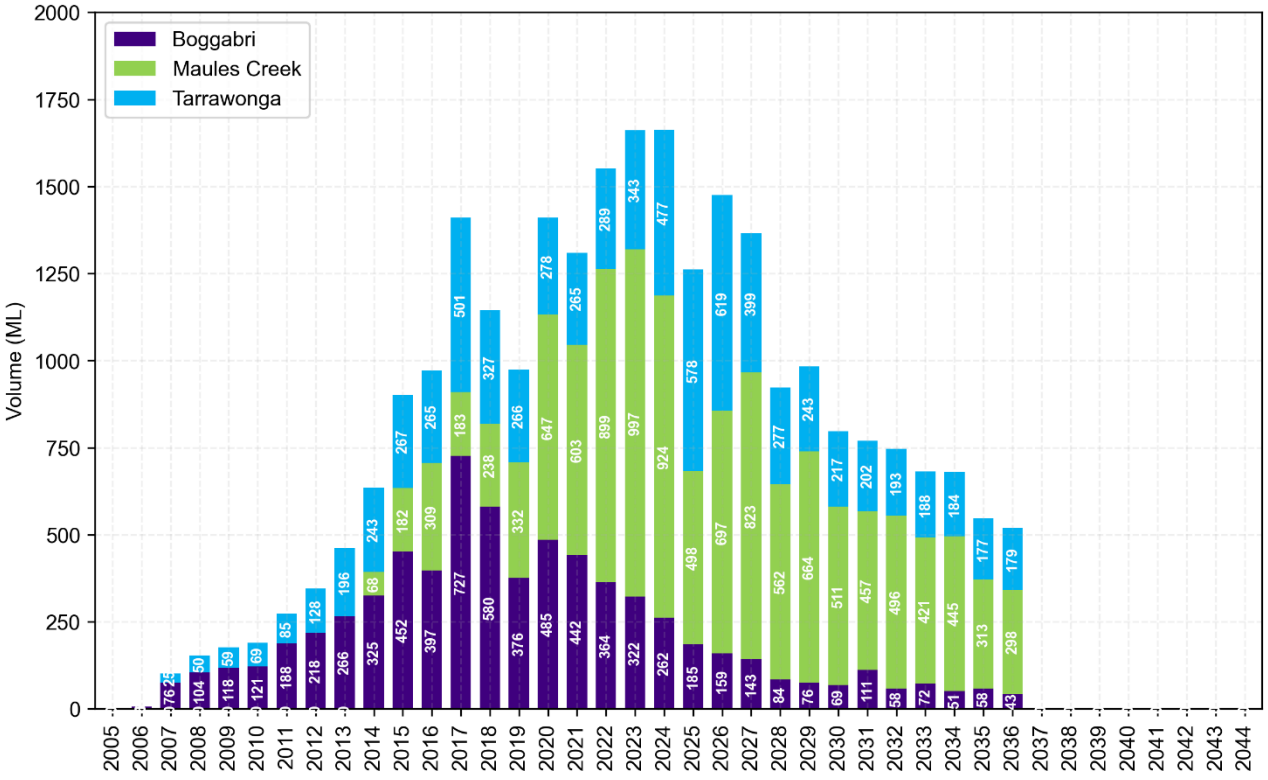

Figure F 72 Predicted groundwater directly intercepted in BTM Complex mines – AGE (2022)

It should be noted that the previous model (AGE, 2022) did not simulate mine closures according to their designated mine plans but instead, kept mines completely open until the last mine in operating in the BTM complex reached closure. At that point all mines transitioned to closure simultaneously. Inflows were therefore reported for mines that would have reached closure by then.

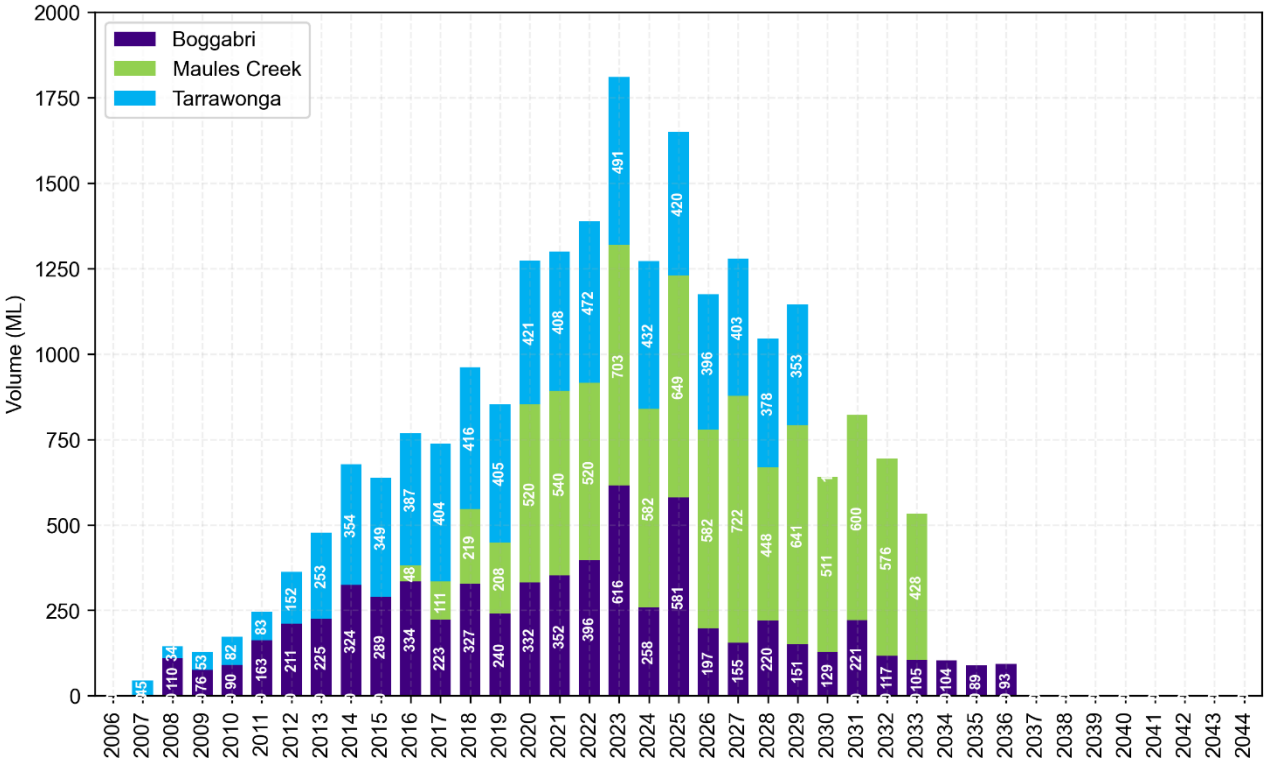

Figure F 73 Predicted groundwater directly intercepted in BTM Complex mines – cumulative approved (Scenario 2)

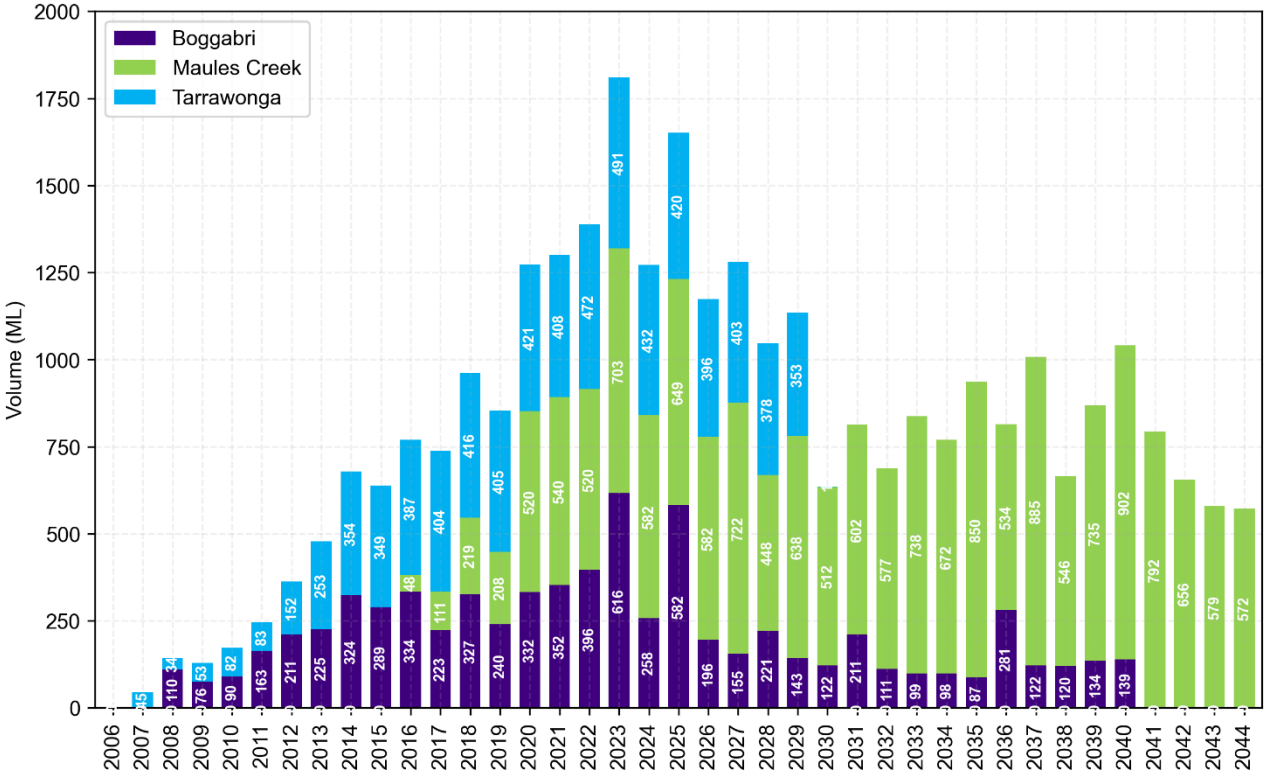

Figure F 74 Predicted groundwater directly intercepted in BTM Complex mines – cumulative proposed (Scenario 6)

Table F 14 compares the estimated annual volumes of groundwater directly intercepted within each of the BTM Complex mines for the previous model (AGE, 2022), and scenarios 2 and 6 from the current model update.

Table F 14 Predicted total volume for mine inflows within each mining area

Year	Predicted volume of inflow to mining areas (ML/year)								
	Previous model - approved mining AGE (2022)			Approved mining (Scenario 2)			Proposed mining (Scenario 6)		
	Boggabri	Tarra-wonga	Maules Creek	Boggabri	Tarra-wonga	Maules Creek	Boggabri	Tarra-wonga	Maules Creek
2025	185	578	498	581	420	649	582	420	649
2026	159	619	697	197	397	582	196	396	582
2027	143	399	823	155	404	722	155	403	722
2028	84	277	562	220	377	448	221	378	448
2029	76	243	664	151	353	641	143	353	638
2030	69	217	511	129	-	511	122	-	512
2031	111	202	457	221	-	600	211	-	602
2032	58	193	496	117	-	576	111	-	577
2033	72	188	421	105	-	428	99	-	738
2034	51	184	445	104	-	398	98	-	672
2035	58	177	313	89	-	-	87	-	850
2036	43	179	298	93	-	-	281	-	534
2037	-	-	-	-	-	-	122	-	885
2038	-	-	-	-	-	-	120	-	546
2039	-	-	-	-	-	-	134	-	735
2040	-	-	-	-	-	-	139	-	902
2041	-	-	-	-	-	-	-	-	792
2042	-	-	-	-	-	-	-	-	656
2043	-	-	-	-	-	-	-	-	579
2044	-	-	-	-	-	-	-	-	572

F8.8 Water licensing requirements

Water take due to aquifer interference activities can be categorised as either consumptive, incidental, or passive and are defined as follows:

- 'Consumptive water take' is defined as water directly taken from an aquifer by pumping and consumed by the activity. MCCM and BCM have water supply bores for consumptive water use.
- 'Incidental water take' is defined in the AIP as *"water that is taken by an aquifer interference activity that is incidental to the activity; including water that is encountered within and extracted from mine workings…".* This water does not need to be used as part of the activity.
- 'Passive water take' refers to water losses from a groundwater system adjacent to mining activity, but not directly excavated by the mining operation. At the BTM Complex, passive water take occurs from the surrounding alluvial water sources due to depressurisation and changes in flow from the underlying Permian bedrock.

The AIP states that a WAL is required for aquifer interference activity regardless of whether water is taken directly for consumptive use or incidentally. The following sections describe how the groundwater model estimates the incidental and passive water take due to mining. It is important to note that it is not possible to directly measure incidental or passive water take to verify model predictions. This unavoidable inherent element of groundwater modelling should be recognised when interpreting the model predictions.

F8.8.1 Estimate of incidental water take

Incidental water take occurs from the Gunnedah-Oxley NSW Murray Darling Basin Porous Rock Groundwater Sources due to the BTM mining activities. Table F 15 summarises the WALs entitlements the BTM mines hold to account for incidental water take.

Table F 15 Water access licenses and total entitlement held - porous rock WSP

Mine	Water access licenses [1]	Entitlement (units)	Total entitlement (units)
Boggabri	WAL 29473 WAL 29562	142 700	842
Tarrawonga	WAL 31084 WAL 29548 WAL 29461 WAL 29537	250 50 120 120	540
Maules Creek	WAL 29467 WAL 36641	306 800	1106

Note: [1] Gunnedah - Oxley Basin NSW Murray Darling Basin Porous Rock Groundwater Sources.

The volumes of incidental water take that need to be accounted for under the porous rock WSP were estimated as follows:

a) the groundwater directly intercepted by each mining area by drain cells (representing dewatering of the mining voids) was extracted from the model (Table F 14);

b) the change in groundwater flux from the porous rock WSP into the alluvial WSP area due to mining activities was extracted from the model – this volume of water was assigned as 'passive water take' from the alluvial WSP; and

c) the passive alluvial 'water take' was subtracted from the drain cell flux to calculate the 'incidental water take' from the porous rock WSP (a minus b).

This method prevents double accounting of 'incidental water take' from the porous rock with the 'passive water take' from the alluvial WSPs. Table F 16 presents the calculated volume of incidental water from the porous rock WSP.

Table F 16 Predicted volume of incidental water take from each mining area within porous rock WSP (ML)

Year	Previous model (AGE 2022)			Approved mining			Proposed mining		
	Boggabri	Tarra-wonga	Maules Creek	Boggabri	Tarra-wonga	Maules Creek	Boggabri	Tarra-wonga	Maules Creek
2025	155	483	415	478	235	502	479	235	502
2026	137	529	596	49	205	487	48	204	487
2027	120	322	705	83	176	588	83	175	588
2028	63	207	431	156	77	377	157	78	377
2029	58	184	515	105	69	537	97	69	534
2030	50	153	363	80	-	373	73	-	374
2031	77	138	320	177	-	442	167	-	444
2032	38	126	345	81	-	391	74	-	386
2033	46	120	276	68	-	254	60	-	545
2034	32	114	291	41	-	250	31	-	500
2035	32	98	173	51	-	-	45	-	644
2036	23	94	156	47	-	-	229	-	333
2037	-	-	-	-	-	-	82	-	668
2038	-	-	-	-	-	-	67	-	351
2039	-	-	-	-	-	-	93	-	530
2040	-	-	-	-	-	-	79	-	695
2041	-	-	-	-	-	-	-	-	578
2042	-	-	-	-	-	-	-	-	417
2043	-	-	-	-	-	-	-	-	315
2044	-	-	-	-	-	-	-	-	288

Notes: [1] Total number of units for water access licenses held from porous rock WSP.

[2] Entitlements held by each organisation may vary over time due to purchase, sale or transfer of licenses.

Table F 16 shows that the BTM Complex holds sufficient WALs to account for the peak volume of groundwater predicted to be intercepted by mining from the porous rock WSP. Cumulatively, the BTM Complex holds 2,368 ML of WALs, with the estimated annual peak volume of groundwater intercepted by the complex from the porous rock to be at 1,215 ML for the period 2025 for the approved and proposed mining.

F8.8.2 Estimate of passive water take

Passive water take occurs from the Namoi Alluvial Groundwater Sources due to the BTM Complex mining activities. Table F 17 summarise the WALs held by each mining operation within each Namoi Alluvial Groundwater Sources.

Table F 17 Water access licenses and total entitlement held - alluvial WSP

Mine	Water access licenses [1]	Entitlement (units)	Zone	Total entitlement (units)[2]
Boggabri	WAL 15037 WAL 24103 WAL 12767 WAL 12691 WAL 36547 WAL 37519	172 275 3 457 37 84	4	1028
Boggabri	WAL 42234	20	11	20
Tarrawonga	WAL 12716 WAL 36548	43 36	4	79
Tarrawonga	WAL 12479	78*	11	39*
Maules Creek	WAL 27385 WAL 12613 WAL 36548 WAL 12722 WAL 12718	38 50 36 77 102	4	303
Maules Creek	WAL 12479 WAL 12480 WAL 12491 WAL 12473 WAL 12482 WAL 12486 WAL 12489	78* 215 77 241 77 77 28	11	754

Note: [1] Upper and Lower Namoi Groundwater Sources WSP.

[2] Whitehaven may transfer WALs between its Gunnedah mines to meet annual water licensing requirements.

* Planned to be shared with TCM (39 ML each).

Indirect passive water take from the adjacent alluvial water sources was estimated for approved mining using zone budgets from the following model scenarios:

- a no-mining scenario (Scenario 1);
- a scenario with mining at all three of the sites (Scenario 2); and
- three scenarios representing approved mining at each BTM site individually (Scenarios 12, 13 and 14).

The model with all approved mining (Scenario 2) was then run to simulate the change in groundwater flow to the alluvial zones compared to the model with no mining (Scenario 1). The change in groundwater flow to the alluvial zones for each model with only one mine operating was also calculated compared to the no-mining model.

The calculated change in flow from each of the three models with only one mine was then combined to determine the proportion of impact attributable to each operation. A time-varying factor for each mine was then applied to the change in flow calculated by the model, with all three mines operating, to estimate the proportion of the cumulative impact attributable to each operation.

The same method was used to estimate indirect water take from the adjacent alluvial water sources for proposed mining using zone budgets from the following model scenarios instead:

- a no-mining scenario (Scenario 1);
- a scenario with mining at all three of the sites (Scenario 6); and
- two scenarios representing proposed mining at each BTM site individually (Scenarios 10 and 11) and approved TCM mining (Scenario 12).

Zones were defined based on the groundwater management zones detailed in the WSPs for the Namoi Alluvial Groundwater Sources. Table F 18 presents the predicted volume of groundwater removed passively from each alluvial water management zone under the alluvial WSP. Only fluxes during individual mine operations are presented. Table F 18 compares the predicted water take from the previous BTM Complex model (AGE, 2022) with the predictions for approved and proposed mining using the updated model. Table F 18 indicates the need for additional entitlements from some water sources over time to account for the predicted passive water take.

Table F 18 Predicted groundwater take passively intercepted from adjacent alluvial water sources (ML)

Year	Previous model (AGE 2022)						Approved mining (Scenario 2)						Proposed mining (Scenario 6)					
	Boggabri		Tarrawonga		Maules Creek		Boggabri		Tarrawonga		Maules Creek		Boggabri		Tarrawonga		Maules Creek	
	Zone 4	Zone 11	Zone 4	Zone 11	Zone 4	Zone 11	Zone 4	Zone 11	Zone 4	Zone 11	Zone 4	Zone 11	Zone 4	Zone 11	Zone 4	Zone 11	Zone 4	Zone 11
2025	29	1	91	4	79	4	99	4	183	2	139	8	99	4	183	2	139	8
2026	21	1	86	4	96	5	144	4	190	2	84	11	144	4	190	2	84	11
2027	22	1	73	4	112	6	68	4	224	4	123	11	68	4	224	4	123	11
2028	20	1	66	4	123	8	60	4	291	9	61	10	60	4	291	9	61	10
2029	17	1	55	4	139	10	42	4	275	9	91	13	42	4	275	9	91	13
2030	18	1	59	5	137	11	44	5	-	-	122	16	44	5	-	-	122	16
2031	31	3	59	5	126	11	39	5	-	-	137	21	39	5	-	-	137	21
2032	18	2	61	6	138	13	31	5	-	-	159	26	31	6	-	-	160	31
2033	24	2	62	6	132	13	32	5	-	-	147	27	32	7	-	-	149	44
2034	17	2	63	7	139	15	53	10	-	-	122	26	53	14	-	-	124	48
2035	23	3	71	8	126	14	30	8	-	-	-	-	30	12	-	-	141	65
2036	18	2	76	9	127	15	38	8	-	-	-	-	38	14	-	-	125	76
2037	-	-	-	-	-	-	-	-	-	-	-	-	26	14	-	-	133	84
2038	-	-	-	-	-	-	-	-	-	-	-	-	35	18	-	-	110	85
2039	-	-	-	-	-	-	-	-	-	-	-	-	26	15	-	-	110	95
2040	-	-	-	-	-	-	-	-	-	-	-	-	38	22	-	-	103	104
2041	-	-	-	-	-	-	-	-	-	-	-	-	-	-	-	-	98	116
2042	-	-	-	-	-	-	-	-	-	-	-	-	-	-	-	-	111	128

Year	Previous model (AGE 2022)						Approved mining (Scenario 2)						Proposed mining (Scenario 6)					
	Boggabri		Tarrawonga		Maules Creek		Boggabri		Tarrawonga		Maules Creek		Boggabri		Tarrawonga		Maules Creek	
	Zone 4	Zone 11	Zone 4	Zone 11	Zone 4	Zone 11	Zone 4	Zone 11	Zone 4	Zone 11	Zone 4	Zone 11	Zone 4	Zone 11	Zone 4	Zone 11	Zone 4	Zone 11
2043	-	-	-	-	-	-	-	-	-	-	-	-	-	-	-	-	128	136
2044	-	-	-	-	-	-	-	-	-	-	-	-	-	-	-	-	140	144

Notes: [1] Total number of units for water access licenses held from each alluvial WSP management zone.

[#] Entitlements held by each organisation may vary over time due to purchase, sale or transfer of licenses.

F8.8.3 Estimate of consumptive water take

Both MCCM and BCM have water supply bores installed within the Namoi Alluvial Groundwater Sources. Water take from these bores is determined by flow meters installed on each bore. Therefore, it is not necessary to use the groundwater flow model to estimate the consumptive water take, which is reported in each site's Annual Review.

F9 Uncertainty analysis

The sections below describe the methodology and results of the uncertainty analysis. All parameters used in calibration formed part of the uncertainty analysis. This includes all aquifer properties, recharge, fault properties, and elevations, plus the conductance of boundary conditions.

F9.1 Methodology

The overall approach to uncertainty analysis adopted in this project is linear, stochastic analysis with Bayesian probability quantification. Two different methods were used to assess uncertainty for different predictions. First, a constrained Monte-Carlo approach was used to produce drawdown probability surfaces (spatially) of the water table. Second, Data Space Inversion (DSI) was used for assessing uncertainty in value predictions of maximum drawdown at receptors, mine inflow across all mine sites, and cumulative water take from the alluvial zones identified in the Water Sharing Plans (WSPs). The two approaches were required because DSI relies on a surrogate and is, therefore, unable to provide a spatial distribution of drawdown to create a probability surface. DSI is consequently the primary approach for the uncertainty analysis in this project. DSI was selected because it is less prone to the deleterious effects of information loss and/or corruption that can potentially accompany a complex model. The application of both methods, constrained Monte-Carlo and DSI, are fully supported by the IESC Explanatory Note in uncertainty analysis for groundwater modelling (Peeters and Middlemis, 2023). The IESC Note suggests that methods selected for uncertainty analysis should strike a balance between model complexity, the number of parameters, and the number of model evaluations required for the assessment. The Bayesian and ensemble-based approaches (using IESC terminology) implemented in this work meet this trade-off and can accommodate the complexity of the model predictions (QoIs) needed for this project.

Several utilities provided in the PEST (Doherty, 2024a) and PEST-HP (Doherty, 2024) suites were used to implement the uncertainty analysis for this project. For the sake of brevity, more technical details on the approaches used, implementation steps, and tools required for typical uncertainty analysis, the reader is referred to the extensive documentation outlined on the GMDSI website[5].

As the first step, Ensemble Space Inversion (ENSI) was used to calibrate the model. In addition to the minimum error variance model, the ENSI process produces a Jacobian matrix. Performing linear analysis with the Jacobian containing local sensitivities informs their posterior distributions in the Bayesian framework. The parameter sets used in the constrained Monte-Carlo were drawn from their posterior distributions. The overall steps implemented for the uncertainty analysis are listed below:

(i) Calibrate the model with ENSI.

(ii) Perform linear uncertainty analysis following ENSI calibration.

(iii) Use posterior distributions in model parameters obtained via step (ii) to randomly draw realisations of model parameters.

(iv) Execute the model and store the heads file for probability surface creation.

[5] https://gmdsi.org/blog/ensi-and-linear-analysis.

As a second step, to account for uncertainty in predicted drawdowns, 300 model realisations were used, with five models failing to converge, resulting in 295 completed models. The converged models' hydraulic heads files were used to calculate drawdown from a null scenario using the same parameter set. The predicted drawdown of each model's water table at the end of mining operations in 2044 and 200 years post-closure (in 2244) was used to produce drawdown probability surfaces for describing a likelihood of a 2 m exceedance at those times. Outputs from this uncertainty assessment were processed following the risk-based language proposed by Middlemis & Peeters (2018). The ranges adopted are shown in Table F 19. It is important to note that the ranges include outputs from all model runs constrained by the calibration. This does not eliminate the possibility of outlier predictions because not all parameters affecting predictions may be sensitive to the calibration dataset.

DSI was subsequently applied for uncertainty analysis. DSI enables the exploration of a model prediction's posterior distribution without requiring the exploration of the posterior distribution of model parameters. This is achieved by constructing a surrogate model using principal component analysis (PCA) of a covariance matrix of model outputs. This matrix links model outputs corresponding to field measurements with predictions of interest. The resulting predictions are then conditioned on real-world measurements of system behaviour in the latent PCA subspace. The primary input for DSI is a dataset comprising simulated observations of field measurements and predictions from a Monte-Carlo of the prior. It should be noted that DSI can produce near-measurement noise levels of fit with observation data and consequently will also show reduced margins for uncertainty. More information on the method and its limitations are provided in Section F16.

The same prior used in the ENSI calibration was used to draw 300 model realisations. Ensemble draw and creation of the PCA model was accomplished with Pyemu[6], a set of Python modules for model-independent, user-friendly, computer model uncertainty analysis. PESTPP-IES (White, 2018) was used to run the prior Monte-Carlo and collate the simulated field observations and simulated prediction observations for use as a training dataset for DSI.

Table F 19 Language used to describe uncertainty analysis results

Narrative descriptor	Probability class	Description	Colour code
Very likely	90 – 100 %	Likely to occur even in extreme conditions	
Likely	67 – 90 %	Expected to occur in normal conditions	
About as likely as not	33 – 67 %	About an equal chance of occurring as not	
Unlikely	10 – 33 %	Not expected to occur in normal conditions	
Very unlikely	0 – 10 %	Not likely to occur even in extreme conditions	

F9.2 Results

The results obtained from the uncertainty analysis are presented in the following order:

1. Likelihood of water table drawdown to exceed 2 m at the end of operations for the BTM-complex and 200 years post-closure. This was produced by processing hydraulic head output files from the constrained Monte-Carlo.
2. Table of maximum drawdown observed at identified reportable locations, along with accompanying statistics. This was a direct output of DSI.
3. Box plots showing the uncertainty in indirect take from Zone 4 and Zone 11. This was a direct output from DSI.
4. Bar graphs showing the uncertainty in mine inflows. This was a direct output from DSI.

[6] https://github.com/pypest/pyemu.

F9.2.1 Uncertainty in drawdown

Figure F 75 shows the likelihood of the maximum water table drawdown exceeding two metres for Scenario 6. The findings align with the base case scenario, showing that most simulations indicate the water table drawdown exceeding two metres is limited to the Permian during operations. A few simulations indicated that the possible drawdown could extend beyond the Permian, as reflected in the spread of the very unlikely category. The area labelled as "very likely" extends farther north to south than east to west, following the general north-south alignment of the open-cut pits.

At 200 years post-closure, the area experiencing a drawdown of more than two meters expands, particularly toward the east and west, becoming more evenly distributed around the BTM Complex. Noting this expansion in the drawdown area reaches the eastern boundary condition of the model domain. Recall that the east boundary was configured as a GHB condition, but limited to layer 1 in the Permian, aiming to account for flux from the upper catchment area and potential enhanced recharge due to orographic effects. The controlling heads for the GHB were assumed to be distant from the edge of the model at increased elevation in the upper catchment. It is unlikely that drawdown will propagate into the upper catchment, thereby affecting the controlling heads of the GHB. Both the controlling hydraulic head for the GHB and its assigned conductance were included in the uncertainty analysis. No-flow conditions in the lower layers along the eastern boundary align with the conceptualisation of the Hunter-Mooki Thrust Fault as a fixed vertical hydraulic barrier. The no-flow condition dominates the saturated thickness along the east edge of the Permian. Drawdown at this boundary is acceptable, given the conceptualisation.

The long-term likelihood for drawdowns observed in the model simulations is considered to be highly correlated with the pit lakes and other assumptions regarding prevailing climatic conditions. Uncertainty in the long-term pit lake equilibrium stage elevation was not accommodated in the uncertainty analysis. The uncertainty associated with changing climatic conditions was accounted for through mean recharge, which varied by +/-30% in each model realisation compared to the calibrated model. Greater percentage changes for uncertainty in recharge were initially applied at +/-50% but resulted in many model realisations failing to converge.

End of operations

200 years post - operations

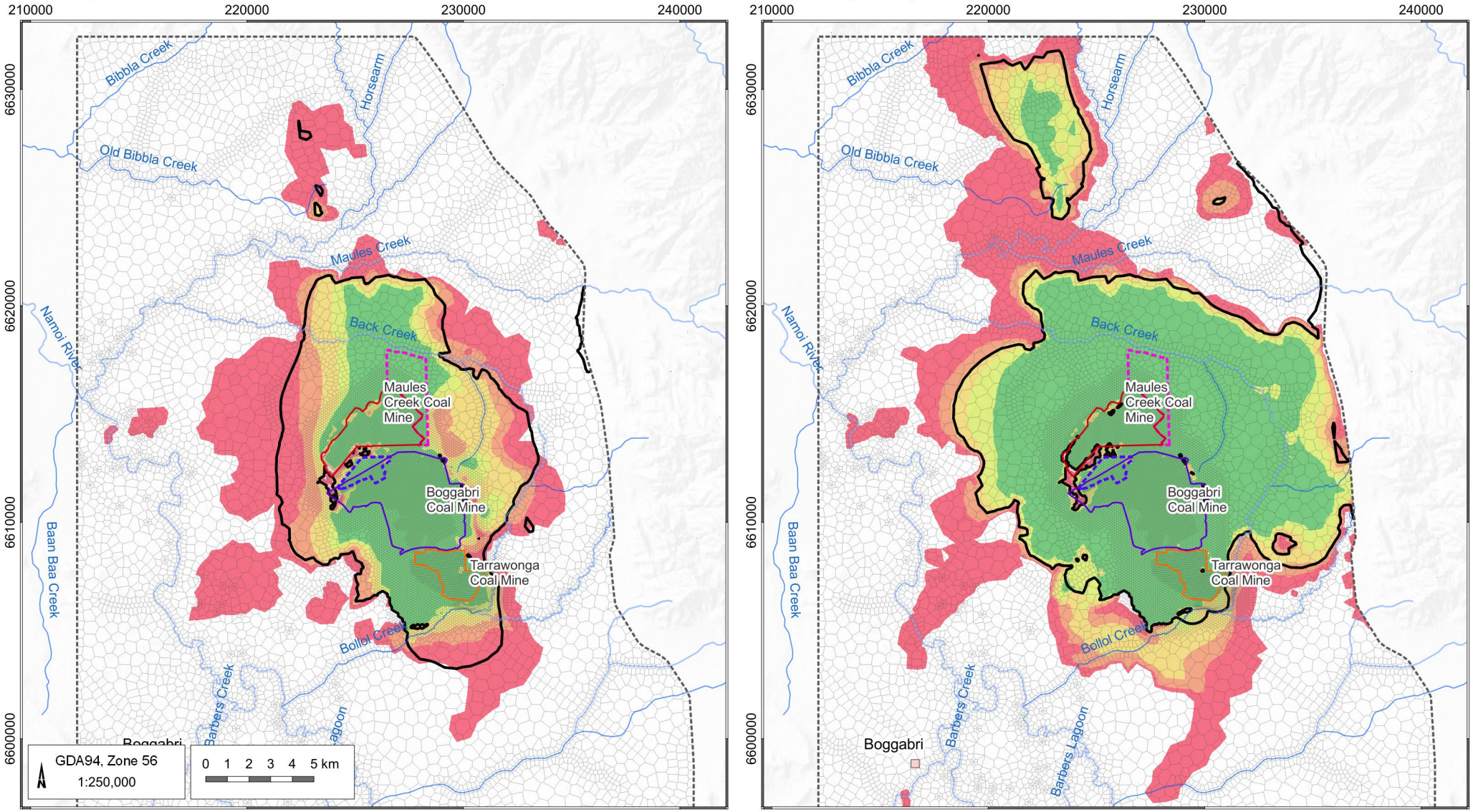

LEGEND

- MCCM Open Cut Extent
- BCM Open Cut Extent
- TCM Open Cut Extent
- BCM Modification Mining Area
- MCCM Continuation Project
- Model Extent
- Model Grid
- Base case 2m drawdown

Likelihood > 2 m drawdown

- 90 - 100 % (Very likely)
- 67 - 90 % (Likely)
- 33 - 67 % (About as likey as not)
- 10 - 33 % (Unlikely)
- 0 - 10 % (Very unlikely)

BTM Complex Groundwater Model Update 2024

AGE

Likelihood of water table drawdown exceeding 2 m at end of operations and after 200 years for Scenario 6

DATE
14/02/2025

FIGURE No:
F 75

©2025 Australasian Groundwater and Environmental Consultants Pty Ltd (AGE) - www.ageconsultants.com.au
Source: 1 second SRTM Derived DEM-S - © Commonwealth of Australia (Geoscience Australia) 2011.; GEODATA TOPO 250K Series 3 - © Commonwealth of Australia (Geoscience Australia) 2006.;
G:\Projects\MCJ5003.001 Maules Creek Continuation Project EIS\3_GIS\Workspaces\003_Stage 3 -EIS Report\Appendix F\F_75_MCJ5003_Likelihood of water table drawdown exceeding 2 m at end of operations and after 200 years for Scenario 6.qgz

F9.2.2 Uncertainty at drawdown in water supply bores

A large number (1247) of reportable locations were assessed for maximum drawdown from the DSI approach. Here, a few selected outputs are provided to demonstrate the prior and posterior histograms from the ensemble of models, thus reporting uncertainty in these predictions. In Figure F 76, the x-axis shows the drawdown in meters, whereas the y-axis shows the frequency/density of the drawdowns. Each plot provides the location ID and its coordinates. In all cases, predictive uncertainty is significantly reduced for each location when comparing the prior and posterior histograms. This reduction is driven by the DSI training process, where the behavioural model runs (i.e., model runs within an acceptable margin of error) inform the uncertainty analysis. Note that these observations are not time-specific but the maximum observed throughout operations and post-closure.

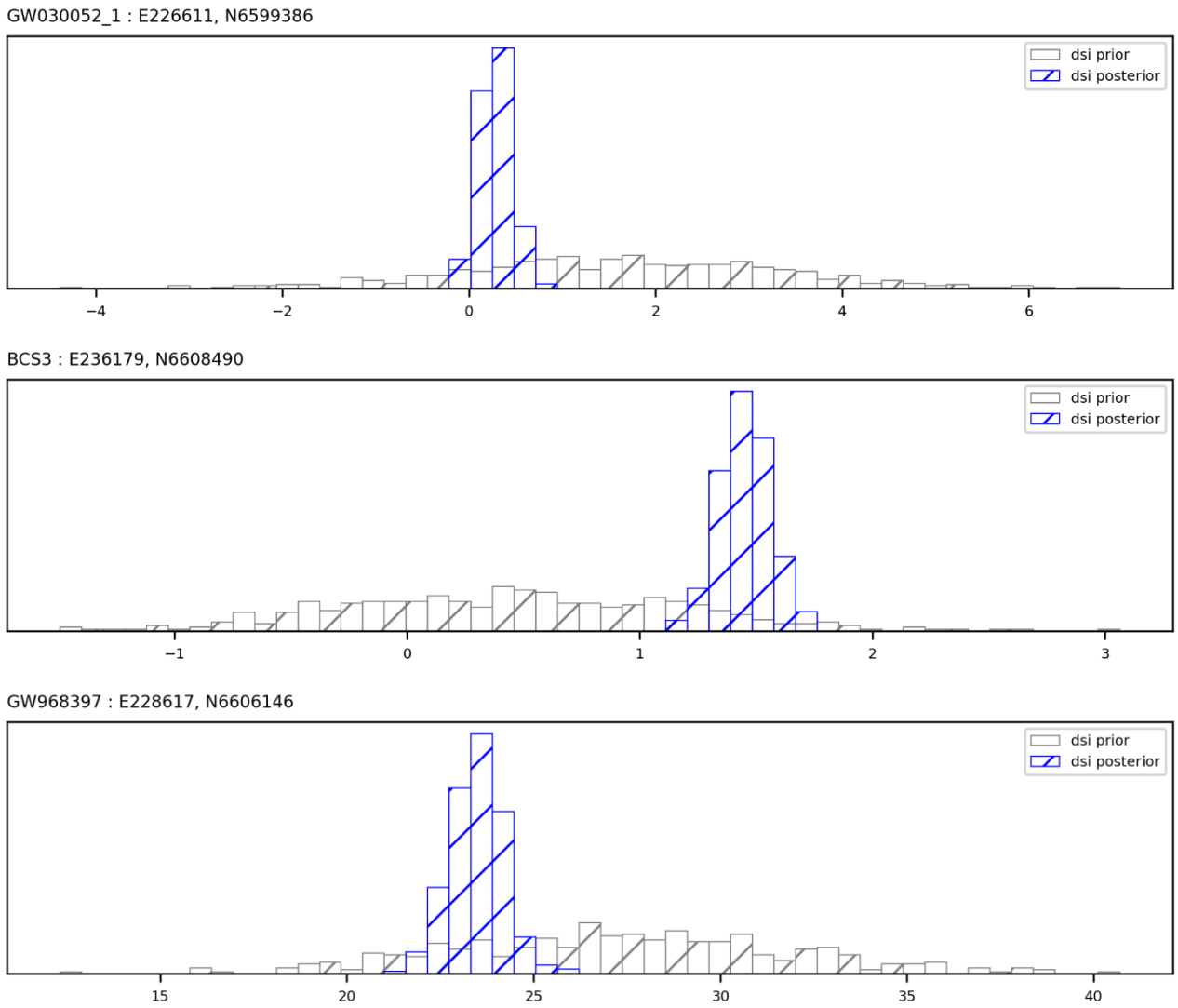

Figure F 76 Examples of maximum drawdown predictions at select locations

Two tables provided in Sections F14 and F15 list the estimated maximum drawdown at existing water supply bores. The table in Section F14 presents the maximum simulated drawdown from the calibrated model and includes the year within the simulation that the maximum drawdown was observed. The table in Section F15 lists the DSI mean prediction for maximum drawdown and the uncertainty associated with each prediction described by standard deviation, interquartile range and maximum and minimum predicted value. Note that zero entries in the table were originally small negative numbers and converted to zero.

F9.2.3 Uncertainty in water take

An uncertainty analysis in water take was included but limited to cumulative fluxes, that is, not apportioned between the different mines in the BTM Complex. In addition, the plots only include fluxes during operational periods. Figure F 77 and Figure F 78 present the water take obtained from DSI as box plots for each year for Zone 4 and Zone 11, respectively. The boxes of the box plots indicate the interquartile range of simulated values, while the whiskers denote the effective maximum and minimum water take. The circles are considered outliers. The fluxes are comparable to those observed in the Scenario 6 model simulation. The uncertainty in the predictions is relatively small, with most interquartile ranges spanning approximately 5 ML to 25 ML or less. It is worth noting that the uncertainty in water take for zone 4, expressed by the interquartile range in the box plots, seems to decrease slightly the further the simulation progresses in time. For zone 11, the contrary is observed.

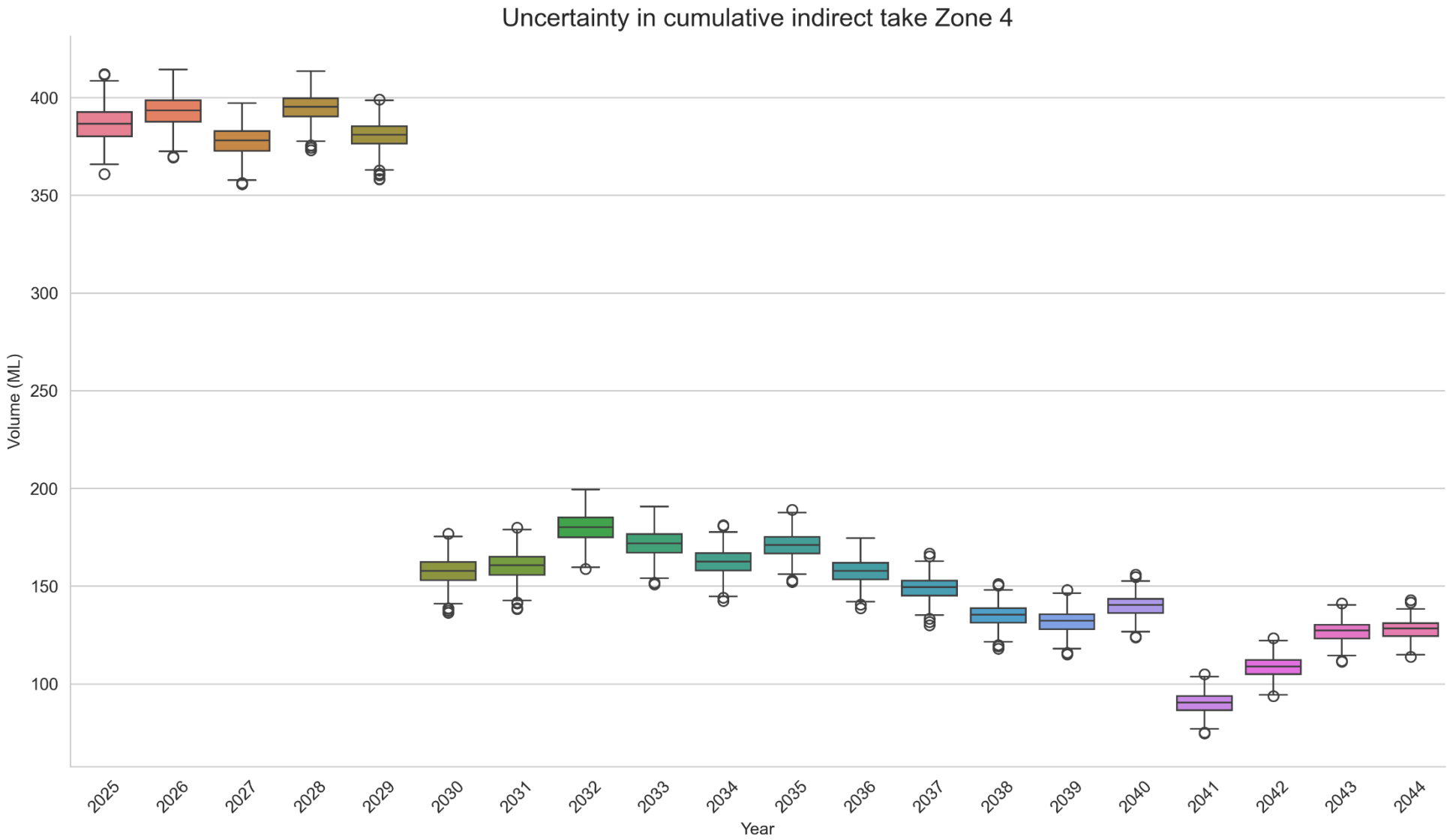

Figure F 77 Uncertainty in indirect take from Zone 4

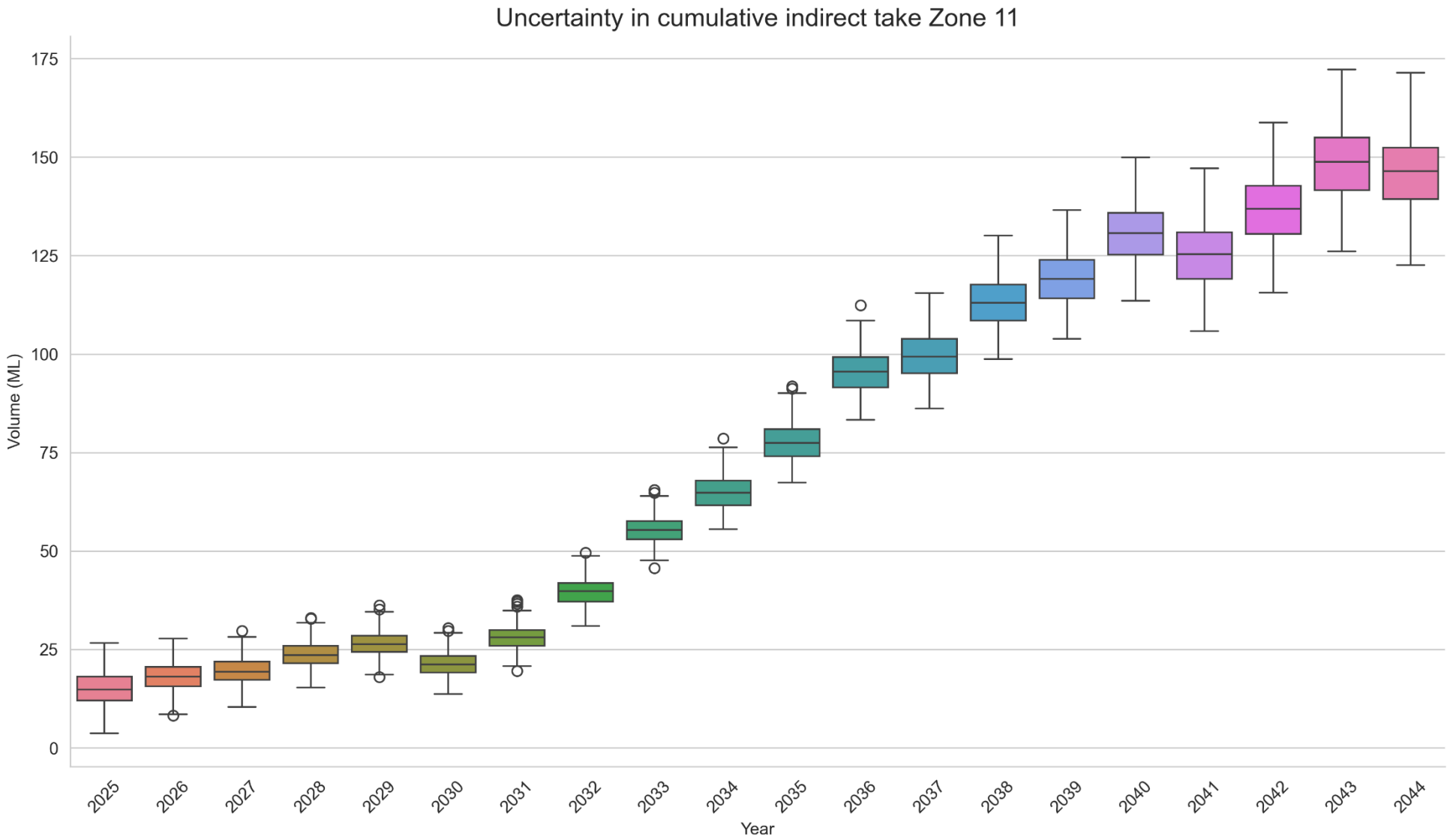

Figure F 78 Uncertainty in indirect take from Zone 11

F9.2.4 Uncertainty in mine inflows

Simulated observations of annual inflow into each mine were also included in the uncertainty analysis with DSI. Note that variability in predicted inflows is mainly related to how the mine plan is implemented as a stress in the model since all other stresses are assigned average values, making them effectively static. Figure F 79 to Figure F 81 show the mean mine inflow predicted as a bar graph for MCCM, BCM and TCM, respectively. At the top of each bar in the bar graphs is an indication of the range in the prediction covered by three standard deviations (0.03 to 99.7 percentiles). Here, there is also reasonable agreement with the predictions from the Scenario 6 model with uncertainties up to 200 ML in inflows at MCCM, up to 275 ML at BCM, and up to 220 ML at TCM. The uncertainty range is comparable to that of a constrained Monte-Carlo style approach, where structural error may play a significant role in predictive variance.

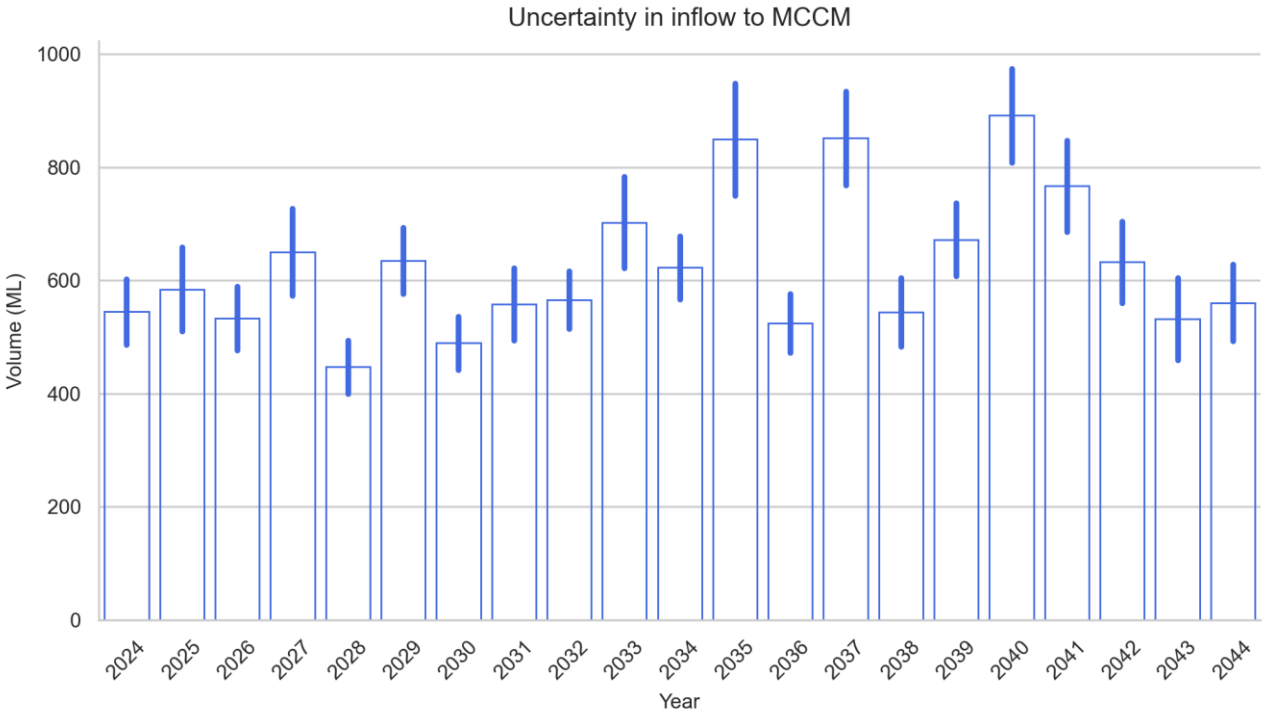

Figure F 79 Uncertainty in inflows to MCCM

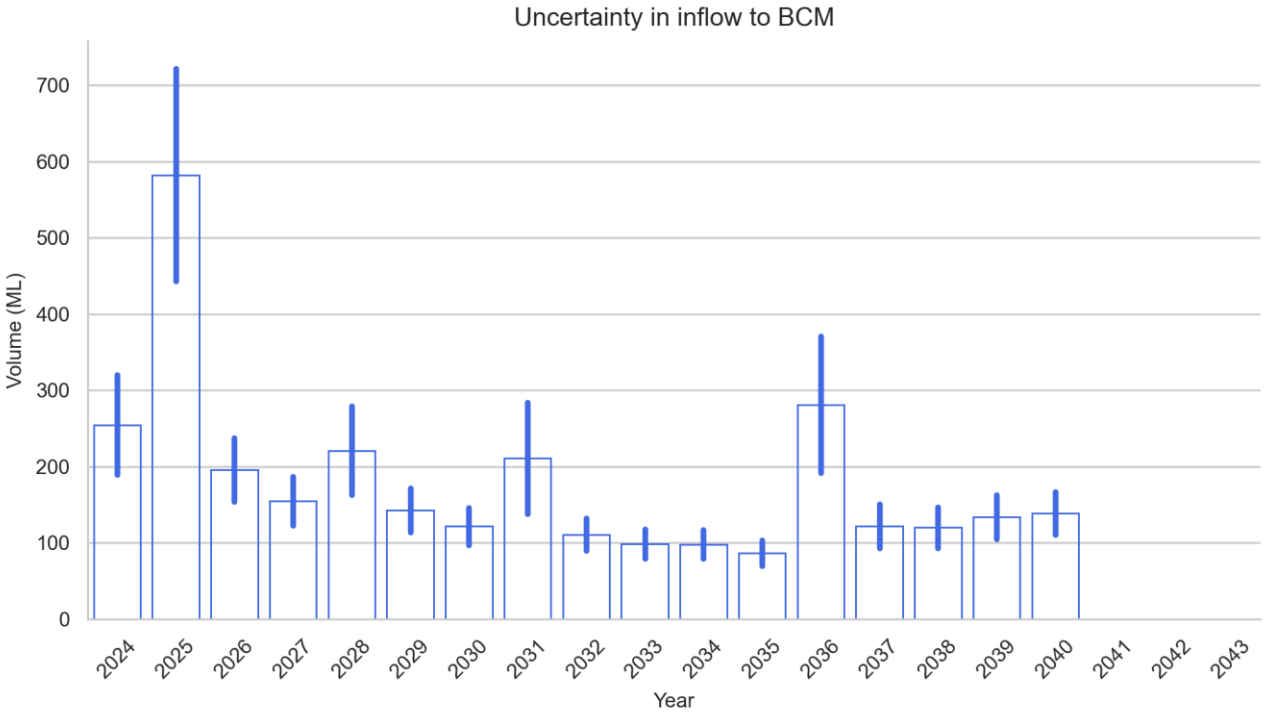

Figure F 80 Uncertainty in inflows to BCM

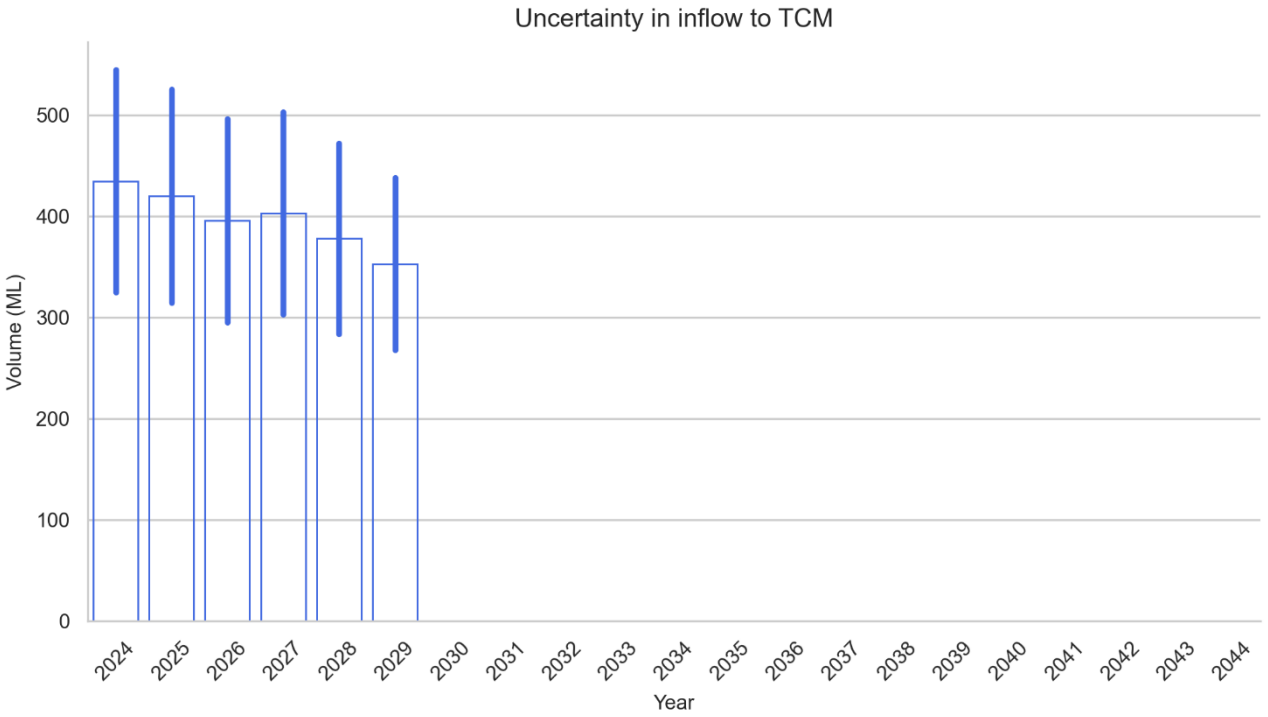

Figure F 81 Uncertainty in inflows to TCM

F10 Climate change considerations

Forecasted changes to mean rainfall and mean temperature are provided by the NSW and Australian regional climate modelling (NARCliM)[7] project for the next 100 years. Predicted increases to mean temperature range between 1.6°C and 4.5°C under low and high emission scenarios, respectively. Average rainfall is predicted to reduce by 11% under low-emission scenarios and 8% under high-emission scenarios.

It is unclear what the combined effect of these changes may have on recharge to the system because diffuse rainfall recharge is not considered a primary driver of the water balance. Mean recharge is more influenced by flow events in the ephemeral creeks. Consequently, assuming a change of +/- 30% to recharge was considered a suitable proxy for the combined effect of predicted future changes to average temperature and rainfall.

The model used for uncertainty analysis simulates post-closure conditions for up to 200 years. This obviates the need for individual scenario simulations to assess climate change effects, as the primary influence on the system associated with climate change is captured in the analysis.

F11 Peer review

The groundwater modelling was independently reviewed by Dr Noel Merrick. Dr Merrick has significant expertise in groundwater modelling and coal mining in NSW and has previously been involved in the independent peer review of the BTM Complex groundwater model. The peer review report is contained within Appendix G.

[7] https://www.climatechange.environment.nsw.gov.au.

F12 References

Australasian Groundwater and Environmental Consultants Pty Ltd (AGE. 2010). *Continuation of Boggabri Coal Mine Groundwater Assessment, Project G1465.* Boggabri Coal Pty Ltd.

Australasian Groundwater and Environmental Consultants Pty Ltd (AGE. 2011). *Maules Creek Coal Project Groundwater Impact Assessment prepared for Aston Resources Limited. Project No. G1508.* Brisbane: AGE Consultants.

Australasian Groundwater and Environmental Consultants Pty Ltd (AGE. 2014). *Maules Creek Coal Project Installation of Monitoring Bore Network and Updating Groundwater Model. Prepared for Whitehaven Coal Project No. G1508/B, January 2014.* Brisbane: AGE Consultants.

Australasian Groundwater and Environmental Consultants Pty Ltd (AGE. 2018). *Boggabri, Tarrawonga, Maules Creek Complex Numerical Model Update, project number G1850A.* Brisbane: Australian Groundwater and Environmental Consultants.

Australasian Groundwater and Environmental Consultants Pty Ltd (AGE. 2022). *Boggabri, Tarrawonga, Maules Creek Complex Groundwater Model Update v04.04, project number G1850P.* Brisbane: Australian Groundwater and Environmental Consultants.

Australasian Groundwater and Environmental Consultants Pty Ltd (AGE. 2023). *Maules Creek Continuation Project EIS Groundwater Modelling Plan.* Brisbane: Australasian Groundwater and Environmental Consultants Pty Ltd.

Allen, R., Pereira, L. S., Raes, D., & Smith, M. (1998). Crop evapotranspiration: guidelines for computing crop water requirements. *Irrigation and Drainage Paper 56*, p. 300.

Barnett, B., Townley, L. R., Post, V., Evans, R. E., Hunt, R. J., Peeters, L., . . . Boronkay, A. (2012). *Australian groundwater modelling guidelines. Waterlines report.* Canberra: National Water Commission.

Boussinesq, J. (1877). *Essai sur la théorie des eaux courantes*. Mémoires présentées par divers savants à l'Académie des Sciences. Paris, France: Imprimerie Nationale.

Commonwealth of Australia. (2024). *Information Guidelines Explanatory Note: Using impact pathway diagrams based on ecohydrological conceptualisation in environmental impact assessment.* Department of Climate Change, Energy, the Environment and Water, Independent Expert Scientific Committee on Unconventional Gas Development and Large Coal Mining Development. Canberra: Commonwealth of Australia.

Commwealth of Australia. (2024). *Information Guidelines Explanatory Note Using impact pathway diagrams based on ecohydrological conceptualisation in environmental impact assessment.* Canberra: Commonwealth of Australia.

de Silva, C. S., & Rushton, K. R. (2007). Groundwater recharge estimation using improved soil moisture balance methodology for a tropical climate with distinct dry seasons. *Hydrological Sciences Journal, 52*(5), 1051-1067.

de Silva, C. S., & Rushton, K. R. (2007). Groundwater recharge estimation using improved soil moisture balance methodology for a tropical climate with distinct dry seasons. *Hydrological Sciences Journal, 52*(5), 1051-1067. doi:https://doi.org/10.1623/hysj.52.5.1051.

Doherty, J. (2024). *PEST_HP.* Watermark Numerical Computing. Retrieved from https://pesthomepage.org/programs.

Doherty, J., & Moore, C. (n.d.). Decision support modelling viewed through the lens of model complexity. *GMDSI Monograph*.

Doody, T. M., & Moore, C. (2019). *Information Guidelines Explanatory Note: Assessing groundwater-dependent ecosystems.* Canberra: Independent Expert Scientific Committee on Coal Seam Gas and Large Coal Mining Development, Department of the Environment and Energy, Commonwealth of Australia. Retrieved from https://www.iesc.gov.au/sites/default/files/2022-07/information-guidelines-explanatory-note-assessing-groundwater-dependent-ecosystems.pdf.

Edelman, F. (1947) Over de berekening van grond water stromingen, Delft University. PhD thesis.

HydroAlgorithmics. (2016). AlgoMesh version 1.2. Retrieved from https://www.hydroalgorithmics.com/algomesh-version-1-2-released.

HydroSimulations. (2018). *Vickery Extension Project Groundwater Assessment, project number WHI013, report HS2018/05g.* Whitehaven Coal Pty Ltd.

IESC. (2023). *Using impact pathway diagrams in environmental impact assessment, IESC information guideline explanatory note.* Commonwealth of Australia. Retrieved from https://www.iesc.gov.au/sites/default/files/2023-08/consultation-info-guideline-en-using-impact-pathway-diagrams-2023.pdf.

Middlemis, H. (2004). *model development is an on-going process of refinement from an initially simple representation of the aquifer system to one with an appropriate degree of complexity.* model development is an on-going process of refinement from an initially simple representation of the aquifer system to one with an appropriate degree of complexity.

Middlemis, H., & Peeters, L. J. (2018). *Information Guidelines Explanatory Note: Uncertainty analysis – guidance for groundwater.* Independent Expert Scientific Committee on Coal Seam Gas and Large Coal Mining Development through the Department of the Environment and Energy, Commonwealth of Australia. Retrieved from https://www.iesc.gov.au/publications/information-guidelines-explanatory-note-uncertainty-analysis.

Murray, T. A., & Power, W. L. (2021). *Information Guidelines Explanatory Note: Characterisation and modelling of geological fault zones.* Independent Expert Scientific Committee on Coal Seam Gas and Large Coal Mining Development through the Department of Agriculture, Water and the Environment, Commonwealth of Australia.

NSW Department of Planning and Envionment. (2022d). *Cumulative Groundwater Impact Assessment Approaches.* NSW Department of Planning and Envionment.

NSW Department of Planning and Environment. (2022a). *Groundwater assessment toolbox for major projects in NSW - Overview document. Technical guideline prepared for the Water group.* NSW Department of Planning and Environment.

NSW Department of Planning and Environment. (2022b). *Guidelines for Groundwater Documentation for SSD/SSI Projects. Technical guideline.* NSW Department of Planning and Environment.

NSW Department of Planning and Environment. (2022c). *Minimum Groundwater Modelling Requirements for SSD/SSI Projects. Technical Guidelines.* NSW Department of Planning and Environment.

Parsons Brinkerhoff. (2005). *Boggabri Coal Project - Groundwater Assessment.* Idemitsu Boggabri Coal Pty Ltd.

Parsons Brinkerhoff. (2008). *Updated Boggabri Model for Boggabri Mine Extension.* Idemitsu Boggabri Coal Pty Ltd.

Peeters, L. J., & Middlemis, H. (2023). *Information Guidelines Explanatory Note: Uncertainty analysis for groundwater modelling, A report prepared for the Independent Expert Scientific Committee on Coal Seam Gas and Large Coal Mining Development through the Department of Climate Change, Energy.* Canberra: Commonwealth of Australia. Retrieved from https://www.iesc.gov.au/sites/default/files/2022-07/information-guidelines-explanatory-note-uncertainty-analysis.pdf.

Rawls, W. J., Ahuja, L. R., Brakensiek, D. L., & Shirmohammadi, A. (1992). Infiltration and soil water movement. In D. R. Maidment, *Handbook of Hydrology* (p. 1424). New York: McGraw-Hill.

Rushton, K. R., Eilers, V. H., & Carter, R. C. (2006). Improved soil moisture balance methodology for recharge estimation. *Journak od Hydrogeology*(318), 379-399.

State Government of NSW and NSW Department of Climate Change, Energy, the Environment and Water. (2012). Hydrologic Soil Groups (HSG) of NSW. *The Sharing and Enabling Environmental Data Portal*. Retrieved from The Sharing and Enabling Environmental Data Portal: https://datasets.seed.nsw.gov.au/dataset/b6af12aa-a167-4486-8092-96a047a1e13d], date accessed 2024-06-19.

Wilson, S. R., & Lu, X. (2011). *Rainfall recharge assessment for Otago groundwater basins, Otago Regional Council technical report.*

F13 Calibration hydrographs

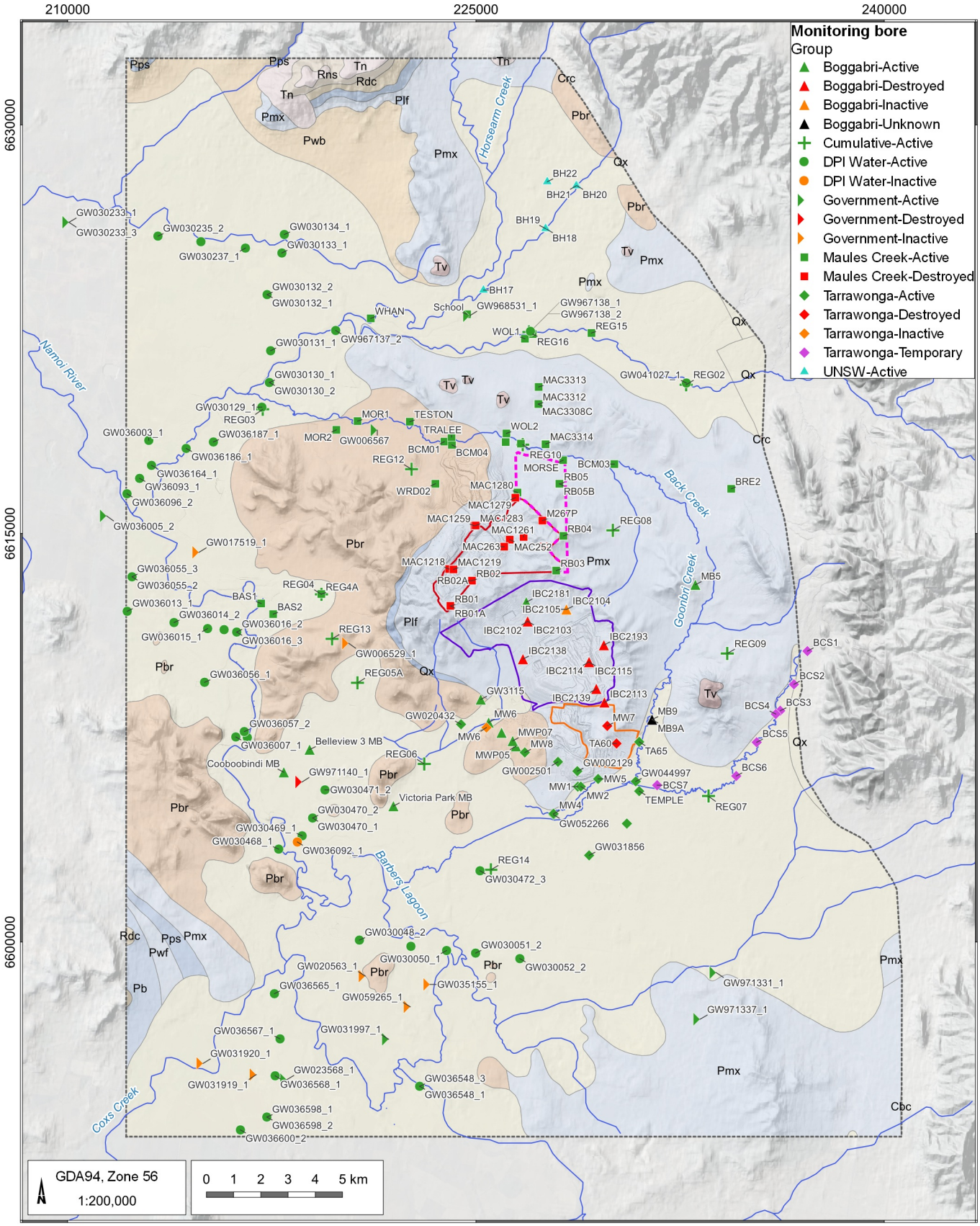

LEGEND

- Drainage
- MCCM Open Cut Extent
- BCM Open Cut Extent
- TCM Open Cut Extent
- MCCM Continuation Project
- BTM Complex numerical model extent

Gunnedah Coalfield rock unit (1:100k)

- Qx - Quaternary Sediments
- Tn - Tertiary Nandewar Volcanics
- Tv - Tertiary Volcanics
- Rns - Napperby Formation
- Rdc - Digby Formation
- Pb - Pamboola Formation
- Pwf - Watermark Formation
- Pps - Porcupine Formation
- Pmx - Maules Creek and Goonbri formations
- Plf - Leard Formation
- Pwb - Werrie Basalt
- Pbr - Boggabri Volcanics
- Cbc - Currabubula Formation
- Crc - Rocky Creek Conglomerate

BTM Complex Groundwater Model Update 2024

Regional groundwater monitoring network

AGE

DATE 26/03/2025

FIGURE No: **F 82**

©2025 Australasian Groundwater and Environmental Consultants Pty Ltd (AGE) - www.ageconsultants.com.au

Source: 1 second SRTM Derived DEM-S - © Commonwealth of Australia (Geoscience Australia) 2011.; GEODATA TOPO 250K Series 3 - © Commonwealth of Australia (Geoscience Australia) 2006.;
G:\Projects\MCJ5003.001 Maules Creek Continuation Project EIS\3_GIS\Workspaces\003_Stage 3 -EIS Report\Appendix F\F_82_MCJ5003.001_Regional groundwater monitoring network.qgz

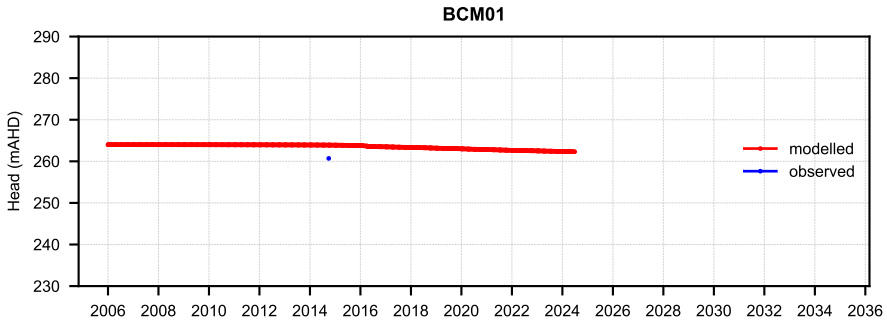
BCM01
Head (mAHD)
290
280
270
260
250
240
230
2006 2008 2010 2012 2014 2016 2018 2020 2022 2024 2026 2028 2030 2032 2034 2036
modelled
observed

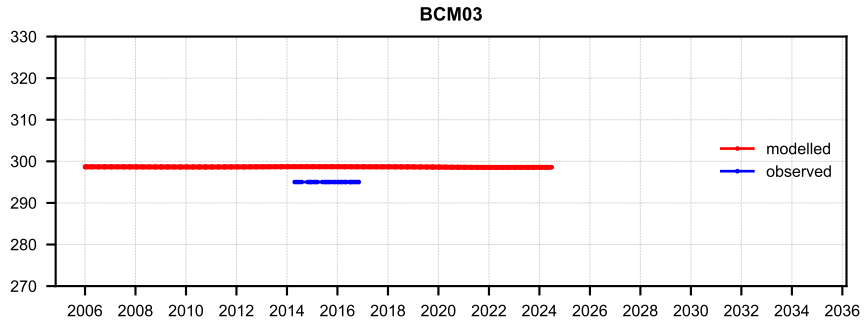
BCM03
330
320
310
300
290
280
270
2006 2008 2010 2012 2014 2016 2018 2020 2022 2024 2026 2028 2030 2032 2034 2036
modelled
observed

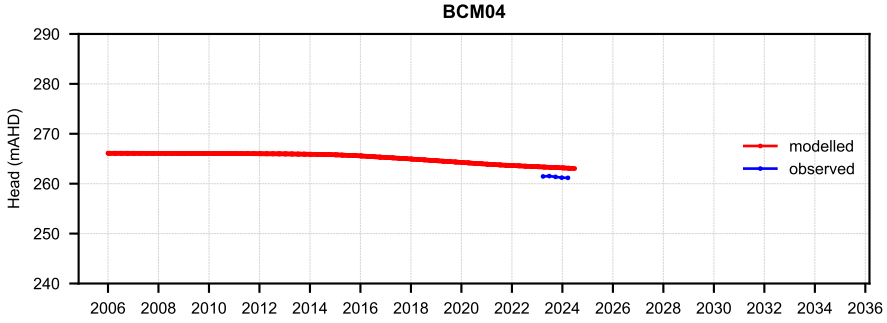
BCM04
Head (mAHD)
290
280
270
260
250
240
2006 2008 2010 2012 2014 2016 2018 2020 2022 2024 2026 2028 2030 2032 2034 2036
modelled
observed

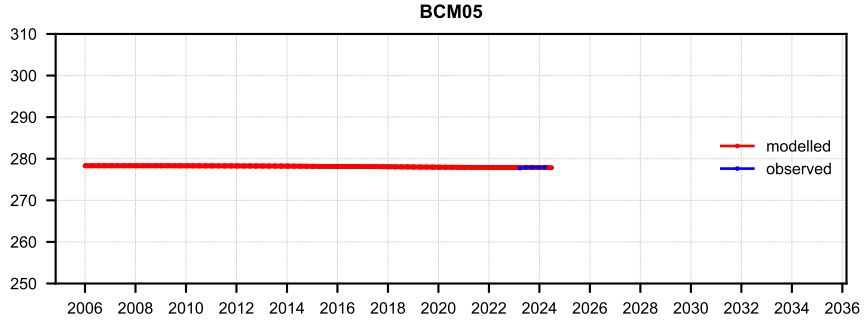
BCM05
310
300
290
280
270
260
250
2006 2008 2010 2012 2014 2016 2018 2020 2022 2024 2026 2028 2030 2032 2034 2036
modelled
observed

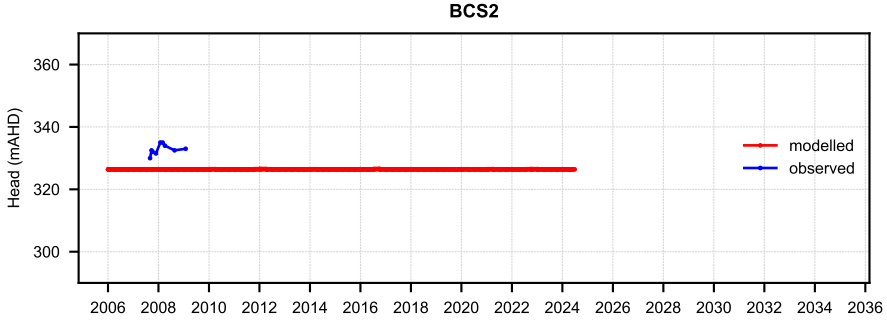
BCS2
Head (mAHD)
360
340
320
300
2006 2008 2010 2012 2014 2016 2018 2020 2022 2024 2026 2028 2030 2032 2034 2036
modelled
observed

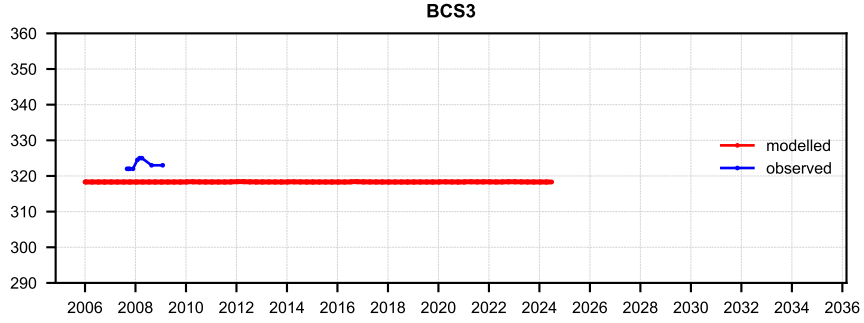
BCS3
360
350
340
330
320
310
300
290
2006 2008 2010 2012 2014 2016 2018 2020 2022 2024 2026 2028 2030 2032 2034 2036
modelled
observed

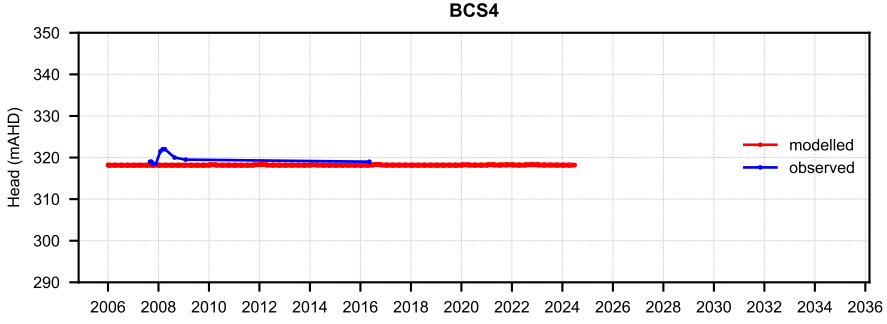
BCS4
Head (mAHD)
350
340
330
320
310
300
290
2006 2008 2010 2012 2014 2016 2018 2020 2022 2024 2026 2028 2030 2032 2034 2036
modelled
observed

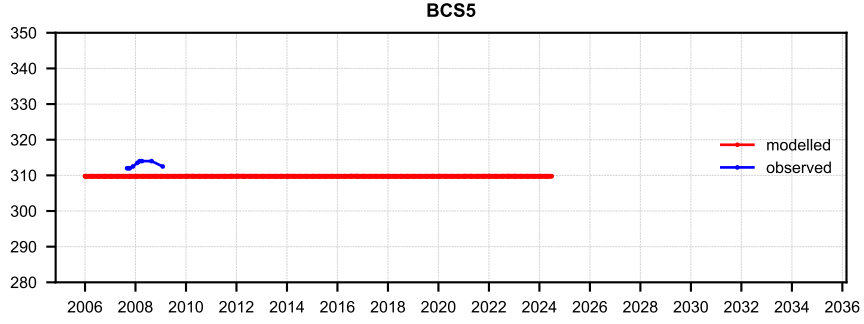
BCS5
350
340
330
320
310
300
290
280
2006 2008 2010 2012 2014 2016 2018 2020 2022 2024 2026 2028 2030 2032 2034 2036
modelled
observed

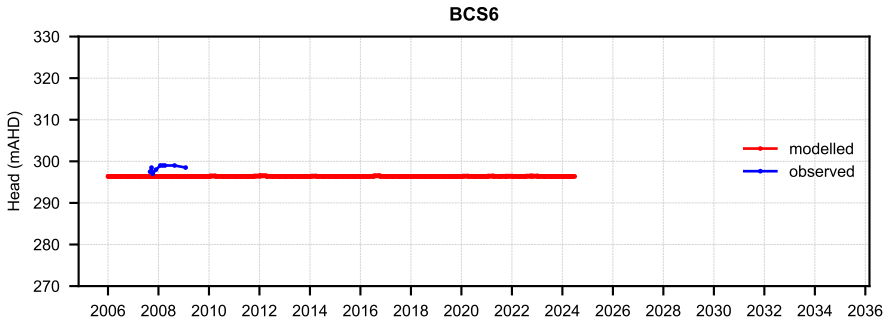
BCS6
Head (mAHD)
330
320
310
300
290
280
270
2006 2008 2010 2012 2014 2016 2018 2020 2022 2024 2026 2028 2030 2032 2034 2036
modelled
observed

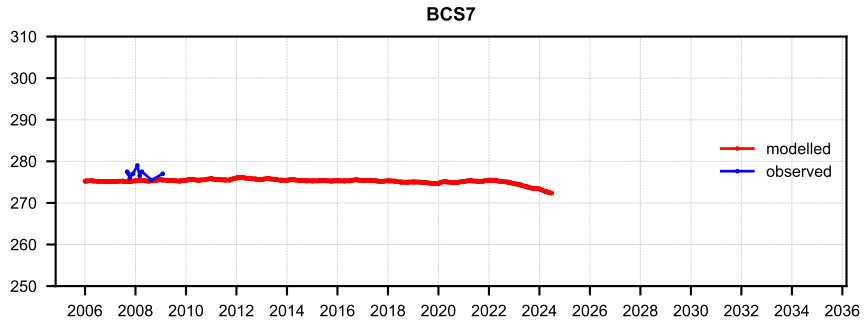
BCS7
310
300
290
280
270
260
250
2006 2008 2010 2012 2014 2016 2018 2020 2022 2024 2026 2028 2030 2032 2034 2036
modelled
observed

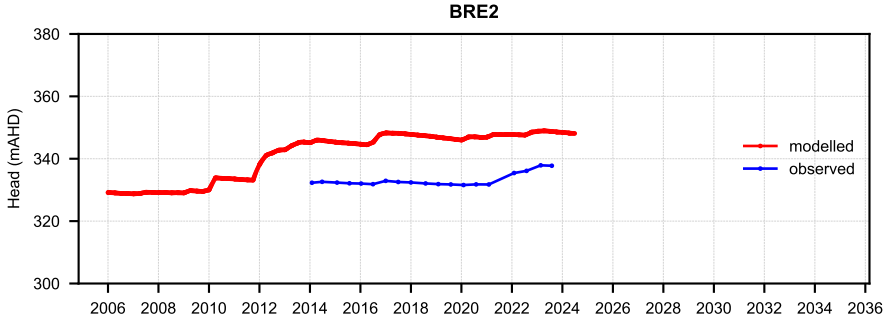
BRE2
Head (mAHD)
380
360
340
320
300
2006 2008 2010 2012 2014 2016 2018 2020 2022 2024 2026 2028 2030 2032 2034 2036
modelled
observed

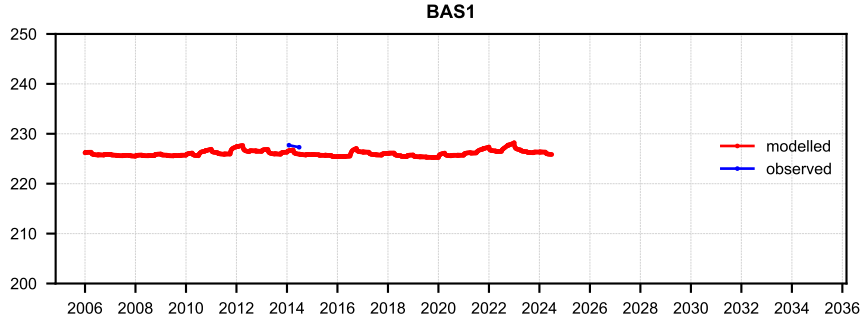
BAS1
250
240
230
220
210
200
2006 2008 2010 2012 2014 2016 2018 2020 2022 2024 2026 2028 2030 2032 2034 2036
modelled
observed

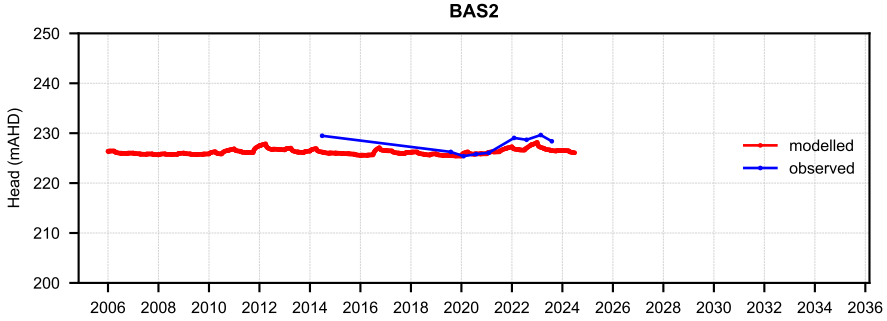
BAS2
Head (mAHD)
250
240
230
220
210
200
2006 2008 2010 2012 2014 2016 2018 2020 2022 2024 2026 2028 2030 2032 2034 2036
modelled
observed

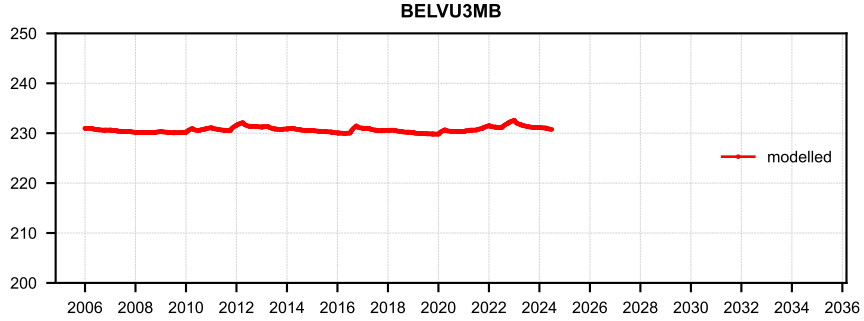
BELVU3MB
250
240
230
220
210
200
2006 2008 2010 2012 2014 2016 2018 2020 2022 2024 2026 2028 2030 2032 2034 2036
modelled

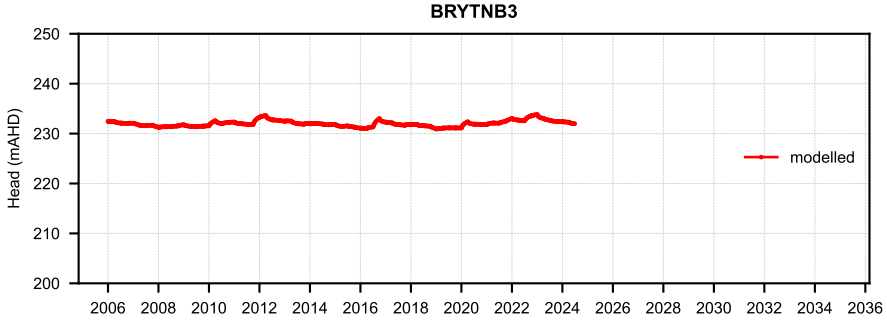
BRYTNB3
Head (mAHD)
250
240
230
220
210
200
2006 2008 2010 2012 2014 2016 2018 2020 2022 2024 2026 2028 2030 2032 2034 2036
modelled

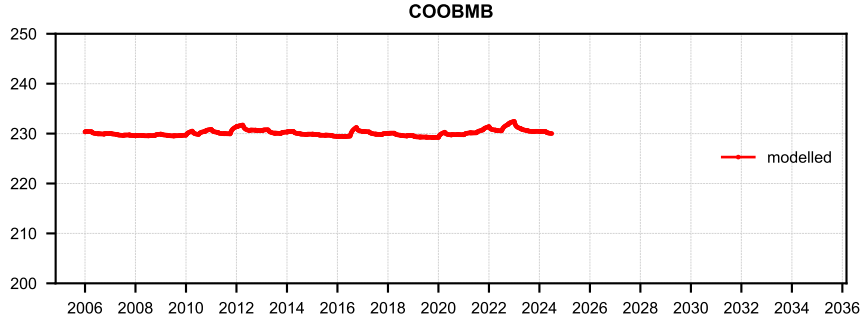
COOBMB
250
240
230
220
210
200
2006 2008 2010 2012 2014 2016 2018 2020 2022 2024 2026 2028 2030 2032 2034 2036
modelled

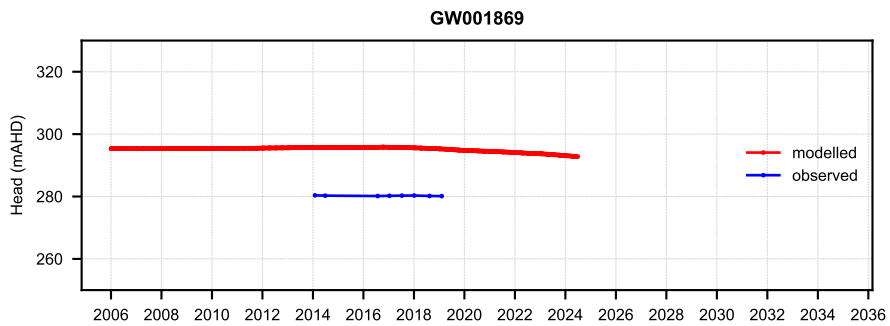
GW001869
Head (mAHD)
modelled
observed

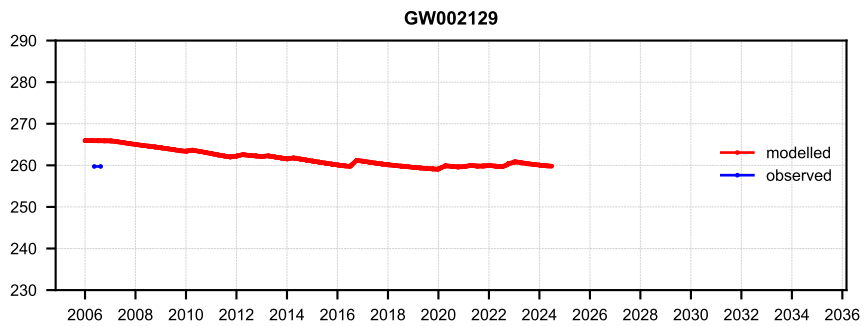
GW002129
modelled
observed

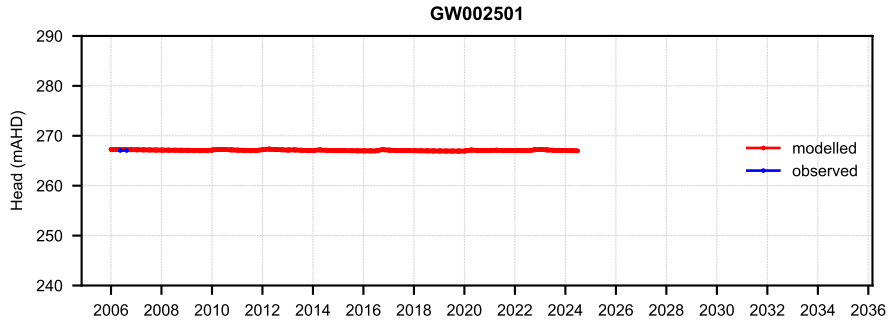
GW002501
Head (mAHD)
modelled
observed

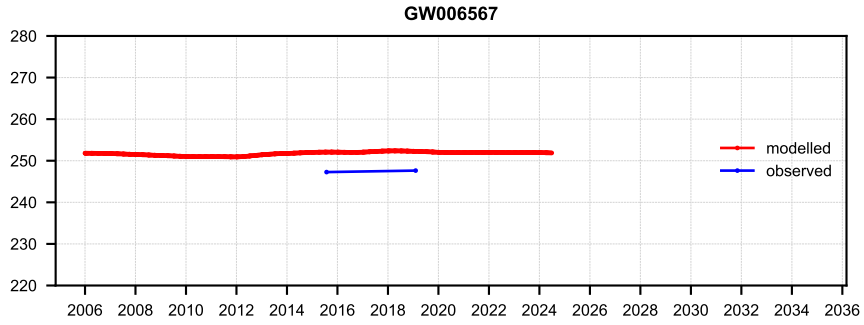
GW006567
modelled
observed

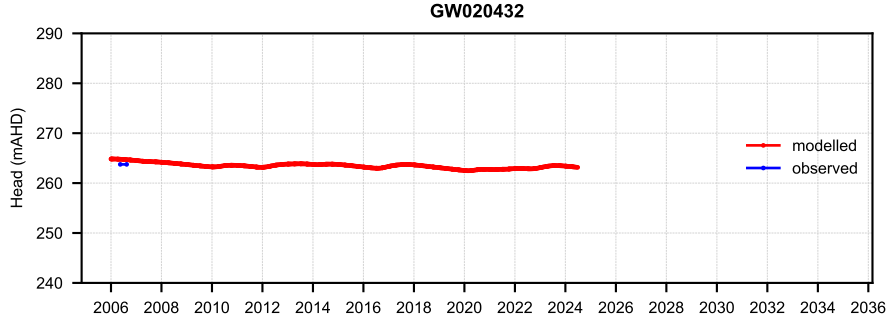
GW020432
Head (mAHD)
modelled
observed

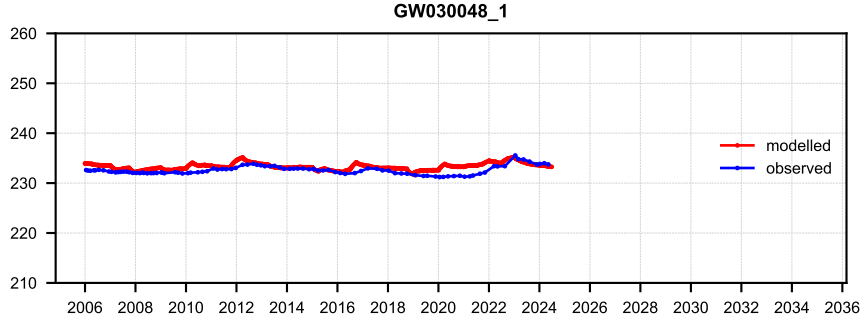
GW030048_1
modelled
observed

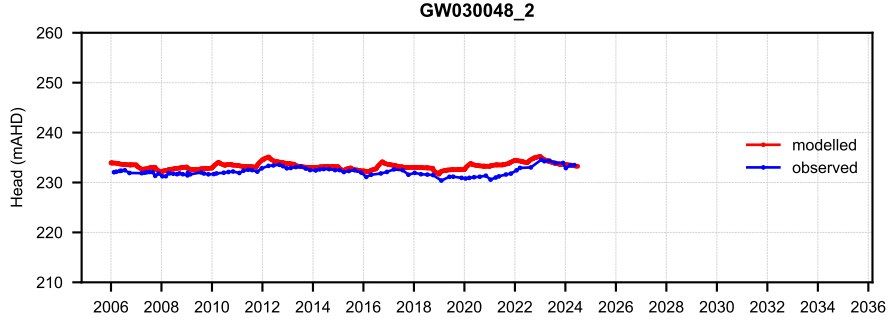
GW030048_2
Head (mAHD)
modelled
observed

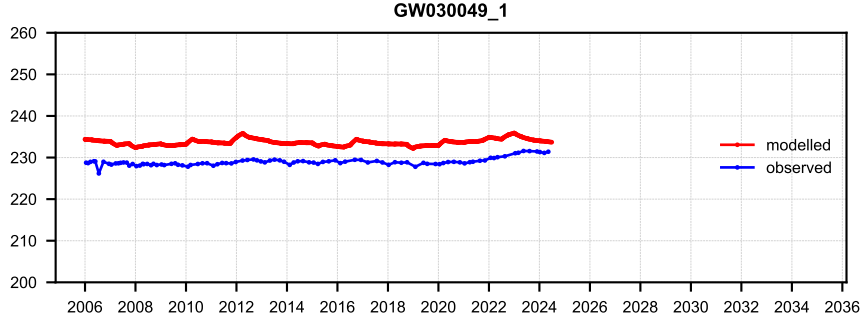
GW030049_1
modelled
observed

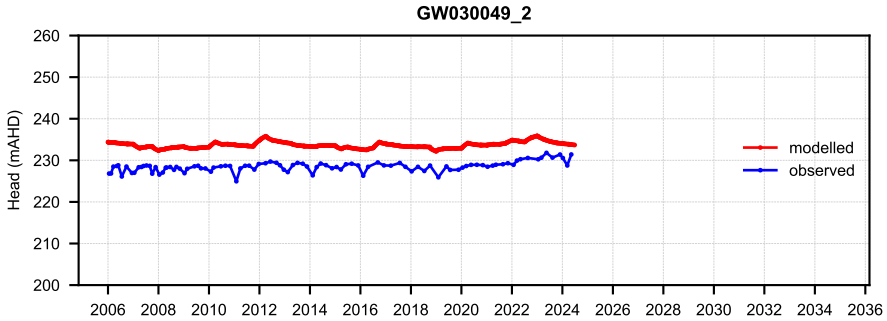
GW030049_2
Head (mAHD)
modelled
observed

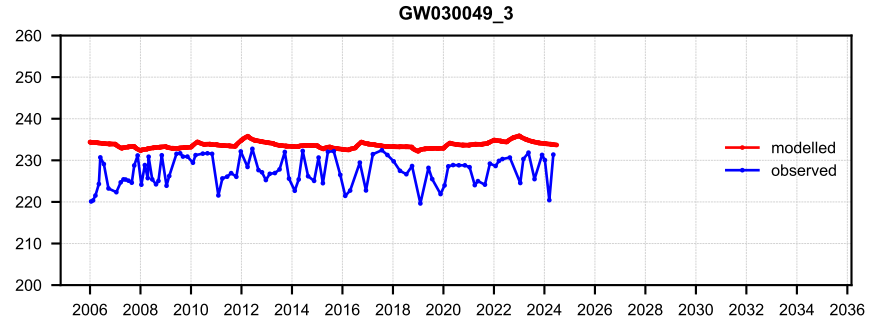
GW030049_3
modelled
observed

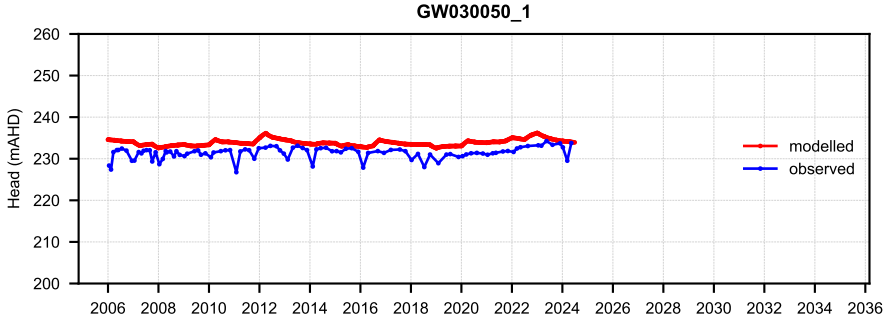
GW030050_1
Head (mAHD)
modelled
observed

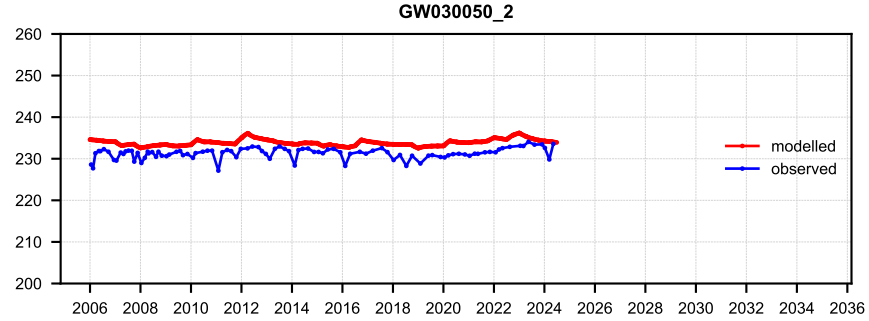
GW030050_2
modelled
observed

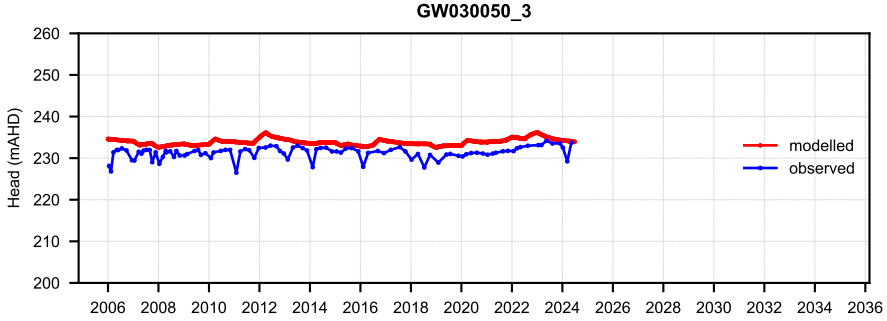
GW030050_3
Head (mAHD)
modelled
observed

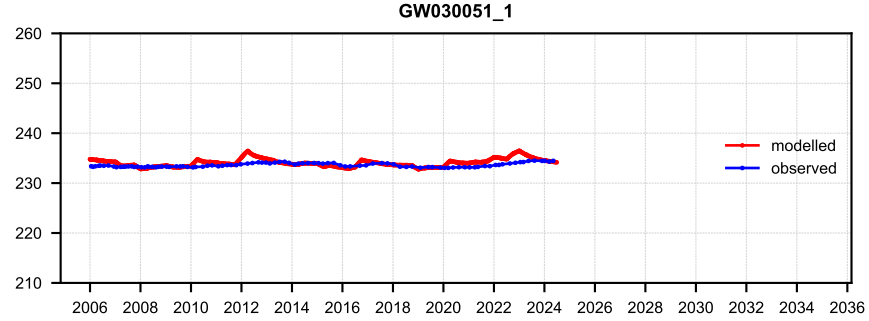
GW030051_1
modelled
observed

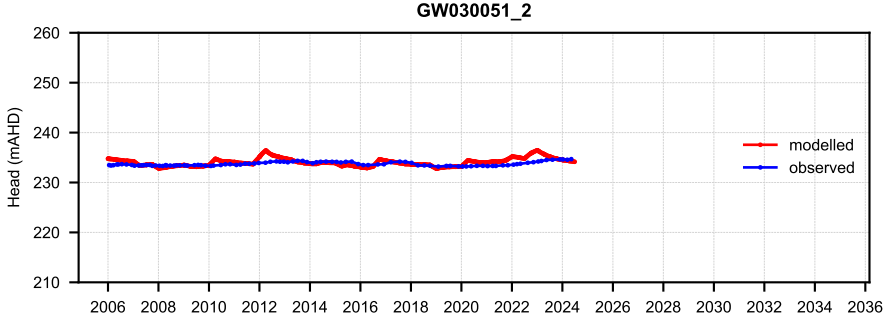
GW030051_2
Head (mAHD)
modelled
observed

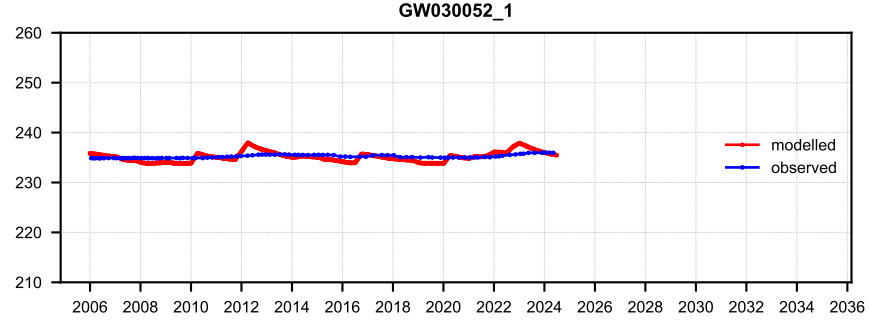
GW030052_1
modelled
observed

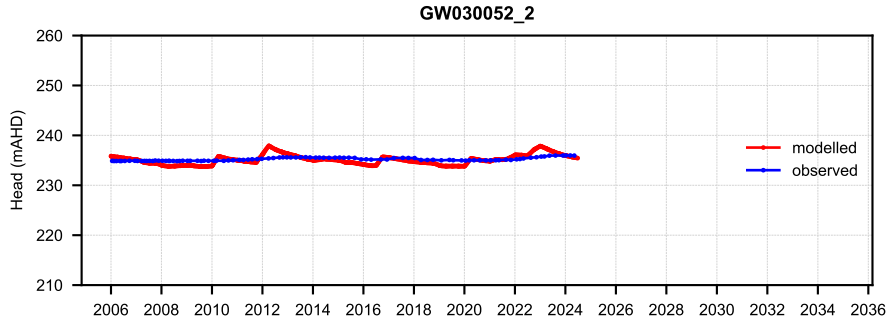
GW030052_2
Head (mAHD)
modelled
observed

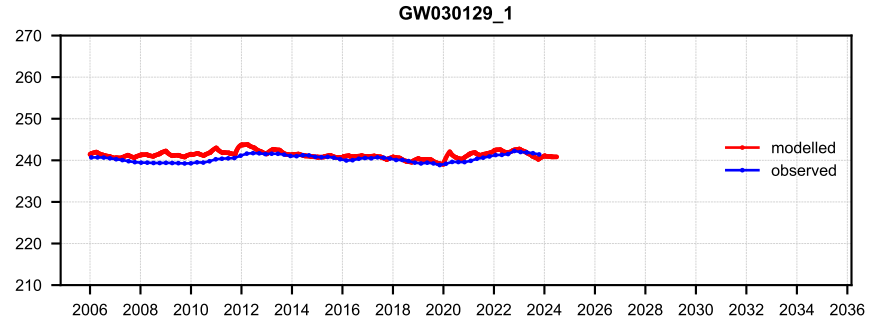
GW030129_1
modelled
observed

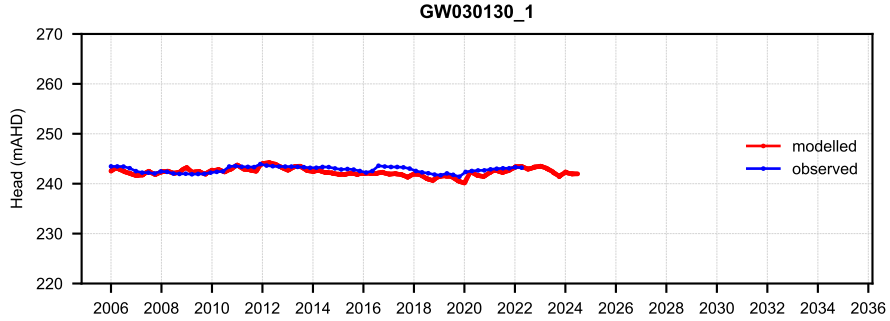
GW030130_1
Head (mAHD)
modelled
observed

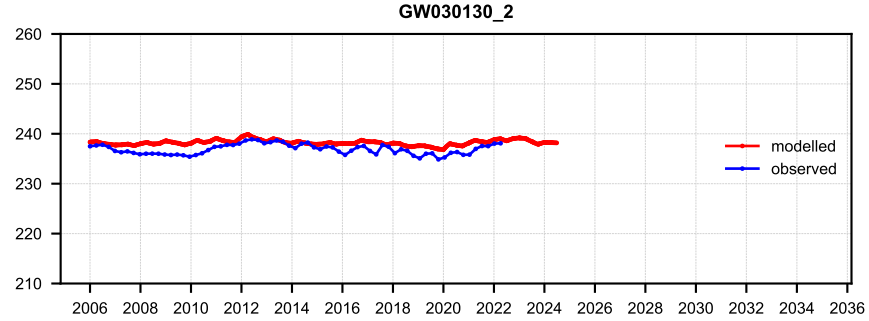
GW030130_2
modelled
observed

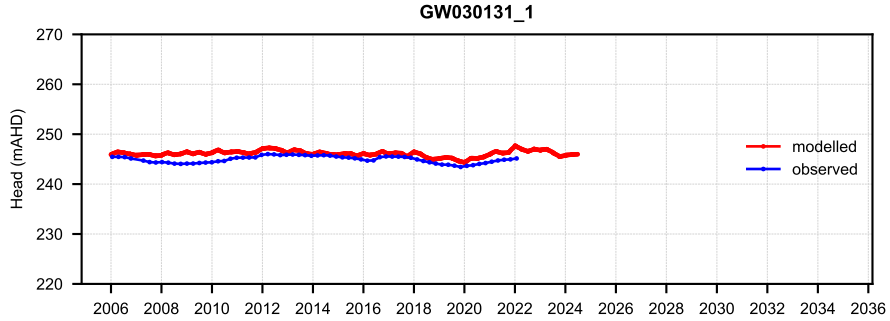
GW030131_1
Head (mAHD)
modelled
observed

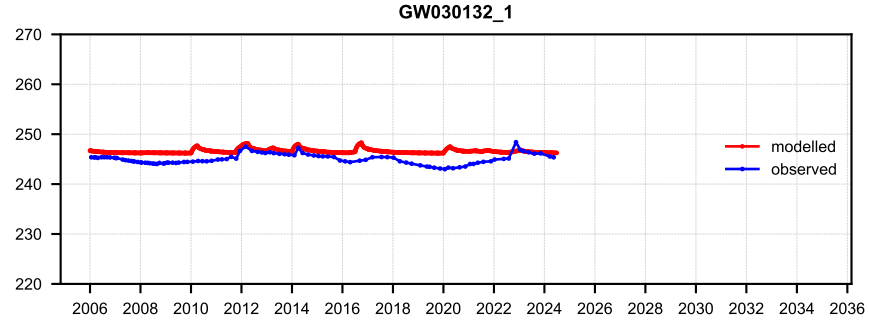
GW030132_1
modelled
observed

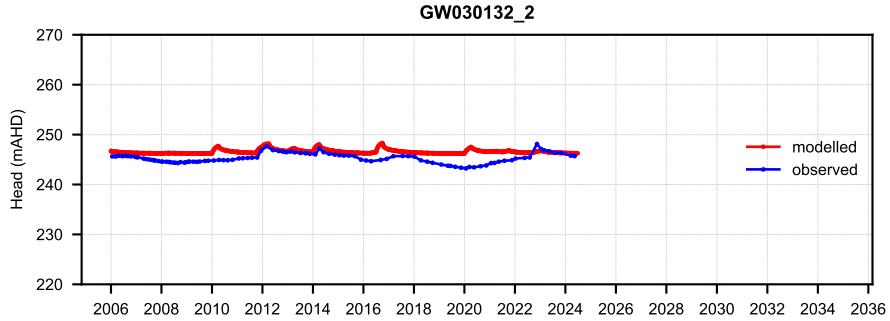
GW030132_2
Head (mAHD)
modelled
observed

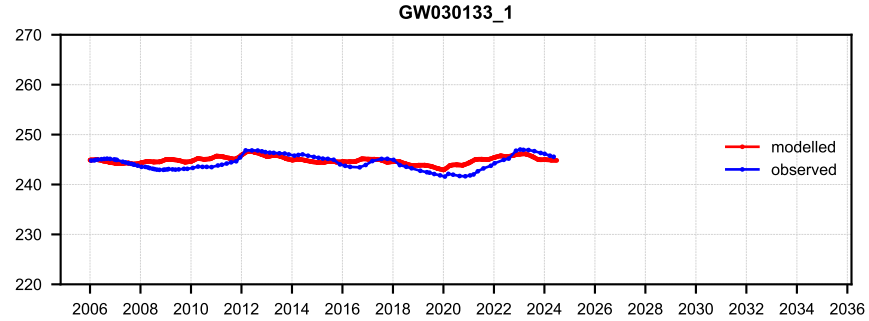
GW030133_1
modelled
observed

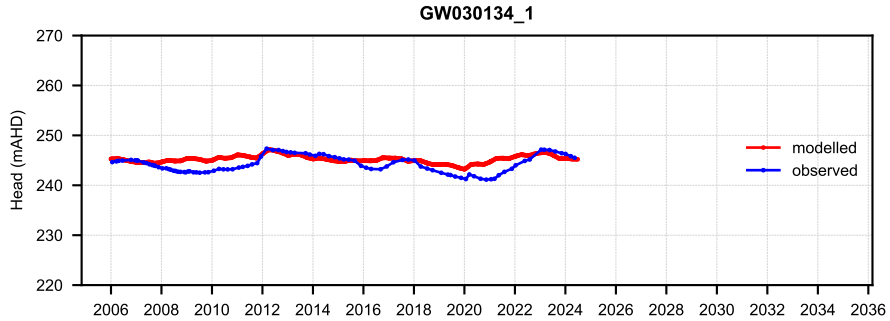
GW030134_1
Head (mAHD)
modelled
observed

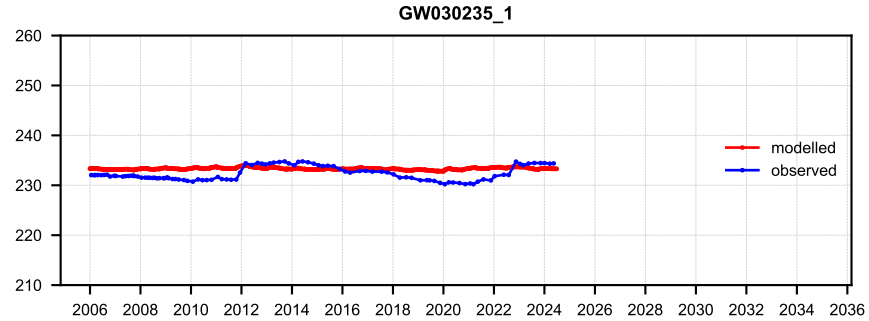
GW030235_1
modelled
observed

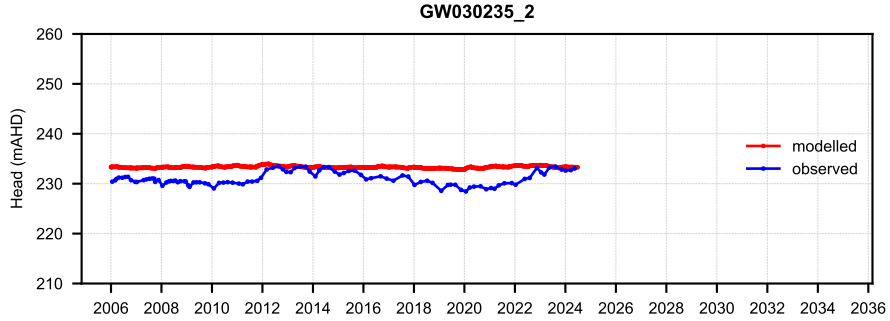
GW030235_2
Head (mAHD)
modelled
observed

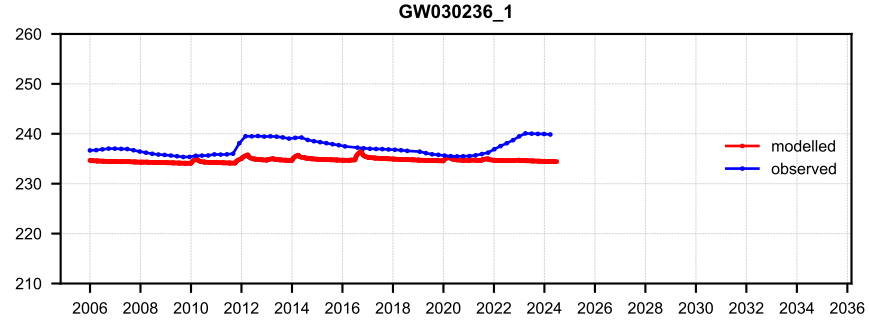
GW030236_1
modelled
observed

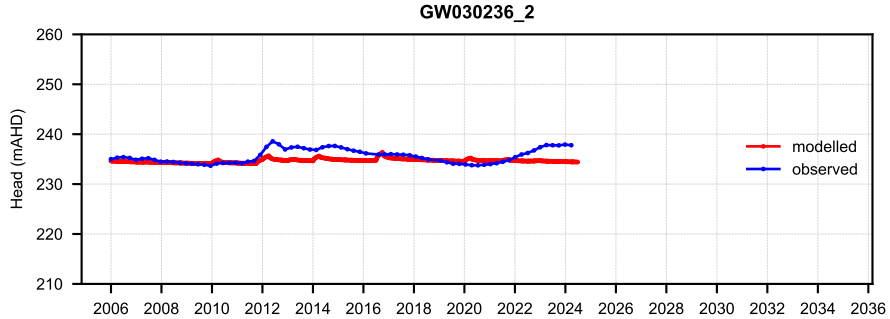
GW030236_2
Head (mAHD)
modelled
observed

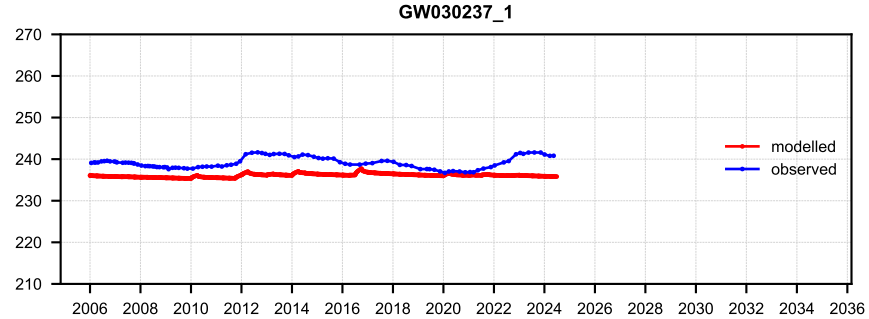
GW030237_1
modelled
observed

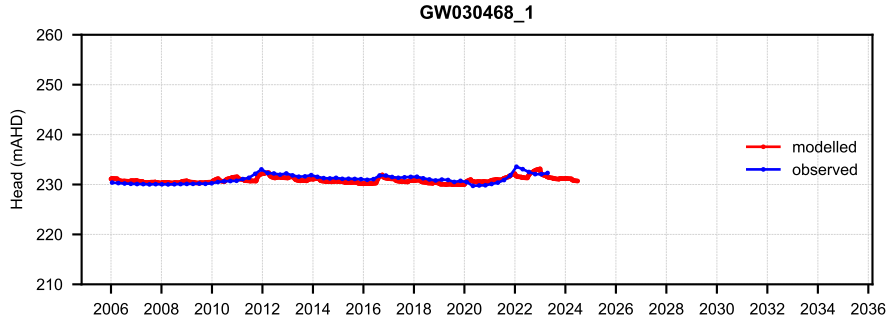
GW030468_1
Head (mAHD)
modelled
observed

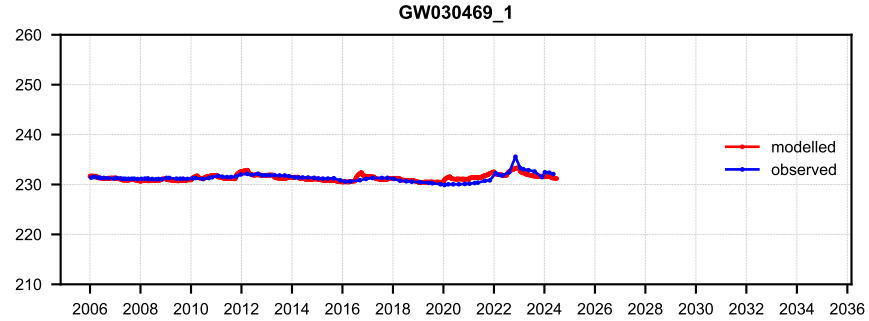
GW030469_1
modelled
observed

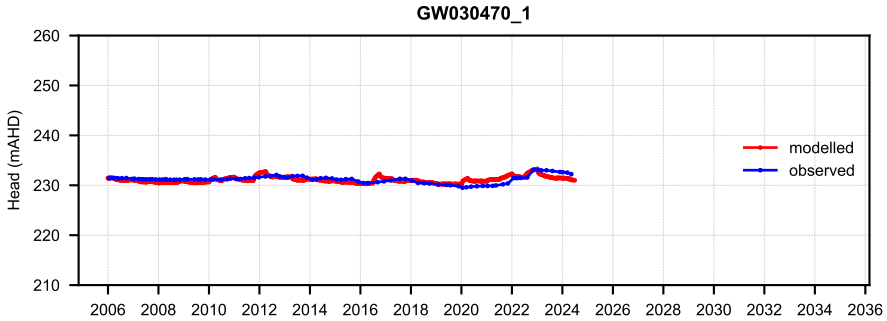
GW030470_1
Head (mAHD)
modelled
observed

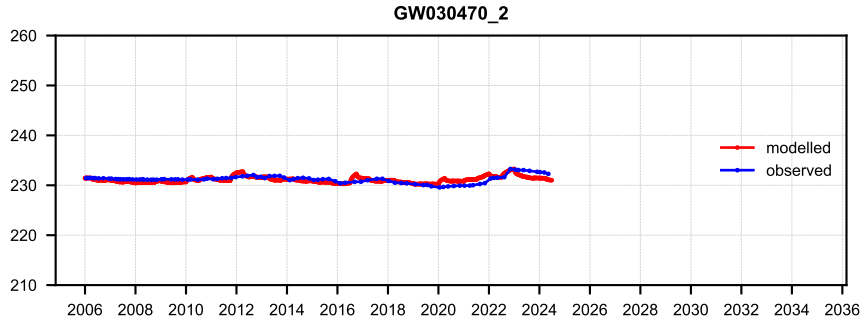
GW030470_2
modelled
observed

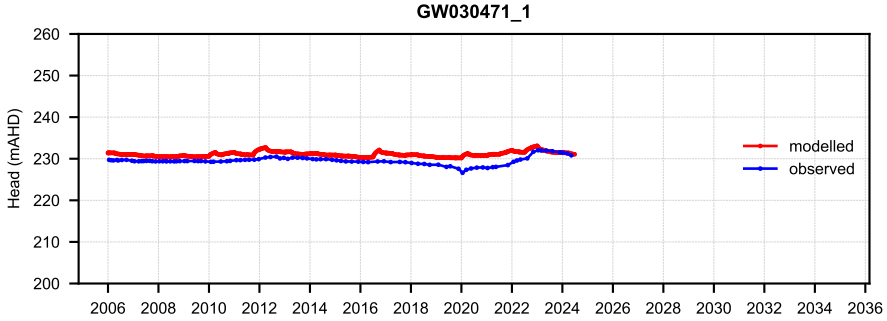
GW030471_1
Head (mAHD)
modelled
observed

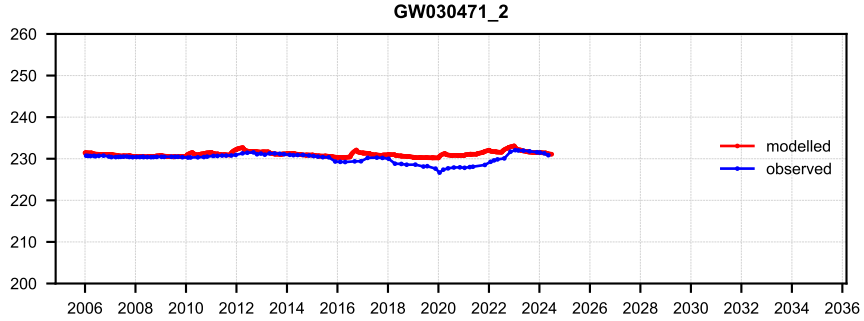
GW030471_2
modelled
observed

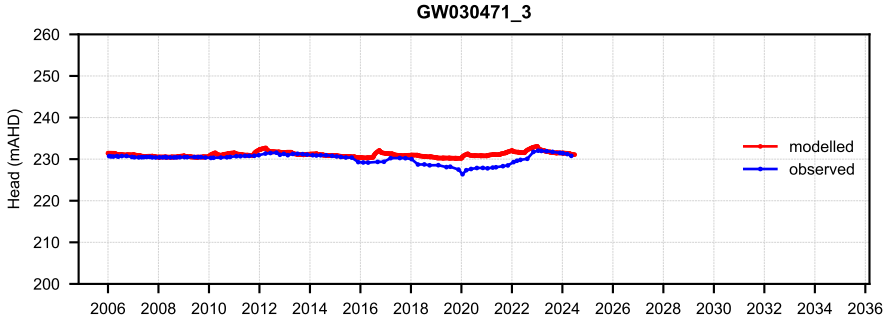
GW030471_3
Head (mAHD)
modelled
observed

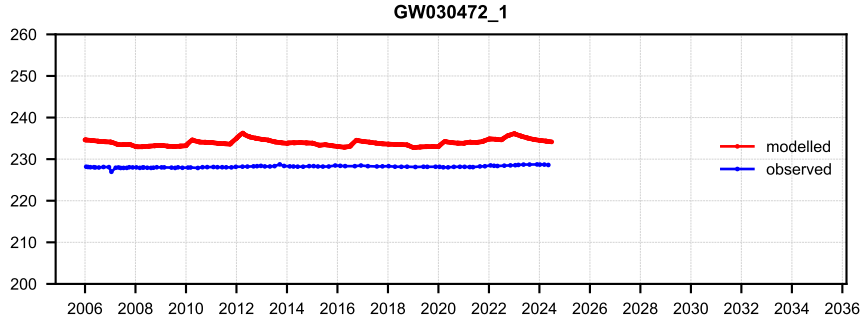
GW030472_1
modelled
observed

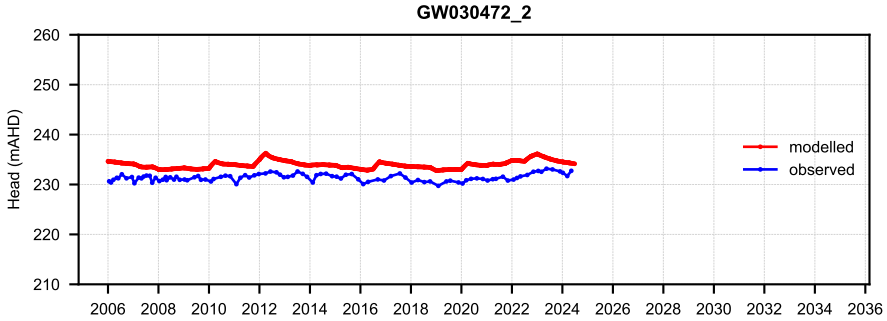
GW030472_2
Head (mAHD)
modelled
observed

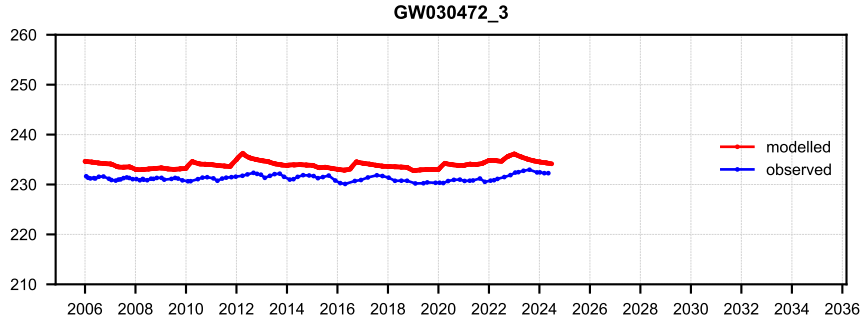
GW030472_3
modelled
observed

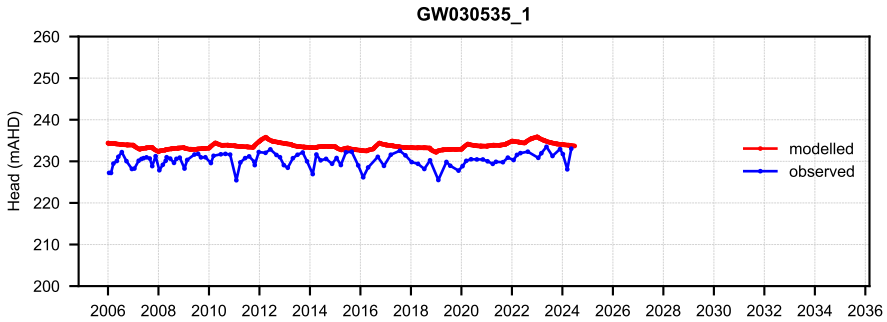
GW030535_1
Head (mAHD)
modelled
observed

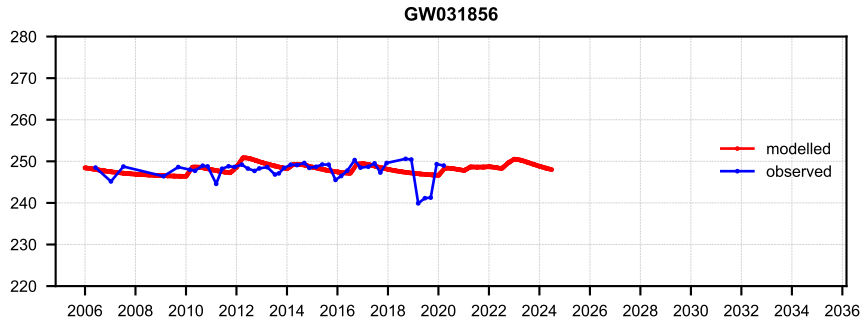
GW031856
modelled
observed

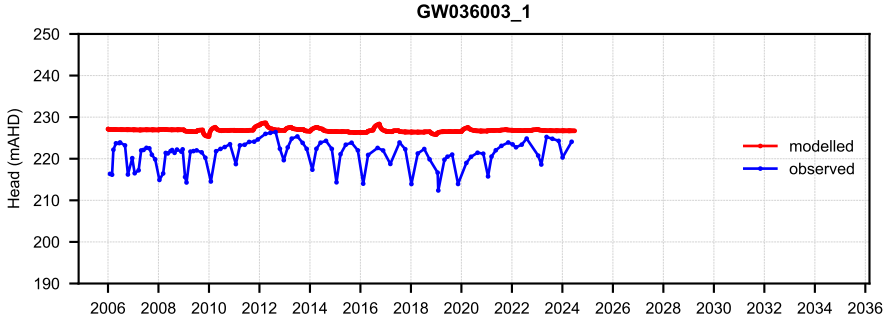
GW036003_1
Head (mAHD)
modelled
observed

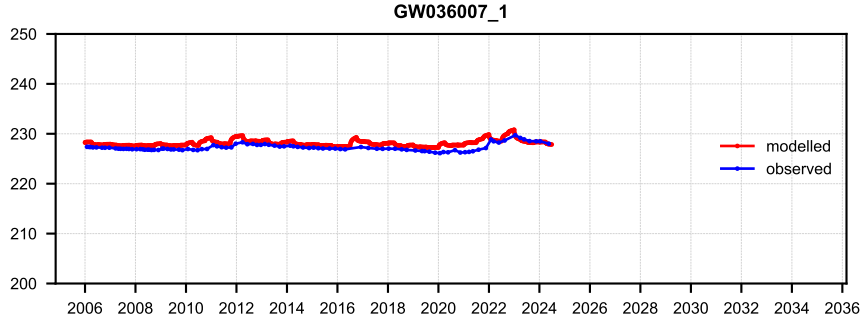
GW036007_1
modelled
observed

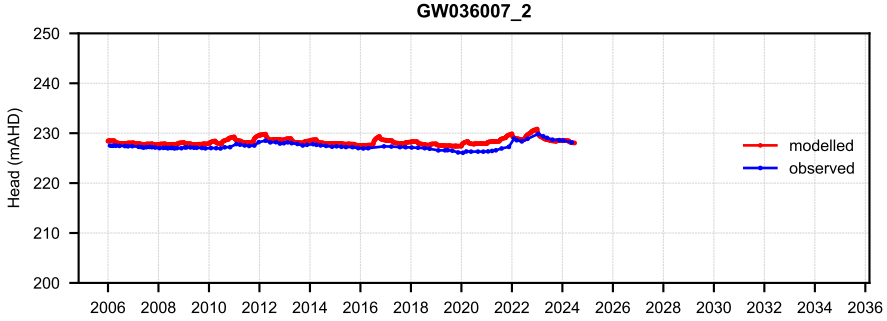
GW036007_2
Head (mAHD)
modelled
observed

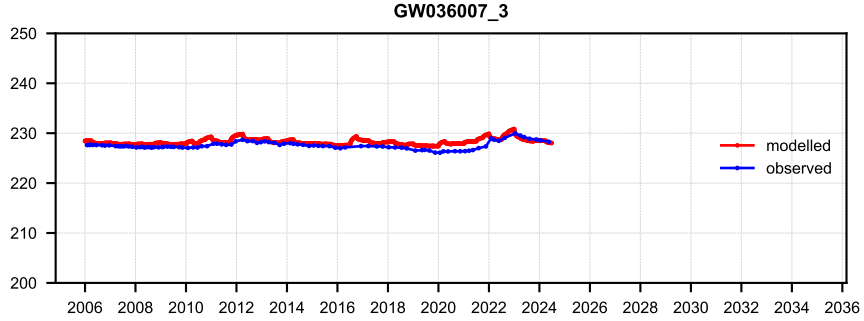
GW036007_3
modelled
observed

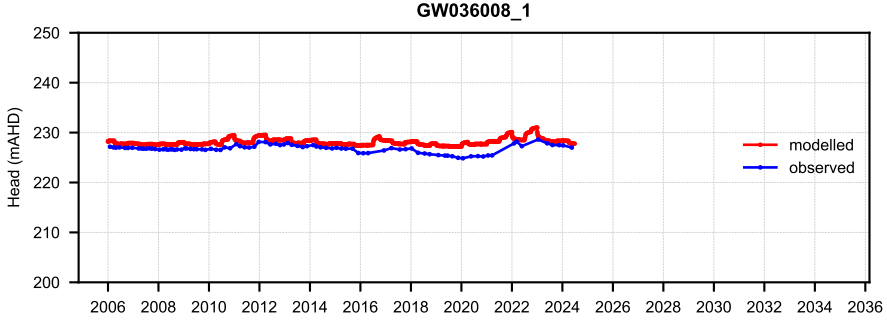
GW036008_1
Head (mAHD)
modelled
observed

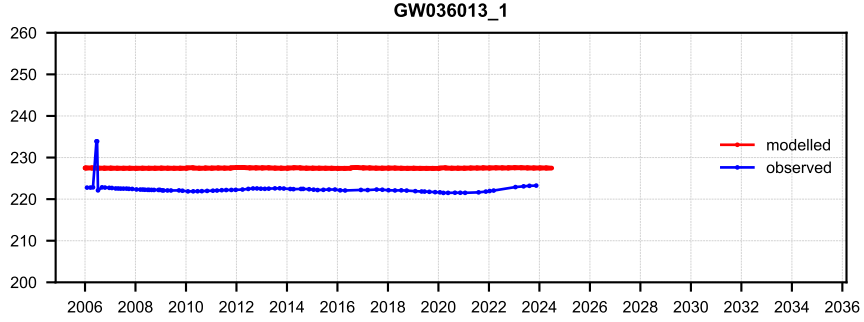
GW036013_1
modelled
observed

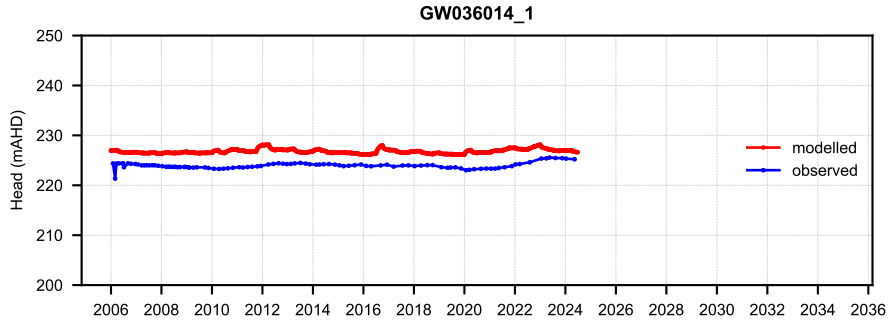
GW036014_1
Head (mAHD)
250
240
230
220
210
200
2006 2008 2010 2012 2014 2016 2018 2020 2022 2024 2026 2028 2030 2032 2034 2036
modelled
observed

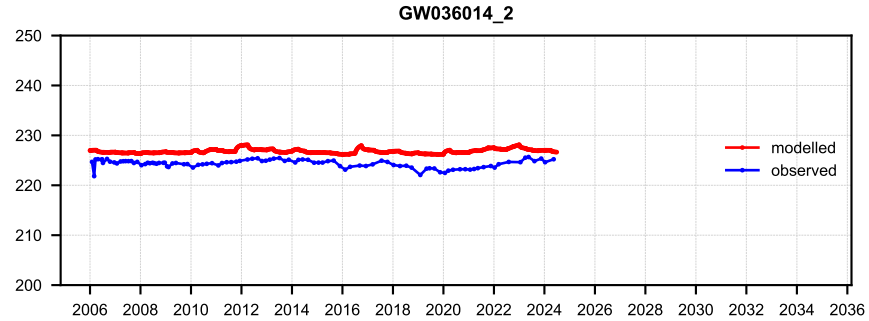
GW036014_2
250
240
230
220
210
200
2006 2008 2010 2012 2014 2016 2018 2020 2022 2024 2026 2028 2030 2032 2034 2036
modelled
observed

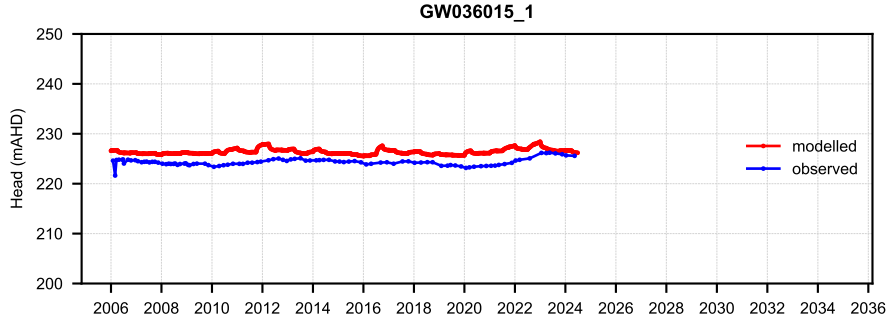
GW036015_1
Head (mAHD)
250
240
230
220
210
200
2006 2008 2010 2012 2014 2016 2018 2020 2022 2024 2026 2028 2030 2032 2034 2036
modelled
observed

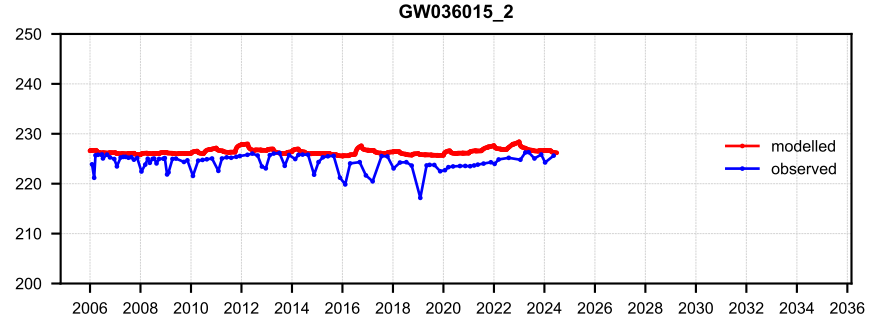
GW036015_2
250
240
230
220
210
200
2006 2008 2010 2012 2014 2016 2018 2020 2022 2024 2026 2028 2030 2032 2034 2036
modelled
observed

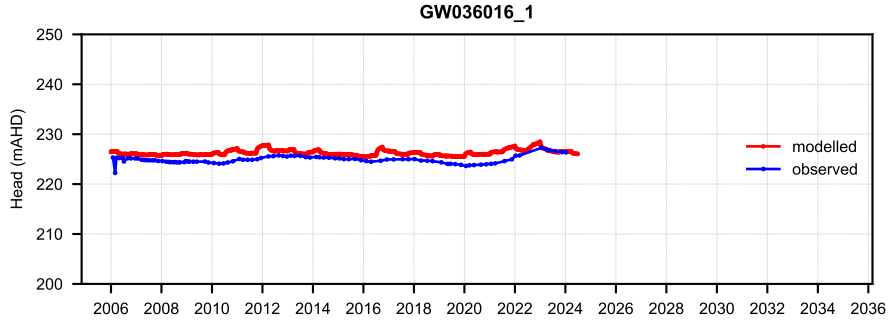
GW036016_1
Head (mAHD)
250
240
230
220
210
200
2006 2008 2010 2012 2014 2016 2018 2020 2022 2024 2026 2028 2030 2032 2034 2036
modelled
observed

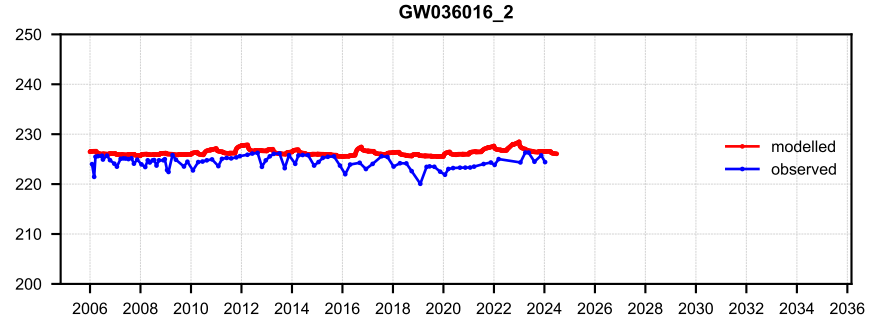
GW036016_2
250
240
230
220
210
200
2006 2008 2010 2012 2014 2016 2018 2020 2022 2024 2026 2028 2030 2032 2034 2036
modelled
observed

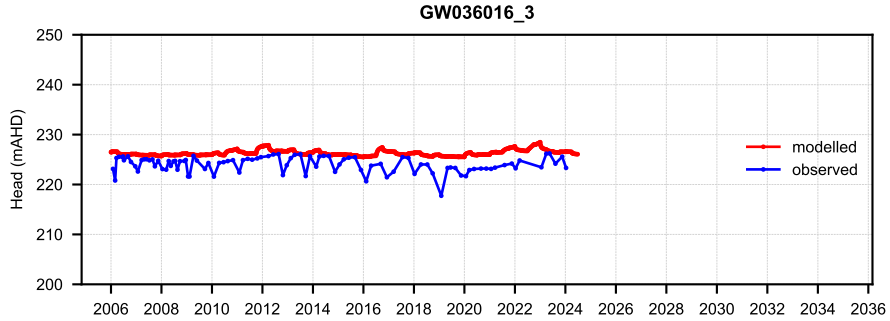
GW036016_3
Head (mAHD)
250
240
230
220
210
200
2006 2008 2010 2012 2014 2016 2018 2020 2022 2024 2026 2028 2030 2032 2034 2036
modelled
observed

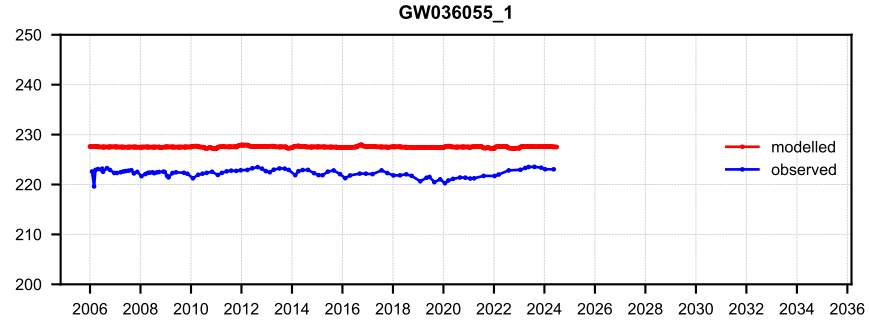
GW036055_1
250
240
230
220
210
200
2006 2008 2010 2012 2014 2016 2018 2020 2022 2024 2026 2028 2030 2032 2034 2036
modelled
observed

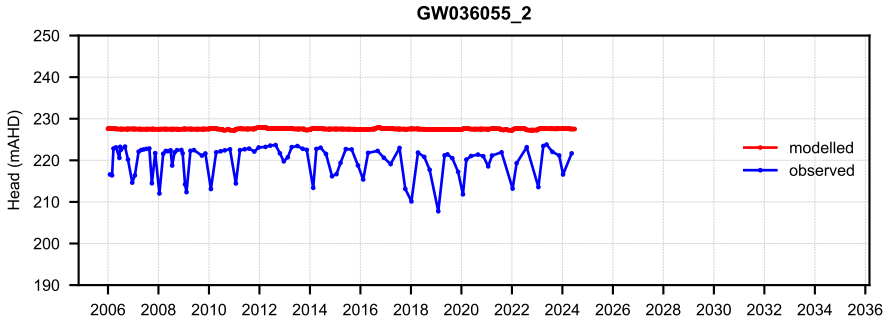
GW036055_2
Head (mAHD)
modelled
observed

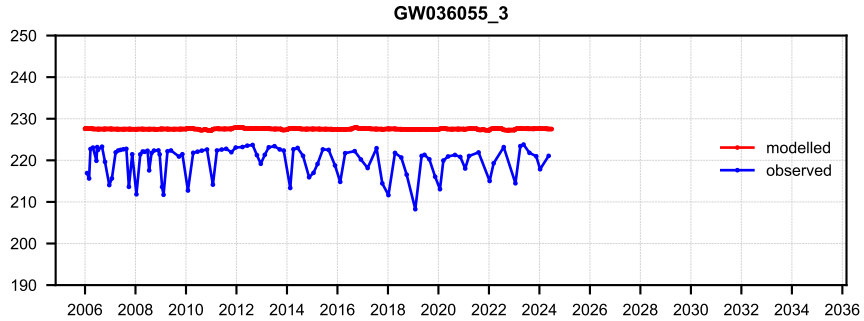
GW036055_3
modelled
observed

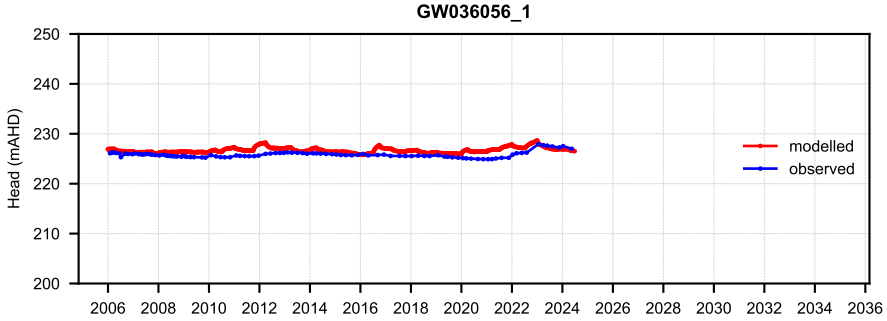
GW036056_1
Head (mAHD)
modelled
observed

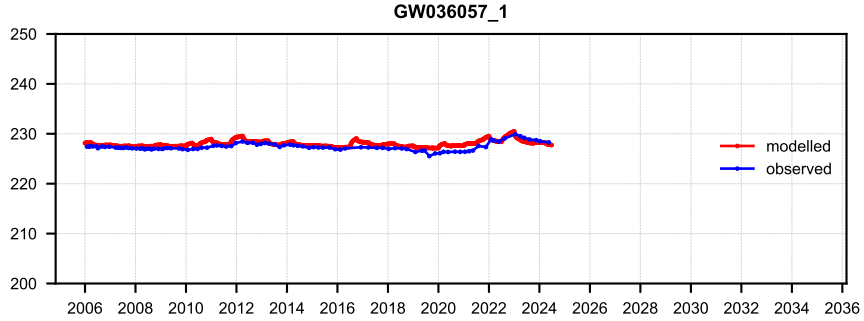
GW036057_1
modelled
observed

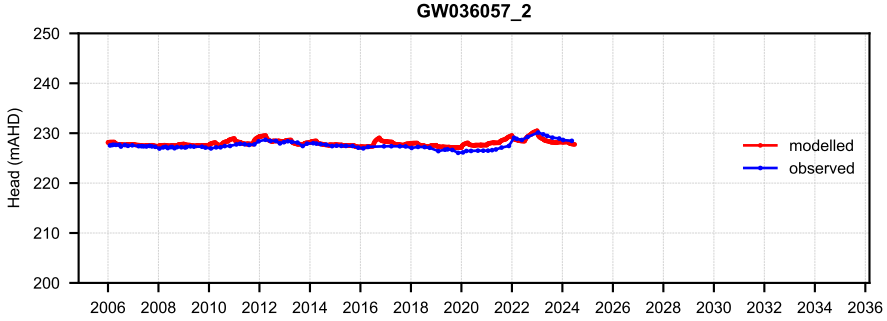
GW036057_2
Head (mAHD)
modelled
observed

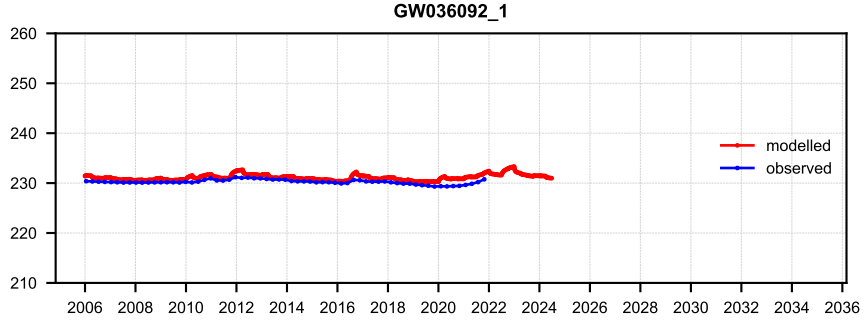
GW036092_1
modelled
observed

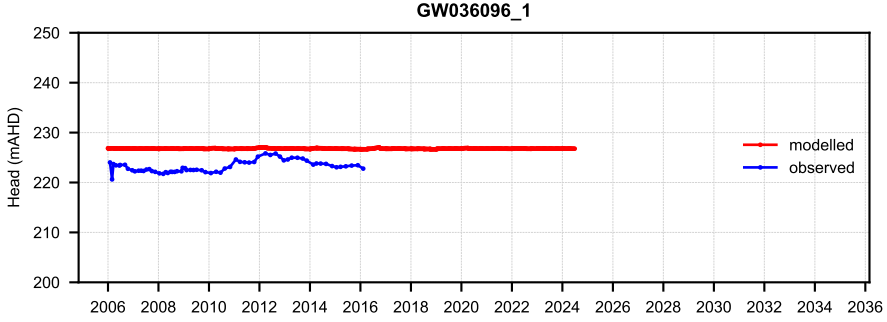
GW036096_1
Head (mAHD)
modelled
observed

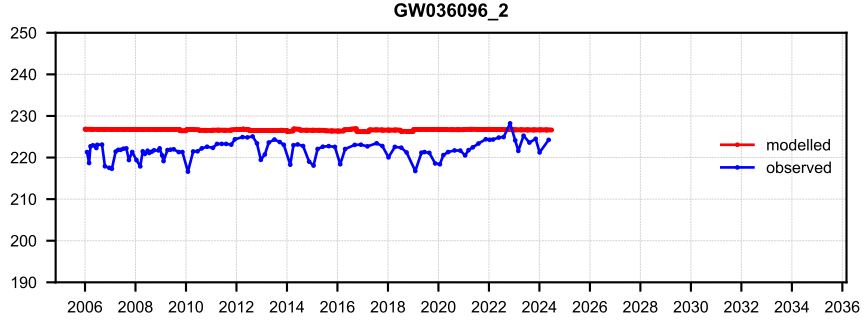
GW036096_2
modelled
observed

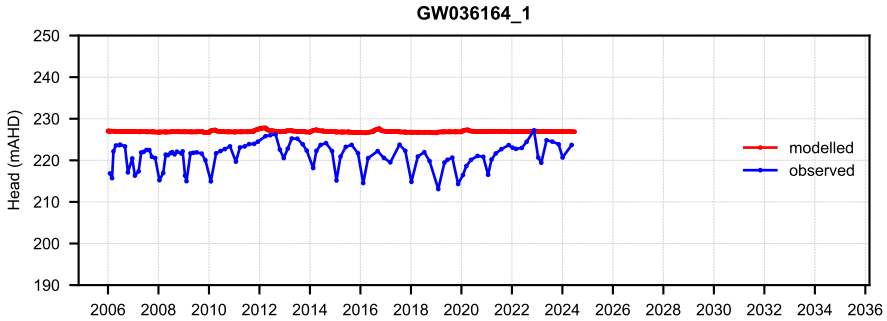
GW036164_1
Head (mAHD)
modelled
observed

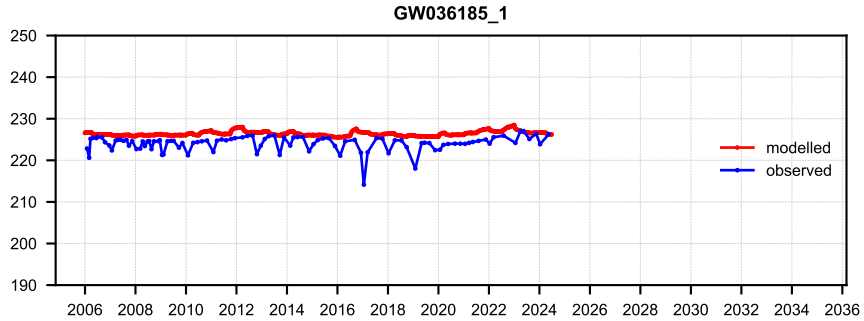
GW036185_1
modelled
observed

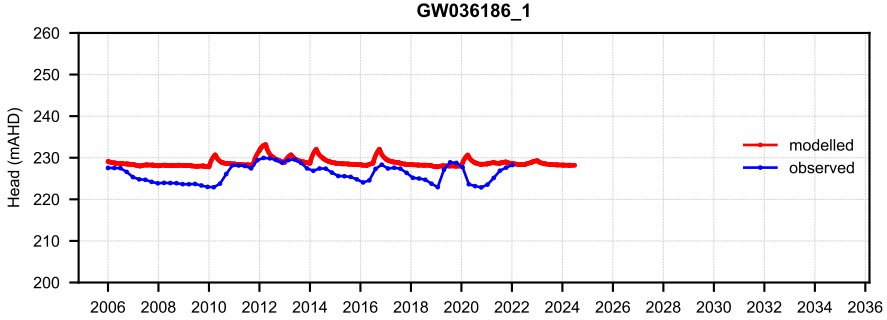
GW036186_1
Head (mAHD)
modelled
observed

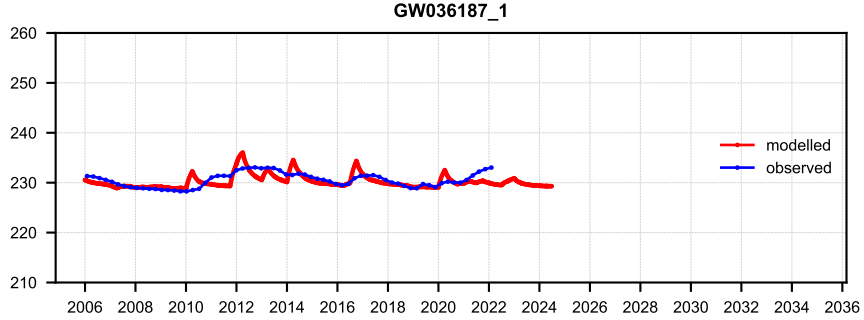
GW036187_1
modelled
observed

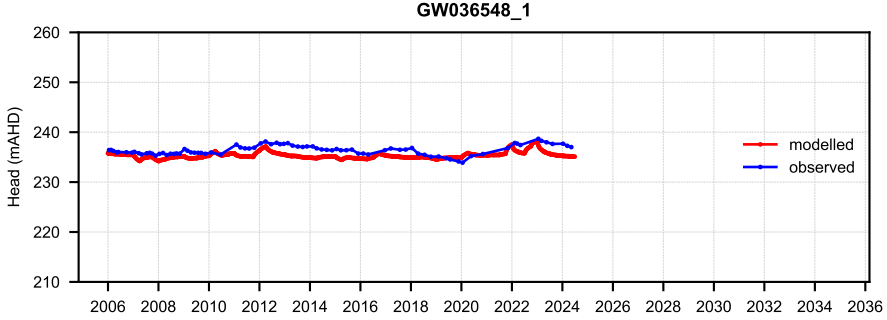
GW036548_1
Head (mAHD)
modelled
observed

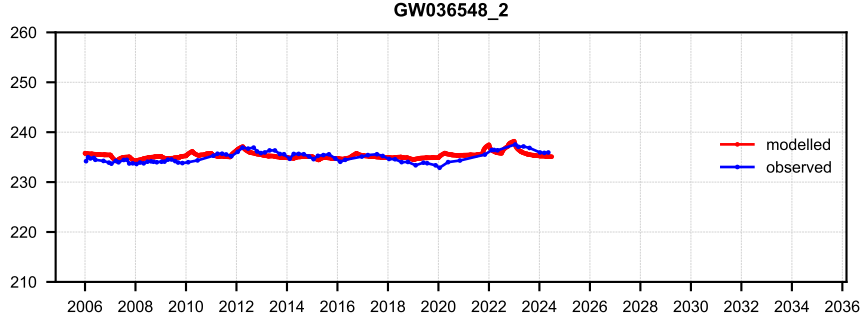
GW036548_2
modelled
observed

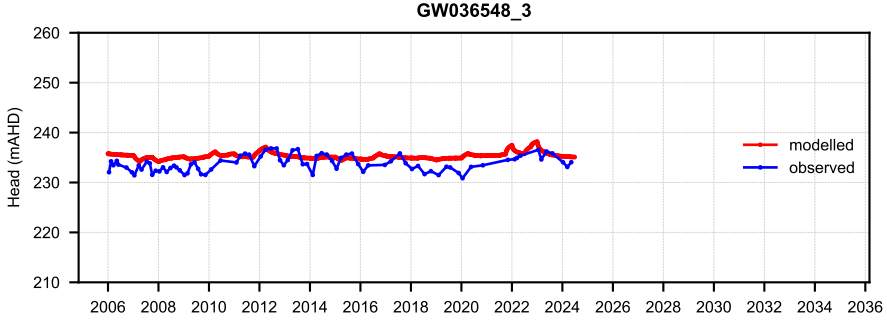
GW036548_3
Head (mAHD)
modelled
observed

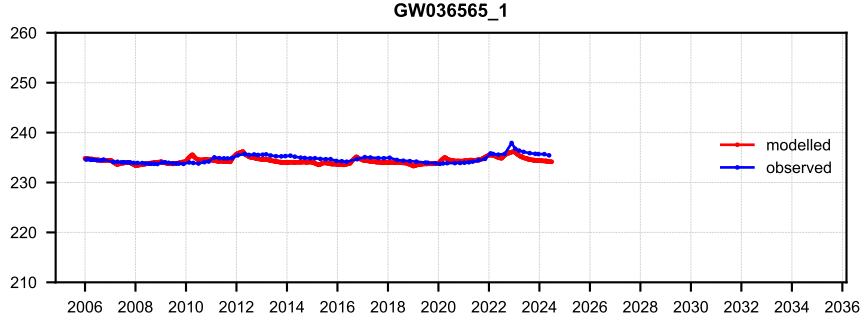
GW036565_1
modelled
observed

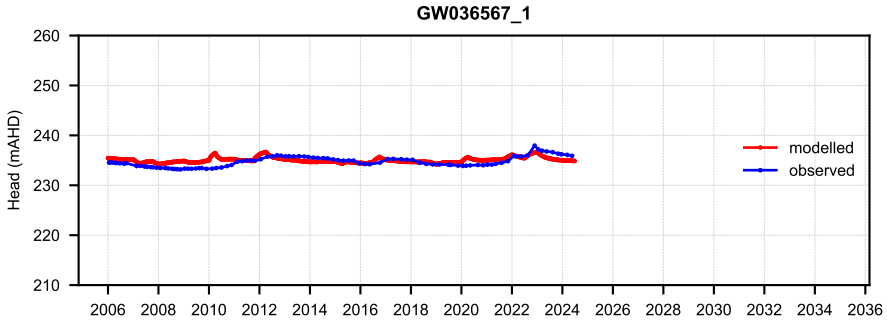
GW036567_1
Head (mAHD)
modelled
observed

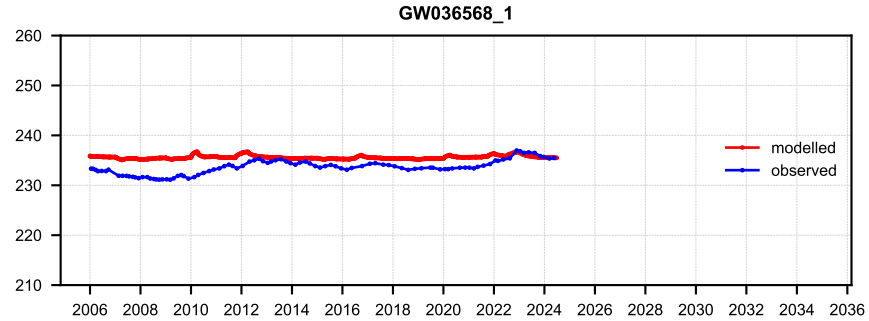
GW036568_1
modelled
observed

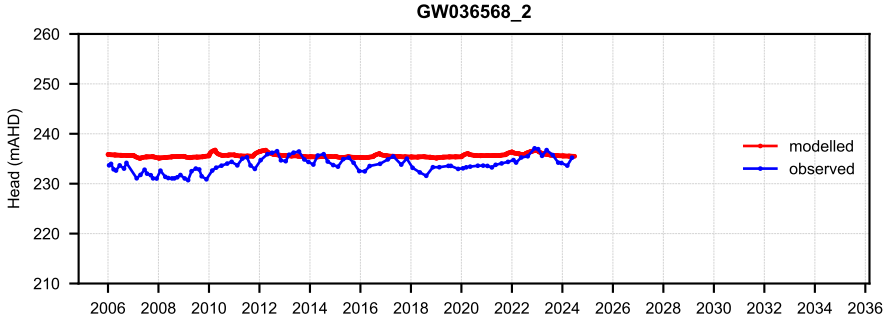
GW036568_2
Head (mAHD)
modelled
observed

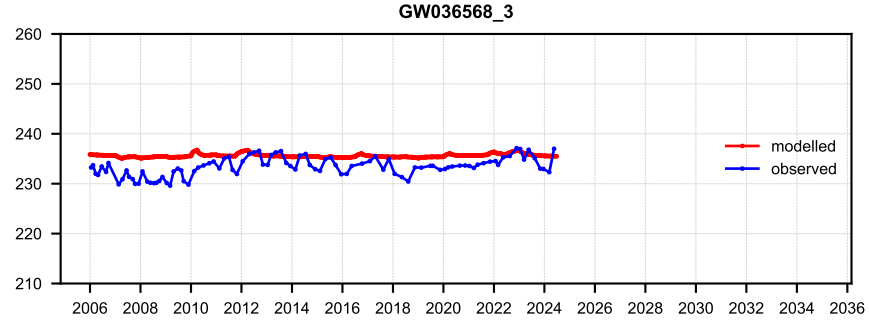
GW036568_3
modelled
observed

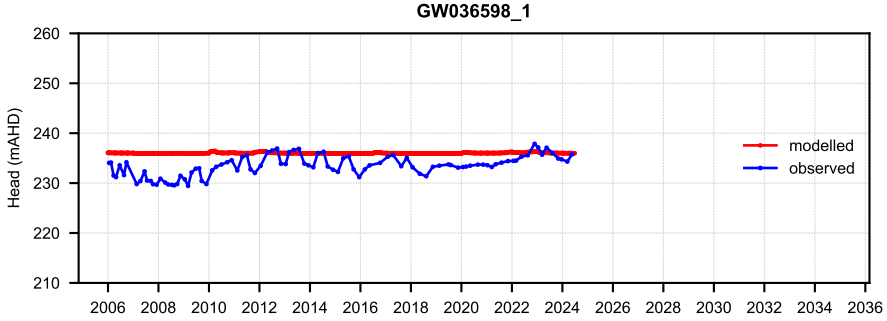
GW036598_1
Head (mAHD)
modelled
observed

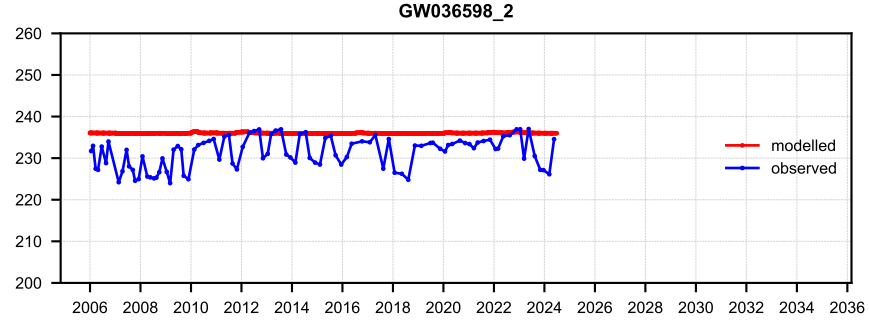
GW036598_2
modelled
observed

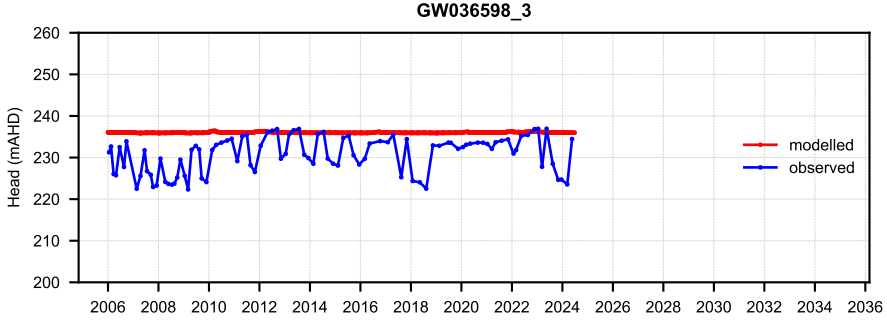
GW036598_3
Head (mAHD)
modelled
observed

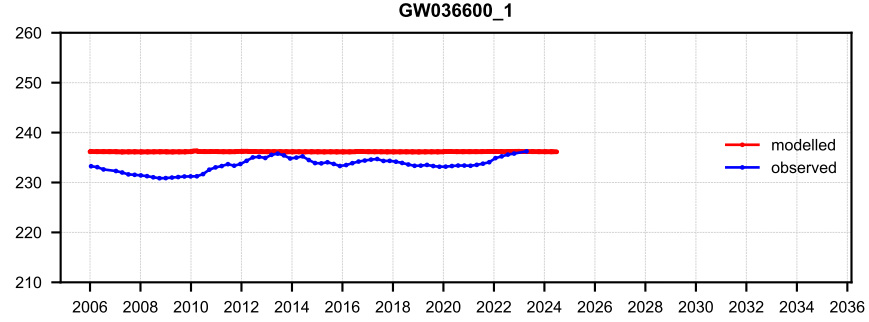
GW036600_1
modelled
observed

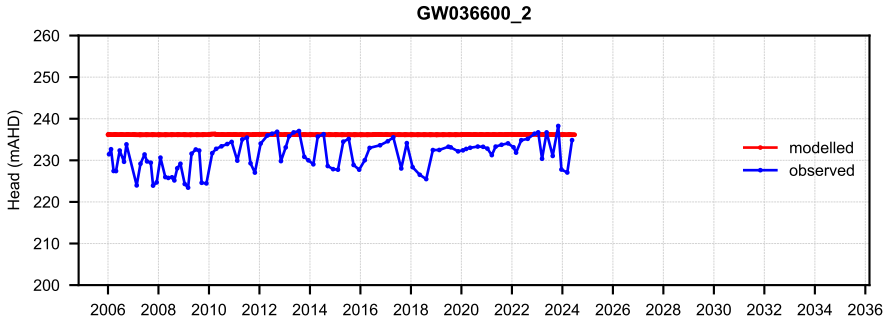
GW036600_2
Head (mAHD)
modelled
observed

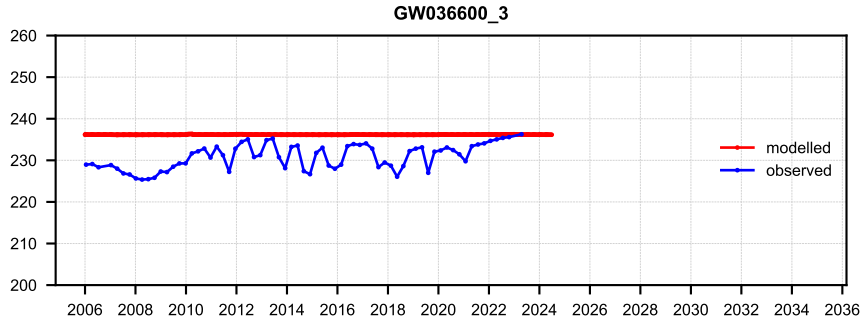
GW036600_3
modelled
observed

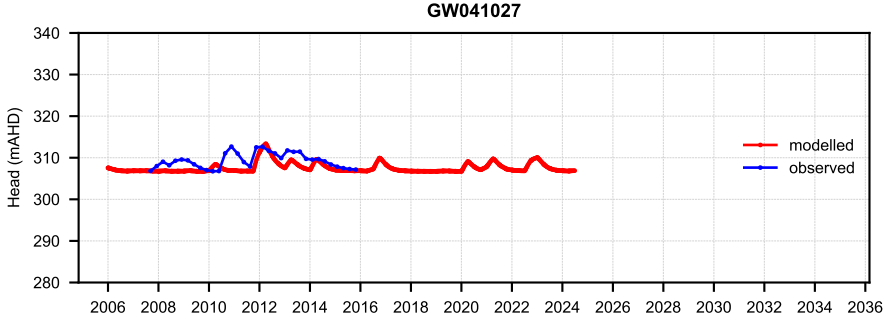
GW041027
Head (mAHD)
modelled
observed

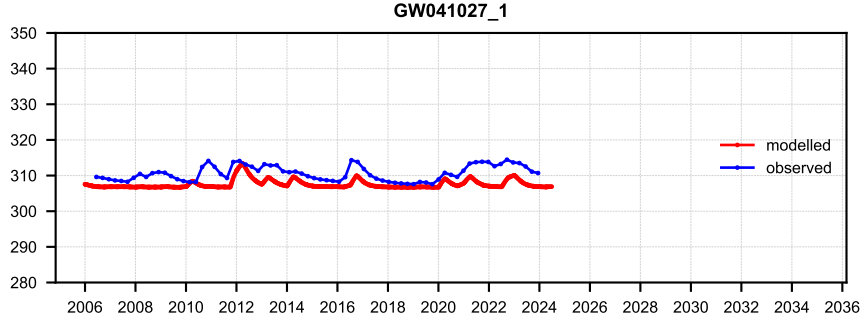
GW041027_1
modelled
observed

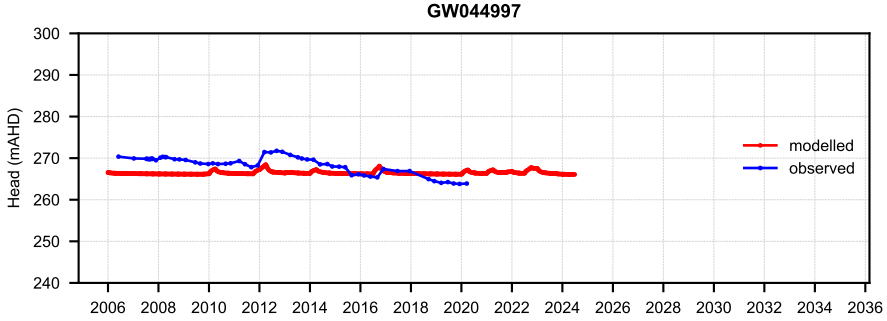
GW044997
Head (mAHD)
modelled
observed

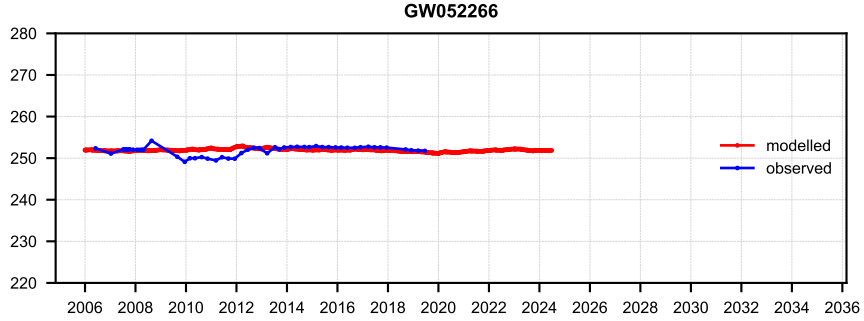
GW052266
modelled
observed

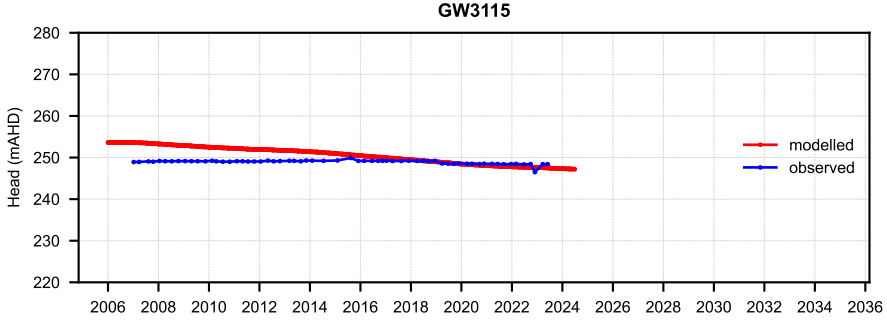
GW3115
Head (mAHD)
modelled
observed

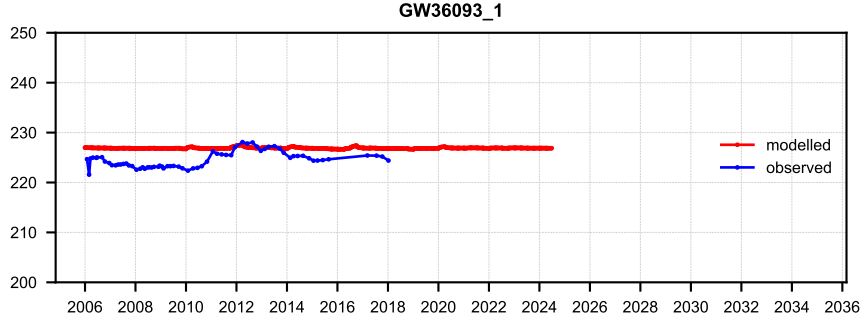
GW36093_1
modelled
observed

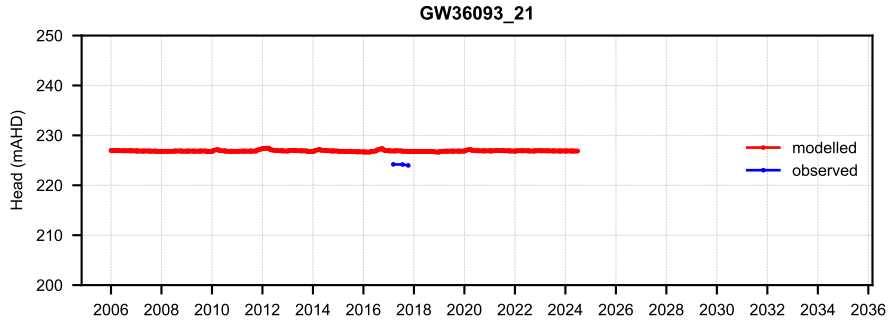
GW36093_21
Head (mAHD)
modelled
observed

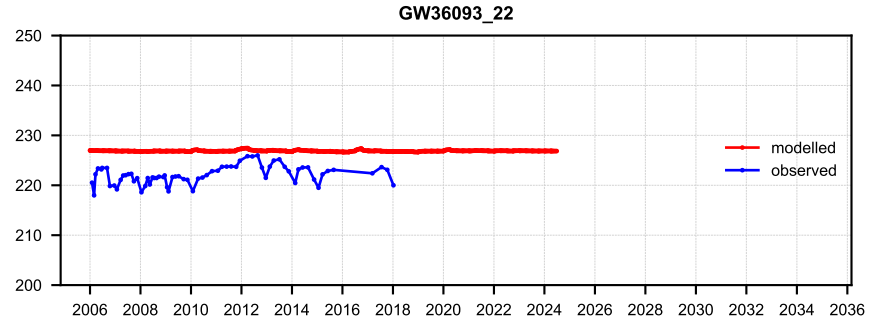
GW36093_22
modelled
observed

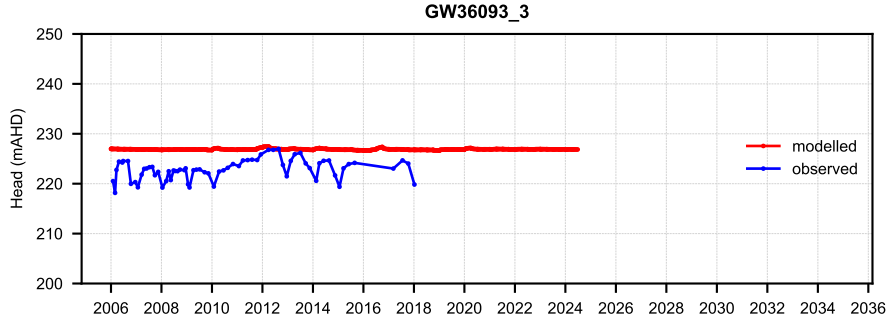
GW36093_3
Head (mAHD)
modelled
observed

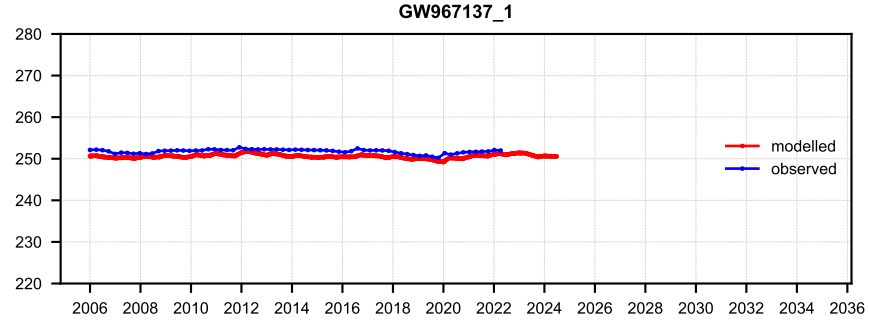
GW967137_1
modelled
observed

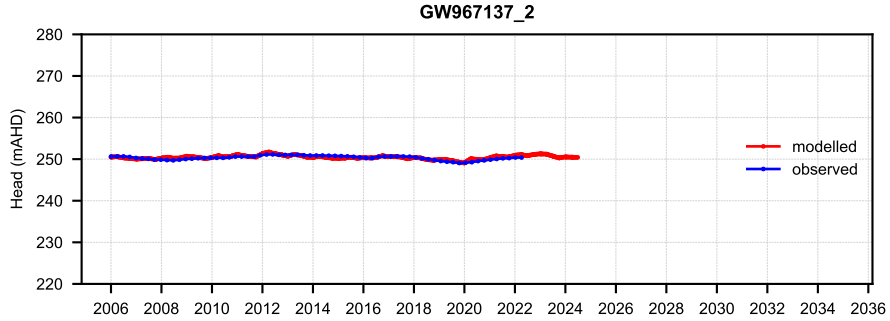
GW967137_2
Head (mAHD)
modelled
observed

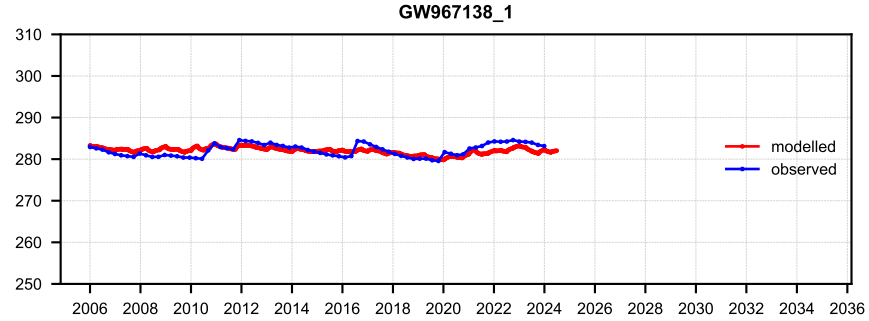
GW967138_1
modelled
observed

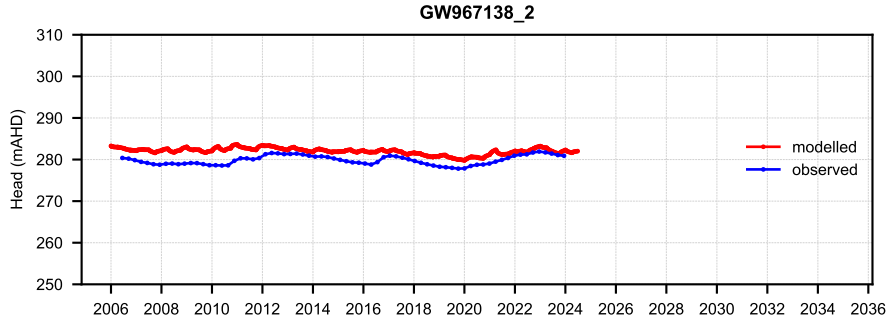
GW967138_2
Head (mAHD)
modelled
observed

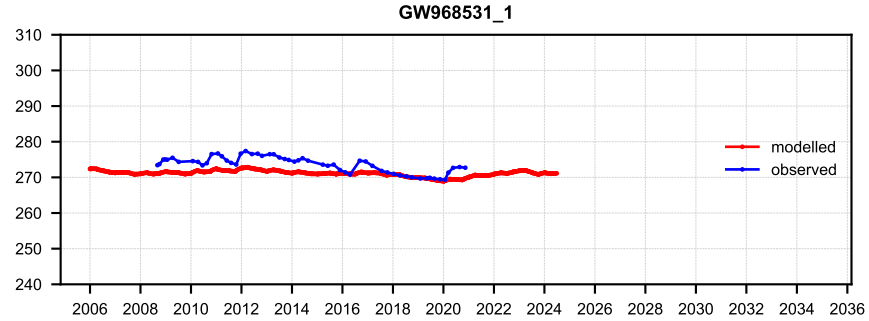
GW968531_1
modelled
observed

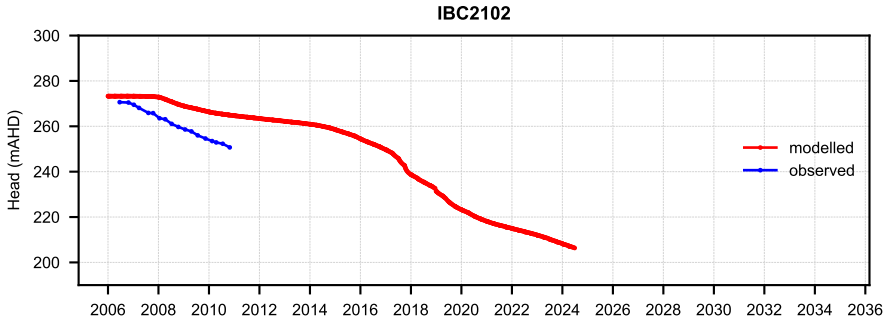
IBC2102
Head (mAHD)
modelled
observed

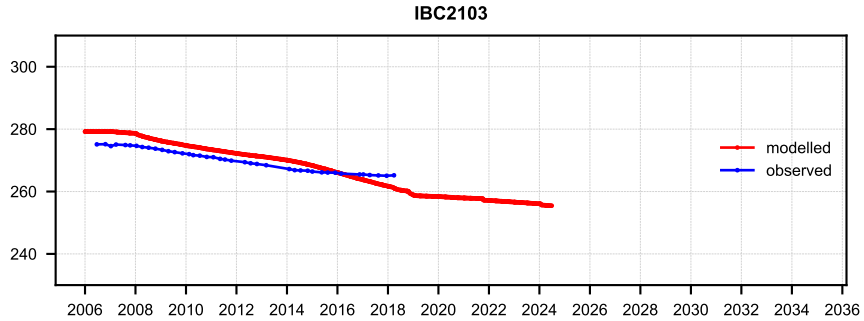
IBC2103
modelled
observed

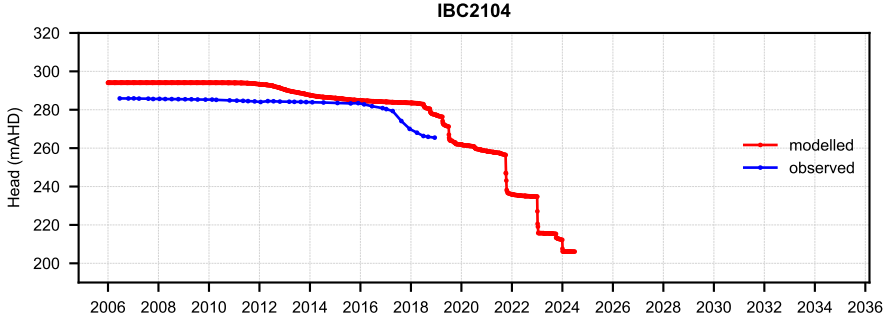
IBC2104
Head (mAHD)
modelled
observed

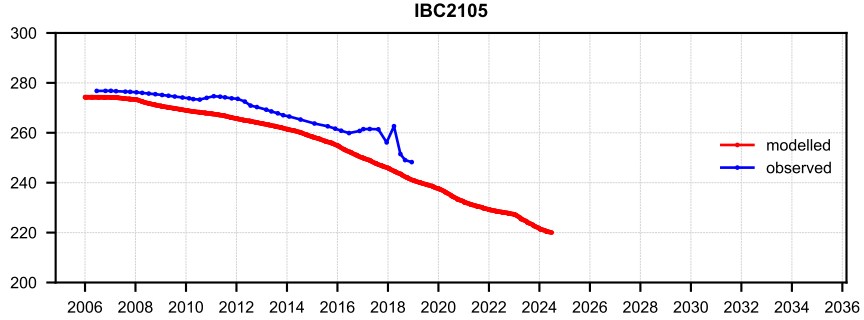
IBC2105
modelled
observed

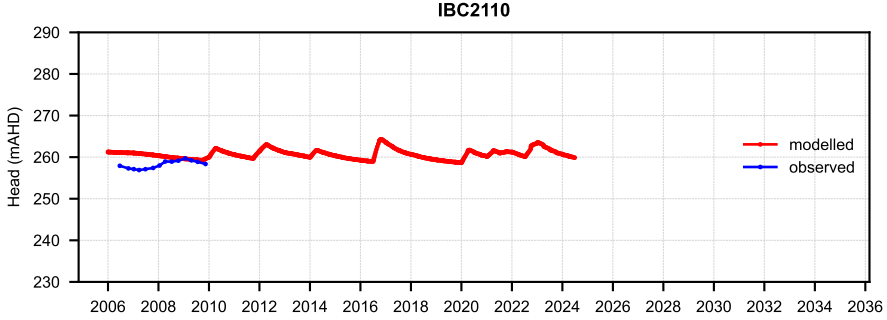
IBC2110
Head (mAHD)
modelled
observed

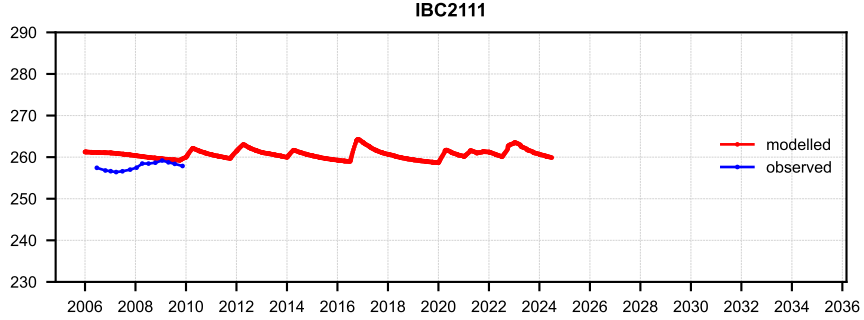
IBC2111
modelled
observed

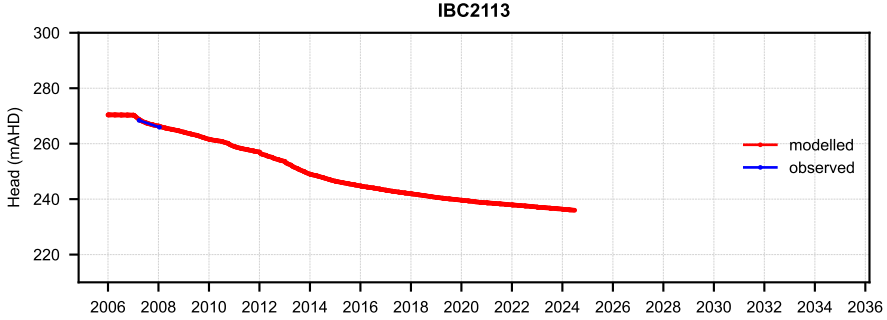
IBC2113
Head (mAHD)
modelled
observed

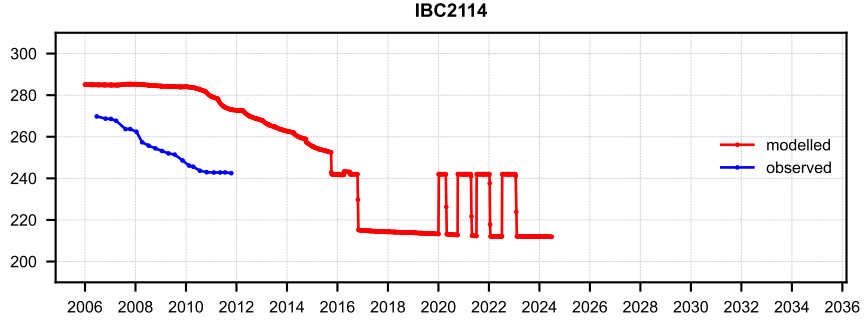
IBC2114
modelled
observed

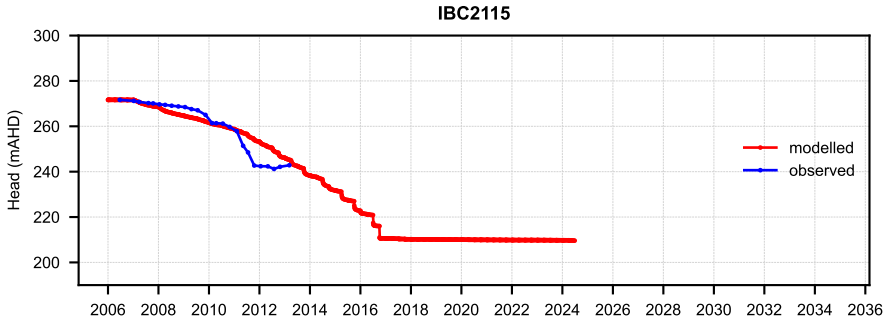
IBC2115
Head (mAHD)
modelled
observed

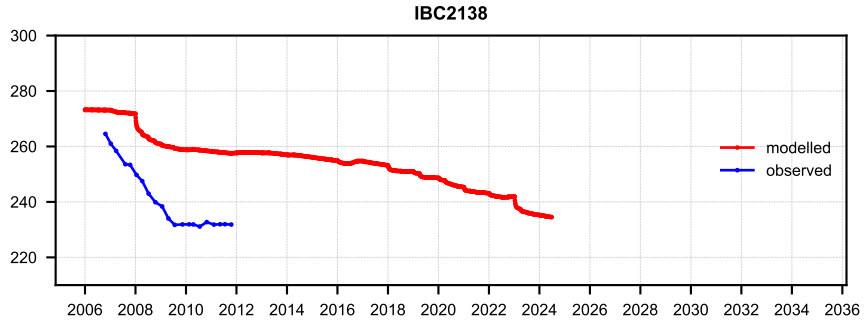
IBC2138
modelled
observed

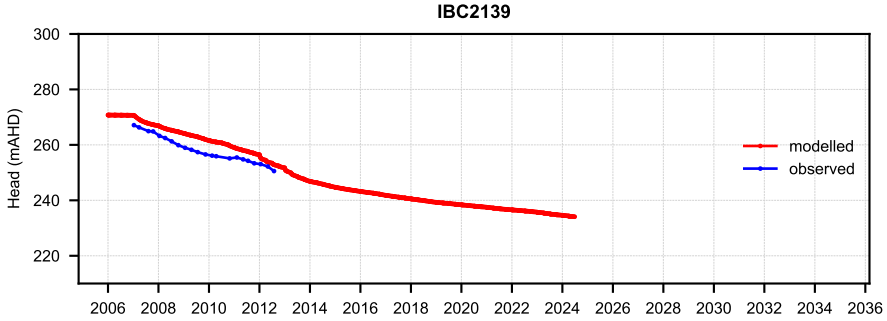
IBC2139
Head (mAHD)
modelled
observed

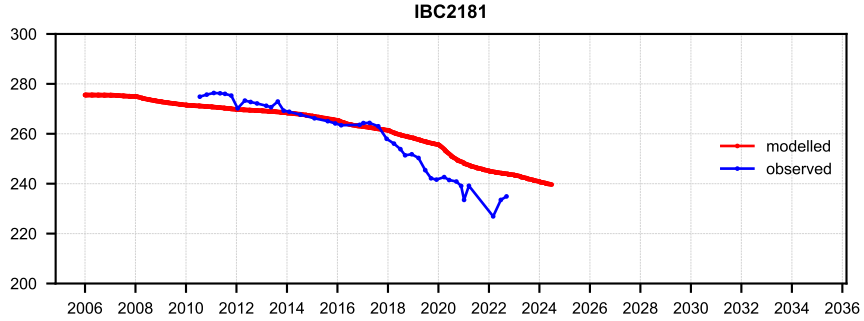
IBC2181
modelled
observed

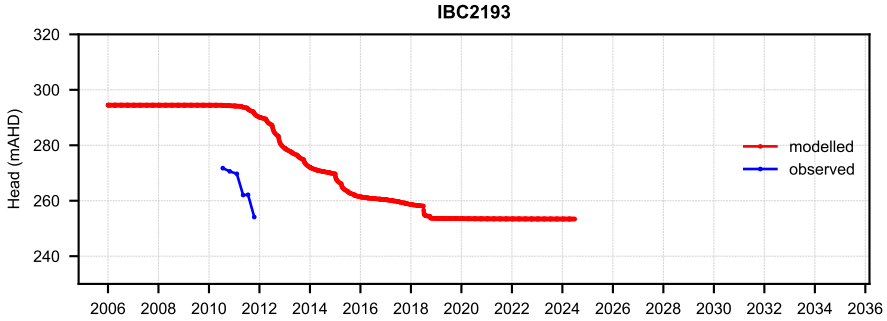
IBC2193
Head (mAHD)
modelled
observed

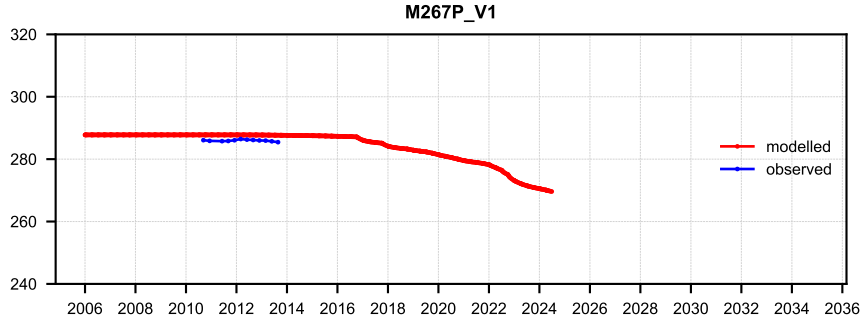
M267P_V1
modelled
observed

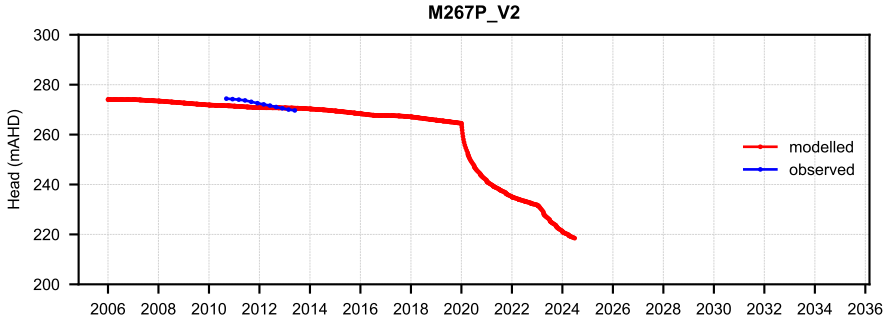
M267P_V2
Head (mAHD)
modelled
observed

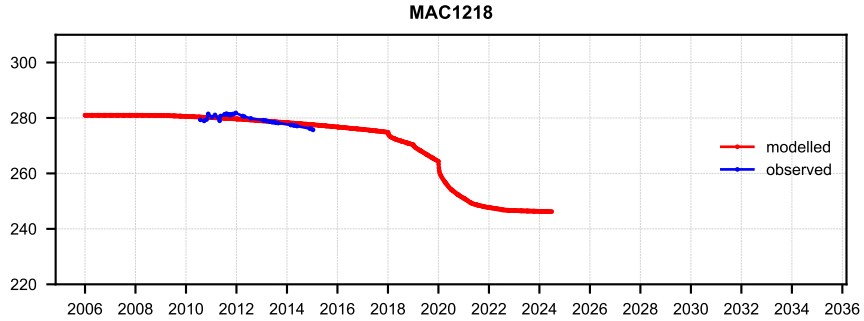
MAC1218
modelled
observed

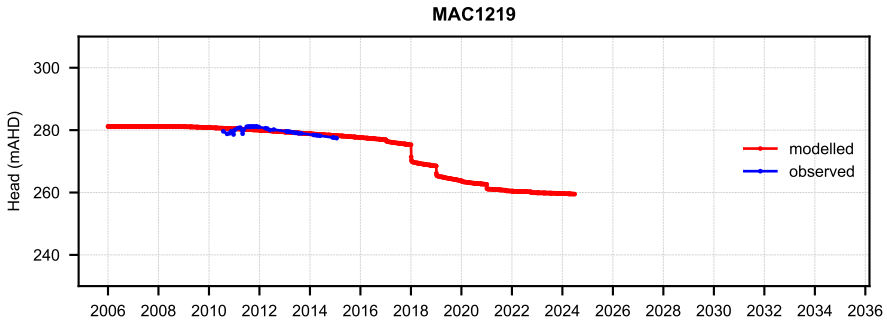
MAC1219
Head (mAHD)
modelled
observed

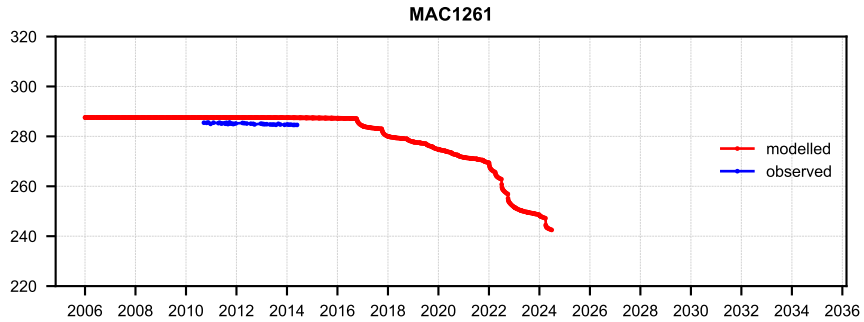
MAC1261
modelled
observed

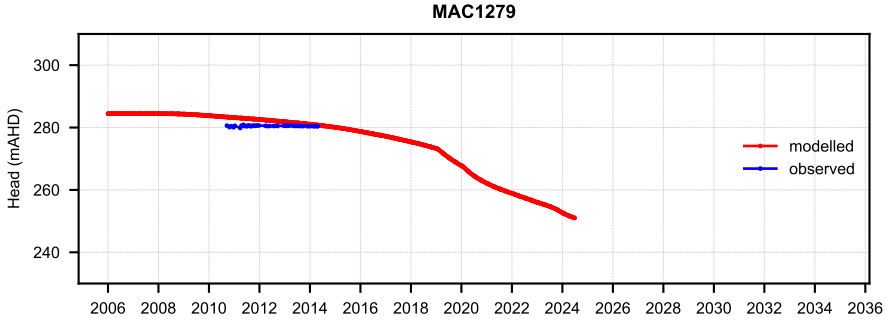
MAC1279
Head (mAHD)
modelled
observed

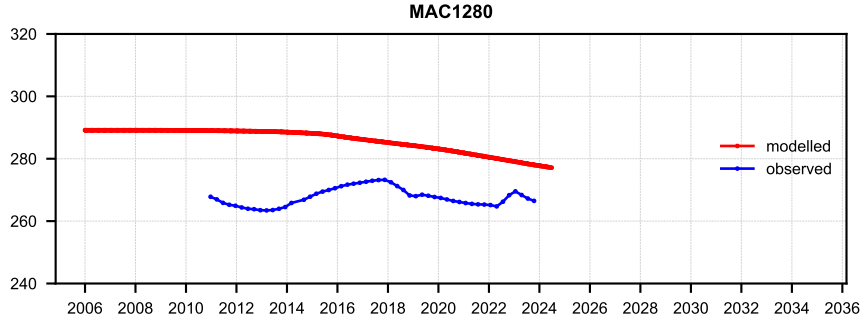
MAC1280
modelled
observed

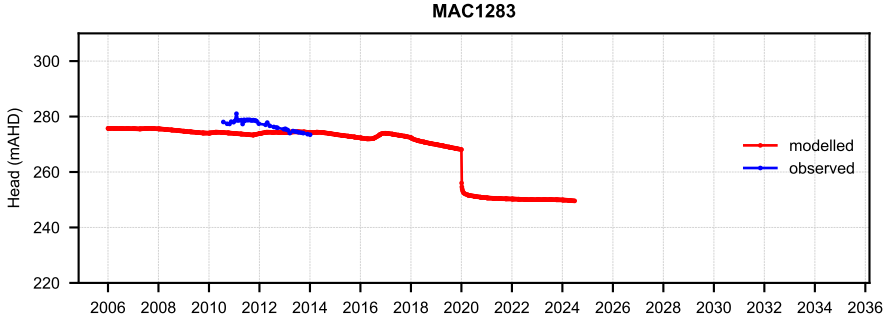
MAC1283
Head (mAHD)
modelled
observed

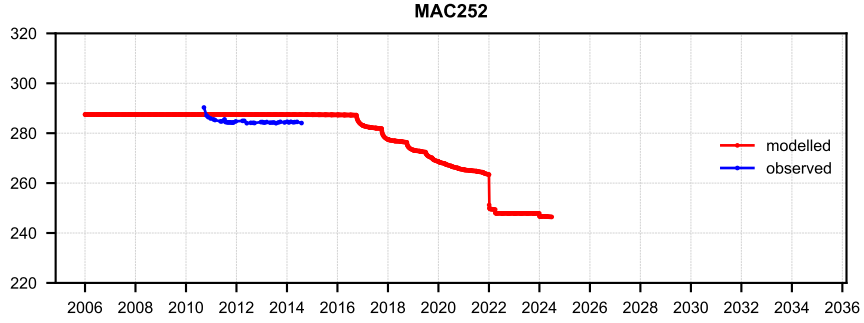
MAC252
modelled
observed

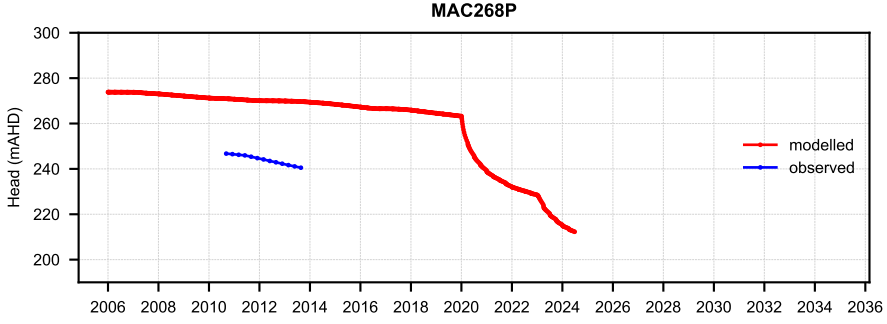
MAC268P
Head (mAHD)
modelled
observed

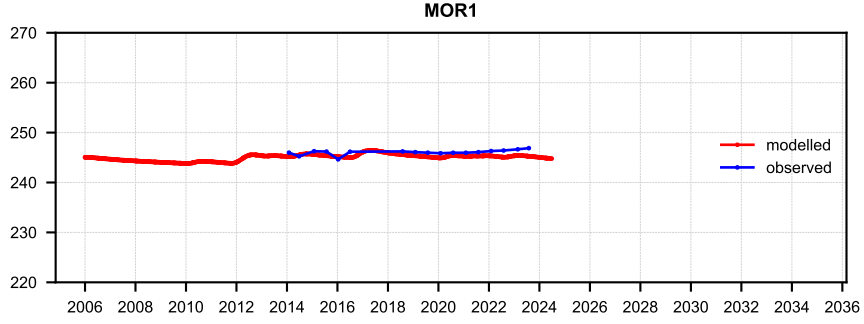
MOR1
modelled
observed

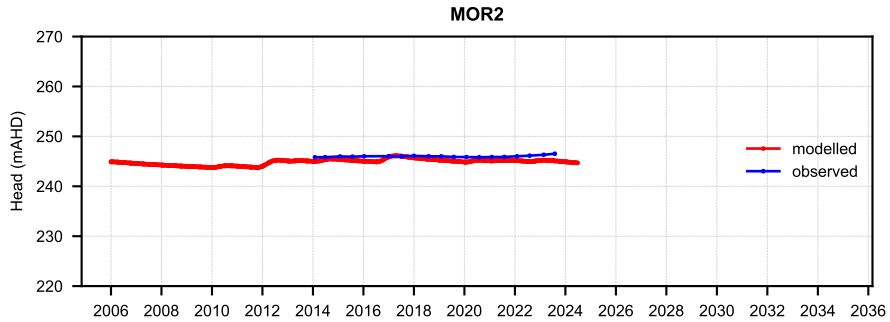
MOR2
Head (mAHD)
modelled
observed

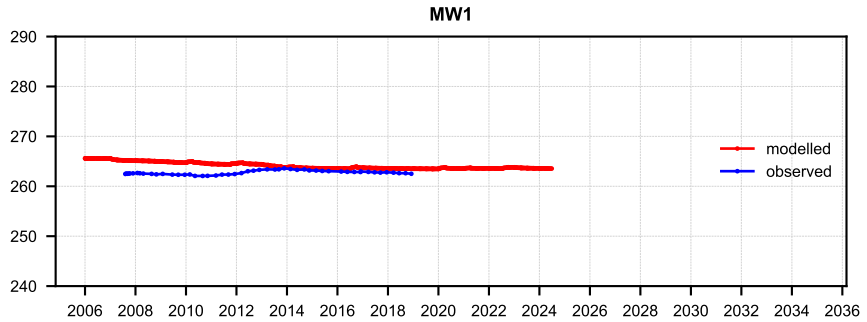
MW1
modelled
observed

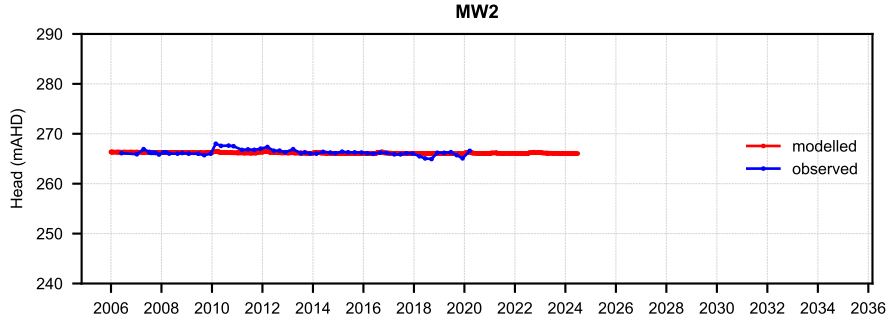
MW2
Head (mAHD)
modelled
observed

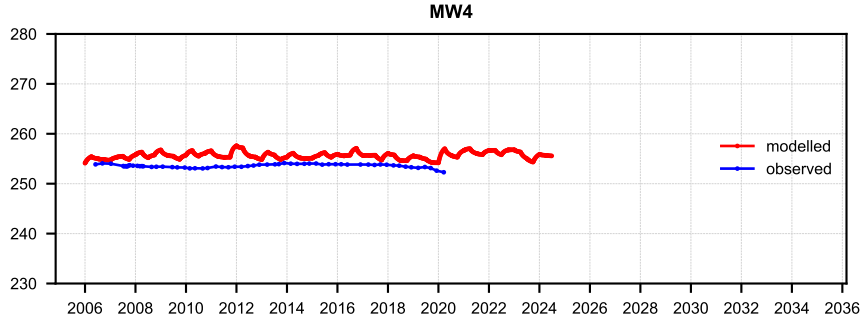
MW4
modelled
observed

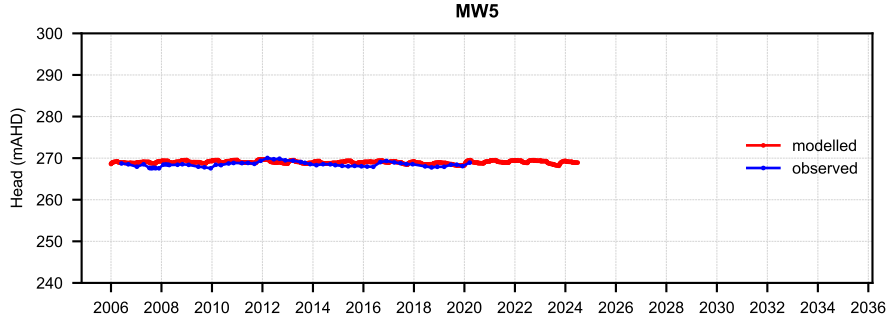
MW5
Head (mAHD)
modelled
observed

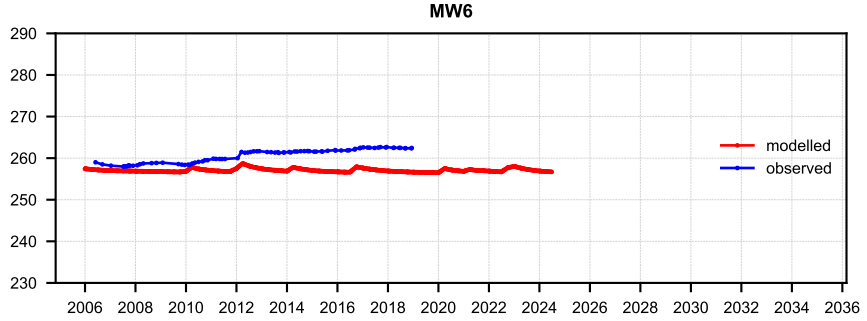
MW6
modelled
observed

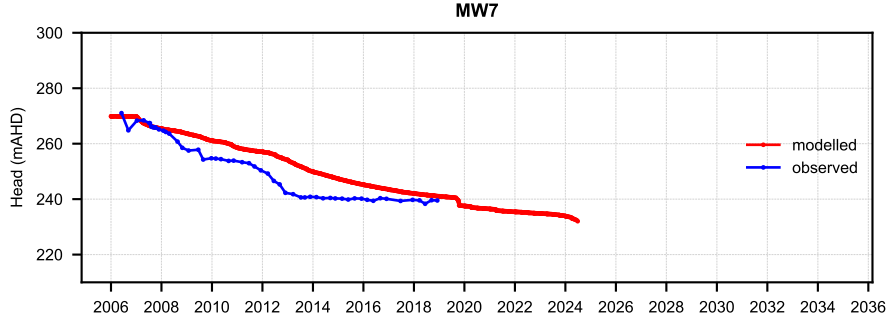
MW7
Head (mAHD)
modelled
observed

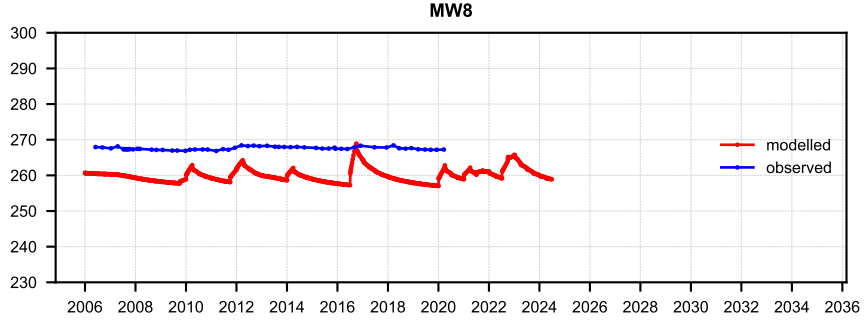
MW8
modelled
observed

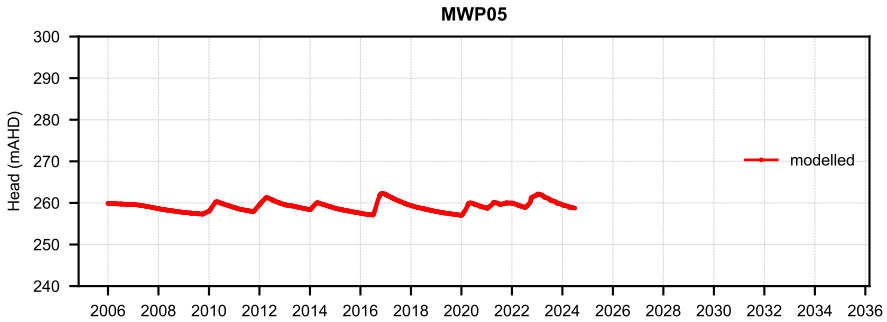
MWP05
Head (mAHD)
modelled

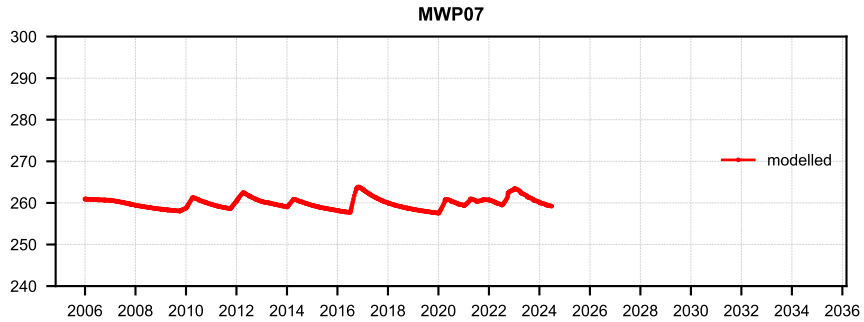
MWP07
modelled

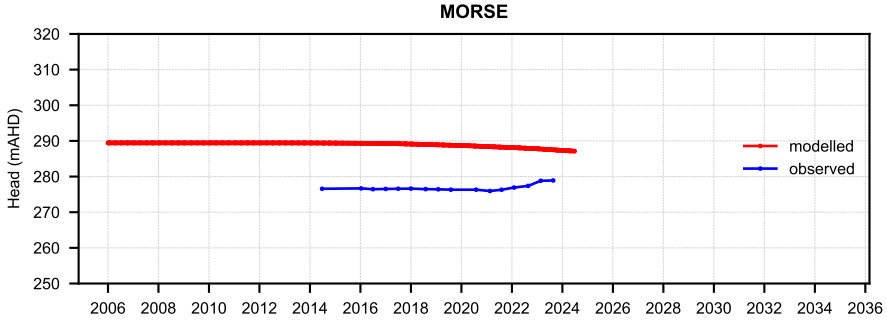
MORSE
Head (mAHD)
modelled
observed

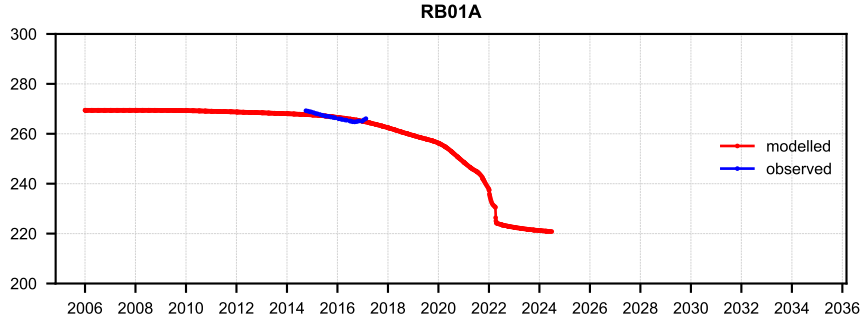
RB01A
modelled
observed

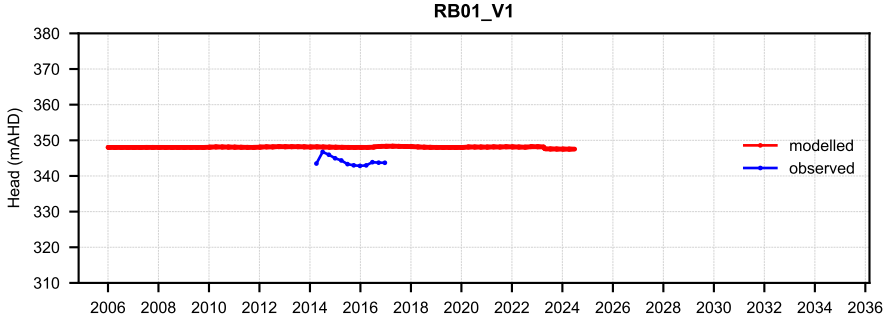
RB01_V1
Head (mAHD)
modelled
observed

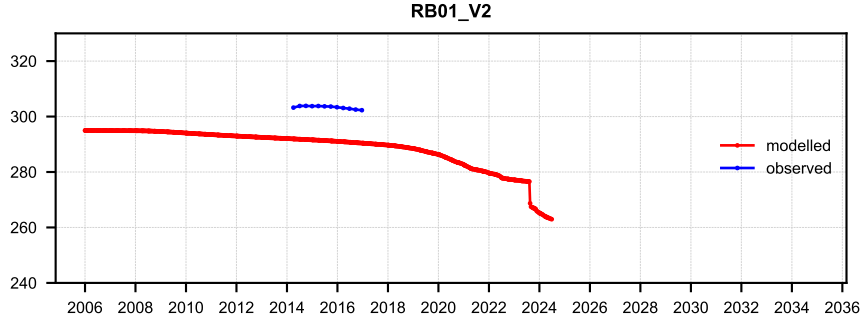
RB01_V2
modelled
observed

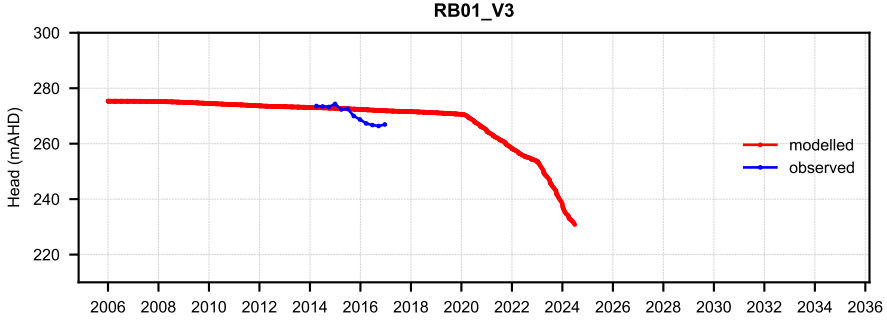
RB01_V3
Head (mAHD)
modelled
observed

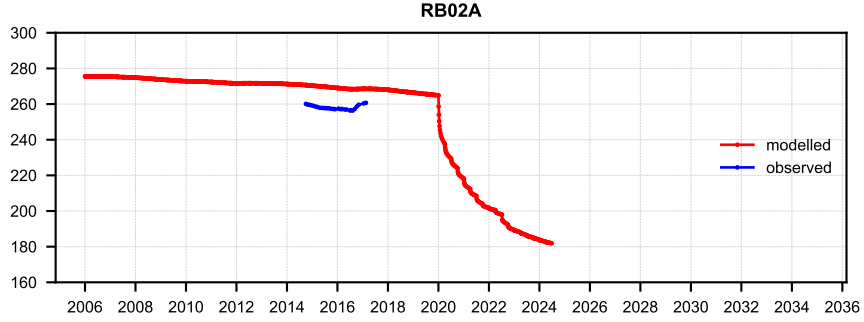
RB02A
modelled
observed

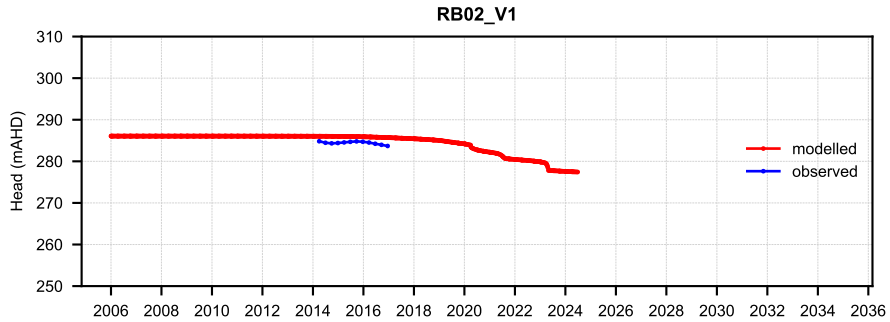
RB02_V1
Head (mAHD)
modelled
observed

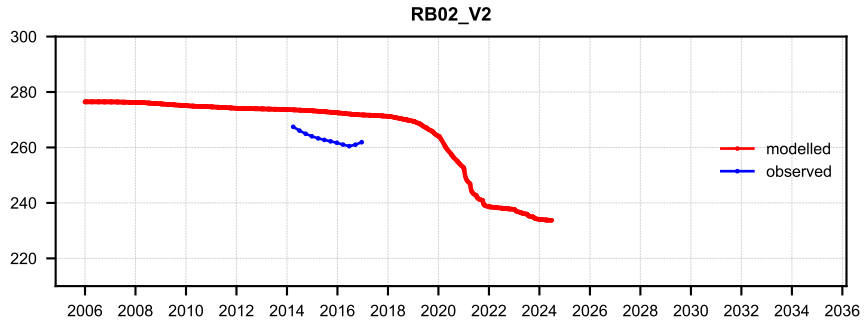
RB02_V2
modelled
observed

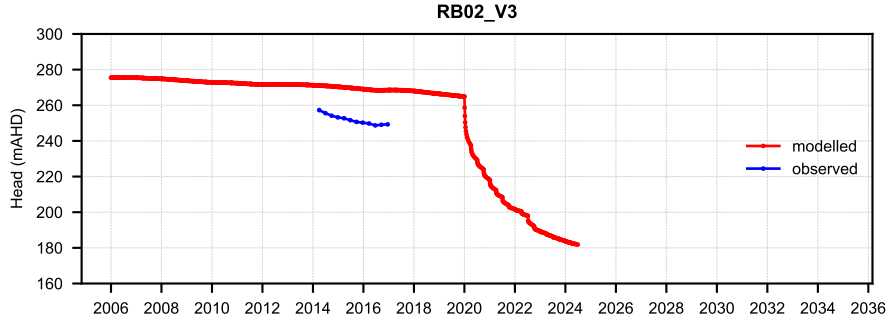
RB02_V3
Head (mAHD)
modelled
observed

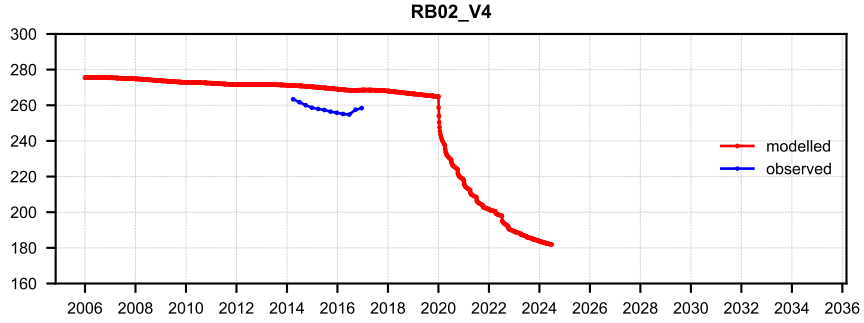
RB02_V4
modelled
observed

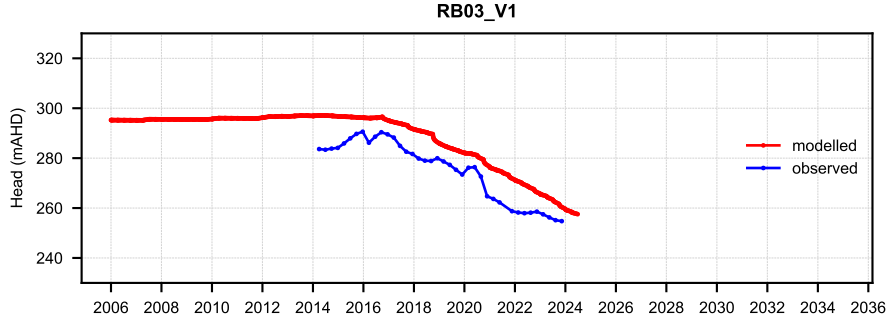
RB03_V1
Head (mAHD)
modelled
observed

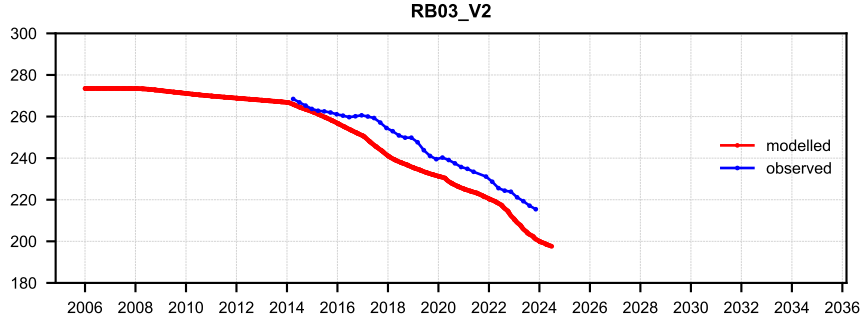
RB03_V2
modelled
observed

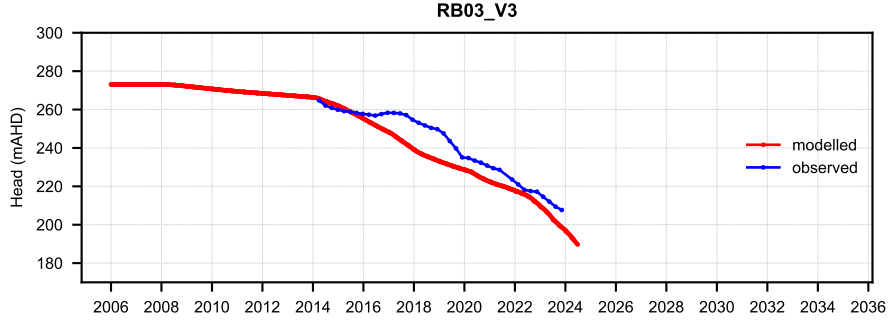
RB03_V3
Head (mAHD)
modelled
observed

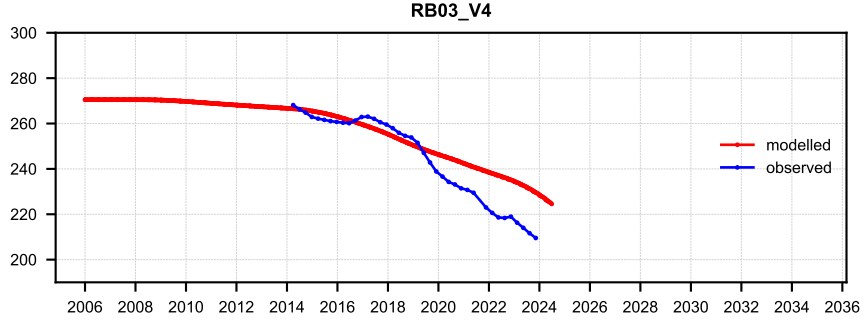
RB03_V4
modelled
observed

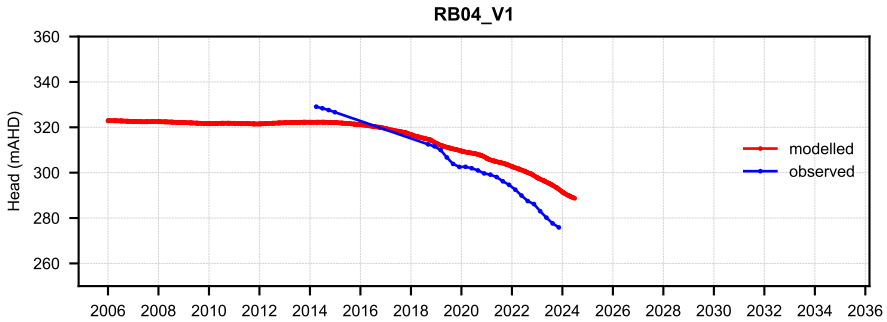
RB04_V1
Head (mAHD)
modelled
observed

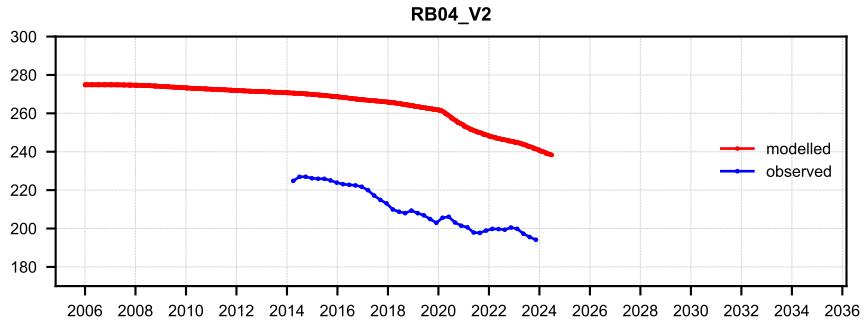
RB04_V2
modelled
observed

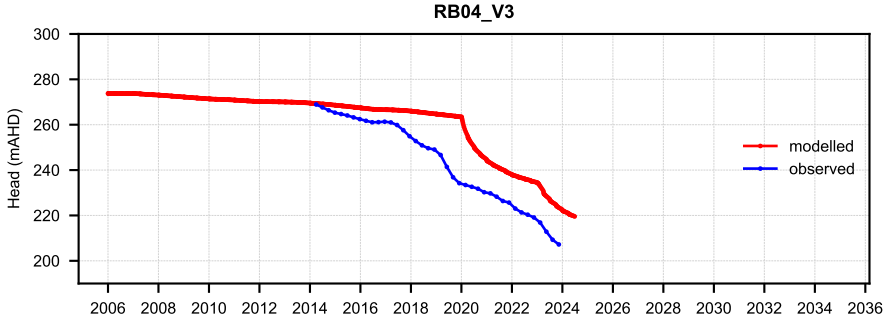
RB04_V3
Head (mAHD)
modelled
observed

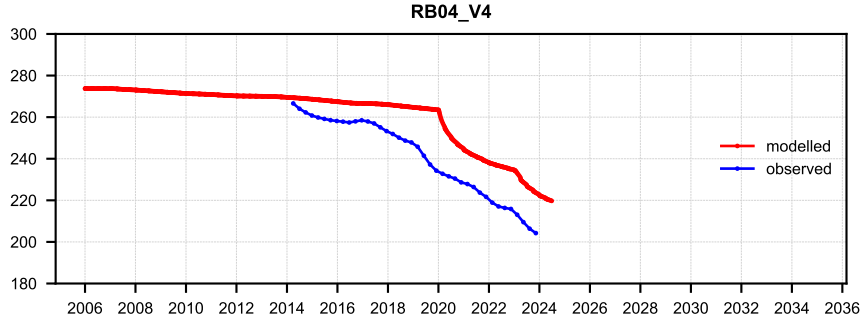
RB04_V4
modelled
observed

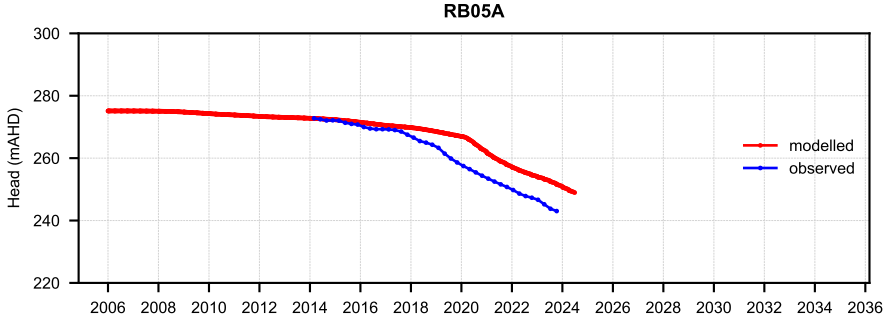
RB05A
Head (mAHD)
modelled
observed

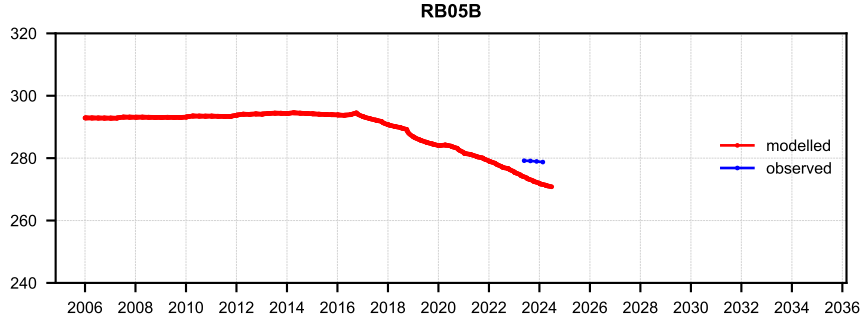
RB05B
modelled
observed

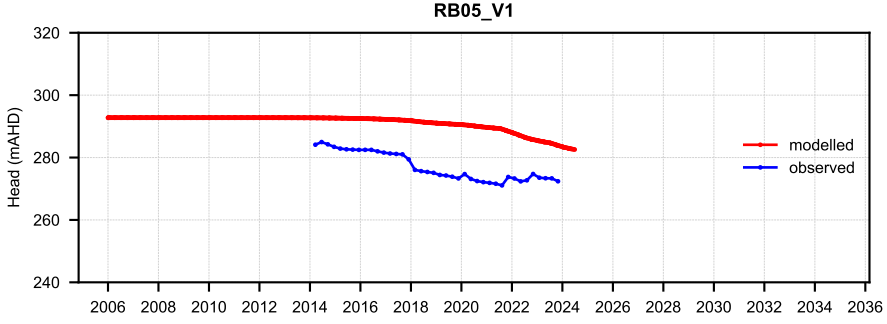
RB05_V1
Head (mAHD)
modelled
observed

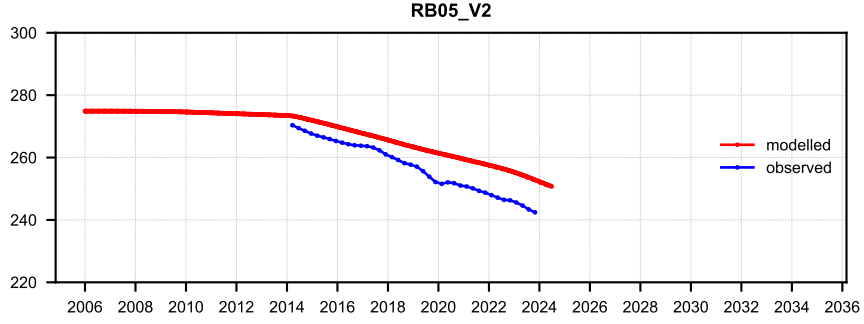
RB05_V2
modelled
observed

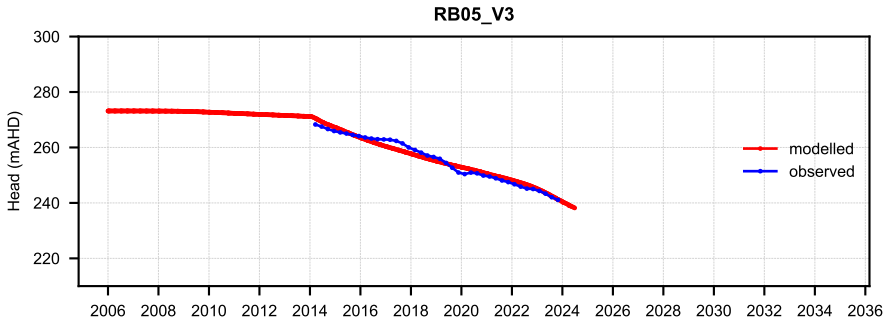
RB05_V3
Head (mAHD)
modelled
observed

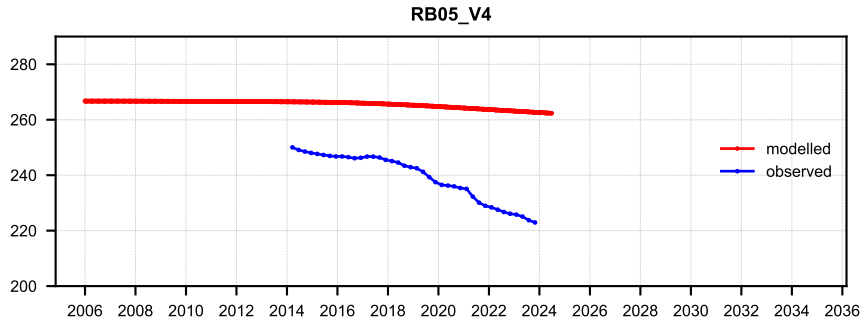
RB05_V4
modelled
observed

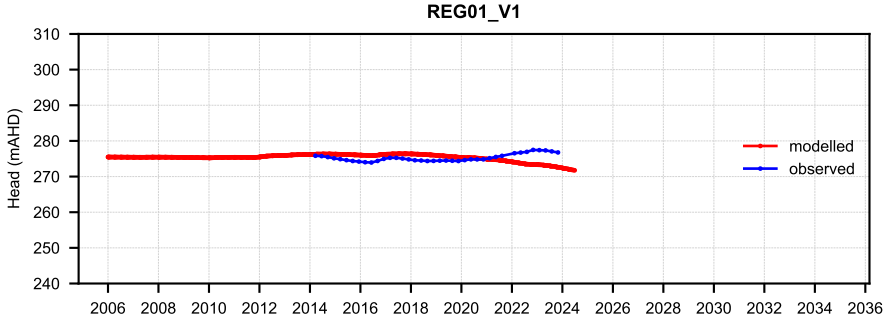
REG01_V1
Head (mAHD)
modelled
observed

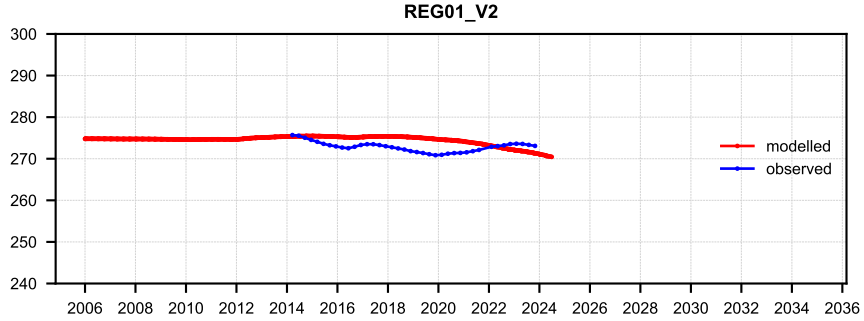
REG01_V2
modelled
observed

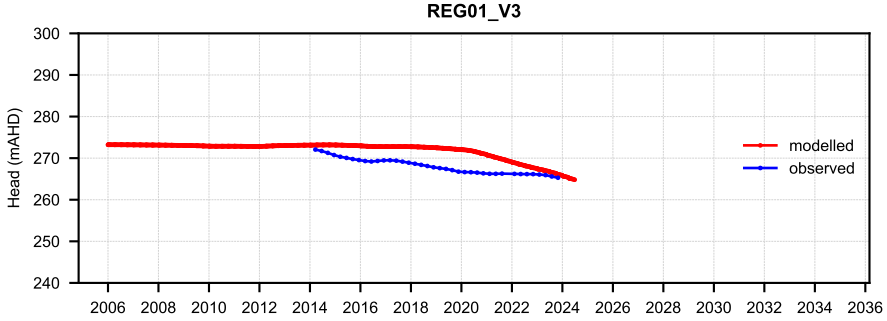
REG01_V3
Head (mAHD)
modelled
observed

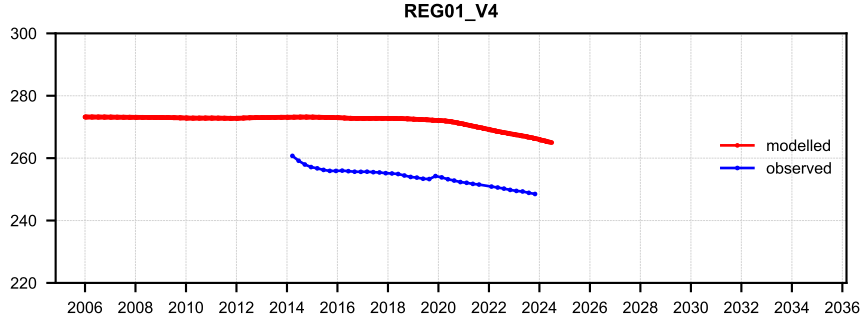
REG01_V4
modelled
observed

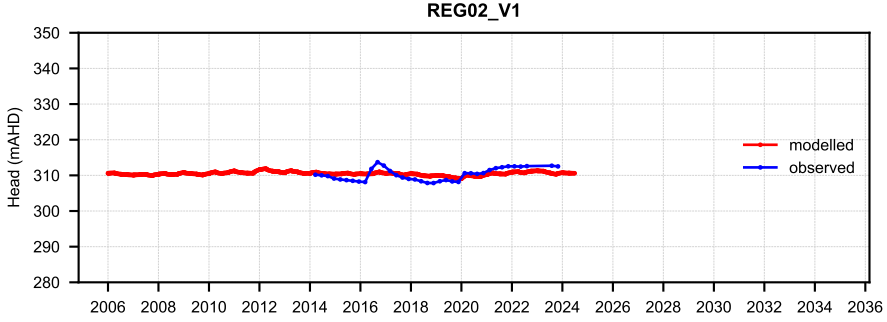
REG02_V1
Head (mAHD)
modelled
observed

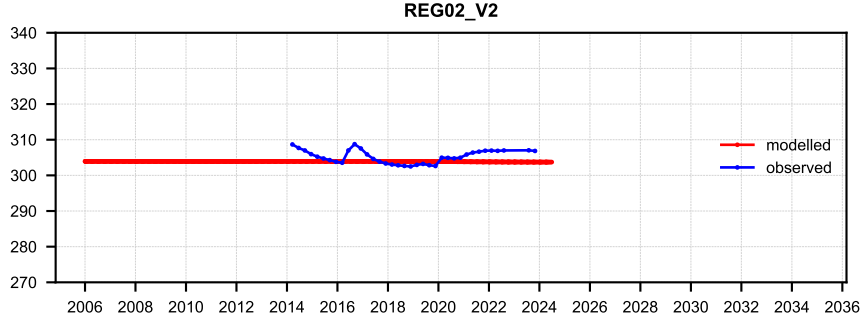
REG02_V2
modelled
observed

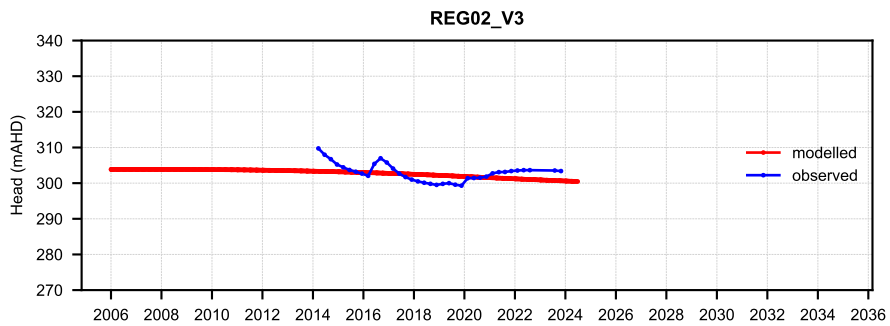
REG02_V3
Head (mAHD)
modelled
observed

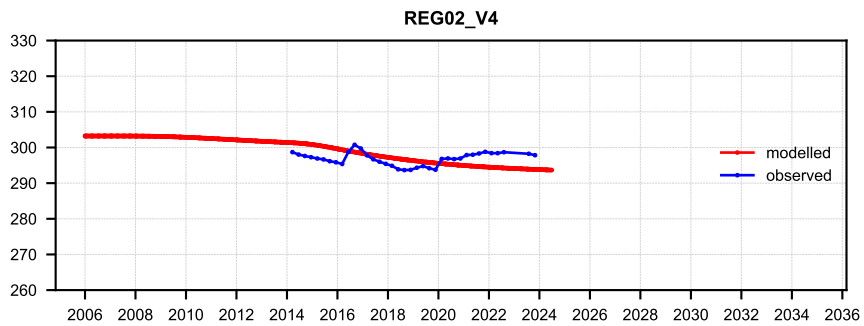
REG02_V4
modelled
observed

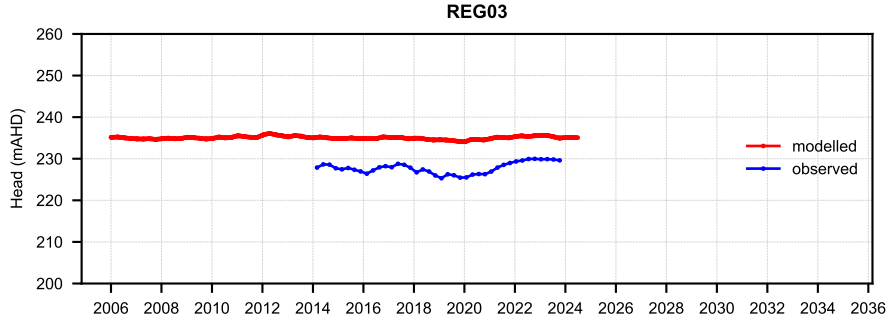
REG03
Head (mAHD)
modelled
observed

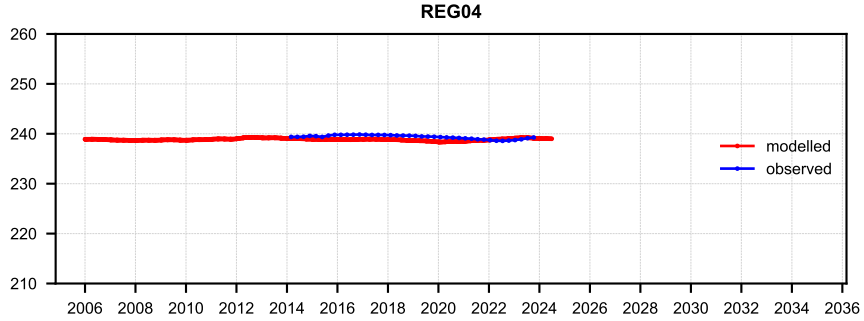
REG04
modelled
observed

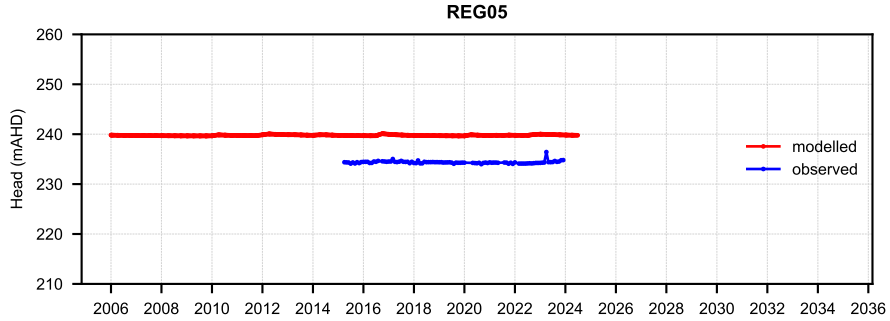
REG05
Head (mAHD)
modelled
observed

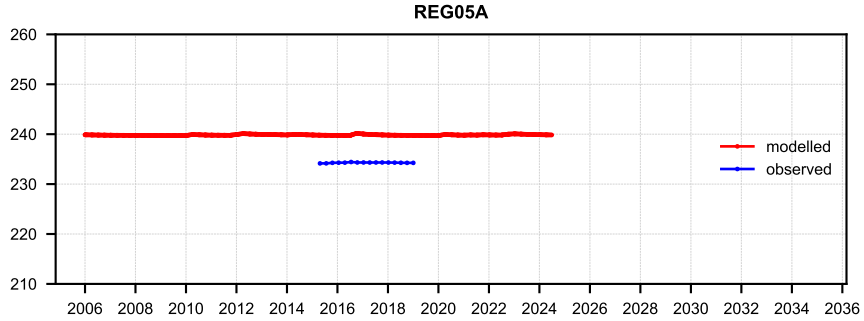
REG05A
modelled
observed

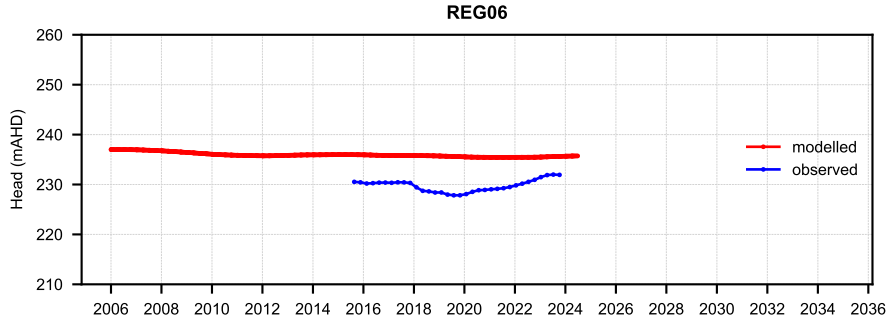
REG06
Head (mAHD)
modelled
observed

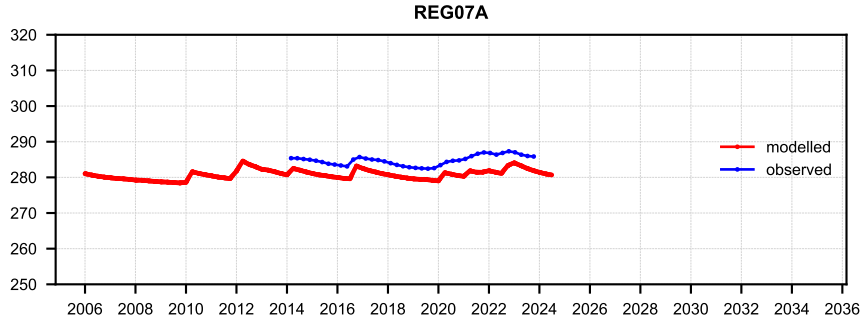
REG07A
modelled
observed

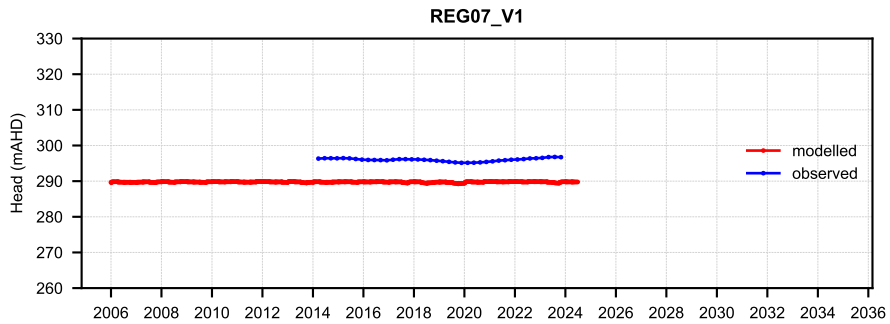
REG07_V1
Head (mAHD)
modelled
observed

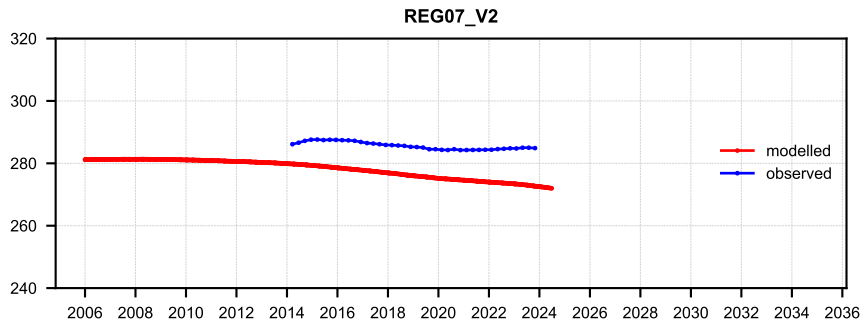
REG07_V2
modelled
observed

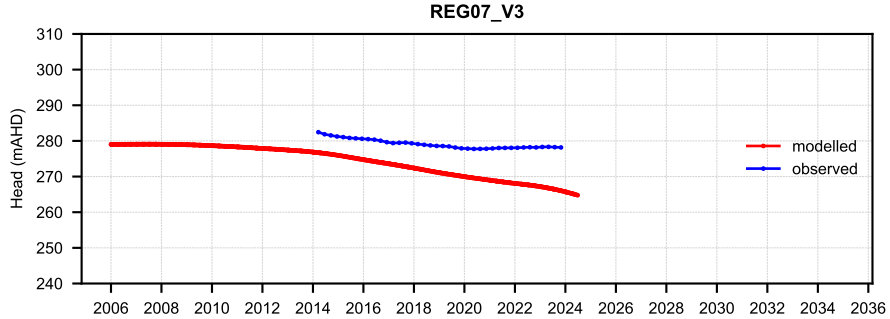
REG07_V3
Head (mAHD)
modelled
observed

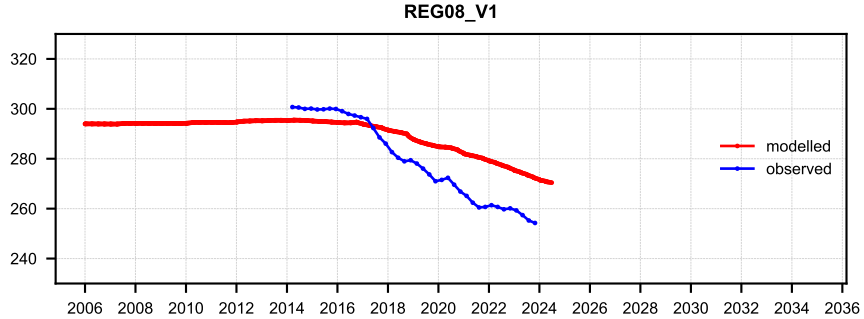
REG08_V1
modelled
observed

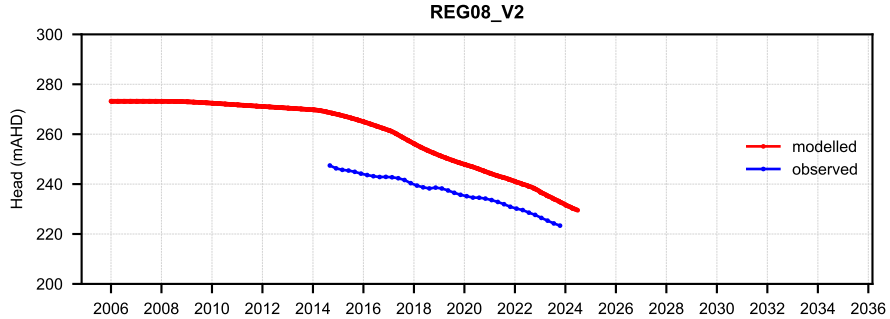
REG08_V2
Head (mAHD)
modelled
observed

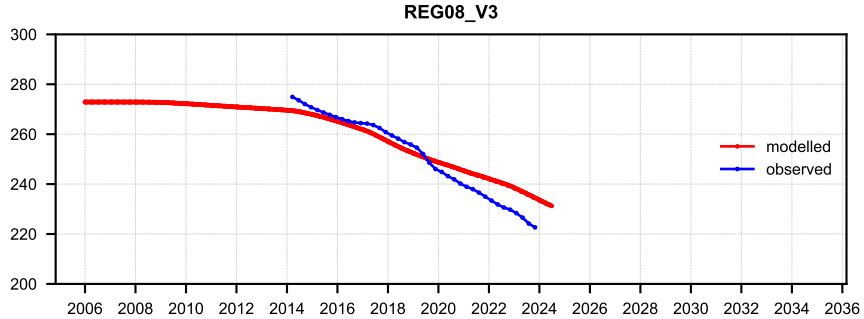
REG08_V3
modelled
observed

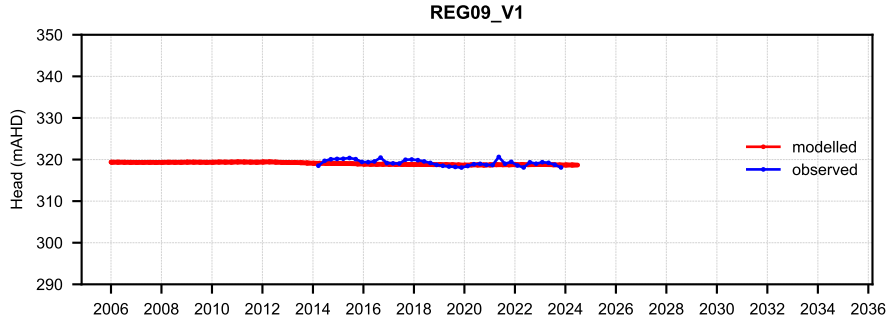
REG09_V1
Head (mAHD)
modelled
observed

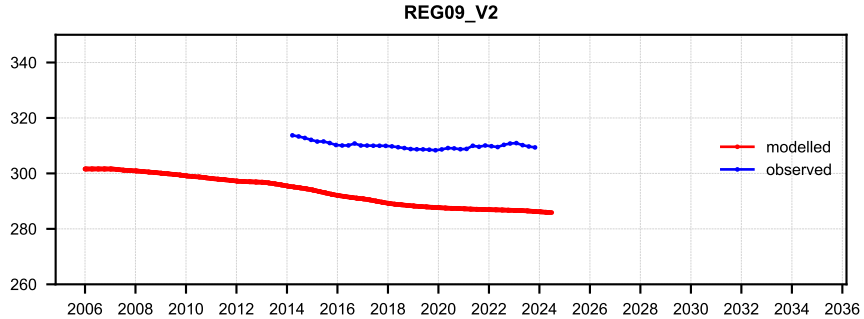
REG09_V2
modelled
observed

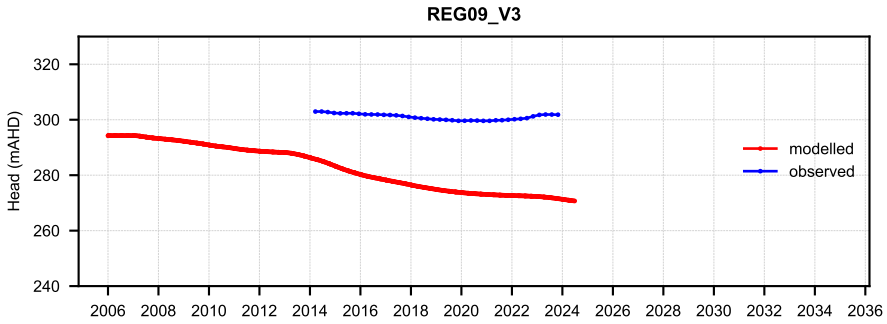
REG09_V3
Head (mAHD)
modelled
observed

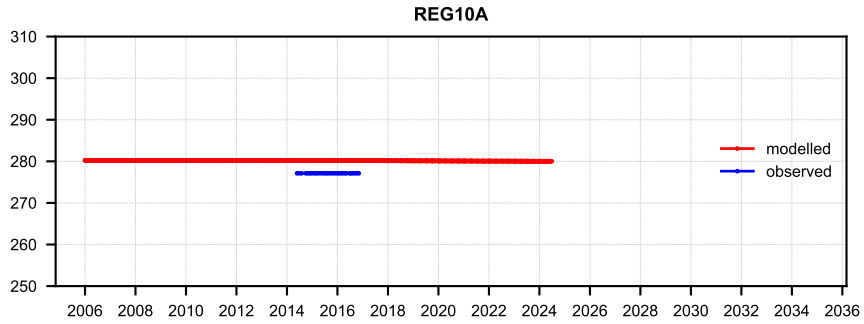
REG10A
modelled
observed

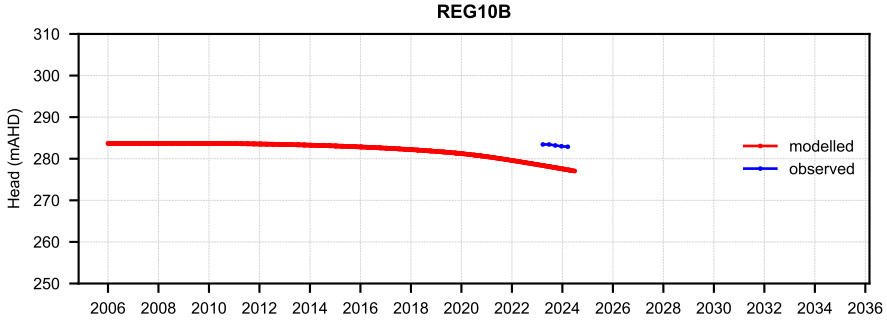
REG10B
Head (mAHD)
modelled
observed

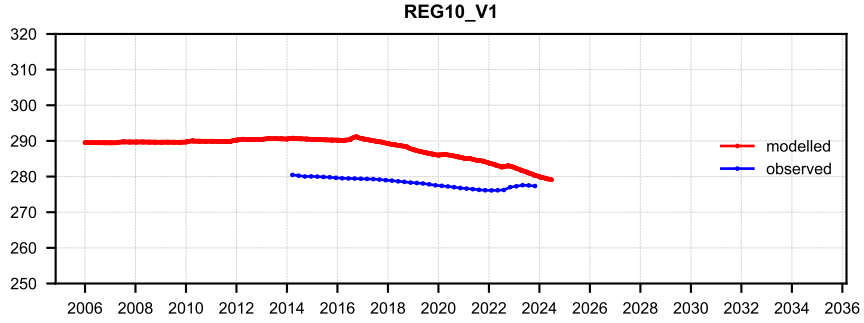
REG10_V1
modelled
observed

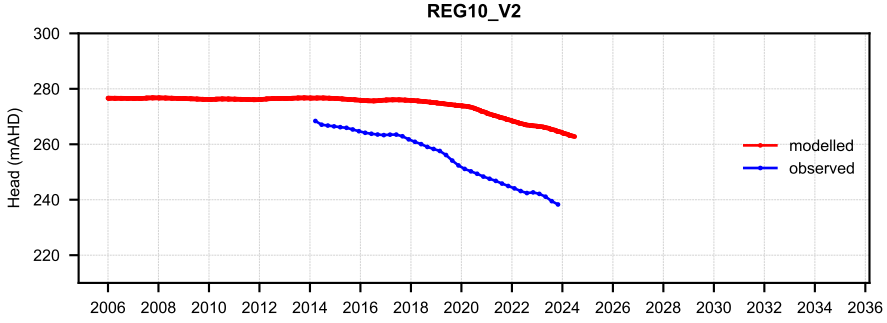
REG10_V2
Head (mAHD)
modelled
observed

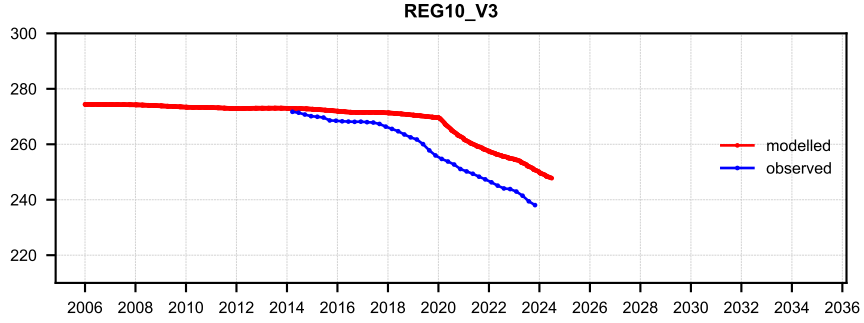
REG10_V3
modelled
observed

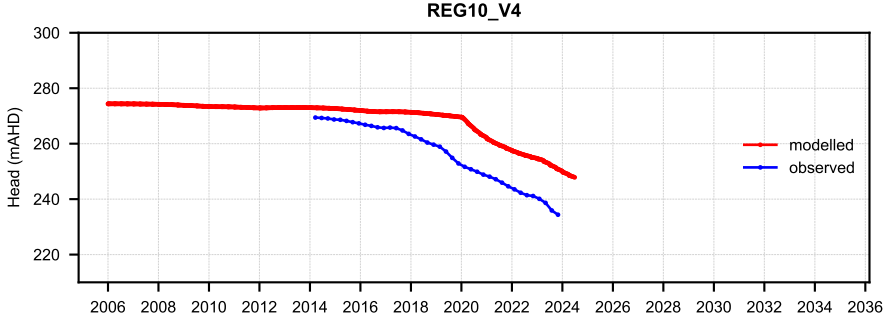
REG10_V4
Head (mAHD)
modelled
observed

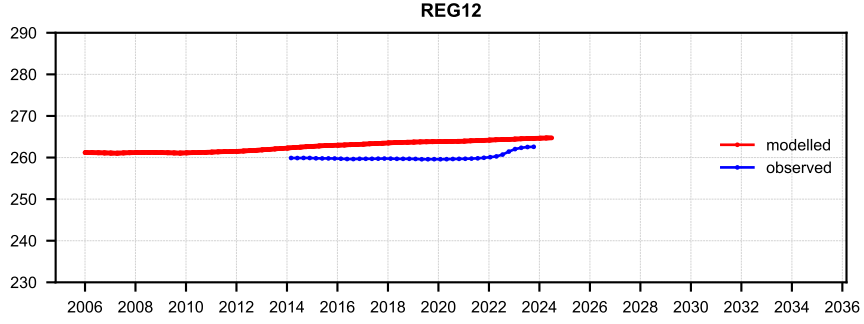
REG12
modelled
observed

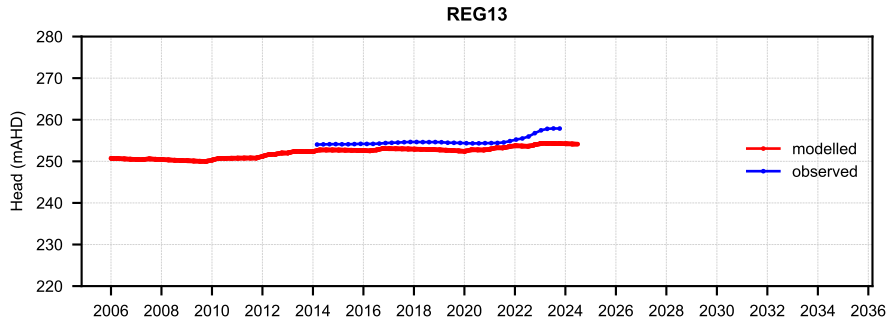
REG13
Head (mAHD)
modelled
observed

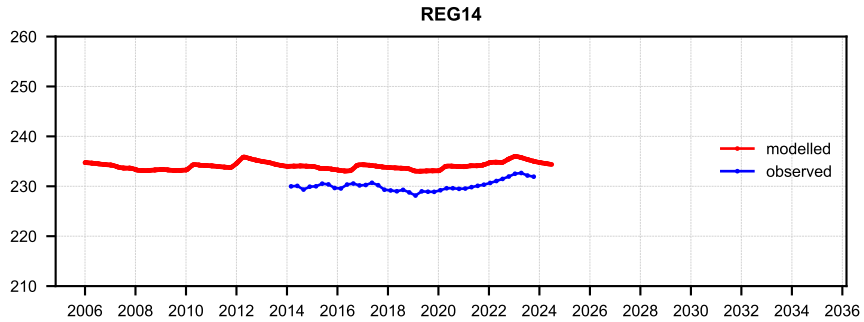
REG14
modelled
observed

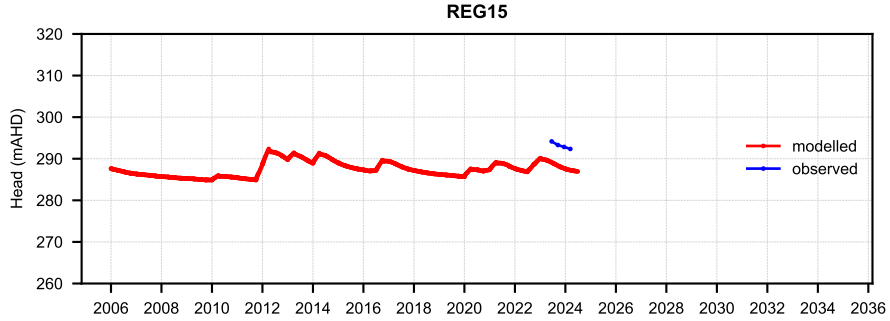
REG15
Head (mAHD)
modelled
observed

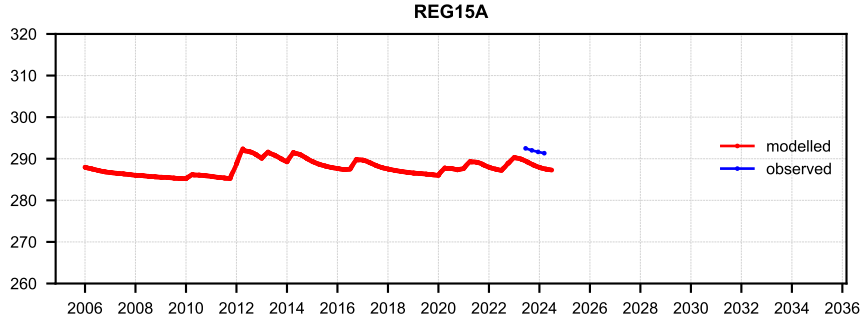
REG15A
modelled
observed

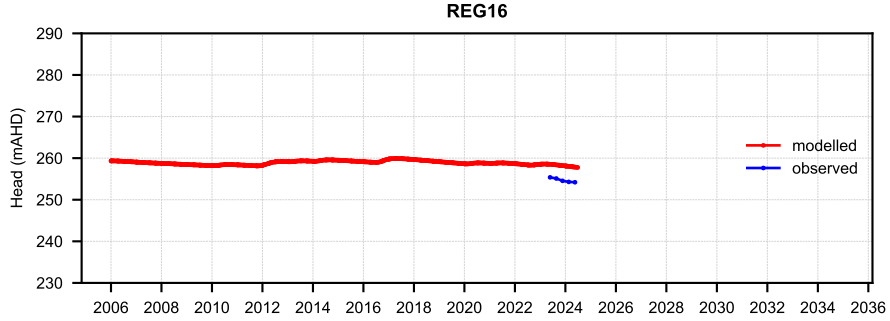
REG16
Head (mAHD)
modelled
observed

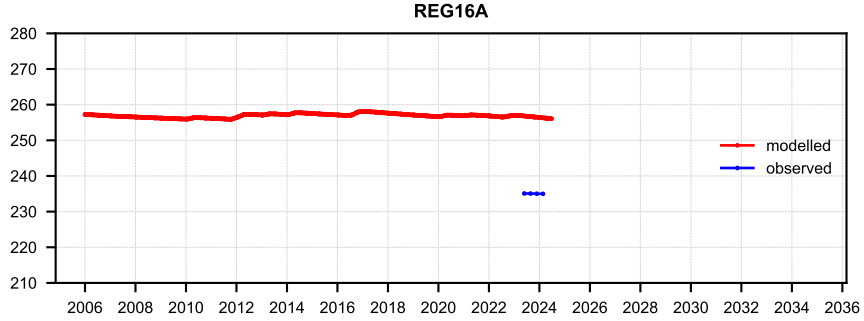
REG16A
modelled
observed

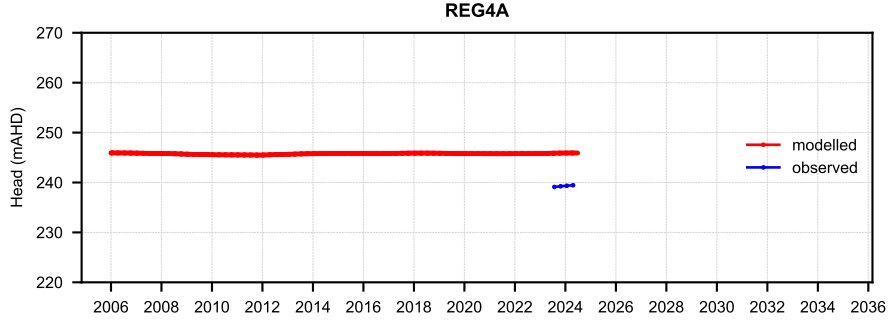
REG4A
Head (mAHD)
modelled
observed

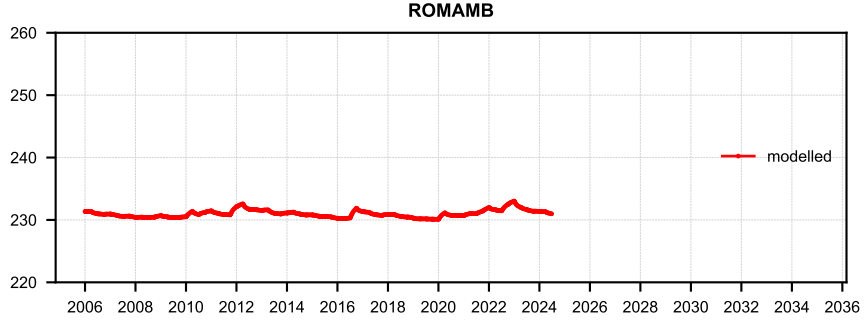
ROMAMB
modelled

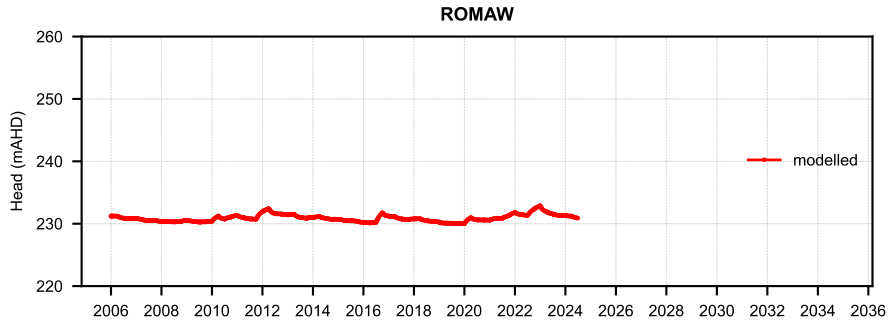
ROMAW
Head (mAHD)
modelled

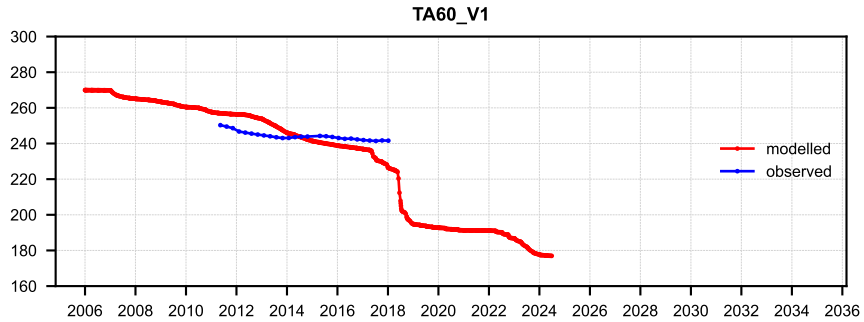
TA60_V1
modelled
observed

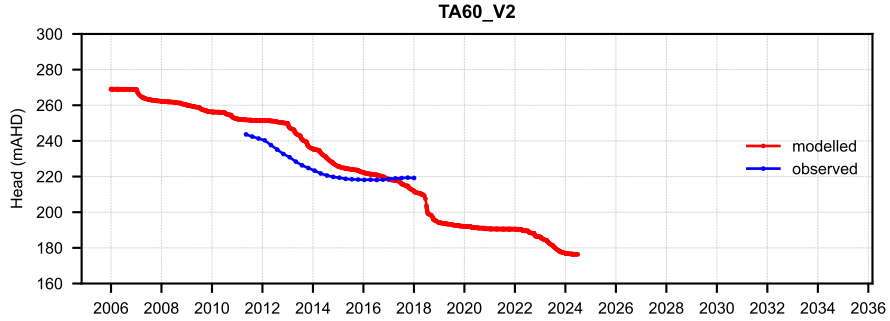
TA60_V2
Head (mAHD)
modelled
observed

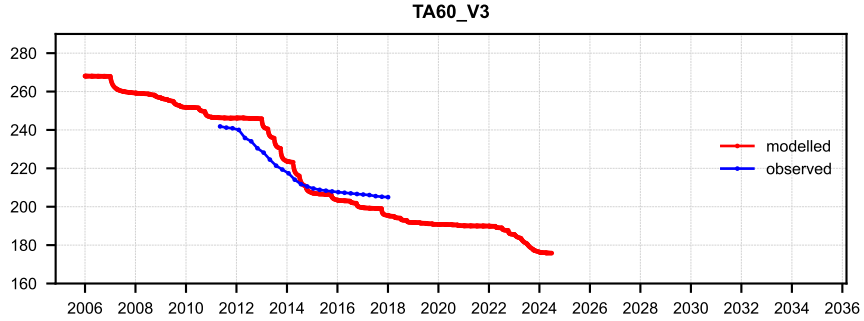
TA60_V3
modelled
observed

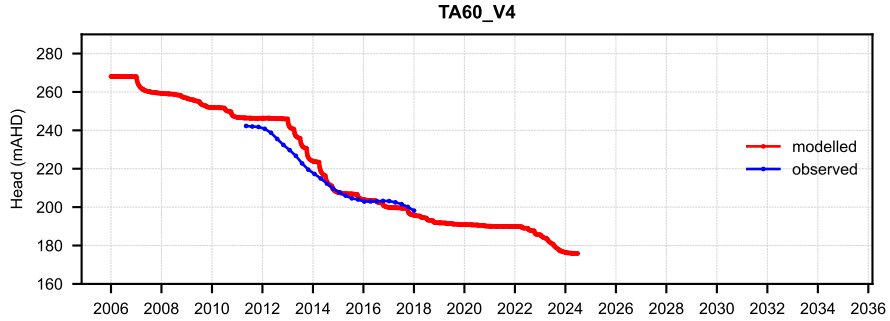
TA60_V4
Head (mAHD)
modelled
observed

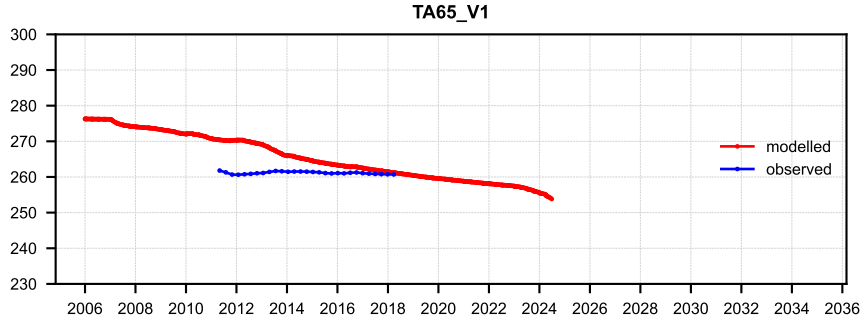
TA65_V1
modelled
observed

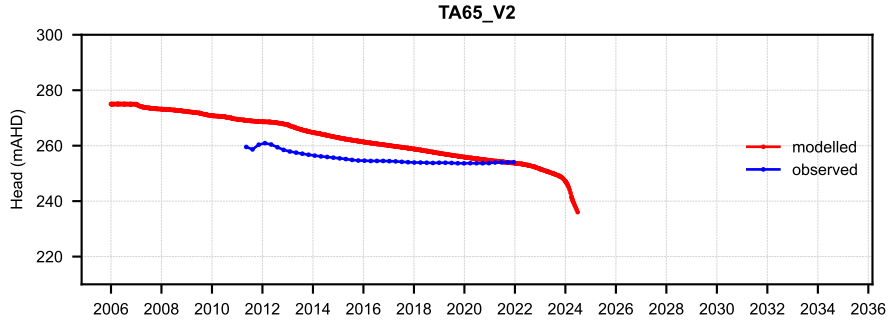
TA65_V2
Head (mAHD)
modelled
observed

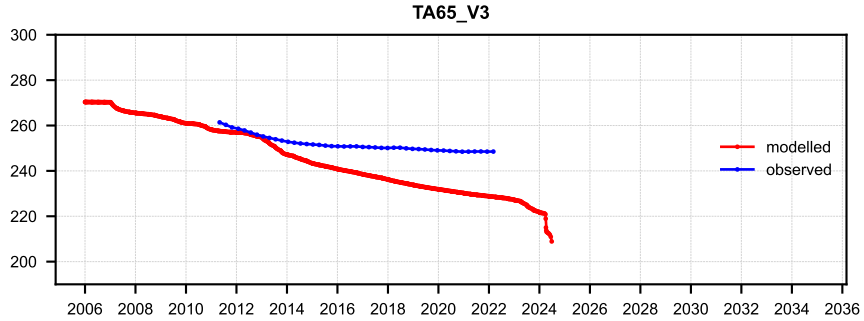
TA65_V3
modelled
observed

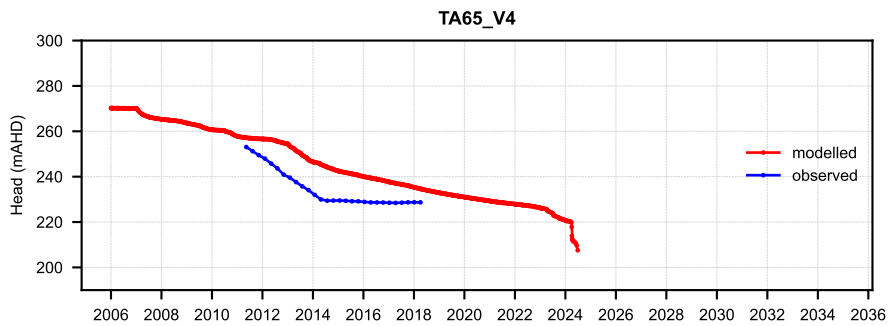
TA65_V4
Head (mAHD)
modelled
observed

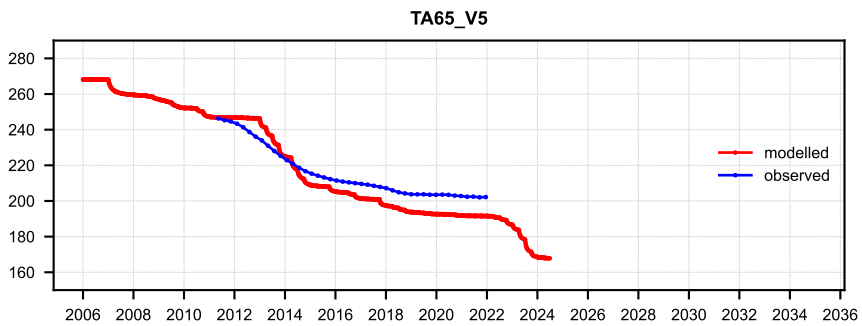
TA65_V5
modelled
observed

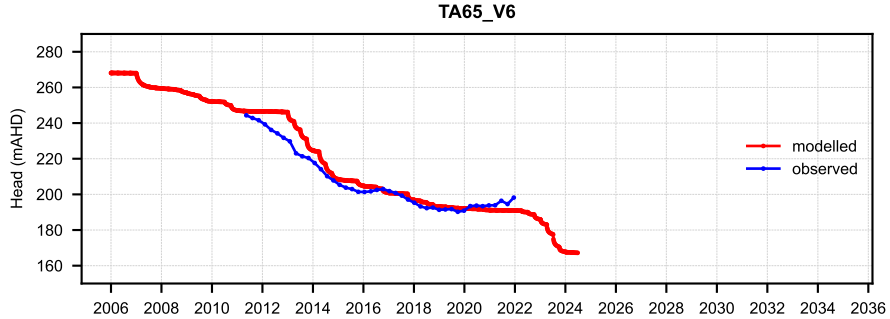
TA65_V6
Head (mAHD)
modelled
observed

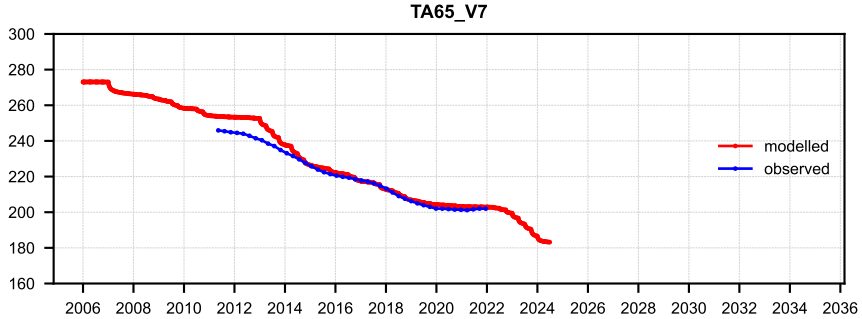
TA65_V7
modelled
observed

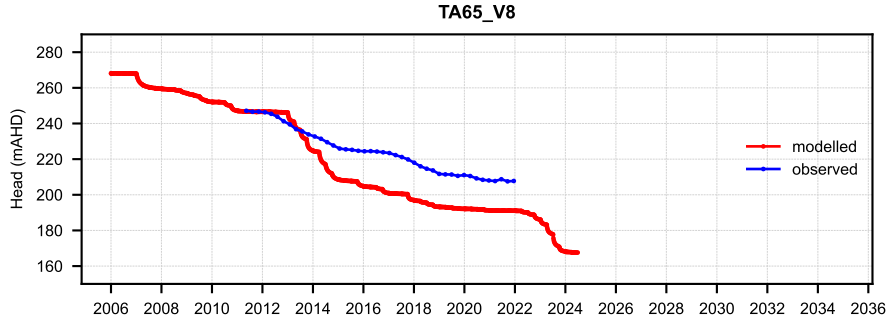
TA65_V8
Head (mAHD)
modelled
observed

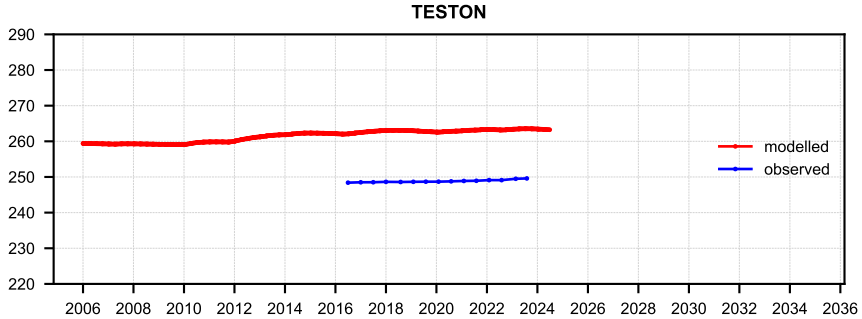
TESTON
modelled
observed

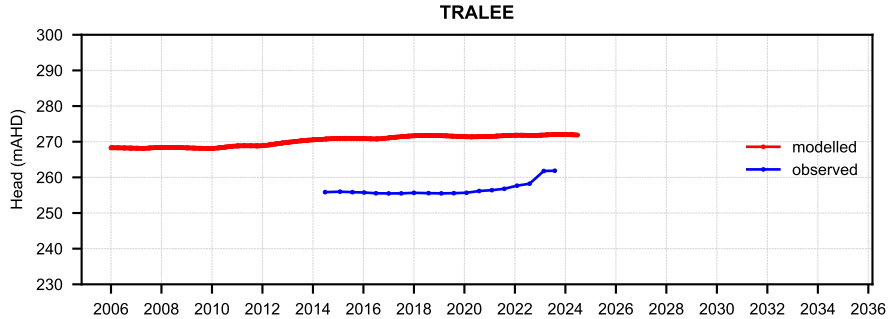
TRALEE
Head (mAHD)
modelled
observed

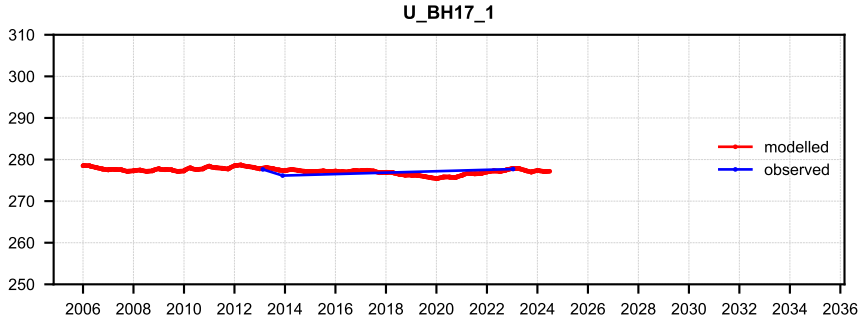
U_BH17_1
modelled
observed

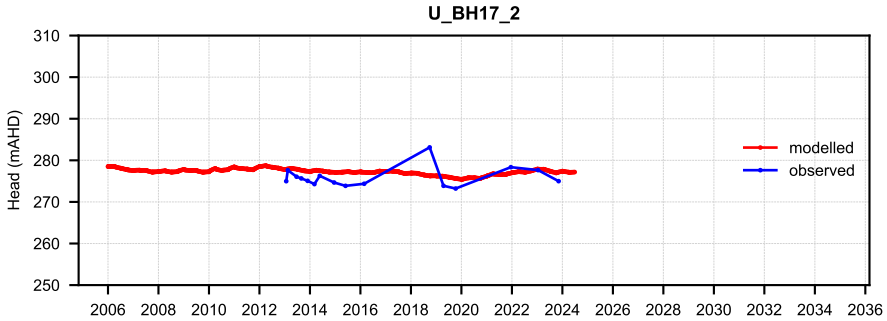
U_BH17_2
Head (mAHD)
modelled
observed

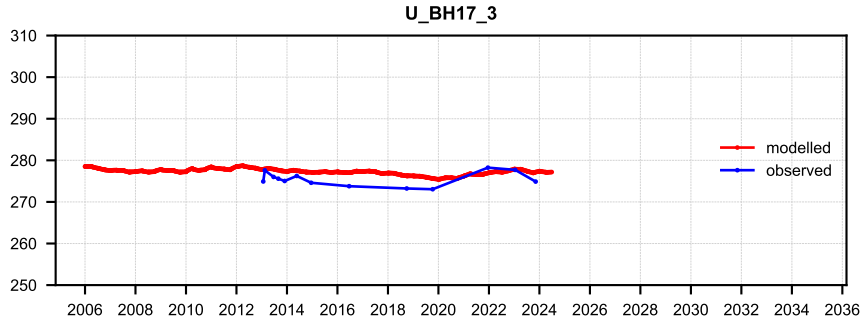
U_BH17_3
modelled
observed

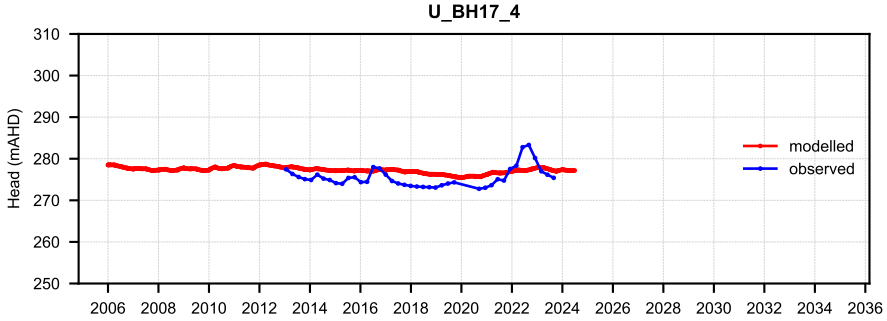
U_BH17_4
Head (mAHD)
modelled
observed

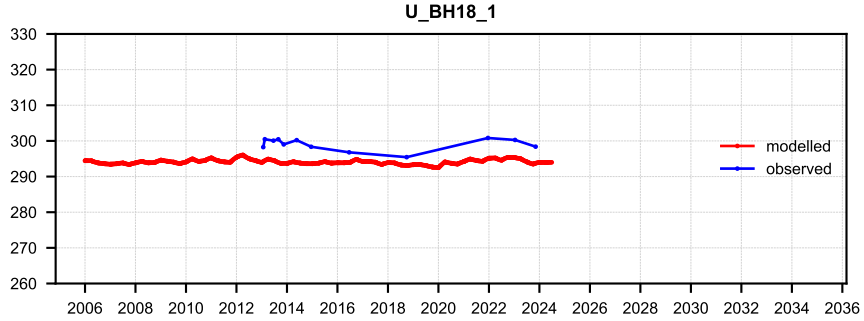
U_BH18_1
modelled
observed

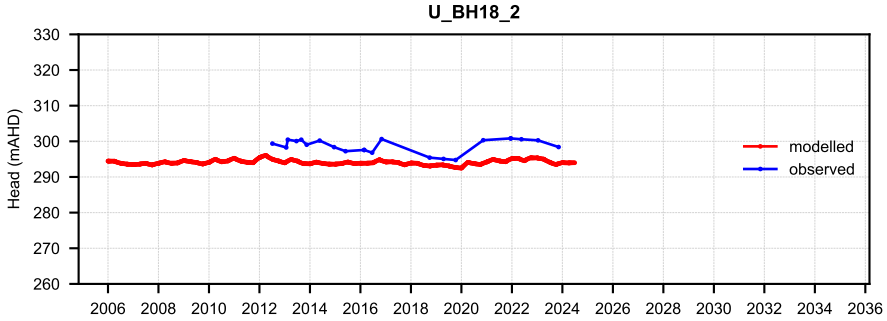
U_BH18_2
Head (mAHD)
modelled
observed

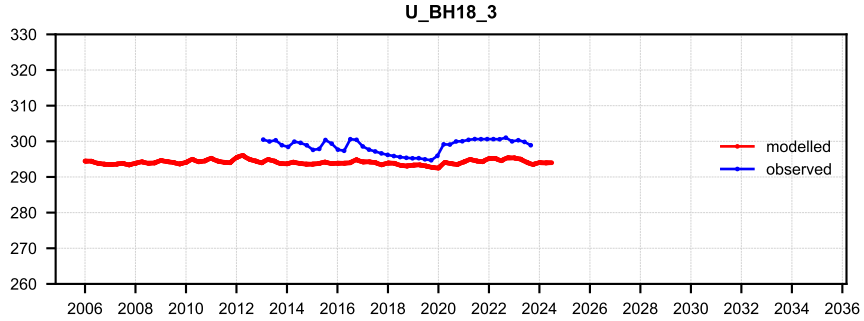
U_BH18_3
modelled
observed

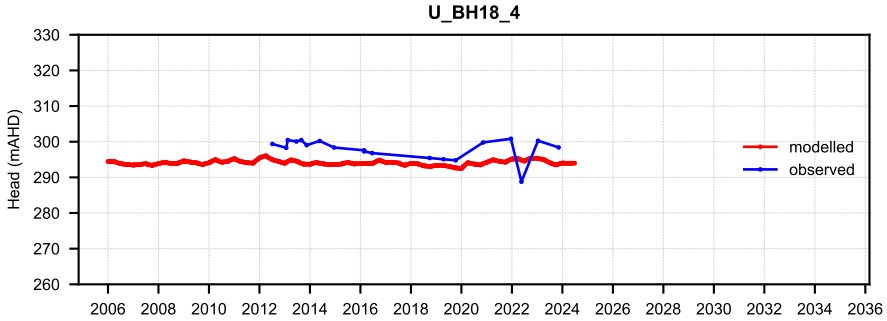
U_BH18_4
Head (mAHD)
modelled
observed

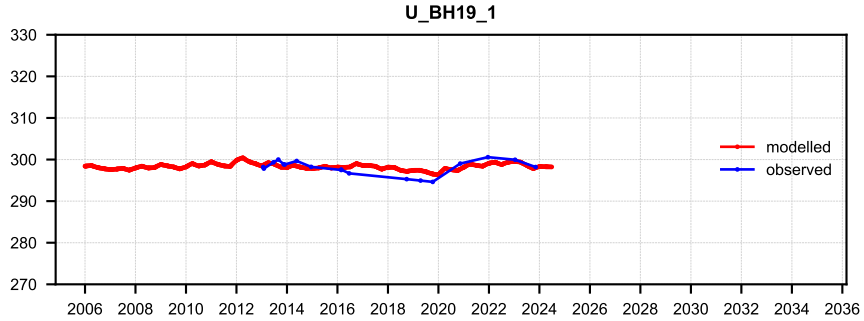
U_BH19_1
modelled
observed

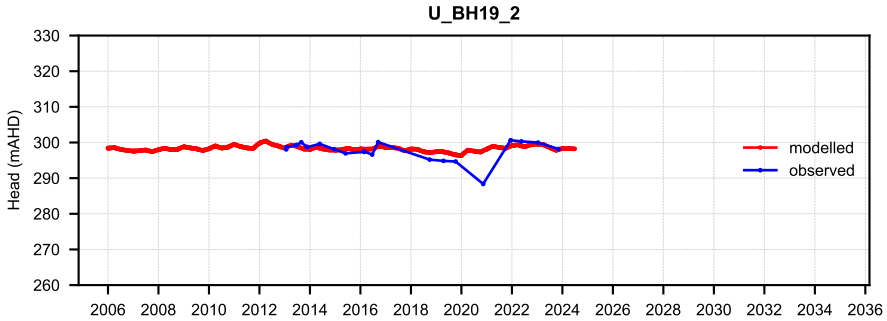
U_BH19_2
Head (mAHD)
330
320
310
300
290
280
270
260
2006 2008 2010 2012 2014 2016 2018 2020 2022 2024 2026 2028 2030 2032 2034 2036
modelled
observed

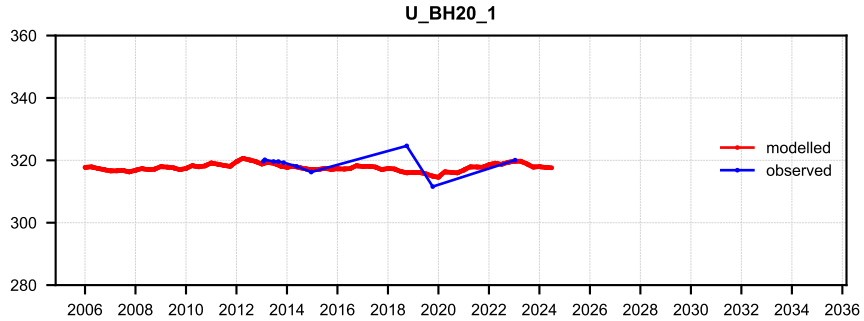
U_BH20_1
360
340
320
300
280
2006 2008 2010 2012 2014 2016 2018 2020 2022 2024 2026 2028 2030 2032 2034 2036
modelled
observed

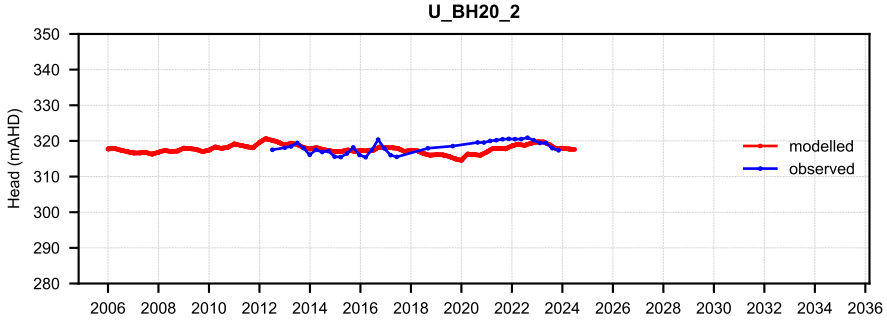
U_BH20_2
Head (mAHD)
350
340
330
320
310
300
290
280
2006 2008 2010 2012 2014 2016 2018 2020 2022 2024 2026 2028 2030 2032 2034 2036
modelled
observed

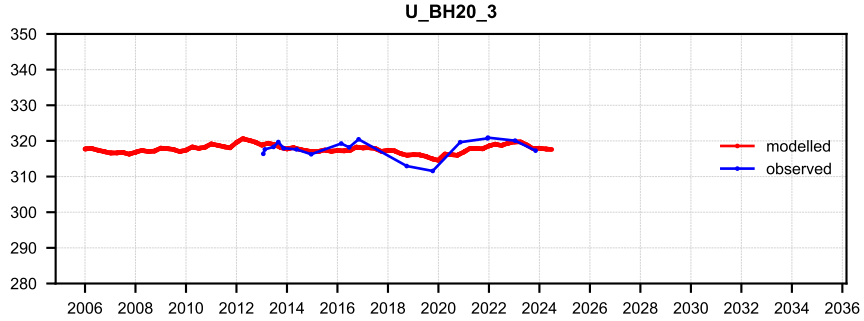
U_BH20_3
350
340
330
320
310
300
290
280
2006 2008 2010 2012 2014 2016 2018 2020 2022 2024 2026 2028 2030 2032 2034 2036
modelled
observed

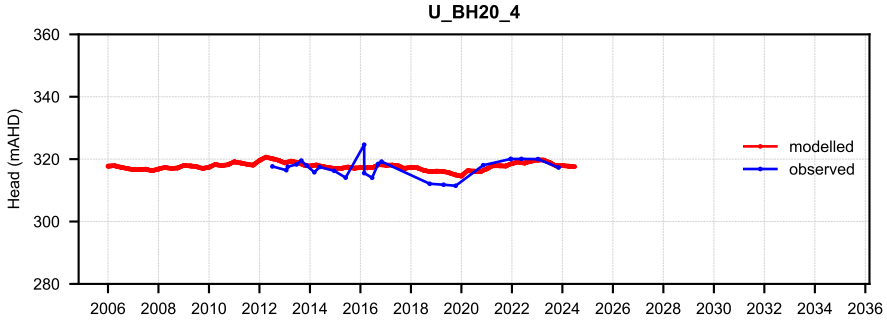
U_BH20_4
Head (mAHD)
360
340
320
300
280
2006 2008 2010 2012 2014 2016 2018 2020 2022 2024 2026 2028 2030 2032 2034 2036
modelled
observed

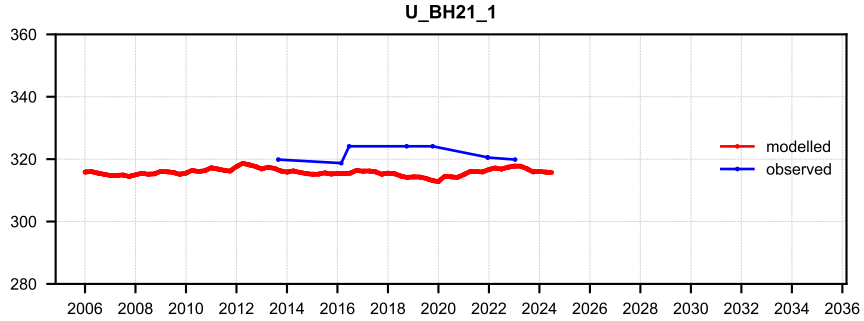
U_BH21_1
360
340
320
300
280
2006 2008 2010 2012 2014 2016 2018 2020 2022 2024 2026 2028 2030 2032 2034 2036
modelled
observed

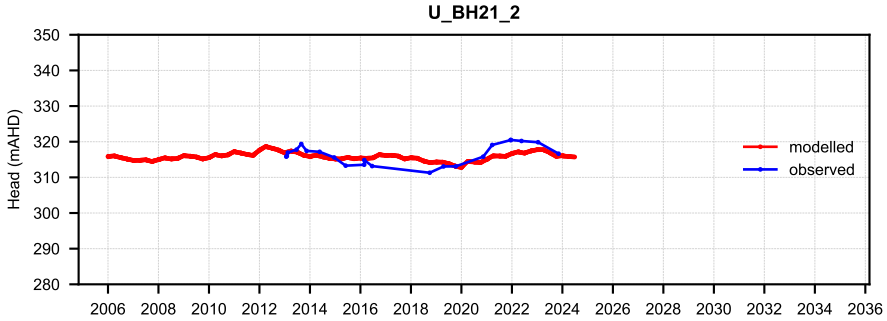
U_BH21_2
Head (mAHD)
350
340
330
320
310
300
290
280
2006 2008 2010 2012 2014 2016 2018 2020 2022 2024 2026 2028 2030 2032 2034 2036
modelled
observed

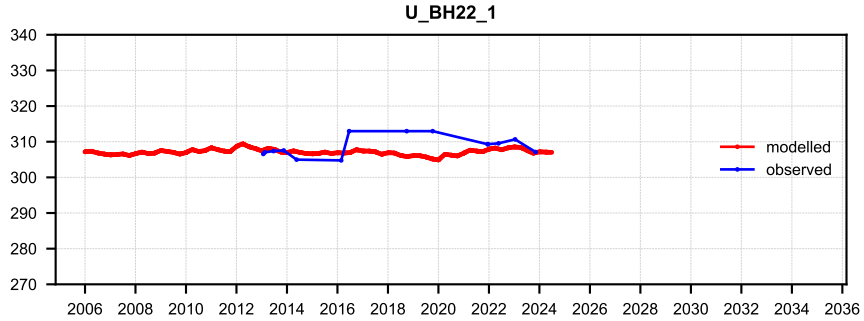
U_BH22_1
340
330
320
310
300
290
280
270
2006 2008 2010 2012 2014 2016 2018 2020 2022 2024 2026 2028 2030 2032 2034 2036
modelled
observed

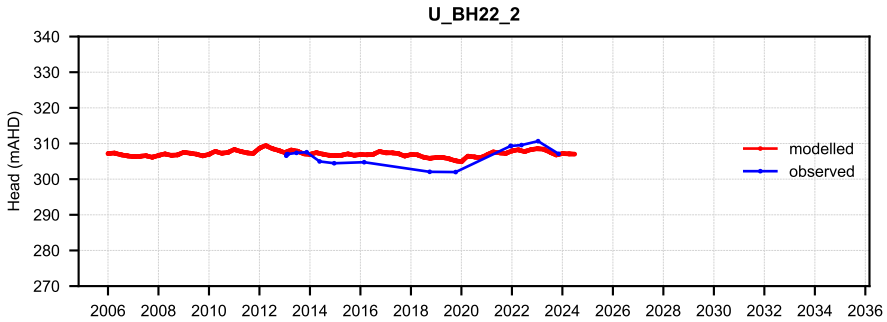
U_BH22_2
Head (mAHD)
modelled
observed

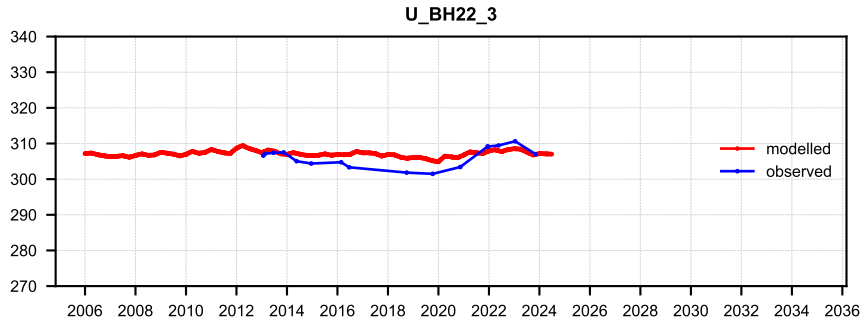
U_BH22_3
modelled
observed

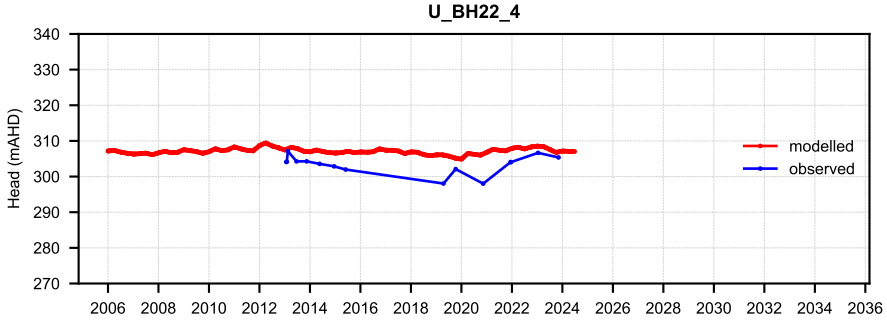
U_BH22_4
Head (mAHD)
modelled
observed

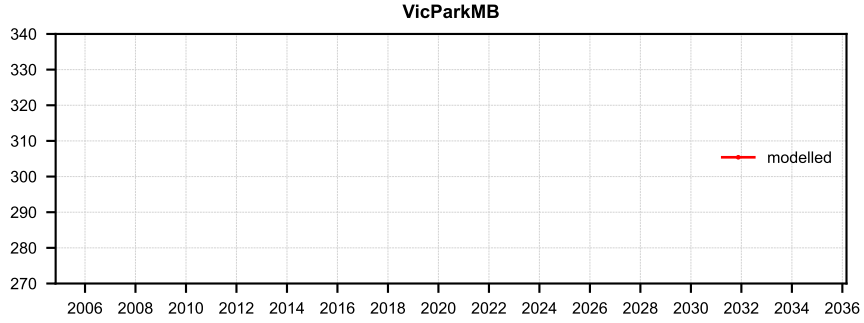
VicParkMB
modelled

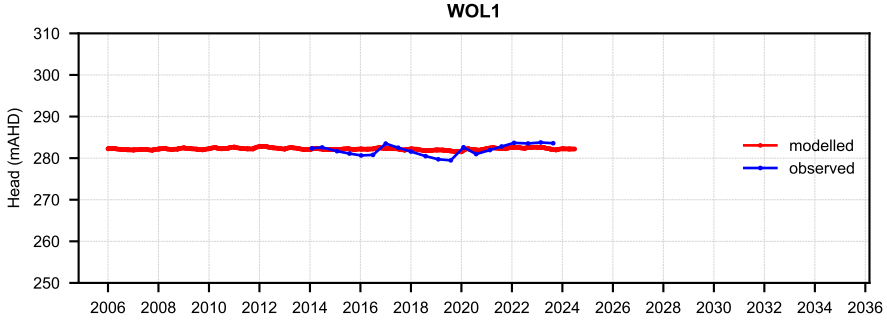
WOL1
Head (mAHD)
modelled
observed

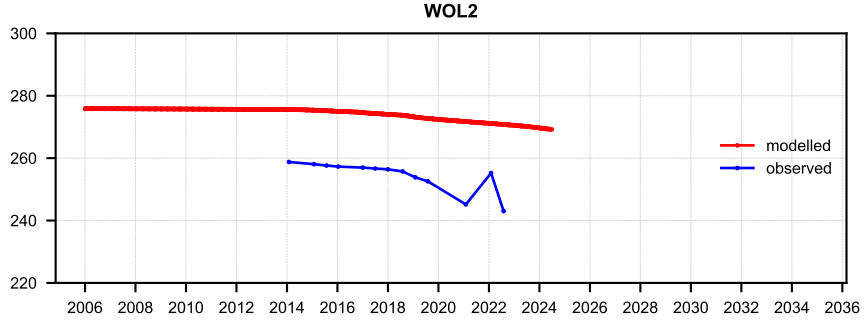
WOL2
modelled
observed

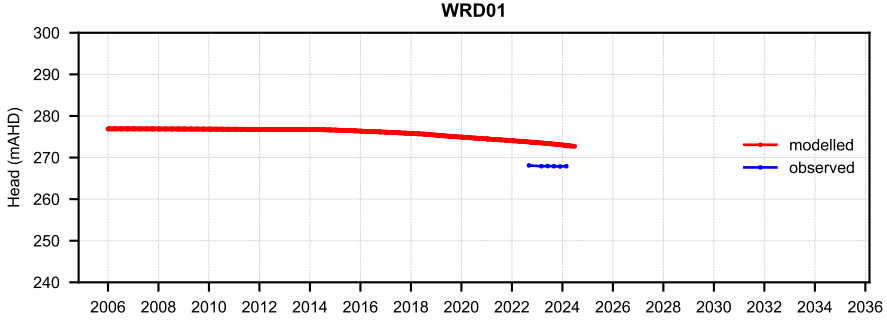
WRD01
Head (mAHD)
modelled
observed

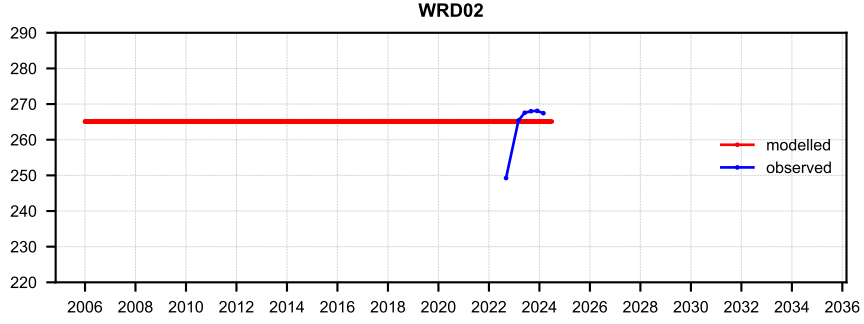
WRD02
modelled
observed

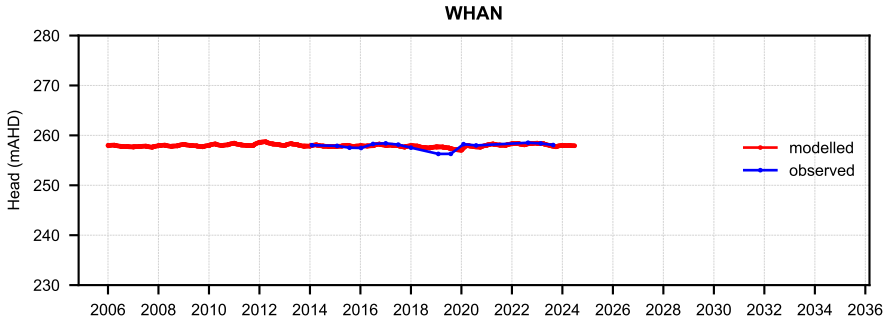
WHAN
Head (mAHD)
280
270
260
250
240
230
2006
2008
2010
2012
2014
2016
2018
2020
2022
2024
2026
2028
2030
2032
2034
2036
modelled
observed

F14 Predicted maximum drawdown

Table F 20 Predicted maximum drawdown that exceeds 2 m on private water supply bores

Bore ID	Bore registered number	Cumulative approved (Scenario 2)		Cumulative proposed (Scenario 6)	
		Maximum predicted drawdown	Year of maximum drawdown	Maximum predicted drawdown	Year of maximum drawdown
gw003520	gw003520	-	-	2.3	2240
gw015715	gw015715	-	-	3.4	2240
gw001928	gw001928	-	-	4.3	2240
gw001799	gw001799	2.4	2240	5.1	2240
gw011459	gw011459	3.3	2095	6.4	2150
gw901162	gw901162	3.4	2145	6.6	2150

Note: - predicted drawdown is less than 2 m.

F15 Uncertainty in maximum drawdown

Table F 21 Uncertainty in maximum drawdown

Location	Easting	Northing	Maximum Predicted Drawdown (metres)						
			mean	Standard deviation	minimum	25%	50%	75%	maximum
gw000891	231254	6597099	0.54	0.07	0.35	0.49	0.54	0.59	0.73
gw000921	227360	6595244	0.07	0.25	0	0	0.08	0.23	0.82
gw000965	230334	6593439	0	0	0	0	0	0	0
gw001799	235262	6609236	5.10	0.21	4.44	4.87	5.01	5.21	5.73
gw001928	235304	6617540	3.56	0.43	2.04	3.29	3.54	3.83	5.18
gw001999	221656	6626474	1.44	0.26	0.55	1.27	1.44	1.61	2.32
gw003073	234792	6603659	0	0	0	0	0	0	0
gw003150	220516	6628263	0	0	0	0	0	0	0
gw003520	235256	6618414	2.30	0.21	1.74	2.17	2.31	2.44	3.03
gw003530	230844	6621882	0.16	0.02	0.1	0.15	0.16	0.18	0.24
gw005749	229726	6594317	0	0	0	0	0	0	0
gw008205	215622	6628506	1.54	0.16	1.05	1.44	1.54	1.64	1.95
gw008236	233773	6621025	0	0	0	0	0	0	0
gw008238	231073	6621411	1.01	0.21	0.44	0.87	1.01	1.14	1.73
gw010751	220552	6626847	0.84	0.29	0	0.67	0.83	1.01	1.79

Location	Easting	Northing	Maximum Predicted Drawdown (metres)						
			mean	Standard deviation	minimum	25%	50%	75%	maximum
gw011043	219085	6628874	0	0	0	0	0	0	0
gw011044	219277	6629680	0	0	0	0	0	0	0
gw011070	212262	6626291	0.34	0	0.34	0.34	0.34	0.34	0.34
gw011459	221833	6629992	6.40	0.86	3.92	5.61	6.41	6.79	8.88
gw012804	215146	6621219	0.17	0.11	0	0.09	0.17	0.24	0.46
gw013065	216735	6629861	0	0	0	0	0	0	0
gw013066	217301	6629660	0	0	0	0	0	0	0
gw013946	215128	6626983	0	0	0	0	0	0	0
gw015055	225320	6599013	0.33	0.08	0.08	0.28	0.33	0.37	0.58
gw015715	223627	6631918	3.40	0.03	3.32	3.39	3.40	3.42	3.46
gw016139	235127	6603051	3.80	0.06	3.67	3.8	3.84	3.87	4
gw016328	213063	6631367	0	0	0	0	0	0	0
gw016874	238943	6594022	0.33	0.03	0.24	0.31	0.33	0.35	0.41
gw017285	213551	6617363	1.14	0.02	1.09	1.13	1.14	1.16	1.20
gw017521	216657	6629797	0	0	0	0	0	0	0
gw020251	216899	6595188	0.35	0	0.34	0.34	0.35	0.35	0.35
gw021703	216934	6596884	0.32	0	0.30	0.32	0.32	0.32	0.34
gw022097	215553	6624004	0.01	0.17	0	0	0.01	0.12	0.41

Location	Easting	Northing	Maximum Predicted Drawdown (metres)						
			mean	Standard deviation	minimum	25%	50%	75%	maximum
gw022098	216067	6624788	0	0	0	0	0	0	0
gw022104	215954	6622997	0	0	0	0	0	0	0
gw022905	213220	6617377	1.18	0.02	1.13	1.16	1.17	1.19	1.22
gw025637	217086	6615444	0	0	0	0	0	0	0
gw026032	217778	6600236	1.70	0.06	1.53	1.66	1.70	1.74	1.86
gw026498	234705	6603749	0	0	0	0	0	0	0
gw027653	224653	6623068	0	0	0	0	0	0	0
gw030540	222475	6599865	1.24	0.06	1.07	1.20	1.24	1.27	1.41
gw031340	234582	6603904	0	0	0	0	0	0	0
gw031900	221424	6593180	0.35	0	0.34	0.35	0.35	0.35	0.35
gw031919	216927	6595127	0.35	0	0.34	0.34	0.35	0.35	0.35
gw032080	218913	6602670	1.00	0.05	0.87	0.96	1.00	1.03	1.15
gw032093	217754	6598108	0.26	0.01	0.24	0.25	0.26	0.26	0.28
gw032265	215302	6602205	0	0	0	0	0	0	0
gw032712	219617	6622627	0	0	0	0	0	0	0
gw032925	219214	6600304	1.54	0.06	1.37	1.5	1.54	1.57	1.70
gw035920	218274	6621068	0.83	0.20	0	0.69	0.85	0.98	1.40
gw037136	220944	6597298	0.39	0.01	0.37	0.38	0.39	0.39	0.41

Location	Easting	Northing	Maximum Predicted Drawdown (metres)						
			mean	Standard deviation	minimum	25%	50%	75%	maximum
gw038675	214698	6626078	0	0	0	0	0	0	0
gw043067	226774	6600499	0.51	0.11	0.18	0.43	0.51	0.58	0.80
gw043142	216150	6628736	0.81	0.09	0.54	0.76	0.82	0.87	1.05
gw043458	214251	6617712	0.82	0.04	0.73	0.79	0.82	0.85	0.92
gw045596	213938	6631606	0	0	0	0	0	0	0
gw054311	212929	6601248	0	0	0	0	0	0	0
gw054713	216603	6602362	0	0	0	0	0	0	0
gw055081	216159	6602012	0.81	0.07	0.63	0.77	0.81	0.85	1
gw056932	225981	6628619	0.28	0.06	0.09	0.23	0.28	0.32	0.46
gw056945	213138	6617436	1.19	0.02	1.14	1.18	1.19	1.20	1.23
gw056948	212890	6617738	1.17	0.02	1.12	1.16	1.17	1.18	1.21
gw057438	222163	6597514	0.43	0.01	0.41	0.43	0.43	0.44	0.46
gw060823	218011	6598454	0.23	0.01	0.21	0.22	0.23	0.23	0.24
gw060867	237482	6596082	0.40	0.03	0.32	0.39	0.40	0.42	0.46
gw060920	237120	6605763	9.55	0.56	8.18	9.13	9.54	9.92	11.04
gw062727	220683	6623069	0	0	0	0	0	0	0
gw062728	223394	6623252	0	0	0	0	0	0	0
gw062729	223444	6623376	0	0	0	0	0	0	0

Location	Easting	Northing	Maximum Predicted Drawdown (metres)						
			mean	Standard deviation	minimum	25%	50%	75%	maximum
gw062730	223912	6623379	0	0	0	0	0	0	0
gw062731	222268	6624109	0	0	0	0	0	0	0
gw062732	222232	6623256	0	0	0	0	0	0	0
gw062733	223138	6622882	0	0	0	0	0	0	0
gw062734	222245	6623315	0	0	0	0	0	0	0
gw062735	221870	6623367	0	0	0	0	0	0	0
gw062736	224423	6621644	0	0	0	0	0	0	0
gw062737	225941	6627131	0.02	0.03	0	0	0.02	0.05	0.12
gw062738	227049	6627132	1.15	0.10	0.87	1.08	1.15	1.22	1.43
gw062739	227395	6626528	0.21	0.02	0.17	0.20	0.21	0.23	0.26
gw062740	227931	6626449	0.24	0.02	0.18	0.23	0.24	0.26	0.30
gw062741	226433	6626596	0.39	0.03	0.26	0.36	0.38	0.41	0.47
gw062742	226211	6625738	0.39	0.03	0.30	0.37	0.39	0.41	0.47
gw062743	226155	6624894	0.28	0.03	0.20	0.26	0.28	0.30	0.36
gw062744	226606	6625028	0.82	0.05	0.65	0.79	0.83	0.85	0.95
gw062745	227250	6624891	0.18	0.01	0.14	0.17	0.18	0.18	0.21
gw062746	225568	6624527	0	0	0	0	0	0	0
gw062747	225970	6624867	0.24	0.03	0.15	0.22	0.24	0.26	0.33

Location	Easting	Northing	Maximum Predicted Drawdown (metres)						
			mean	Standard deviation	minimum	25%	50%	75%	maximum
gw062748	216935	6620187	0.26	0.15	0	0.16	0.27	0.36	0.72
gw062749	217536	6619673	0.52	0.16	0	0.4	0.52	0.62	1.03
gw062750	217215	6619671	0.36	0.15	0	0.25	0.36	0.47	0.84
gw062751	220884	6622336	0	0	0	0	0	0	0
gw062775	224438	6624172	0	0	0	0	0	0	0
gw062776	223185	6624140	0	0	0	0	0	0	0
gw062781	232413	6621002	0	0	0	0	0	0	0
gw062782	232480	6621723	0.23	0.21	0	0.08	0.24	0.38	0.84
gw062783	232120	6621074	0.22	0.19	0	0.09	0.24	0.35	0.76
gw062784	231830	6621456	0.53	0.20	0	0.39	0.54	0.66	1.12
gw062788	235028	6621058	0	0	0	0	0	0	0
gw062789	232788	6620782	0	0	0	0	0	0	0
gw062792	228855	6626872	0.12	0.03	0.03	0.10	0.12	0.14	0.21
gw062793	228638	6625942	0.17	0.02	0.10	0.16	0.17	0.18	0.23
gw062794	218822	6622517	0	0	0	0	0	0	0
gw062795	217909	6622740	0	0	0	0	0	0	0
gw063742	217325	6627718	0.53	0.19	0	0.39	0.54	0.67	1.05
gw065669	213793	6625961	0.21	0.01	0.19	0.21	0.21	0.22	0.25

Location	Easting	Northing	Maximum Predicted Drawdown (metres)						
			mean	Standard deviation	minimum	25%	50%	75%	maximum
gw065672	231289	6598887	0	0	0	0	0	0	0
gw065733	222540	6601500	1.07	0.06	0.92	1.03	1.07	1.11	1.24
gw066211	214775	6619113	0.26	0.08	0.06	0.2	0.26	0.31	0.46
gw068150	224601	6600171	0.90	0.07	0.71	0.85	0.89	0.94	1.10
gw069109	220492	6623140	0	0	0	0	0	0	0
gw069131	215002	6592969	0.35	0	0.35	0.35	0.35	0.35	0.35
gw069132	214205	6593083	0.34	0	0.34	0.34	0.34	0.34	0.35
gw070540	233919	6623424	6.22	0.86	3.92	5.61	6.21	6.79	8.88
gw071936	215331	6608904	0.14	0.03	0.06	0.12	0.14	0.16	0.22
gw273200	219974	6622727	0	0	0	0	0	0	0
gw273201	219974	6622737	0	0	0	0	0	0	0
gw273202	219964	6622709	0	0	0	0	0	0	0
gw900000	217321	6627714	0.53	0.19	0	0.39	0.54	0.67	1.05
gw900363	224502	6623072	0	0	0	0	0	0	0
gw900381	215336	6609136	0.17	0.03	0.09	0.15	0.16	0.18	0.25
gw900409	214799	6619635	0.29	0.08	0.09	0.23	0.29	0.35	0.50
gw900493	225718	6626772	0.07	0.02	0.02	0.05	0.06	0.08	0.12
gw901067	217828	6598031	0.26	0.01	0.24	0.26	0.26	0.27	0.28

Location	Easting	Northing	Maximum Predicted Drawdown (metres)						
			mean	Standard deviation	minimum	25%	50%	75%	maximum
gw901091	221571	6595102	0.44	0.01	0.42	0.44	0.44	0.45	0.46
gw901099	215268	6619762	0	0	0	0	0	0	0
gw901162	222105	6630238	6.60	0.56	5.24	6.19	6.6	6.98	8.10
gw901940	217536	6598286	0.23	0.01	0.21	0.23	0.23	0.24	0.25
gw902049	217608	6598174	0.24	0.01	0.22	0.24	0.24	0.24	0.26
gw902074	224127	6632139	0	0	0	0	0	0	0
gw902408	213593	6625536	0.27	0.01	0.25	0.27	0.27	0.27	0.29
gw902849	220915	6598702	0.24	0	0.23	0.24	0.24	0.24	0.26
gw965430	233269	6598076	0.23	0.02	0.18	0.22	0.23	0.24	0.27
gw965935	215839	6620080	0	0	0	0	0	0	0
gw966829	213361	6618337	1.11	0.02	1.04	1.09	1.11	1.12	1.17
gw967252	218812	6602643	1.08	0.05	0.94	1.05	1.08	1.12	1.24
gw967471	215409	6613167	0.69	0.01	0.66	0.68	0.69	0.70	0.72
gw968531	224772	6622994	0	0	0	0	0	0	0
gw968645	214111	6617675	0.92	0.03	0.83	0.89	0.92	0.94	1.01
gw968706	226425	6592875	0.22	0.01	0.19	0.21	0.22	0.23	0.25
gw969277	214876	6619406	0.09	0.10	0	0.03	0.09	0.16	0.32
gw970204	232367	6594263	2.40	0.26	1.55	2.27	2.44	2.61	3.32

Location	Easting	Northing	Maximum Predicted Drawdown (metres)						
			mean	Standard deviation	minimum	25%	50%	75%	maximum
gw970209	239356	6597419	0.11	0.22	0	0	0.11	0.26	0.75
gw970269	214630	6624965	0.28	0.15	0	0.18	0.28	0.37	0.70
gw970797	223158	6603885	0.94	0.06	0.77	0.90	0.94	0.98	1.14
gw970900	227570	6632352	0	0	0	0	0	0	0
gw971159	224884	6629137	0.50	0.07	0.31	0.45	0.5	0.55	0.69
gw971331	233826	6598872	4.20	0.56	2.18	3.13	4.24	4.92	6.04
gw971337	233231	6597160	2.70	0.06	1.92	2.03	2.70	3.11	3.24

F16 Data space inversion

Note that the following section is an excerpt from the PEST manual and is provided here as a reference for anyone seeking more information on the application of the method used for the uncertainty analysis. Note that the PEST implementation of DSI has several versions. Moreover, none of these were used in this assessment; instead, the Pyemu implementation, which is similar to DSI2 in PEST, was employed. An abridged description of DSI2 is now presented, as outlined in the PEST manual.

"*DSI2 computes an empirical covariance matrix that effectively links the past to the future without involving model parameters. It obtains numbers on which to base this matrix from a CSV file that includes many realisations of model outputs, presumably based on many different model parameter sets. This CSV file may have been written by PESTPP-SWP, PESTPP-IES or other PEST utilities. Or it may have been written by another program altogether. Furthermore, in accordance with data space inversion theory, there is no reason for parameter sets on which model runs were based to be samples of a Gaussian probability distribution. Nor is there any need for model outputs to be continuous with respect to stochastic model parameters, for the DSI process does not require parameter adjustment.*

DSI2 reads a PEST control file (or simply the "observation data" section of a partial PEST control file), which ascribes values and weights to model outputs of interest. (As is described below, it can also ascribe measurement noise standard deviations to model outputs of interest.) Model outputs with which weights of zero are associated are deemed to be predictions. Those with which non-zero weights are associated are deemed to be observations of system state. Unless a standard deviation is specifically assigned to each observation, each such weight is presumed to be equal to the inverse of the standard deviation of measurement noise that is associated with the corresponding field observation.

Note that DSI2 ignores the "observed" values that are ascribed to model predictions. Nevertheless, it transfers the contents of the "observation data" section of this (partial) PEST control file to a new PEST control file. This file can be used by PEST, PEST_HP or PESTPP-IES for history-matching purposes. None of these programs subject zero-weighted model outputs to history-matching."

The following section presents a detailed discussion of the algorithmic aspects specific to the approach employed in this work.

"*DSI2 writes a PEST input dataset. Adjustable parameters pertain to PCA space. Each parameter has a prior mean of zero and a prior standard deviation of 1.0. There may be far fewer of these parameters than there are model outputs that are used in the DSI process. There will almost certainly be far fewer PCA parameters than model parameters. The model that is cited in the DSI2-generated PEST control file is DSIMOD. This is a surrogate model that is history-matched against past measurements of system states and fluxes while predicting future system states and fluxes. DSIMOD calculates surrogate model outputs (both past and future) from these PCA parameters.*

As PCA parameters are adjusted by PEST/PEST_HP or by PESTPP-IES, surrogate values of model predictions are also altered. History-matching of surrogate model outputs to their non-zero-weighted field-measured counterparts ensures that surrogate predictions are constrained by field data. If history-matching is undertaken using PESTPP-IES, then the posterior probability distributions of model predictions are thereby sampled."

Some notable academic journals where this method was applied to groundwater-related problems are summarised below with a reference and brief outline:

- *Sun, W. and Durlofsky, L.J., (2017). A new data-space inversion procedure for efficient uncertainty quantification in subsurface flow problems. Math. Geosci. 49:679-715.*

  It is considered a seminal paper on the application of DSI in groundwater flow problems. Here, DSI was used to estimate uncertainty in several subsurface flow problems featuring stochastically generated geological models. Comparisons were made to a Monte-Carlo style rejection sampling analysis, yielding good agreement in outcomes.

- *Lima et al., (2020) Data-space inversion with ensemble smoother. Comp. Geosci. 24:1179-1200.*

  This paper introduces a DSI implementation based on the use of an iterative ensemble smoother (IES). It demonstrates, with examples, that this new implementation is computationally faster and more robust than earlier methods based on principal component analysis and gradient-driven optimisation. The method was applied to a large reservoir model with long production history and many wells. The results were comparable to those obtained with traditional ensemble smoother approaches.

- *Delottier et al., (2023) Data space inversion for efficient uncertainty quantification using an integrated surface and sub-surface hydrologic model. Geosci. Model Dev. 16:4213-4231.*

  This paper examines the application of DSI in conjunction with linear analysis to conduct a data worth analysis. It also investigates the effectiveness and efficiency of using existing and future monitoring networks. Uncertainty analysis using traditional approaches with the numerical model Hydro-geosphere is compared to the uncertainty obtained in forecasts with DSI. The paper acknowledges some of the shortcomings of DSI as well, specifically the model's inability to inform the modeller of extreme outcomes.

- *Jiang et al., (2020) A data-space inversion procedure for well optimisation and closed loop reservoir management. Comp. Geosci. 24:361-379.*

  This paper uses DSI to perform non-linear optimisation of a reservoir well field. Substantial reductions to uncertainty are demonstrated in this paper. The method is then applied for data assimilation combined with production optimisation under uncertainty, as well as for closed-loop reservoir management, which entails a sequence of data assimilation and optimisation steps.